

University of Warwick institutional repository: <http://go.warwick.ac.uk/wrap>

A Thesis Submitted for the Degree of PhD at the University of Warwick

<http://go.warwick.ac.uk/wrap/34645>

This thesis is made available online and is protected by original copyright.

Please scroll down to view the document itself.

Please refer to the repository record for this item for information to help you to cite it. Our policy information is available from the repository home page.



**Reducing Catalyst Loadings in Radical Cyclisation Reactions and
Investigating Atropisomerism in Enamides**

By

Paul Wilson

A thesis submitted in partial fulfilment of the requirements for the degree of
Doctor of Philosophy in Chemistry

University of Warwick, Department of Chemistry

June 2010

Contents

Acknowledgements	vi
Declaration	viii
Abstract	ix
Abbreviations	xi
Chapter 1 Introduction	1
1.1 Traditional Radical Cyclisation	1
1.2 Origins of Atom Transfer Radical Cyclisation (ATRC)	3
1.3 Copper Mediated ATRC	7
1.3.1 <i>5-Exo Trig</i> ATRC	8
1.3.2 <i>5-Exo Dig</i> ATRC	13
1.3.3 <i>4-Exo</i> and <i>5-Endo Trig</i> Radical Cyclisation	15
1.3.4 Other Ring Sizes by ATRC	19
1.3.5 Rearrangement Reaction	22
1.4 Recent Developments in Transition Metal Mediated ATRC	24
1.4.1 Di-Ttin Derivatives	24
1.4.2 Solid Supported Copper Catalysed ATRC	25
1.4.3 ATRC Using Perfluorous Catalysts	28
1.4.4 Reducing Catalyst Loadings in Atom Transfer Radical Reactions	29
1.4.5 Alternative Transition Metal Mediated ATRC	33
1.4.5.1 Ruthenium	33
1.4.5.2 Titanium	37

	1.4.5.3 Zinc	38
1.5	Synthetic Application of Radical Cyclisation	39
	1.5.1 Natural Product Synthesis Using Di-Tin Reagents	40
	1.5.2 Natural Product Synthesis Using Copper Mediated ATRC	41
1.6	Summary	45
Chapter 2	Radical Cyclisation Reactions Using 1,4-Dimethylpiperazine	47
2.1	Introduction	47
2.2	Results and Discussion	51
	2.2.1 1,4-Dimethylpiperazine Mediated Radical Cyclisation	53
	2.2.2 Radical Trapping	62
	2.2.3 Conclusion	66
Chapter 3	Copper Mediated Atom Transfer Radical Cyclisation Using AIBN and Other Additives	67
3.1	Introduction	67
	3.1.1 The Use of Additives in Atom Transfer Radical Addition And Polymerisation	67
3.2	Results and Discussion	72
	3.2.1 Screening Potential Additives for Copper Mediated ATRC	72
	3.2.2 Scope of Copper Atom Transfer Radical Cyclisation Using AIBN	79
	3.2.2.1 5-Exo Trig ARGET-ATRC	80
	3.2.2.2 5-Exo Dig ARGET-ATRC	85
	3.2.3 Conclusion	88

Chapter 4	Copper Mediated Radical Cyclisation in the Presence of Borohydrides	90
4.1	Introduction	90
4.1.1	Classical Borohydride Chemistry	91
4.1.2	Radical Reactions Involving Sodium Borohydride	92
4.1.3	Copper Borohydride (CuBH ₄)	94
4.2	Results and Discussion	97
4.2.1	The Effect of Borohydride Addition	97
4.2.2	The Effects of Copper Salt and Ligand	101
4.2.3	UV Experiments	105
4.3	Scope and Limitation of Cu(TPA)SO ₄ /KBH ₄ Mediated Cyclisation	110
4.3.1	<i>5-Exo Trig</i> AGET ATRC	112
4.3.2	<i>5-Exo Dig</i> AGET ATRC	116
4.3.3	<i>4-Exo Trig</i> AGET ATRC	118
4.3.4	<i>5-Endo Trig</i> Radical Cyclisation	120
4.3.5	Tetralone Enamides	122
4.4	Conclusion	124
Chapter 5	Atropisomeric Enamides. A Route to Asymmetric <i>5-Endo Trig</i> Radical Cyclisation?	126
5.1	Introduction	126
5.1.1	Early Evidence of Atropisomerism	126
5.1.2	Chiral Induction in Radical Cyclisation	133
5.1.3	Atropisomerism in Enamides	136
5.2	Results and Discussion	142

5.2.1	Barriers to Rotation for Cycloalkenyl Enamides – Effect of α -Halogen	143
5.2.2	General Appearance of ^1H NMR of Enamide Substrates	146
5.2.3	Effect of Ring Size	149
5.2.4	Tetralone Enamides	152
5.2.5	Effect of Solvent	154
5.2.6	Barriers to Rotation for Cyclohexenyl Enamides, Varying the Acyl Group	156
5.2.7	Tetrasubstituted Enamides	163
5.2.8	Conclusion	176
5.3	Future Work	177
Chapter 6	Experimental	179
6.1	General Information and Procedures	179
6.2	General Procedures	181
6.2.1	General Procedures for Substrates Synthesised in Chapter 2	181
6.2.2	General Procedures for 1,4-DMP Mediated Radical Cyclisation	189
6.2.3	General Procedures for 1,4-DMP Mediated Radical Cyclisation Using the Freeze-Pump-Thaw Technique	191
6.2.4	1,4-DMP Mediated Radical Cyclisation in a Microwave	196
6.2.5	General Procedures for Substrates Synthesised in Chapter 3	198
6.2.6	General Procedures for Copper Mediated ATRC Using AIBN in Chapter 3	202

6.2.7	General Procedures for Substrates Synthesised in Chapter 3	211
6.2.8	General Procedures for the Synthesis of Enamides in Chapter 4	213
6.2.9	General Procedures for Copper Mediated ATRC Using KBH_4 in Chapter 4	220
6.2.10	General Procedures for the Synthesis of Enamides in Chapter 5	233
6.2.11	General Procedures for the Synthesis of Tetrasubstituted enamides in Chapter 5	243
6.2.12	General Procedures for the Alkylation of Enamides	250
6.2.13	Products of Attempted Cyclisations Performed in Chapter 5	256
Appendices		259
Appendix A	<i>N</i> -Cycloalkenyl Bond Rotation Studies	259
Appendix B	Chiral HPLC Reports	291
Appendix C	X-Ray Crystallography Data	295
References		297

Acknowledgements

Firstly I would like to thank and extend my utmost respect to my academic supervisor Dr Andrew Clark for putting his faith in me to deliver on the number of projects we have worked on. His guidance and the working environment he provides has proved ideal for my development as a synthetic chemist able to achieve personal and team goals, and that will not be forgotten throughout my career, wherever it takes me. I would also like to thank the ever expanding Clark group, in particular Dr Stuart Coles who was my only companion and a fountain of air sensitive knowledge in the first year of my research. Thanks also to my advisory committee academics, Prof Peter Scott and Dr Guy Clarkson who provided priceless guidance in the development of my research. Thanks also to Guy for the number of X-ray crystal structures he was able to elucidate for me. I would also like to thank Dr David Fox for a number of insightful exchanges which proved influential in the direction of my research into copper mediated atom transfer radical cyclisation, contributing to the progress reported in chapter 4. Throughout the department there are countless people that deserved credit for the excellent jobs they do. Dr Lijiang Song runs an efficient mass spec service and I am grateful to him for all the high resolution mass spectra he performed. Special thanks must go to the NMR service run by Dr Adam Clarke and Dr Ivan Prokes who performed numerous, time consuming, variable temperature NMR experiments. Without them chapter 5 would have been impossible. Concerning chapter 5, Professor Dennis Curran, Dr Dave Guthrie and a number of co-workers at the University of Pittsburgh are thanked for sharing their ideas in a really interesting and rewarding collaboration.

Away from the University there are far too many to people to thank individually. My friends are an extremely important part of my life and I dedicate this work to them. Special thanks go to William Hanna, whose unwavering belief inspired me to set my sights above and beyond my own modest expectation.

Finally I would like thank those closest to me. An eternity of thanks is offered to my long suffering thesis widow girlfriend Sally. Her love and support and the dream of a happy, comfortable future have driven me on through challenging times. My family are without doubt the most important and influential people in my life. I am lucky to have such a close relationship with my brother and sisters and I am extremely proud of them, I hope they equally as proud of me. Finally that leaves me to thank my parents. Words cannot do justice to the job they have done with all four of us. They have sacrificed and worked their entire lives to provide us with the priceless opportunity of education, which we all chose to pursue. I hope they are pleased with their investment and that this work and all that I can endeavour to achieve throughout the remainder of my career can make them as proud of me as I am of them. I love them dearly, from the bottom of my heart.

Declaration

The work presented in this thesis is the original work of the author. References to previous related results and ideas have been fully acknowledged. All work was performed in the Department of Chemistry at the University of Warwick between October 2006 and October 2009 and has not been submitted for a degree at any other institution.

Paul Wilson

Abstract

The bulk of the work presented in this thesis represents an evolution of copper-mediated atom transfer radical cyclisation. Chapter 1 provides introduction to radical cyclisation methods and applications and is followed by the shortest results chapter that discusses the outcome of 1,4-dimethylpiperazine mediated radical cyclisation of monobromoacetamides. Cyclisation was possible but competing reduction and elimination pathways are prevalent when less reactive substrates are used.

Chapters 3 and 4 focus on the evolution of copper-mediated atom transfer radical cyclisation. A number of additives were screened in the hope of achieving catalyst regeneration which would allow catalyst loadings to be reduced without loss of efficiency and negate the need for an inert atmosphere throughout the reaction. In chapter 3, AIBN was found to be the optimum additive and efficient cyclisation was possible using copper (I) (Cu(TPA)Br) and copper (II) (Cu(TPA)Br₂) complexes (1 mol%) in DCM and toluene (at 50 and 110 °C respectively) suggesting AIBN could activate and reactivate the catalyst *in situ*.

In chapter 4 an alternative, highly efficient process was developed using copper (II) in the presence of potassium borohydride in MeOH. Reaction times were significantly reduced (10-30 min) and reactions were performed at room temperature even at decreased catalyst loadings (0.1 mol%). The mechanism for the process is likely to differ from that of conventional atom transfer radical cyclisation. UV analysis of the catalyst complex and the reactions progress, compared to literature data, suggest the active catalyst could be a copper borohydride (CuBH₄) complex.

Finally chapter 5 compiles a structural analysis of a variety of enamides to determine the feasibility of chiral induction during *5-endo trig* radical cyclisation. A number of *N*-cycloalkenyl and *N*-cyclohexenyl enamides, which share an axis of chirality about the N-C(cycloalkenyl) bond, were analysed by variable temperature NMR to determine the rate and barrier of rotation of the chiral axis. Although none of the enamides studied had barriers great enough to achieve chiral induction it was recognised that the barrier to rotation could be significantly increased if tetrasubstituted enamides were accessible. Tetrasubstituted enamides were prepared and their barriers were determined by chiral HPLC, with barriers predicted to be great enough for chiral induction. Cyclisation was attempted but to no avail with unexpected oxidation products being obtained. Despite this, a more comprehensive understanding of the enamide structure has paved the way for potential chiral induction in *5-endo trig* radical cyclisation.

Abbreviations

Ac	Acetyl
acac	Acetyl acetate
AIBN	Azobisisobutyronitrile
AGET-	Activators generated by electron transfer
Ar	Aryl
ARGET-	Activators regenerated by electron transfer
ATRA	Atom transfer radical addition
ATRC	Atom transfer radical cyclisation
ATRP	Atom transfer radical polymerisation
Bipy	Bipyridine
Bn	Benzyl
br	Broad
Bu	Butyl
^t Bu	<i>tert</i> -Butyl
BuLi	Butyl lithium
Conv	Conversion
d	Doublet
dd	Doublet of doublets
ddd	Doublet of doublet of doublets
ddt	Doublet of doublet of triplets
dt	Doublet of triplets
DCE	Dichloroethane
DCM	Dichloromethane

de	Diastereomeric excess
DMAP	Dimethylaminopyridine
DMF	Dimethylformamide
1,4-DMP	1,4-Dimethylpiperazine
D ₂ O	Deuterium Oxide
EI	Electron Ionisation
eq	Equivalents
ESI	Electrospray Ionisation
Et	Ethyl
Et ₃ B	Triethylborane
Et ₃ N	Triethylamine
Et ₂ O	Diethyl ether
EtOH	Ethanol
<i>h</i>	Planck's Constant
ΔH^\ddagger	Enthalpy (of rotation)
HPLC	High Performance Liquid Chromatography
HRMS	High Resolution Mass Spectroscopy
Hz	Hertz
ΔG^\ddagger	Gibbs Free Energy (of rotation)
IR	Infra-red
k_c	Rate Constant of Cyclisation
k_b	Boltzmann Constant
k_{elim}	Rate Constant of Elimination
k_{rot}	Rate Constant of Rotation
m	Multiplet

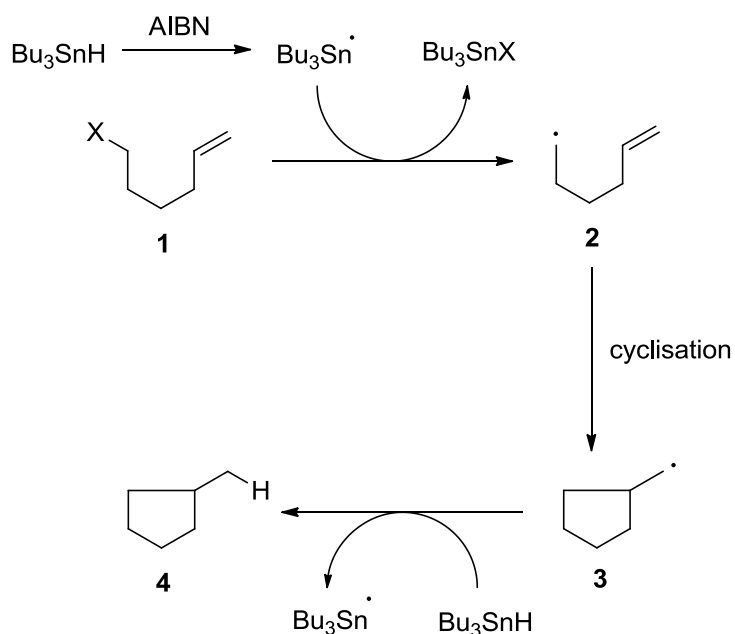
maj	Major
MB	Mass Balance
Me	Methyl
MeCN	Acetonitrile
MeOH	Methanol
Me ₆ -Tren	<i>N,N,N',N',N'',N''</i> -hexamethyltriethylenetetramine
Mg	Magnesium
min	Minor
mpt	Melting Point
MW	Microwave
NHC	<i>N</i> -heterocyclic carbene
nm	Nanometers
NMPI	Pyridine-imine ligand
NMR	Nuclear magnetic resonance
Ph	Phenyl
PMB	<i>para</i> -Methoxybenzyl
PMDETA	<i>N,N,N',N',N''</i> -pentamethyldiethylenetriamine
PhNEt ₂	Diethylaniline
ppm	Parts per million
q	Quartet
RCM	Ring closing metathesis
rt	Room temperature
<i>R</i>	Gas Constant
s	Singlet
ΔS^\ddagger	Entropy (of rotation)

Sept	Septet
SET	Single electron transfer
SET-LRP	Single electron transfer living radical polymerisation
SM	Starting Material
t	Triplet
t _{1/2}	Half-life
TBDMS	<i>tert</i> -Butyldimethylsilyl
Temp	Temperature
THF	Tetrahydrofuran
TLC	Thin Layer Chromatography
TMEDA	Tetramethylethylenediamine
TMS	Trimethylsilyl
Tol	Toluene
Tp	Trispyrazoloylborate
TPA	Tripyridylamine
Ts	Tosyl
V70	2,2'-azobis-(4-methoxy-2,4-dimethyl) valeronitrile
W	Watts
VTNMR	Variable Temperature Nuclear Magnetic Resonance

1.0 Introduction

1.1 TRADITIONAL RADICAL CYCLISATION

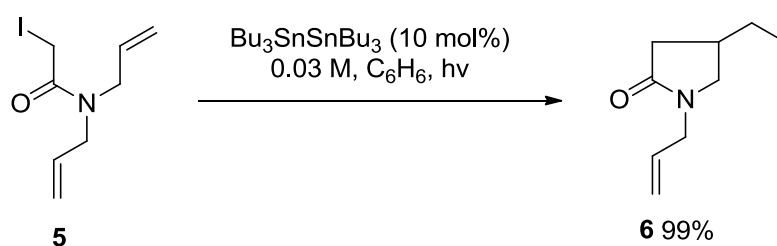
Traditionally, radical cyclisation reactions are achieved using organostannane and organosilane reagents (Bu_3SnH or $(\text{SiMe}_3)_3\text{SiH}$)^{1,2,3} in the presence of radical initiators (peroxides, AIBN) in refluxing benzene or toluene to generate tin or silicon centered radicals. These radicals take advantage of weak $\sigma\text{-C-X}$ ($\text{X} = \text{halogen}$) bonds in the precursor **1** to produce radical **2** that cyclises onto a radical sink (alkene or alkyne) to form a third radical **3**, which abstracts a hydrogen atom from the organostannane or organosilane reagent to furnish the cyclised product **4** and another reactive radical to continue the radical chain (Scheme 1.1).



Scheme 1.1: Reductive Radical Cyclisation Mechanism

Although this has been shown to be a synthetically useful transformation, there are a number of disadvantages associated with organostannane and organosilane reagents. The principal drawback for both methods is that they are reductive in nature. On a laboratory scale this is not always a problem, but quenching the cyclised radicals **3** with hydrogen atoms can be limiting as it leads to the loss of two functional groups in the product **4**. Additional disadvantages include the need for stoichiometric amounts (high cost), and organostannane reagents and their byproducts are particularly toxic, which cause problems and complicate the purification process. All of these issues are magnified on scale-up, making such reactions industrially unattractive.

A non-reductive, non-stoichiometric, alternative organostannane mediated radical cyclisation was developed in the late 80's and early 90's by Curran.^{4,5} The possibility of reductive termination was removed by replacing Bu_3SnH with hexabutylditin ($\text{Bu}_3\text{SnSnBu}_3$), which also allowed the loading of the organostannane reagent to be reduced to the catalytic level of 10 mol% (Scheme 1.2).



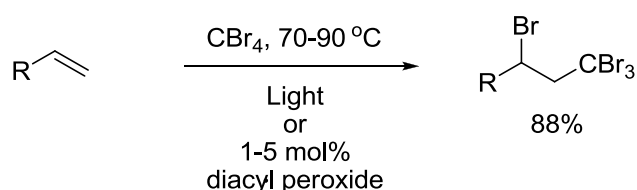
Scheme 1.2: Hexabutylditin Mediated ATRC

The reaction was initiated by photolysis of the Sn-Sn bond and the reaction was found to be terminated by iodine atom transfer from the substrate **5**. Radical cyclisations of this sort are commonly known as atom transfer radical cyclisation reactions (ATRC). The preservation of functionality and the catalytic nature of the

ditin reagent represented significant improvements in organostannane mediated radical cyclisation. However, the toxicity of the tin reagents and byproducts remained a major drawback of these radical cyclisation protocols.

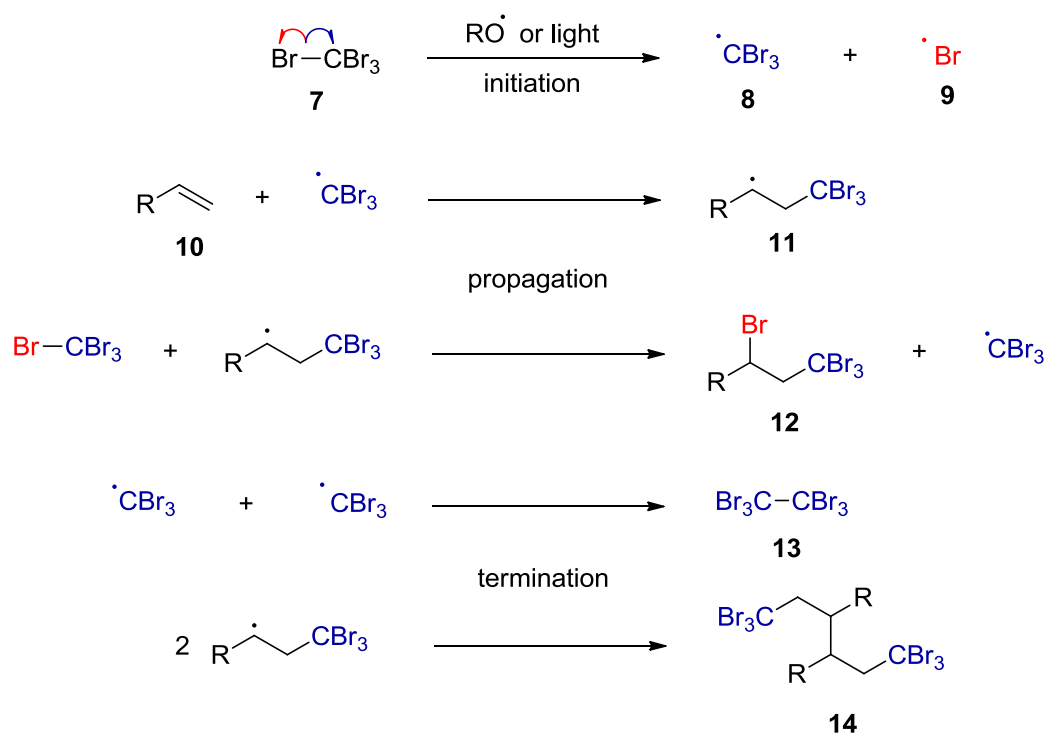
1.2 ORIGINS OF ATOM TRANSFER RADICAL CYCLISATION

In 1945-46,^{6,7,8} Kharasch performed a number experiments resulting in the addition of carbon tetrahalides and haloforms across alkenes. When the halogens present were chlorine atoms, a catalytic amount of diacyl peroxide was required to afford addition. However, when the halogens present were bromine atoms, addition was observed in the absence of peroxides, but in the presence of visible light.



Scheme 1.3: Kharasch Addition of CBr₄ to Terminal Alkenes

Mechanistically, Kharasch proposed that addition proceeded through a radical chain reaction, initiated by homolysis of a C-X (halogen) bond to form a carbon centered radical **8**, and a halogen radical **9**. Addition of the carbon radical **8** to the less substituted end of the alkene **10** then formed a second radical **11**. This could then react with another molecule of CX₄ to form the addition product **12**, and another carbon centered radical that could react with another alkene molecule. Initiation of this transformation can be achieved chemically or photolytically depending on the nature of the initiator, and propagation relies on the preservation of a reactive radical upon product formation.

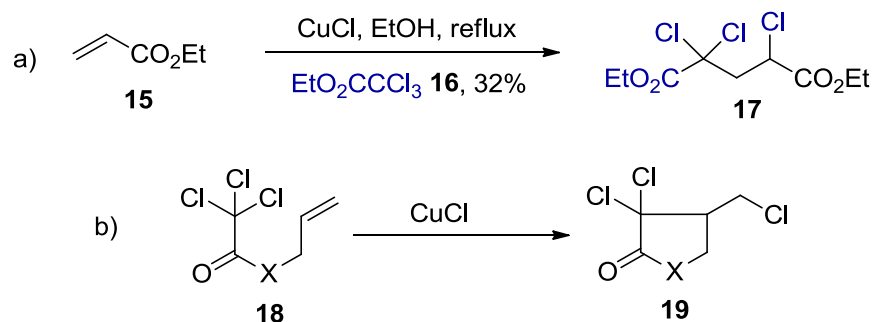


Scheme 1.4: Radical Chain Mechanism

In order for the radical chain to propagate, termination pathways must be avoided. Kharasch addition (Scheme 1.4) can be identified as the first example of intermolecular atom transfer radical addition (ATRA). Substrate and reagent concentrations dictate the relative propensities of propagation and termination. Altering the reactivity of the radicals present during reaction can dictate the product identity, as telomers and polymers, as well as monoadduct products, can be obtained. This is discussed in more detail in section 3.1.

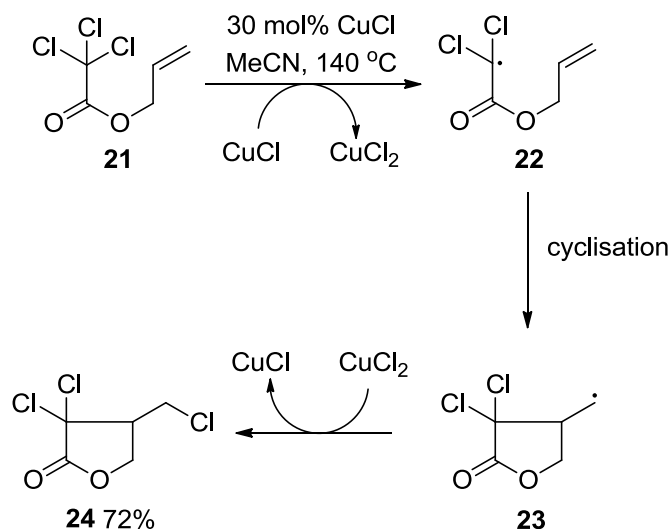
A less toxic, oxidative route to cyclisation (**18** → **19**, Scheme 1.5b) has been developed. The intermolecular version of this reaction, namely addition of **16** to ethyl acrylate **15** to give functionalized monoadduct products **17** (Scheme 1.5a), is also known.⁹ These reactions were mediated using transition metal catalysis, in particular cuprous (CuCl) and cupric chloride (CuCl₂). The authors predicted that

the transition metal catalysed process was unlikely to follow the radical chain mechanism of Kharasch addition, with an alternative catalytic redox mechanism thought to be more likely (Scheme 1.6).



Scheme 1.5: a) Copper Mediated Intermolecular Addition
b) Copper Mediated Intramolecular Addition

The copper-mediated intramolecular addition reaction was achieved by Nagashima in 1983 when they heated activated trichloroacetate **21**, in the presence of CuCl in MeCN (140 °C) in a pressurized bottle for 1 hour to give lactone **24** in 72% yield.¹⁰ With greater confidence they proposed that the reaction followed a catalytic redox mechanism in which CuCl interacted with the substrate **21** to furnish a tertiary radical **22**. This then cyclised to give a more reactive primary radical **23** which could react with CuCl₂ to furnish a functionalised lactone **24** and regenerate the CuCl catalyst (Scheme 1.6).



Scheme 1.6: Intramolecular Radical Addition Mechanism (ATRC)

The redox mechanism allows the reaction to be oxidatively quenched, preserving a degree of functionality in the cyclised products for additional chemistry. Furthermore, the transition metal reagents are relatively cheap, easily handled and purified (*via* filtration through a silica plug) and most importantly the process is catalytic as sub-stoichiometric amounts of copper salts are used. It should also be noted that mechanistically **24** could also be formed from atom transfer from the reaction substrate **21** ($\text{23} + \text{21} \rightarrow \text{24}$). If the desired product **24** is furnished in this way, the failure of the final redox process ($\text{CuCl}_2 \rightarrow \text{CuCl}$) would lead to an accumulation of CuCl_2 , and this would lead to the retardation of reaction initiation; however, in the hands of Nagashima and at 30 mol% catalyst loading this potential problem was not evident.

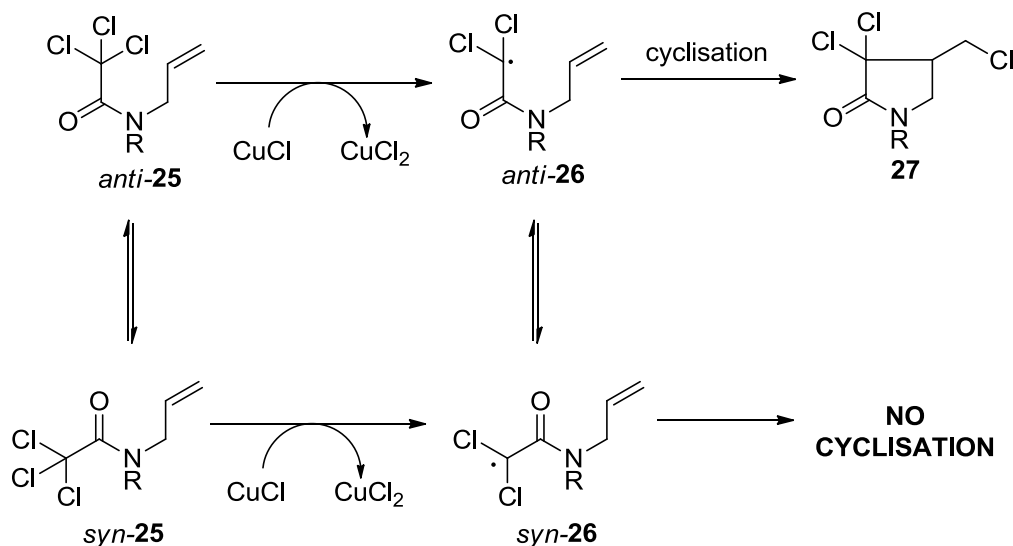
1.3 COPPER MEDIATED ATOM TRANSFER RADICAL CYCLISATION

The cyclisation of trichloroacetate **21** is an example of copper (I) mediated 5-*exo trig* ATRC, which is the most facile and abundantly studied mode of radical cyclisation. A number of factors that influence the rate and outcome of copper (I) mediated ATRC must be considered. Firstly, cyclisation is initiated by homolysis of the C-X (halogen) bond, the rate of which is dependent upon the bond dissociation energy of the bond in question.^{11,12,13} Stronger bonds are more difficult to homolyse than weaker ones and as a result the ease of C-X bond homolysis follows the order C-F < C-Cl < C-Br < C-I. In addition, adjacent halogen substituents weaken the bond dissociation energy further so for homolysis $\text{CCl}_3 > \text{CHCl}_2 > \text{CH}_2\text{Cl}$.

Once the radical is formed the rate and outcome of cyclisation is determined by the radical stability, stereoelectronic effects of ring formation and the radical conformation. Like their ionic counterparts (carbocations R_3C^+), carbon-centered radicals are stabilized by adjacent electron donating substituents. Therefore carbon-centered radicals show the following order of stability $\text{R}_3\text{C}\cdot > \text{R}_2\text{HC}\cdot > \text{RH}_2\text{C}\cdot$. Additionally, and unlike carbocations, radicals can also be stabilized by electron withdrawing groups such as halogens and carbonyl groups.

Some radical precursors are not predisposed for cyclisation, existing in conformations that prevent the required orbital overlap between the radical and the unsaturated carbon of the radical sink. Trichloroacetamides and the radicals derived from them, such as **25** and **26**, can exist as two amide conformers due to slow rotation about the amide (N-CO) bond. When unprotected (R = H) the least sterically hindered *syn* amide conformer is preferred which cannot cyclise. However

addition of bulky or electron withdrawing R groups pushes the equilibrium towards the *anti* conformer which can undergo cyclisation (Scheme 1.7).¹⁴



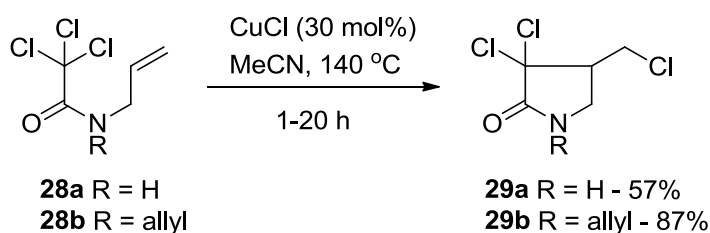
Scheme 1.7: Amide Bond Rotation Giving Rise to *Syn* and *Anti* Acetamide Rotamers

Two other factors that affect the outcome of the radical cyclisation are the nature of the reaction solvent and the addition of additives. Hydrogen donating solvents, such as THF,¹⁵ can intercept intermediate radicals (e.g. **22** or **23**, Scheme 1.6) leading to reduction and as a result poor donor solvents tend to be used for ATRC (toluene, DCM). The addition of amine and pyridine based ligands to the reaction mixture has been shown to significantly accelerate the rate of cyclisation by improving the solubility of the copper salts and/or altering the redox potential of the catalyst system.^{16,17}

1.3.1 5-*Exo* Trig ATRC

The development of copper-mediated ATRC during the end of the last century and the beginning of this one has been summarized in a comprehensive

review by Clark.¹⁸ Initial reactions of trichloroacetamides such as **28a/b** utilized CuCl as a catalyst in MeCN to afford γ -lactams^{19,20} such as **29a/b** via 5-*exo trig* cyclisation. However, in order to achieve synthetically useful yields, high reaction temperatures, and in some cases long reaction times, were required to overcome unfavourable conformer populations (Scheme 1.8).



Scheme 1.8: CuCl Catalysed ATRC

Reactions were improved following the discovery of ligand-accelerated ATRC. Originally, nitrogen containing bidentate ligands including bipyridine (bipy, **30**),^{16,17} pyridine-imine ligands (NPMI's, **31**)^{15,21,22,23,24,25} and tetramethylethylenediamine (TMEDA, **32**)^{26,27,28,29} were shown to significantly improve the efficiency of copper-mediated ATRC.

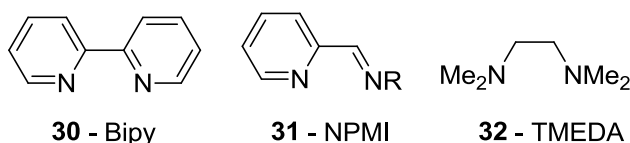
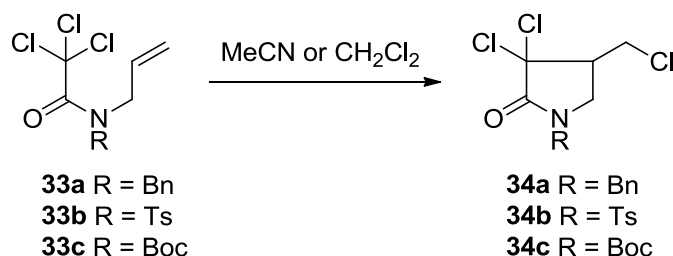


Figure 1.1: Bidentate Ligands Used in Copper Mediated ATRC

It was proposed that these ligands accelerated the atom transfer process by either improving the solubility of the copper salt (CuCl), by altering the redox potential of catalyst system, or by both.^{16,17} For example, the addition of bipy reduced both the reaction time and temperature of the cyclisation of acetamides

33a/b/c. In addition, the formation of such a copper complex allowed the reaction to be carried out in a variety of solvents such as DCM, in which CuCl alone is insoluble (Table 1.1).¹⁷

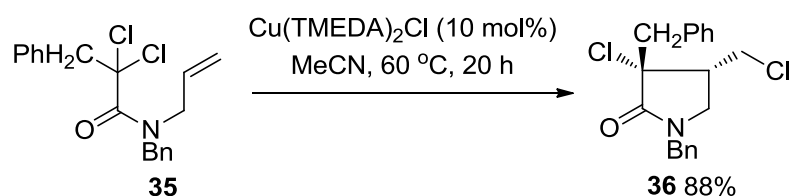


Entry	Substrate	Catalyst (30 mol%)	Temp °C	Time h	Yield
1	33a	CuCl	80	18	68%
2	33a ^a	Cu(30)Cl	rt	1	98%
3	33b	CuCl	rt	24	97%
4	33b ^a	Cu(30)Cl	rt	0.2	91%
5	33c	CuCl	80	4	80%
6	33c ^a	Cu(30)Cl	rt	2	78%

^a Reactions performed in DCM

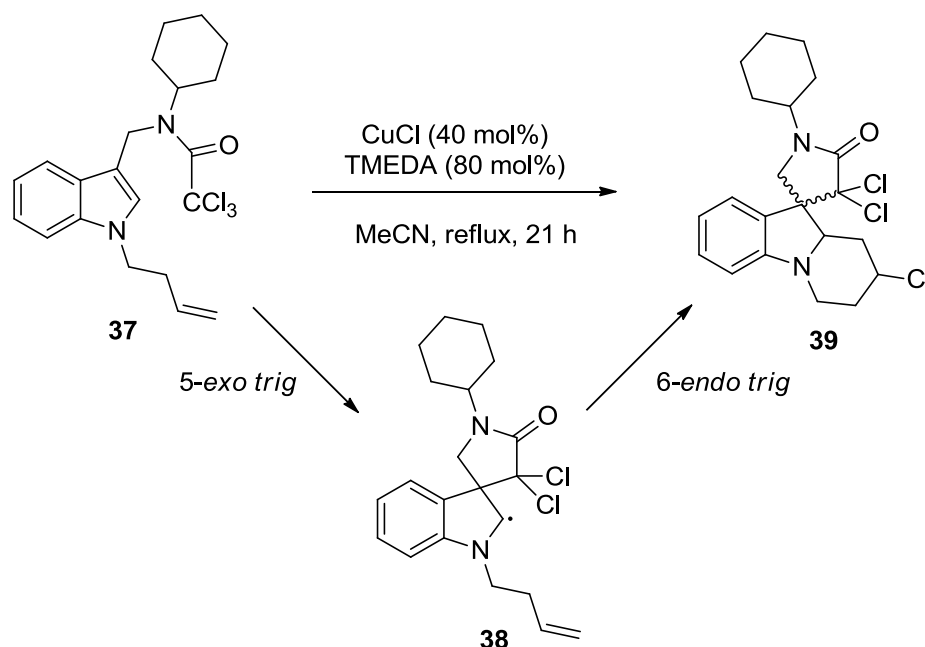
Table 1.1: The Effect of Bipy and Protecting Group (R) on Copper Catalysed ATRC

The use of TMEDA (**32**) as a ligand was found to furnish a more reactive catalyst complex (Cu(TMEDA)₂Cl) than the bipy (**30**) and NPMI (**31**) ligands, improving reaction yields even at reduced catalyst loadings. Cyclisation of dichloroacetamide **35** was unsuccessful using Cu(bipy)Cl, however in the presence of 10 mol% Cu(TMEDA)₂Cl cyclisation was observed to afford an 88% yield of **36** as a single diastereomer (Scheme 1.9).²⁶



Scheme 1.9 Cu(TMEDA)₂Cl Mediated ATRC

More recently, TMEDA (**32**) has been used as the ligand for the copper-catalysed formation of benzospiro-indolizidinepyrrolidinones **39**.³⁰ These compounds occur as a result of sequential carbon-carbon bond forming reaction *via* 5-*exo* (**37** → **38**) then 6-*endo trig* (**38** → **39**) cyclisations. For optimal conversions, the substrate was refluxed in acetonitrile with a 1 : 2 mixture of CuCl (40 mol%) and TMEDA (80 mol%), resulting in formation of the desired product **39** in 40% yield as a mixture of diastereomers (Scheme 1.10).



Scheme 1.10: Tandem Copper Mediated ATRC as a Route to Spiro-Cyclised Indoles

Ghelfi and coworkers reported that the optimum TMEDA (**32**) to copper ratio was 2 : 1, stipulating that 2 equivalents of the bidentate ligand were required to form an active complex.²⁶ As a result alternative ligands *N,N,N',N',N''*-pentamethyldiethylenetriamine (PMDETA **40**),³¹ *N,N,N',N',N'',N''*-hexamethyltriethylenetetramine (Me₆-Tren **41**),^{15,21,25, 32} and tetradentate pyridine ligand tri-pyridylamine (TPA **42**),³³ have been developed to form complexes with a 1 : 1 copper/ligand ratio (Figure 1.2).

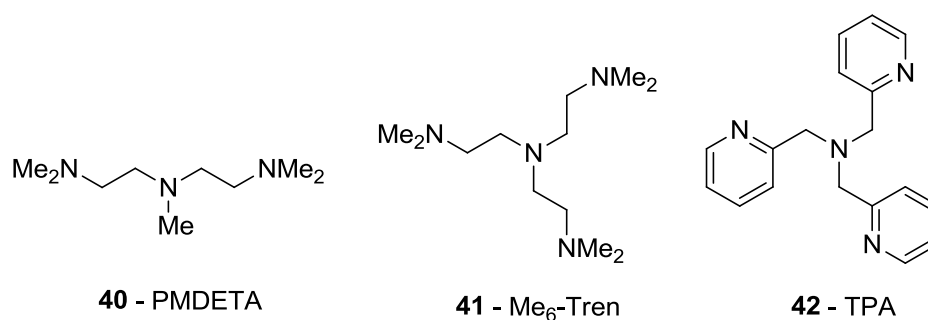
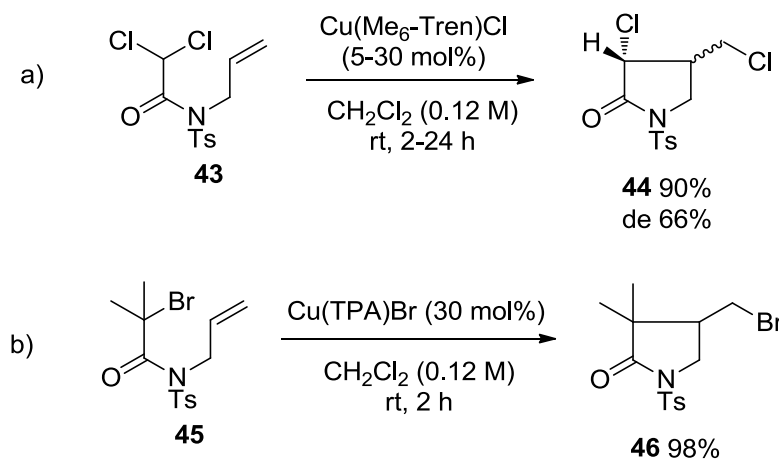


Figure 1.2: Amine and Pyridine Based Ligands That Form Highly Active Complexes

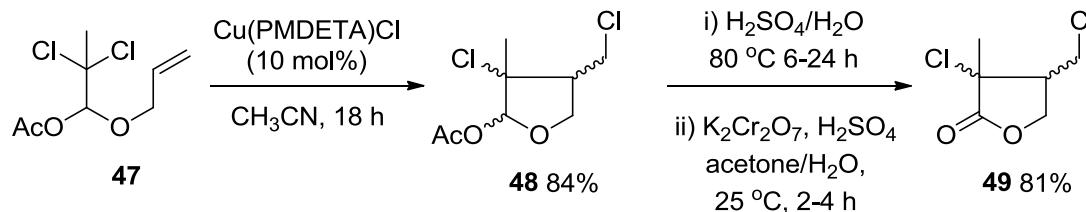
The Cu(Me₆-Tren)X and Cu(TPA)X complexes were found to be significantly more active than any of the bidentate ligand complexes. The more activated nature of the Cu(Me₆-Tren)Cl catalyst allowed the cyclisation of activated dichloroacetamide **43** with a catalyst loading as low as 5 mol% in good yield (Scheme 1.11a).^{21,32} Similarly, Cu(TPA)Br efficiently catalysed the cyclisation of relatively deactivated monobromoacetamide **45** (Scheme 1.11b).³³



Scheme 1.11: a) Cu(Me₆-Tren)Cl Mediated ATRC
b) Cu(TPA)Br Mediated ATRC

In a recent study by Ghelfi and co-workers, a related dichlorohemiacetal acetate **47** was shown to undergo facile Ueno-Stork ATRC using Cu(PMDETA)Cl, in a one pot, multi step reaction (Scheme 1.12).³¹ The cyclic product **48** was

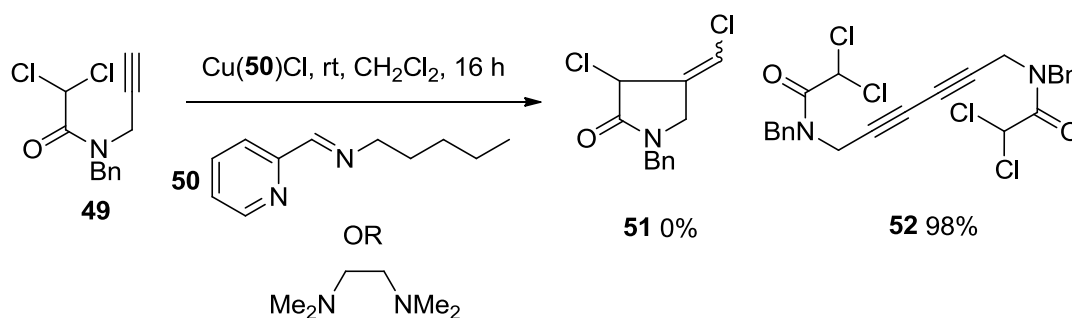
obtained in 84% yield, and the lactone product **49** was easily obtained *via* subsequent oxidation processes.



Scheme 1.12: Cu(PMDETA)Cl Mediated Ueno-Stork ATRC

1.3.2 5-Exo Dig ATRC

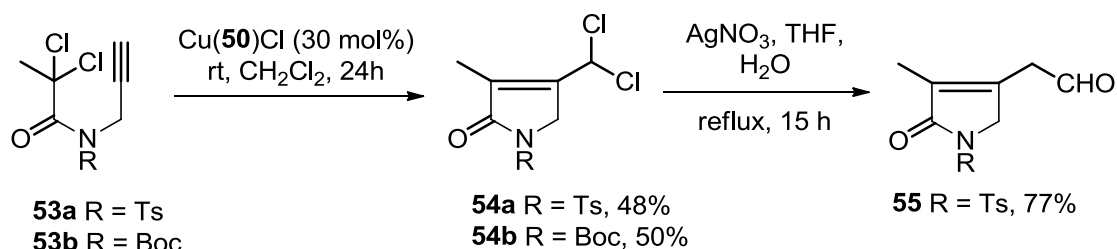
5-Exo dig ATRC reactions of propargylic acetates and acetamides leading to the formation of highly reactive vinyl radicals have been found to be more difficult than the corresponding 5-*exo trig* reactions.¹⁵ In some cases where bidentate ligands such as NPMI's (**31**) and TMEDA (**32**) are used, reactions can be complicated by facile oxidative dimerisation.¹⁵



Scheme 1.13: Oxidative Coupling of Terminal Alkynes

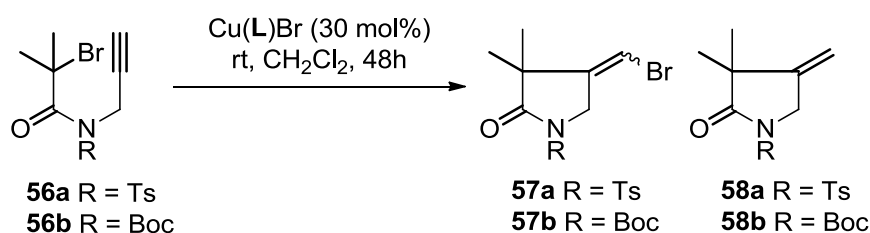
Consequently, the successful 5-*exo dig* radical cyclisation of acetamides has been shown to be dependent on the nature of the protecting group. For example, *N*-

benzyl propargylic acetamides (**49**) tend to undergo dimerisation¹⁵ to give **52** (Scheme 1.13), whereas bulky or electron-withdrawing groups such as *N*-Boc (**53a/b**) or *N*-Ts acetamides can undergo ATRC (**54a/b**) (Scheme 1.14).¹⁵



Scheme 1.14: 5-Exo Dig ATRC

Cyclisation of less activated monobromide acetamides **56a/b** has also been achieved.^{15,21} Stereoisomeric products **57a/b** are obtained in addition to a third product characterized as the reduced compound **58a/b**. The product distribution and stereochemistry (**57a/b**) have been shown to be dependent upon the R group, ligand and solvent used (Table 1.2).



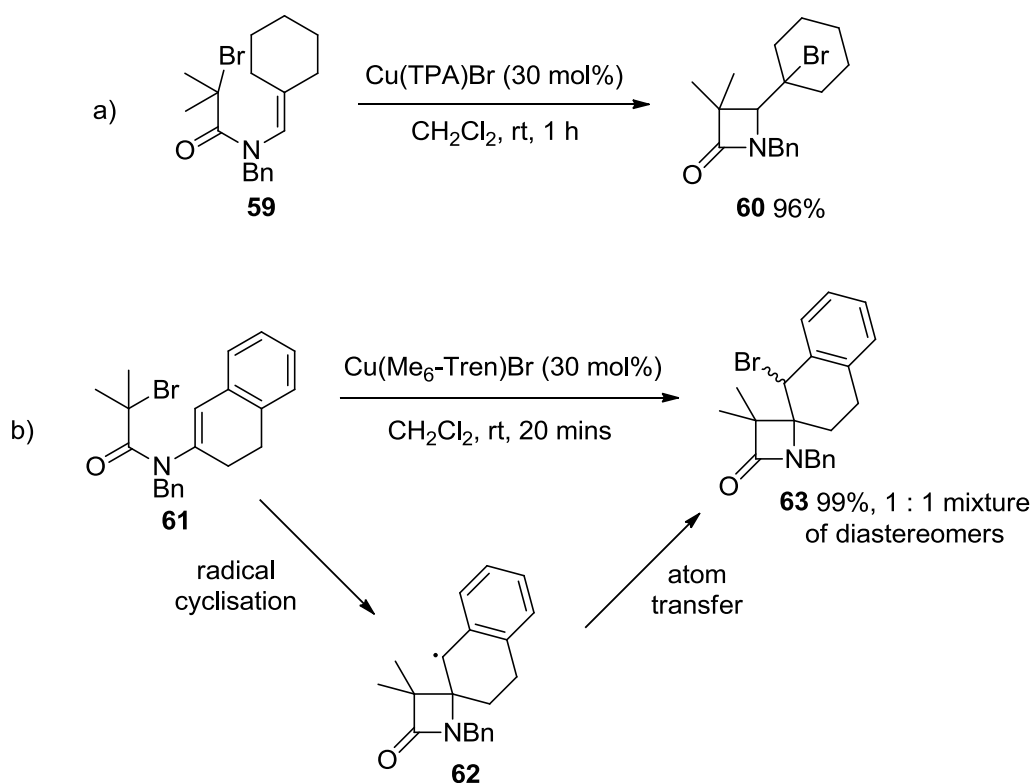
Entry	Ligand	Solvent	R	Ratio 57:58	Yield	57 E:Z
1 (56a)	50	CH ₂ Cl ₂	Ts	25 : 1	96%	2 : 5
2 (56a)	50	Benzene	Ts	74 : 1	94%	1 : 4
3 (56a)	42	THF	Ts	1 : 20	95%	1 : 4
4 (56b)	50	CH ₂ Cl ₂	Boc	10 : 1	96%	1 : 2

Table 1.2: Ligand and Solvent Effects on 5-Exo Dig ATRC

Conducting the reactions in a poor hydrogen donor solvent such as benzene (entry 2) gave a greater proportion of the atom transfer products (**57**). Conversely, when the reaction was repeated using Cu(Me₆-Tren)Br and with a good hydrogen donor solvent such as THF (entry 3), the ratio of the reduced product **58** significantly increased.

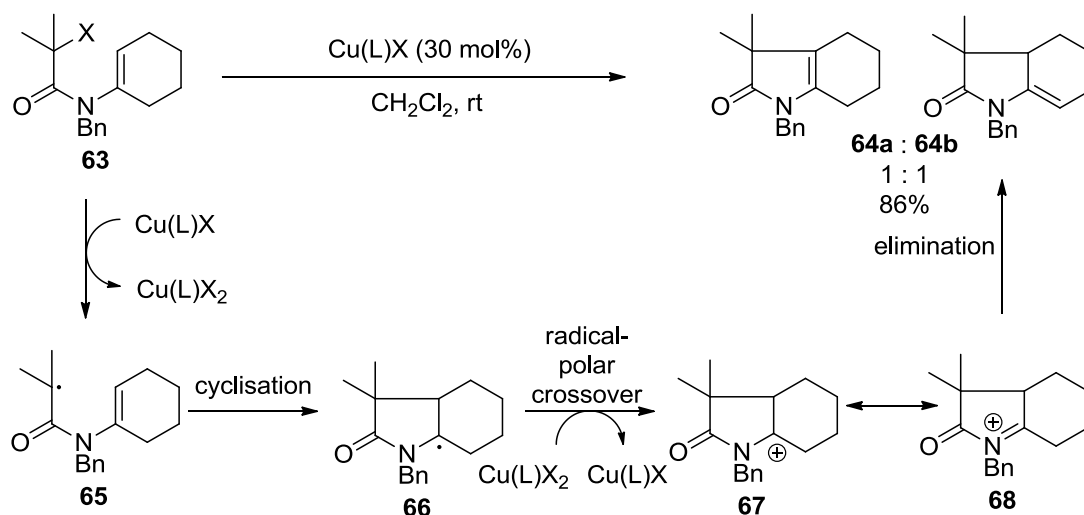
1.3.3 4-Exo and 5-Endo Trig Radical Cyclisation

The more active catalyst complexes, containing tetradentate ligands Me₆-Tren **41** and TPA **42**, have also been shown to facilitate 4-*exo* and 5-*endo trig* radical cyclisations of enamides.^{34,35} For substituted enamides, the two reaction pathways are competitive. 4-*Exo trig* ATRC is often quicker, but reversible, forming the kinetic product, while 5-*endo trig* cyclisation produces a less strained thermodynamic product. Enamides substituted at the β -position of the enamide alkene functional group (e.g. **59**) tend to undergo 4-*exo trig* ATRC furnishing the β -lactam product **60**³⁵ (Scheme 1.). This has also been shown to be the case when intermediate radicals are stabilized,²⁵ for example by conjugation, as demonstrated by the benzylic radical **62** formed from radical cyclisation of enamide **61** leading to formation of β -lactam **63** (Scheme 1.15b).

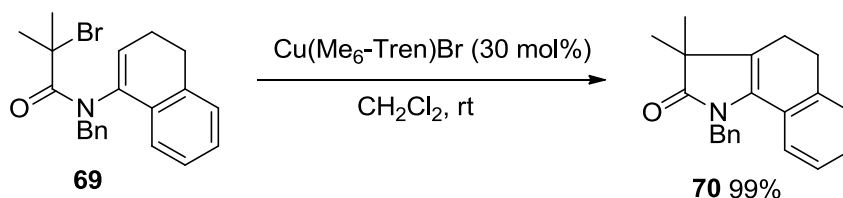


Scheme 1.15: a) Cu(TPA)Br Mediated 4-*Exo Trig* ATRC
 b) Cu(Me₆-Tren)Br Mediated 4-*Exo Trig* ATRC via Stabilised Benzyl Radical

Conversely, if the α -position of the enamide alkene is substituted then 5-*endo trig* radical cyclisation prevails. However, rather than atom transfer products, unsaturated products such as **64a/b** are obtained under copper-mediated ATRC conditions.²⁵ This implies that the mechanism differs from that established for 4- and 5-*exo trig* ATRC. Radical cyclisation of enamides such as **63** have been proposed to form tertiary radicals that are stabilised by the adjacent nitrogen atom **66**. Cu(L)X₂ mediated oxidation can convert the stabilised radical into a cation *via* a radical-polar cross over reaction to form a *N*-acyliminium ion **67**. Subsequent elimination of a proton furnishes the unsaturated cyclised products (Scheme 1.16). This reaction has been found to be general for a variety of ring sizes and substitutions.^{25,36,37}

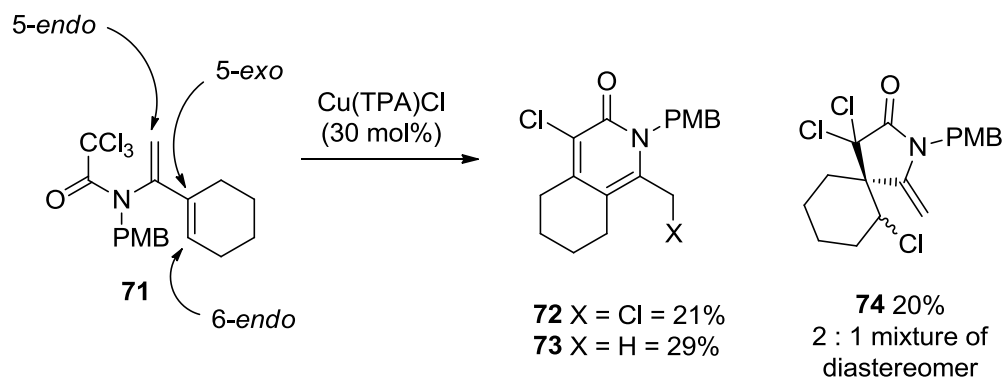
Scheme 1.16: 5-Endo Trig Radical Cyclisation via an *N*-Acyliminium Ion

Upon 5-*endo trig* radical cyclisation α -tetralone enamide **69** forms an extremely stable tertiary radical stabilised by adjacent nitrogen and aromatic groups. Consequently, this reaction is highly efficient occurring at room temperature to give **70** in quantitative yield.

Scheme 1.17: $\text{Cu}(\text{Me}_6\text{-Tren})\text{Br}$ Mediated 5-Endo Trig Radical Cyclisation

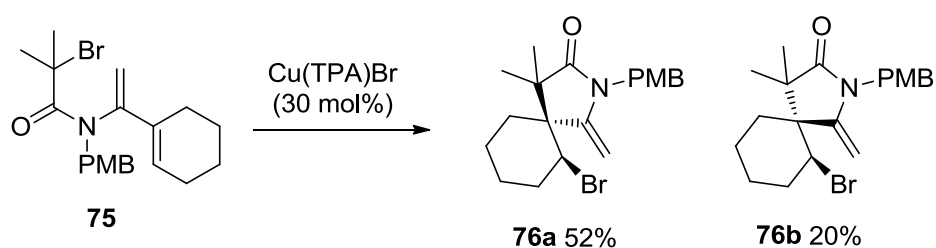
The regiochemistry of competing 5-*exo* and 6-*endo trig*, and 4-*exo* and 5-*endo trig* radical cyclisation reactions of dienamides, catalysed by a $\text{Cu}(\text{TPA})\text{X}$ complex, has been investigated by Clark and co-workers.³⁸ 2-Substituted dienamides were found to undergo 5-*exo* or 6-*endo trig* ATRC depending on the nature of the initiating group. Dienamide **71**, containing the trichloro initiating functionality was expected to undergo 5-*endo trig* radical cyclisation so it was surprising that the relatively rare mode of 6-*endo trig* cyclisation was observed.

Cyclic products **72** and **73** (50% combined yield) were identified as the major products, with the minor product being characterised as the *5-exo trig* product **74** (Scheme 1.18).



Scheme 1.18: Regiochemistry of Dienamide ATRC

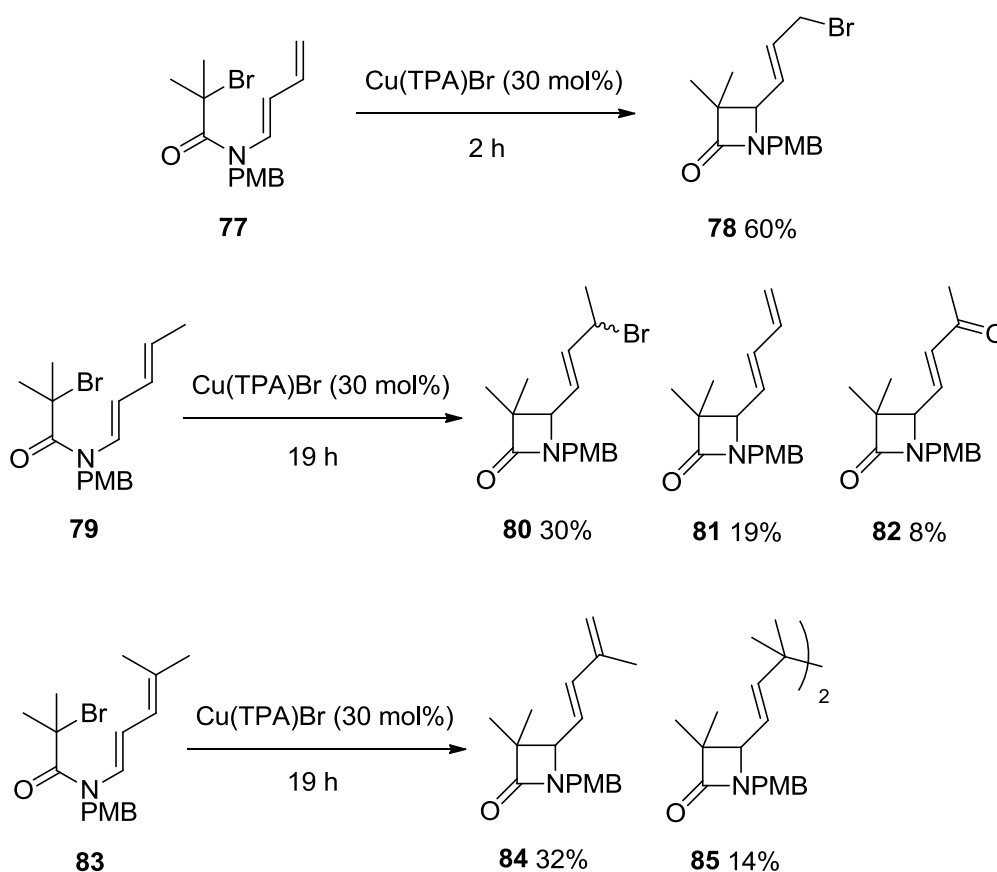
Alternatively, dienamide **75**, containing the less reactive monobromide initiating group exclusively underwent *5-exo trig* radical ATRC to furnish spirocyclic products **76a/b** in a combined yield of 72% (Scheme 1.19). Again, no *endo trig* cyclisation was observed.



Scheme 1.19: Regiochemistry of Dienamide ATRC

3-Substituted dienamides were found to undergo exclusive *4-exo trig* ATRC which could be terminated *via* a variety of pathways to produce β -lactam products. The termination pathway was found to be dependent upon the nature of the diene. Substrate **77** furnished the atom transfer terminated β -lactam product **78** in 60%

yield in 2 hours. Alternatively, dienes **79** and **83**, both substituted at the terminal carbon of the diene functional group, required longer reaction times (19 hours) and led to an array of products arising from atom transfer **80**, elimination **81**, **84**, oxidation **82** or dimerization **85** (Scheme 1.20).

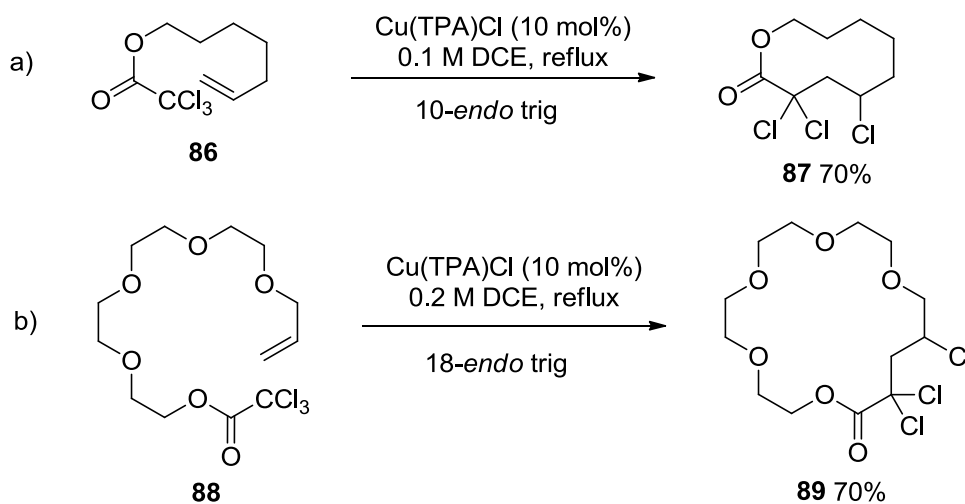


Scheme 1.20: Regiochemistry of Dienamide ATRC

1.3.4 Other Ring Sizes by ATRC

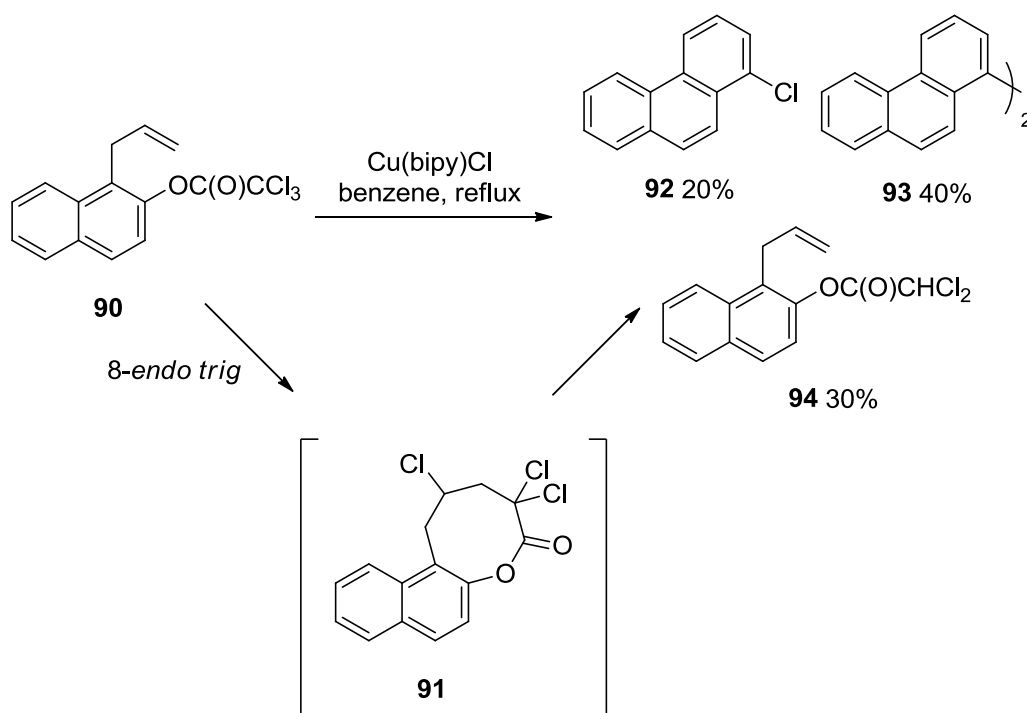
Tetradentate ligand complexes have also been used to facilitate macrolactonisation of trichloroacetates, such as **86**. For example, Verlhac *et al.* discovered that the highly active complex, Cu(TPA)Cl, could catalyse 8-, 9- and 10-*endo trig* ATRC reactions, to form macrocyclic lactones (Scheme 1.21a).³⁹

Furthermore, with respect to synthetic application, radical macrocyclisation by ATRC has been utilized in the synthesis of synthetically useful crown ethers such as **89** (Scheme 1.21b).⁴⁰



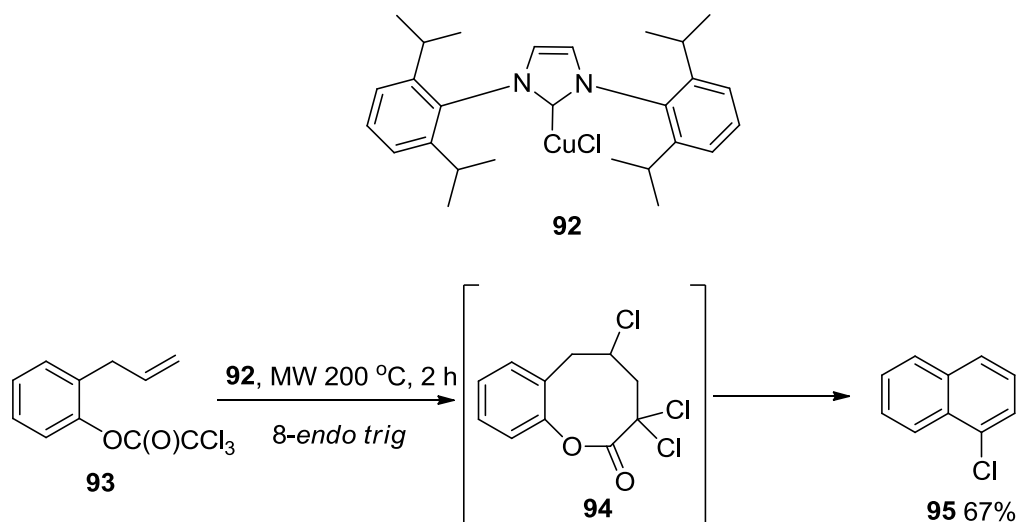
**Scheme 1.21: a) Macrocyclisation by Copper-Mediated ATRC
b) Crown Ether Synthesis by ATRC**

Ram *et al.* have used the copper-bipy complex (Cu(bipy)Cl) for the formation of benzannulated compound **92** via an 8-*endo trig* ATRC intermediate **91**.⁴¹ However, one equivalent of the copper complex was required and yields were poor as the reaction is complicated by the formation of two other products **93** and **94** (Scheme 1.22).



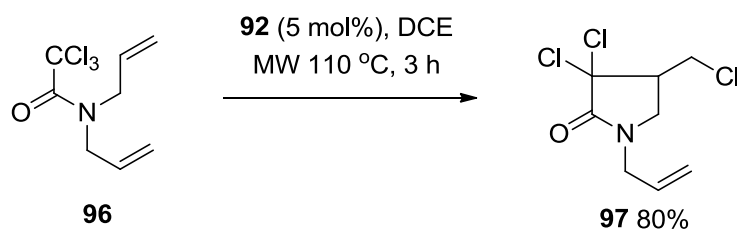
Scheme 1.22: Cu(Bipy)Cl Mediated Benzannulation via an 8-endo trig Intermediate

N-Heterocyclic carbenes (NHC)⁴² have emerged as potential ligands for copper-catalysed processes. These substrates have been identified as phosphane surrogates in transition metal catalysis with potentially greater stability and reactivity. Buchwald⁴³ and Nolan⁴⁴ have shown that stable copper-NHC complexes can efficiently catalyse hydrosilylation,⁴⁴ C-H activation⁴⁵ and Huisgen cycloaddition ('click') reactions.⁴⁶ Subsequently, Quayle *et al.* have reported that copper-NHC complexes such as **92** (5 mol%) can catalyse a regioselective benzannulation reaction that proceeds *via* the initial *8-endo trig* ATRC of aryl trichloroacetate **93** (Scheme 1.23).⁴⁷



Scheme 1.23: NHC Mediated Benzannulation via 8-endo trig Intermediate

Quayle has had success in constructing a number of benzannulated products using **92** and related complexes. Additionally, the use of microwave radiation has allowed the catalyst system to be extended to the familiar ATRC of trichloroacetamide **96** to form **97** in 80% yield (Scheme 1.24).

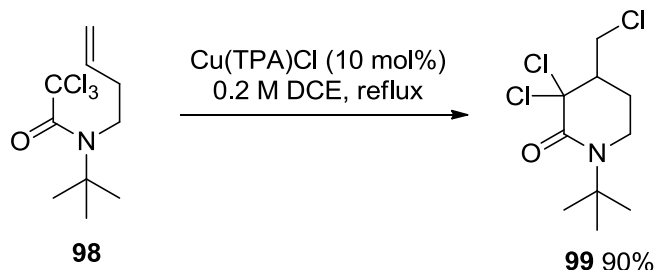


Scheme 1.24: NHC Mediated ATRC

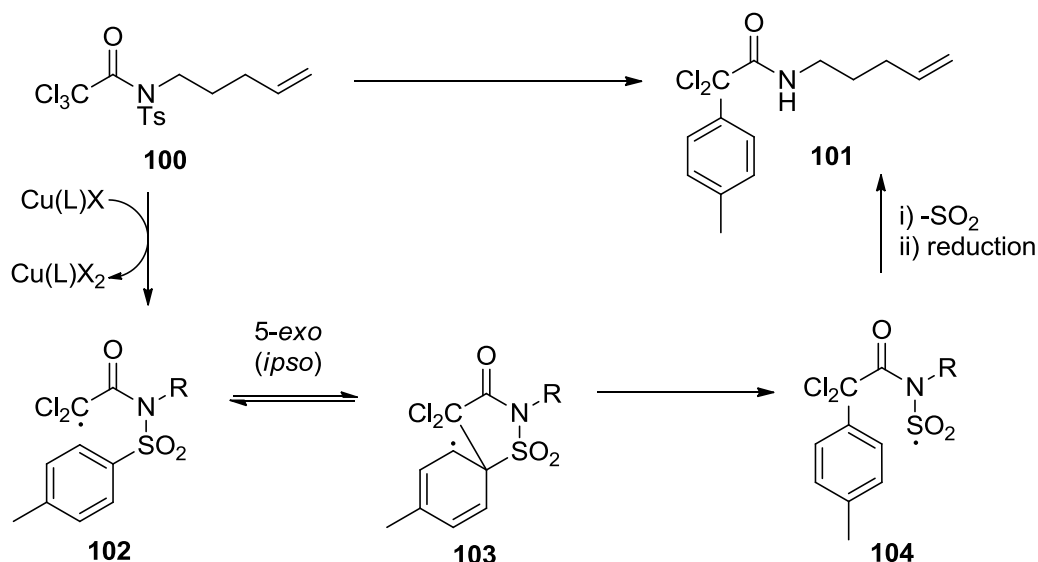
1.3.5 Rearrangement Reactions

Under ATRC conditions (Cu(L)X, 30 mol%) the synthesis of larger ring lactams from acetamides and enamides has been met with limited success. δ -Lactams such as **99**, are accessible using more activated copper complexes (Cu(TPA)Cl) via 6-*exo trig* ATRC (Scheme 1.25).²¹ However, attempts to mediate

8-*endo trig* ATRC of trichloroacetamides like **100** have been unsuccessful, leading to the isolation of rearranged products such as **101** (Scheme 1.26).²¹

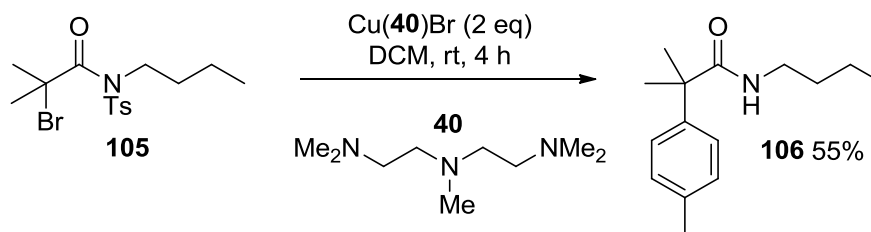


Scheme 1.25: 6-*Exo Trig* ATRC of Acetamides



Scheme 1.26: 5-*Exo Ipsso* Substitution of Acetamides

It has been postulated that this reaction occurs *via* a 5-*exo ipso* aromatic radical substitution^{48,49,50,51} *via* the radical intermediate **102** to give cyclised radical **103**. The rearrangement is then driven by re-aromatization (rather than atom transfer) which produces sulphur radical **104**. Observed loss of SO_2 from **104** and subsequent reduction of the resulting amide radical gives **101**. This rearrangement reaction has been investigated by the Clark group for a number of *N*-alkyl sulfonamides which have been shown to follow this reaction pathway (Scheme 1.27).^{52,53}



Scheme 1.27: 5-Exo Ipsso Substitution of Monobromide Acetamides

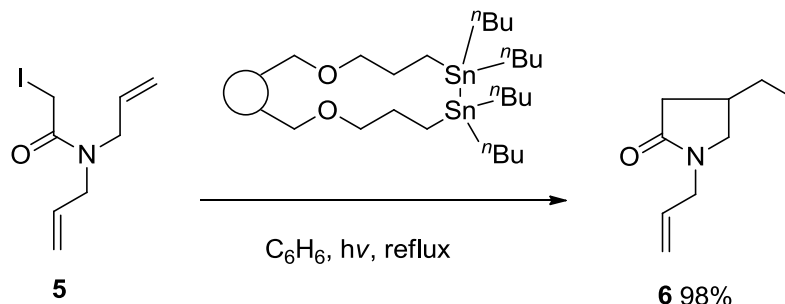
1.4 RECENT DEVELOPMENTS IN TRANSITION METAL MEDIATED ATRC

1.4.1 Di-tin Derivatives

The Clark review¹⁸ comprehensively establishes copper-mediated radical cyclisation as a synthetically useful process, and since its publication numerous advances and applications have been achieved. The principal drawback of the copper-mediated ATRC reaction is that despite being a catalytic process, relatively large amounts (30 mol%) of catalyst are often required. Consequently, it is often difficult to ensure complete removal of the copper complexes from the cyclised products and on scale-up the process could become expensive. As a result heterogeneous methods, and methods designed to improve catalyst efficiency have been developed.^{54,55,56,57}

In homogeneous reactions, hexabutylditin-mediated cyclisations are known to furnish atom transfer products. The use of solid-supported hexabutylditin has recently been shown to facilitate efficient radical cyclisations, with the expected preservation of functionality.⁵⁴ For example, resin-bound hexabutylditin has been

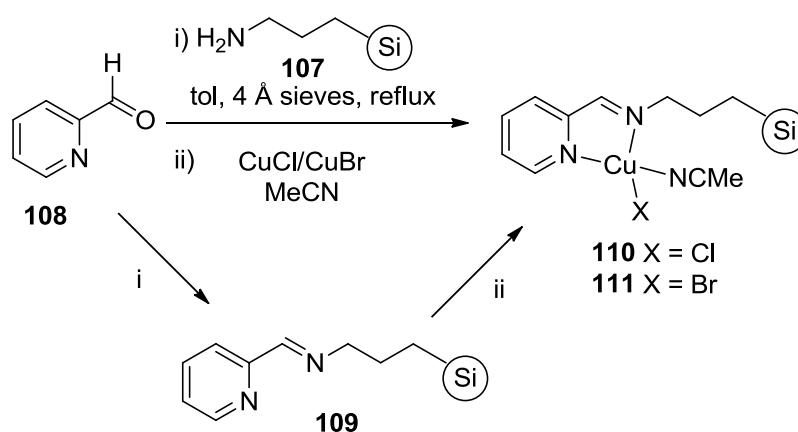
shown to catalyse the iodine ATRC reaction of **5** to give γ -lactam **6** in excellent yield (Scheme 1.28).



Scheme 1.28: Solid-Supported Tin Mediated ATRC

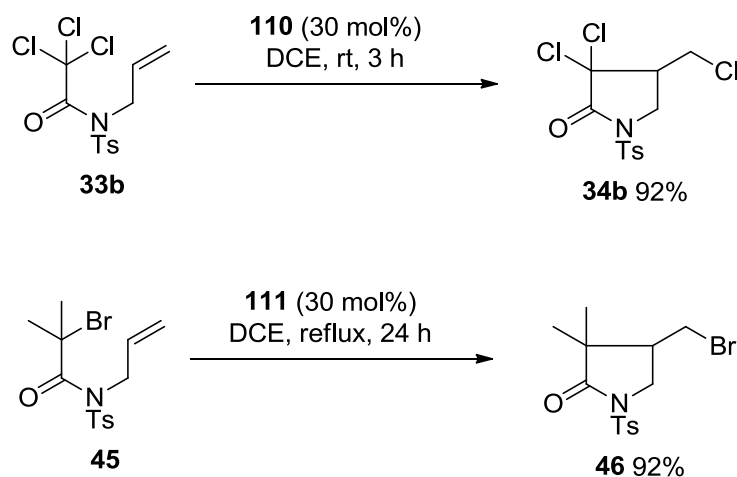
1.4.2 Solid Supported Copper Catalysed ATRC

A range of desirable solid-supported copper catalysts, which are oxidative in nature and preserve functionality, have also been developed.⁵⁵ These are prepared by immobilizing amine and pyridine based ligands onto various solid supports and then stirring them, under an inert atmosphere, with the relevant copper salt (Scheme 1.29). The prime advantage of solid-supported catalysis is that following reaction and product separation, the catalyst can be isolated and re-used.



Scheme 1.29: Preparation of Solid-Supported Copper/Pyridine-Imine Catalyst

Applying the heterogeneous catalysts **110** and **111** to ATRC reactions of a variety of activated and relatively deactivated acetamides successfully furnishes cyclised products between 75-96%.⁵⁵ Activated trichloroacetamides such as **33b** undergo facile cyclisation at room temperature within 1 hour, whereas deactivated monobromoacetamides like **45** require higher temperatures (80 °C) and longer reaction times (24 h) (Scheme 1.30). Heterogeneous NPMI complexes are less active than their homogeneous counterparts but this is compensated for by the ease in which the heterogeneous catalysts can be separated from the cyclised products (filtration) and re-used.

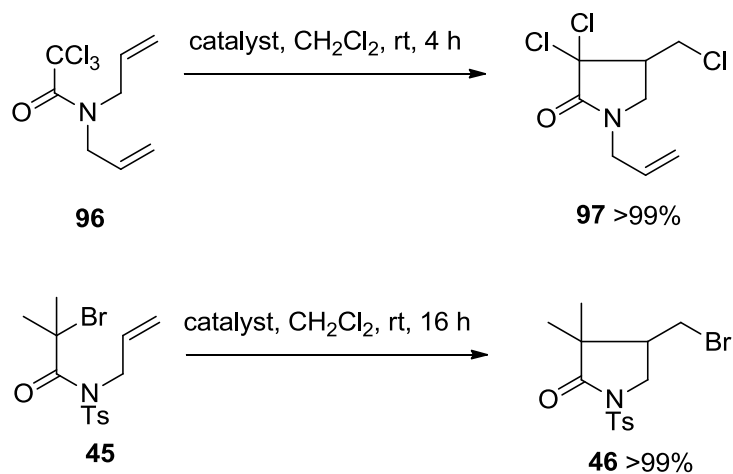


Scheme 1.30: Solid-Supported Copper Mediated ATRC

The concept of catalyst recycling was examined for the cyclisation of activated trichloroacetamide **33b**. The result displayed in Scheme 1.30 represents the yield for the first cyclisation attempt. The catalyst was then isolated by filtration and used under identical conditions with a fresh batch of **33b**. Cyclisation was observed in 18-24 hours and a comparable yield (90%) of **34b** was obtained. After filtration the catalyst was recycled a third time and in order to obtain a comparable

yield (86%) a reaction time of 24-36 hours was required. The longer reaction times and gradual reduction in the yields of this reaction reflects a steady deactivation of the catalyst complex. It was recognized that the catalyst could be deactivated either by leeching of the copper from the solid support or by accumulation of deactivated CuX_2 . In a later publication⁵⁶ 5-*exo trig* and *dig*, as well as disfavoured 5-*endo trig* and 4-*exo trig* radical cyclisations were achieved using a range of solid supported NPMI's and polyamines. In all examples, the heterogeneous method was found to be slower than the homogeneous counterpart and catalyst recycling was possible but with gradual loss of activity.

In 2010, Nagashima applied a novel polysiloxane gel-encapsulated $\text{Cu}(\text{bipy})\text{Cl}$ species as a reusable catalyst system for the ATRC of α -halogenated acetamide derivatives.⁵⁷ Trichloroacetamide **96** was cyclised in quantitative yield within 4 hours using a substrate/catalyst ratio of 220. Upon recycling, identical conversion was obtained but a longer reaction time was required. Less activated monobromoacetamide **45** could also be cyclised in quantitative yield using the polysiloxane gel encapsulated $\text{Cu}(\text{bipy})\text{Cl}$ catalyst, in 16 hours (Scheme 1.31).



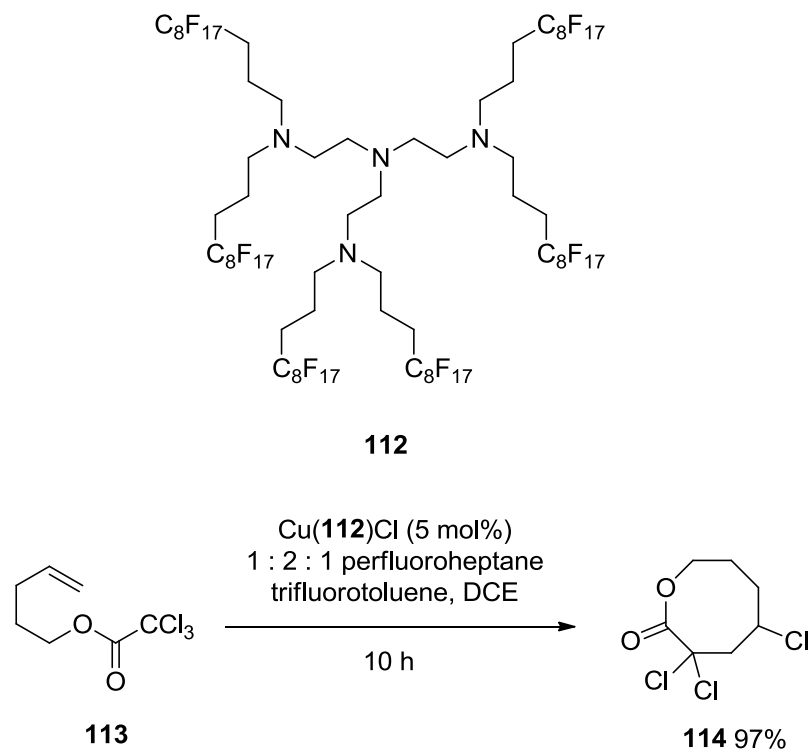
Scheme 1.31: Polysiloxane Gel-Encapsulated $\text{Cu}(\text{Bipy})\text{X}$ Mediated ATRC

The principal advantage of this novel catalyst system is that there is little evidence to suggest that any metal, ligand and/or metal-ligand complex is leaking from the polysiloxane gel supports. Consequently, quantitative conversions to the cyclic products allow facile purification by simple filtration to separate the catalyst from the desired product.

1.4.3 ATRC Using Perfluorous Catalysts

Perfluorous catalysts have found application in a number of organic transformations.^{58,59,60} In principle, these reactions consist of two phases, an organic phase that contains a reaction substrate, and a perfluorous phase that contains the catalyst. At elevated temperatures the phases are miscible and catalysis is possible. However, when the reaction is complete and the temperature is reduced (to ambient temperature) the phases separate again and the catalyst can be easily removed from the reaction product by decanting off the perfluorous phase.

In the field of ATRC, Verlhac *et al.* have employed a perfluorous analogue **112** of Me₆-Tren **41**, generally soluble in perfluorous alkanes, to catalyse the 8-*endo* *trig* ATRC of trichloroacetate **113**.⁶¹ With a catalyst loading of 5 mol% and a solvent system of perfluoroheptane, trifluorotoluene and dichloroethane (1 : 2 : 1), 8-membered lactone **114** was obtained in 97% yield (Scheme 1.36).



Scheme 1.32: ATRC Using Perfluorous Catalysis

As with the solid-supported heterogeneous reactions, perfluorous catalysed ATRC was found to be slower than the analogous homogeneous reaction. However this is compensated for by the recyclability of the catalyst, which is isolated after reaction by decantation and subsequently reused with little loss of efficiency (97%, 95%, 93%, 91% in successive cycles) at the cost of a slight decrease in rate.

1.4.4 Reducing Catalyst Loadings in Atom Transfer Radical Reactions

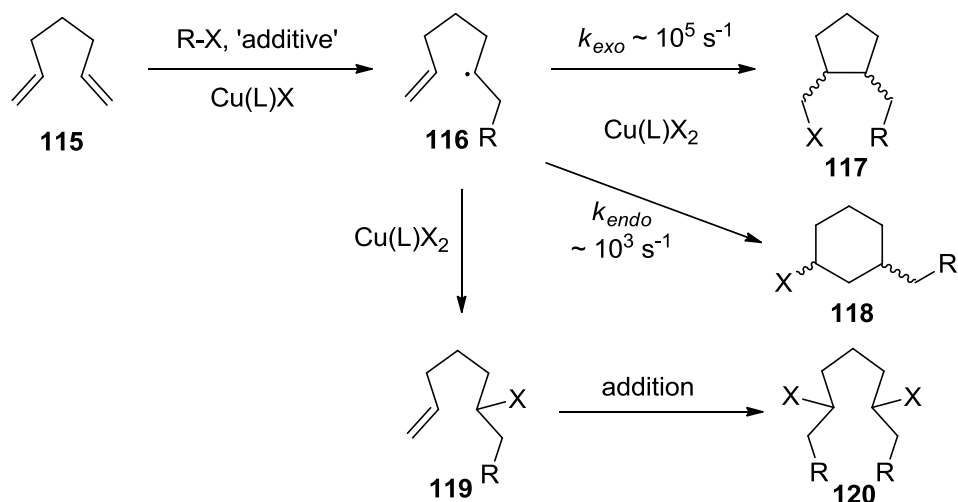
The first examples of reduced catalyst loadings were reported in the field of atom transfer radical polymerisation (ATRP),^{62,63} which is discussed in more detail in chapter 3. Perhaps the most common and successful processes are the activator generation/regeneration methods that utilize common additives, reductive in nature, to continuously regenerate the active catalyst (Cu(L)X) from the deactivator

(Cu(L)X₂). Common reducing agents include phenols,⁶⁴ monosaccharides,^{65, 66} ascorbic acid,^{67,68} hydrazine,⁶⁴ tin(II) 2-ethylhexanoate^{66,67} and diazo compounds.⁶⁴ The principal benefit of the inclusion of such additives is the ability to perform efficient polymerizations in the presence of as little as 5 ppm copper.

Application of similar processes to ATRA reactions has been met with similar success as monoadduct products were accessible with impressive turnover numbers using both ruthenium⁶⁹ and copper catalysts.^{70,71,72} Significantly, the most impressive results were obtained using Cu(TPA)Br₂ from which the active catalyst (Cu(TPA)Br) was formed *in situ* in the presence of diazo initiators.^{70,71,72} The concept of copper-mediated ATRP and ATRA at reduced catalyst loadings has been recently reviewed by Matyjaszewski and Pintauer.⁷³

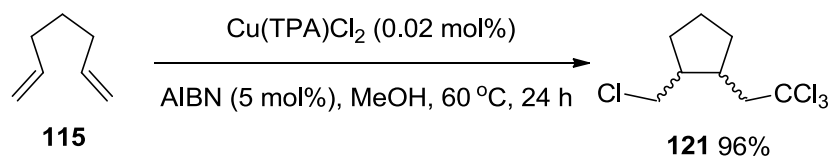
Given the compatibility of the Cu(TPA)Br catalyst and its previous success in ATRC reactions, the concept of reducing loadings by catalyst regeneration was contemplated. For ATRC the advantage of catalyst regeneration is thought to be two-fold. The amount of metal catalyst could be significantly reduced and as a consequence the rate of radical trapping by the deactivator would decrease relative to the rate of ring closure.

Subsequent research into this field has been fruitful. The success of the Clark group at copper-mediated ATRC in the presence of reduced catalyst loadings³³ is discussed in chapters 3 and 4, and similar success has been achieved in ATRA and ATRC cascade reactions by Pintauer and co-workers (Scheme 1.33).⁷⁴ Sequential addition and cyclisation mediated by Cu(TPA)Cl₂ and facilitated by diazo initiators has provided an efficient route to functional carbo- and heterocyclic systems from a range of 1,6-dienes.



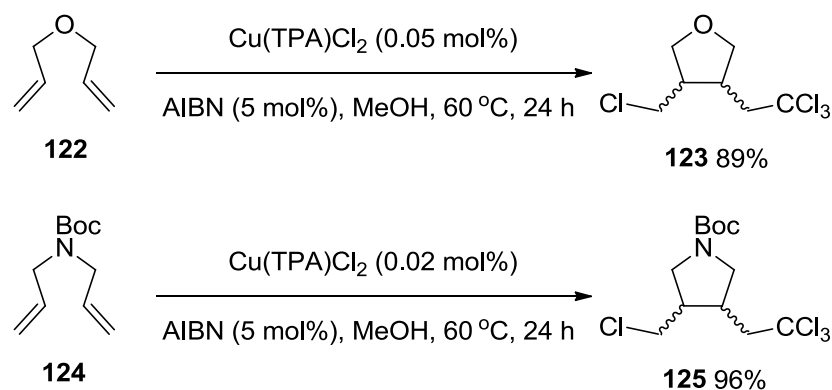
Scheme 1.33: Possible Reaction Pathways of Radical Addition to 1,6-Dienes

Initially, diazo- initiators AIBN and V70 (2,2'-azobis-(4-methoxy-2,4-dimethyl valeronitrile)) were used to initiate ATRA of CCl_4 to 1,6-hexadiene **115** in the absence of any catalyst (20% yield), but no cyclisation was observed. However, upon addition of $\text{Cu}(\text{TPA})\text{Cl}_2$ in conjunction with the diazo initiator, carbocycle **121** was obtained in excellent yield (96%) *via* an addition, cyclisation cascade catalysed by as little as 0.02 mol% catalyst (Scheme 1.34).



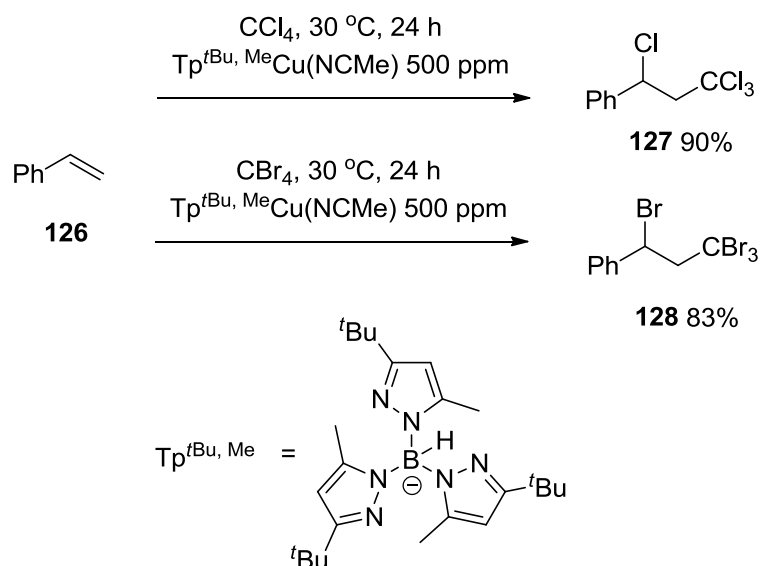
Scheme 1.34: $\text{Cu}(\text{TPA})\text{Cl}_2$ Mediated Cascade Radical Addition and Cyclisation

Additionally, functionalized tetrahydrofuran derivative **123** and pyrrolidine **125** were efficiently prepared under similar conditions (Scheme 1.35). This represents a significant increase in the efficiency of radical cyclisation, and if it could be coupled with the solid support protocol it would result in an industrially amenable process.



Scheme 1.35: Heterocycles From Cascade ATRA/ATRC Reactions

In the ATRA literature there are examples of efficient monoadduct formation at reduced catalyst loading in the absence of any additional reducing agents.⁷⁵ Efficient copper catalysts for ATRA containing trispyrazolylborate ligands (Tp^xCu) have been reported,⁷⁶ with $\text{Tp}^{t\text{Bu, Me}}\text{Cu}(\text{NCMe})$ giving the best results. Both carbon tetrachloride and carbon tetrabromide can be efficiently added to a variety of alkenes in the presence of 500 ppm catalyst (Scheme 1.36).



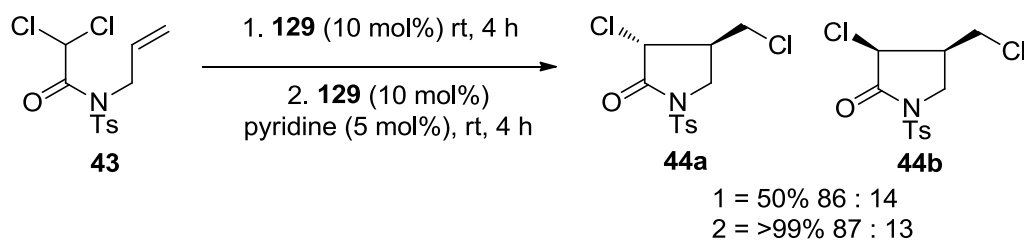
Scheme 1.36: ATRC at Reduced Catalyst Loadings Using Trispyrazolylborate Ligands

1.4.5 Alternative Transition Metal Mediated ATRC

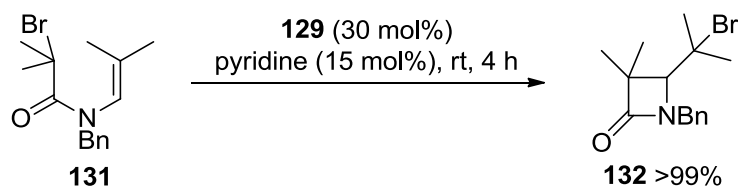
A range of other transition metals have been shown to mediate radical cyclisation reactions. Early research in the 80's and 90's utilized cobalt salen complexes^{77,78,79,80} and functional products were obtainable using radical traps. The emergence of the ATRC process inspired the development of transition metal mediators and catalysts including Ni metal,⁸¹ RuCl₂(PPh₃)₃,⁸² and FeCl₂(P(OEt)₃)₃.⁸² It is feasible to predict that any transition metal with easily accessible oxidation states could mediate redox-initiated ATRC reactions. In more recent years, a number of efficient methods using ruthenium, titanium and zinc complexes have emerged as alternative catalysts or mediators for ATRC.^{83,84,89,90}

1.4.5.1 Ruthenium

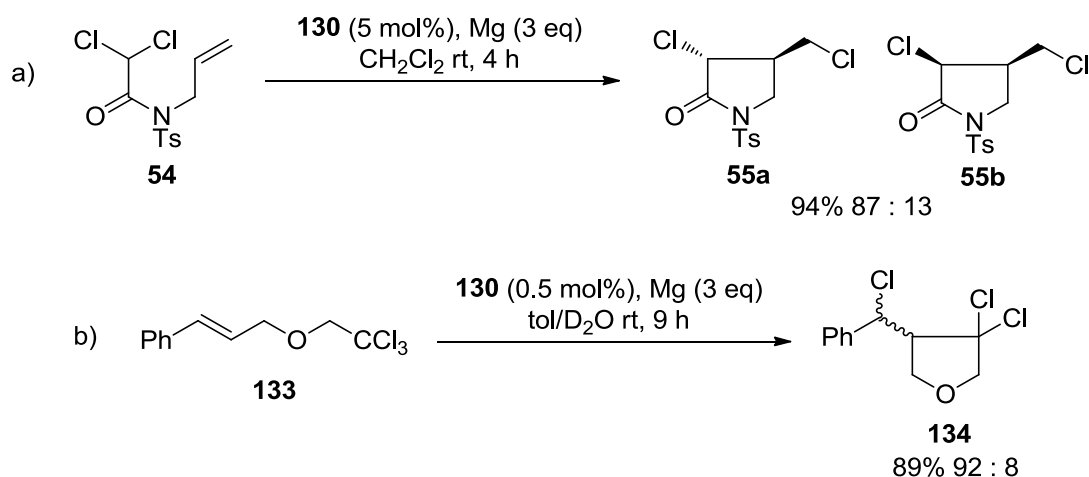
The efficiency of ruthenium complexes closely rival those of copper. Two of the most efficient and recently applied complexes are a ruthenium methoxide complex ([Cp*Ru(OMe)]₂)⁸³ **129** and a ruthenium chloride complex ([RuCl₂Cp*(PPh₃)]⁸⁴ **130**. These complexes can efficiently catalyse ATRC reactions in the presence of reductive additives that enhance the catalyst lifetime and activity. The ruthenium methoxide complex (10 mol%), in the presence of 2-electron donor pyridine (5 mol%), has been shown to exhibit excellent catalytic activity for the cyclisation of *N*-allyl and *N*-vinyl acetamides (**43**) to furnish γ - and β -lactams respectively with good control of diastereoselectivity (**44a/b**) (Scheme 1.37).⁸³

Scheme 1.37: Ruthenium Catalysed 5-*Exo Trig* ATRC

Cyclisation of less activated *N*-vinyl acetamide **131**, which undergoes 4-*exo trig* radical cyclisation was also possible using **129** (30 mol%) and pyridine (15 mol%) (Scheme 1.38), providing an efficient route to functionalized β -lactams such as **132**.⁸³

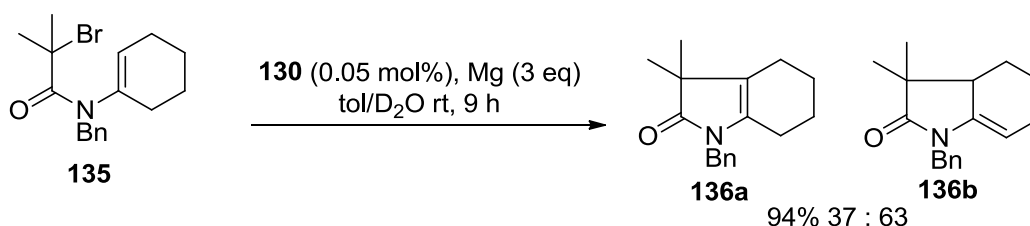
Scheme 1.38: Ruthenium Catalysed 4-*Exo Trig* ATRC

Following this work, Severin and co-workers developed a catalytic procedure using **130** ($[\text{RuCl}_2\text{Cp}^*(\text{PPh}_3)]$) in the presence of activated magnesium powder to mediate ATRA and ATRC under mild conditions with high efficiency.⁸⁴ The same dichloroacetamide **54** underwent cyclisation with as little as 5 mol% **130** and tetrahydrofuran derivative **134** was accessible using only 0.5 mol%. In both cases good diastereoselectivity was observed (Scheme 1.39).



Scheme 1.39: Magnesium-Mediated Ruthenium ATRC
 a) Trichloroacetamides b) Trichloroacetates

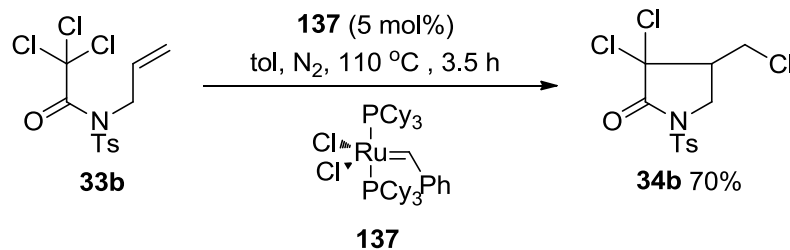
The magnesium present activates **130**, which is a Ru(III) precatalyst complex, to give catalytic Ru(II) *in situ*. The main advantage of this technique was the ability to perform the reaction open to air, as the pre-catalyst was a stable complex. In addition, the magnesium powder could be easily separated from the products by filtration. 5-*Endo trig* radical cyclisation of monobromoacetamide **135** was also possible furnishing regioisomeric products **136a/b** using only 0.05 mol% **130** (Scheme 1.40).⁸⁴



Scheme 1.40: Magnesium Mediated Ruthenium Catalysed 5-*Endo Trig* Radical Cyclisation

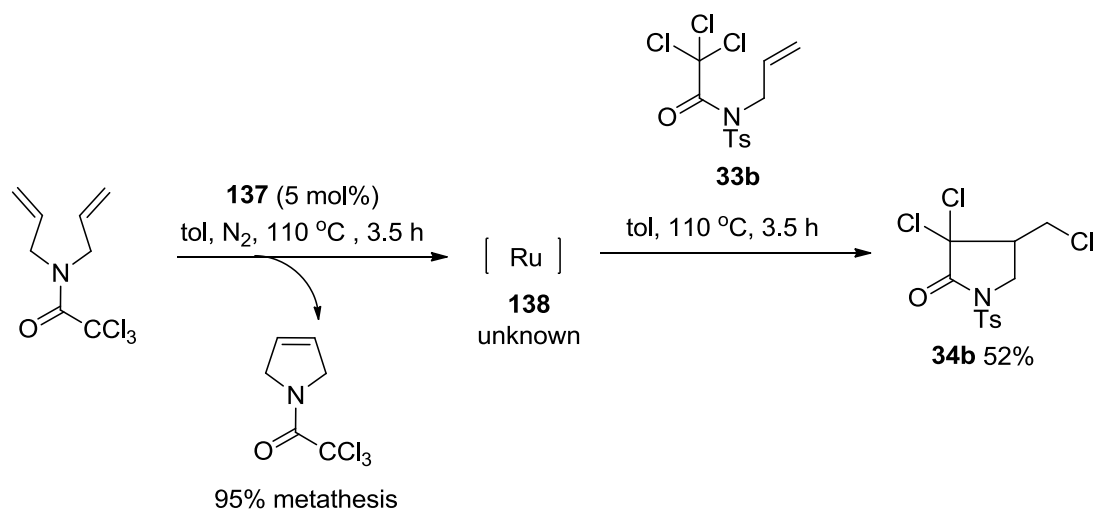
Finally for ruthenium complexes, Quayle and co-workers have developed a method that utilizes Grubbs metathesis catalyst **137** to catalyse ATRC reactions. It

was shown to catalyse ATRC directly⁸⁵ (Scheme 1.41), and sequentially,^{86, 87} following metathesis (Scheme 1.42).



Scheme 1.41: ATRC Using Grubbs Metathesis Catalyst

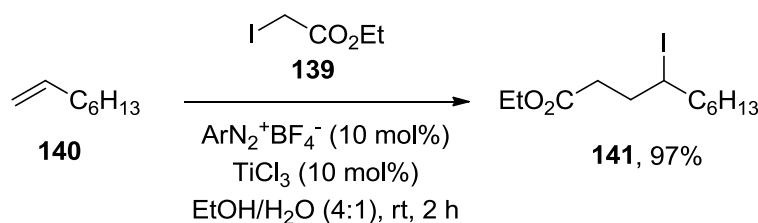
The ATRC activity of this complex is remarkable considering species of this kind are primarily responsible for catalysing ring-closing metathesis (RCM) reactions and analogous decomposition species show activity in alkene isomerisation, redox isomerisation of allylic alcohols and transfer hydrogenation reactions.⁸⁸ For the sequential reactions (Scheme 1.42), it was suggested that **137** acted as a precatalyst for ATRC cyclisation and required denaturation, generating a new ruthenium complex **138** (structure unknown) in which metathesis activity was lost.



Scheme 1.42: Sequential Metathesis and ATRC Using Grubbs Metathesis Catalyst

1.4.5.2 Titanium

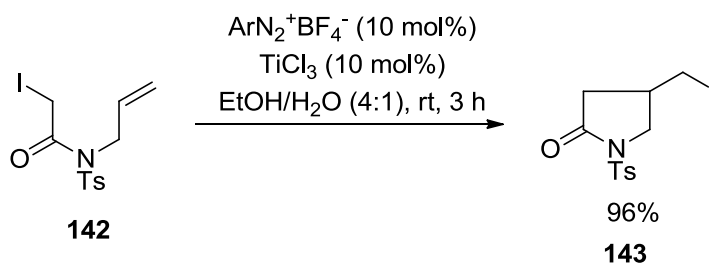
The combination of a *p*-methoxybenzene diazonium salt and TiCl_3 has been shown to mediate a range of efficient atom transfer radical addition and cyclisation reactions in aqueous solutions.⁸⁹ Initially, the reaction was optimized by screening a number of diazonium and transition metal salts for the addition of iodide **139** to alkene **140**. *p*-Methoxybenzene diazonium and TiCl_3 were found to be the best reagents to initiate the transformation to **141** at catalytic loadings (Scheme 1.43).



Scheme 1.43: $\text{TiCl}_3/\text{ArN}_2^+\text{BF}_4^-$ Mediated ATRA

Mechanistically, it is proposed that TiCl_3 acts as a reductant to facilitate the decomposition of the diazonium salt to produce aryl radicals. These then selectively initiate cyclisation by abstraction of a halogen radical, forming a carbon-centred radical equipped for addition or cyclisation. The catalytic nature of the reaction suggests that termination occurs *via* radical abstraction from the starting material **139**, which would re-initiate the reaction. However it is possible that termination could occur from radical abstraction from an aryl halide byproduct. If this was the case, this would reform aryl radicals which could also re-initiate cyclisation.

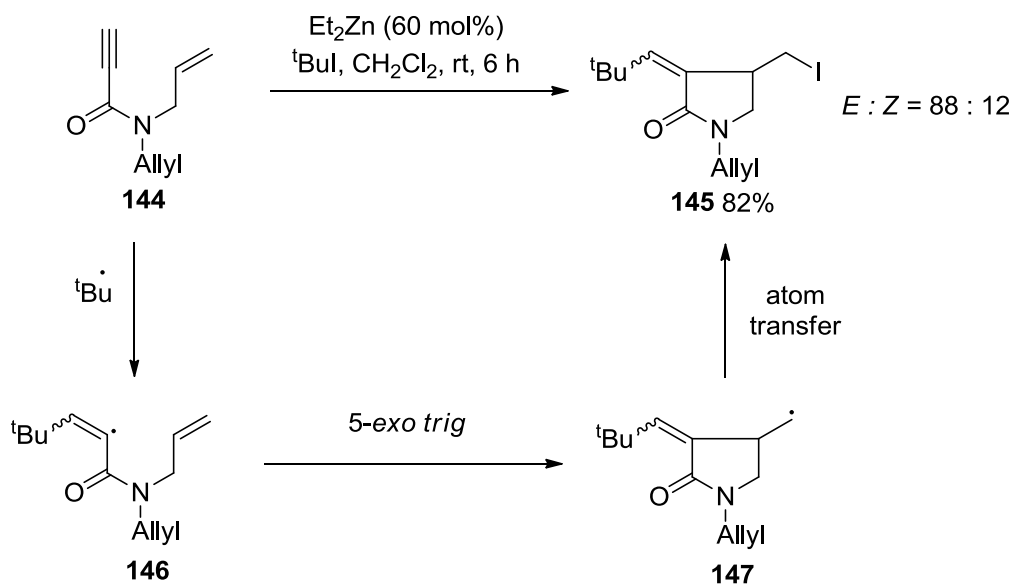
The reaction conditions were applied to the cyclisation of primary iodide **142** which was found to undergo cyclisation within 3 hours at room temperature to give lactam **143** in 96% yield (Scheme 1.44).

Scheme 1.44: $\text{TiCl}_3/\text{ArN}_2^+\text{BF}_4^-$ Mediated ATRC

This reaction represents an alternative, efficient method of ATRC which allows reactions to be performed at room temperature in aqueous solution, as opposed to the organic solvents required for copper mediated ATRC.

1.4.5.3 Zinc

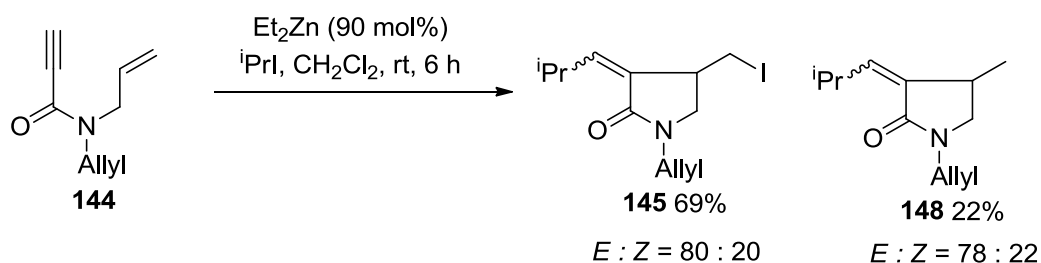
Dialkyl zinc reagents have been used as initiators for sequential radical addition and cyclisation reactions under aerobic conditions.⁹⁰



Scheme 1.45: Zinc Mediated Sequential ATRA/ATRC

The substrates used to demonstrate this method were 1,6-enynes such as *N,N*-diallylpropiolamide **144**, which furnished lactam product **145** (Scheme 1.45). Mechanistically, the reaction was said to be initiated by iodine atom transfer from ^tBuI to the dialkyl zinc derived ethyl radical. The ^tBu radical could then undergo addition to the activated triple-bond followed by *5-exo trig* radical cyclisation of the high reactive vinyl radical **146** leading to primary radical **147** which could undergo iodine atom transfer to give the product **145**.

No competitive reductive zincation was observed when ^tBuI was used. However, when ⁱPrI was used instead, a degree of reduction was observed, as **148** was isolated as well as atom transfer product **145** (Scheme 1.46). Despite this, under the reaction conditions, atom transfer was found to predominate in all examples reported.



Scheme 1.46: Zinc Mediated Sequential ATRA/ATRC

1.5 SYNTHETIC APPLICATIONS OF RADICAL CYCLISATION

Radical cyclisation has proved to be a useful step in a number of total syntheses of biologically interesting compounds. The use of organosilane- and organostannane-mediated radical cyclisation has been extensively reviewed.⁹¹ Most recently, natural products (\pm)-Melinonine-E **149**,⁹² (\pm)-Strychnoxanthine **150**,⁹²

antibacterial natural toxin (\pm)-Botryodiplodin **151**,⁹³ and (+)-Lactacystin **152**^{94,95,96} have been synthesised using these protocols.

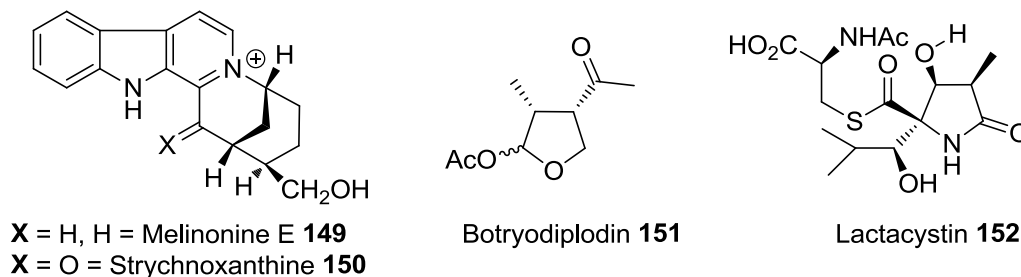


Figure 1.3: Natural Products Recently Synthesised Incorporating Radical Cyclisation as a Key Step

Comparatively, there are fewer examples of total syntheses published utilizing ATRC methodology. However in recent years, to coincide with the development of the ATRC protocol, examples of natural product syntheses using ATRC have started to steadily increase.^{97,106,107,108,110}

1.5.1 Natural Product Synthesis Using Di-tin Reagents

Hexabutylditin has been used in key steps of the total syntheses of sesquiterpenoids (\pm)-Axamide-1 **153** and (\pm)-Axisonitrile-1⁹⁷ **154** that possess a modest number of biological activities.^{98,99}

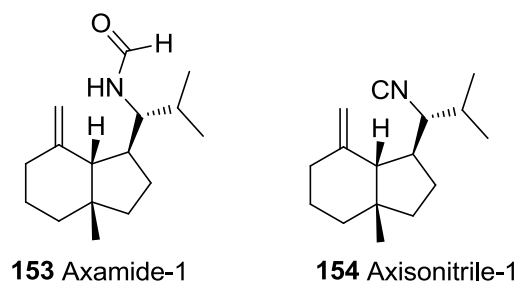
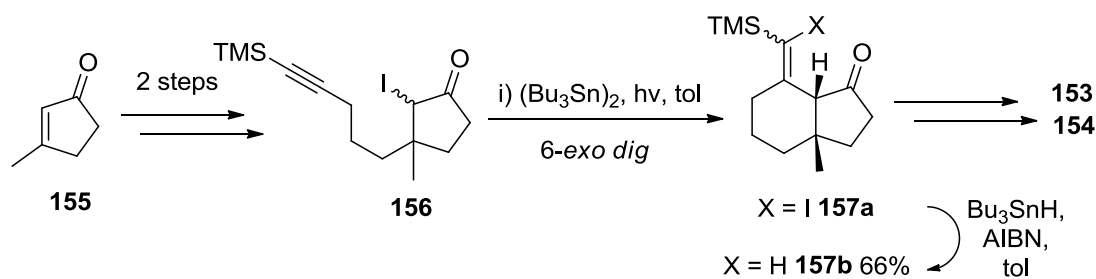


Figure 1.4: Natural Products Obtained Applying ATRC as Key Reaction Step

Previously, Piers *et al.* employed a novel annulation sequence in the construction of the key perhydroindane intermediate^{100,101} **157b**, whilst Hart and co-workers employed intramolecular conjugate additions to reach the same intermediate.^{102,103,104,105} Most recently, Kuo *et al.* have employed hexabutylditin-mediated 6-*exo dig* ATRC of iodo-intermediate **156** to construct the key perhydroindane intermediate **157b** in 66% yield, which can be transformed to **153** and **154** in 5 and 6 additional steps with total yields of 16% and 14% respectively (Scheme 1.47).⁹⁷

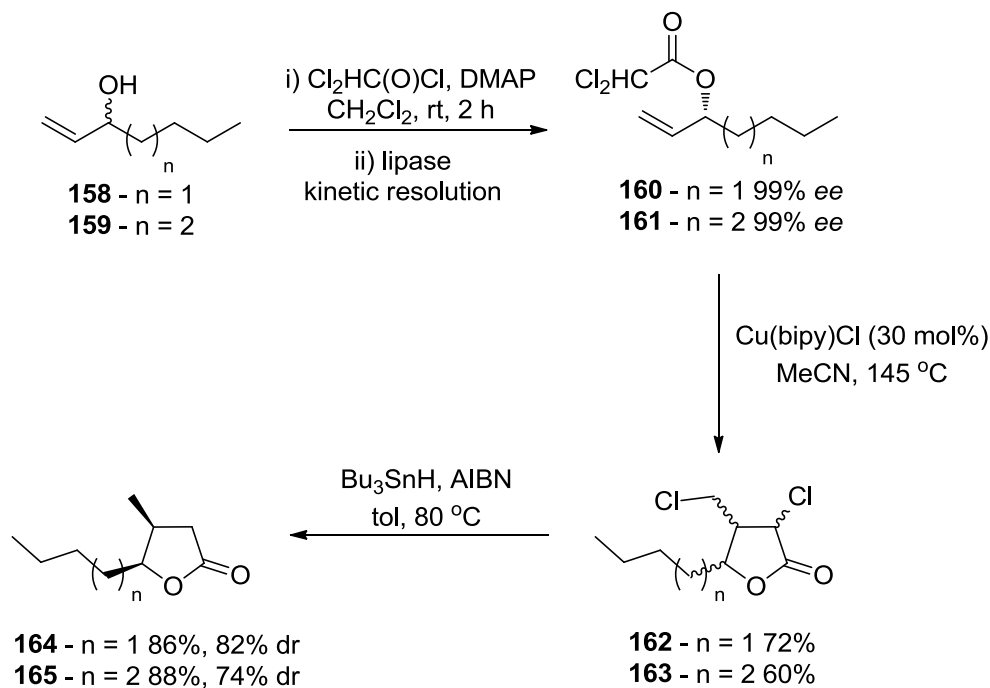


Scheme 1.47: ATRC as a Key Reaction on Route to the Perhydroindane Intermediate

1.5.2 Natural Product Synthesis Using Copper-Mediated ATRC

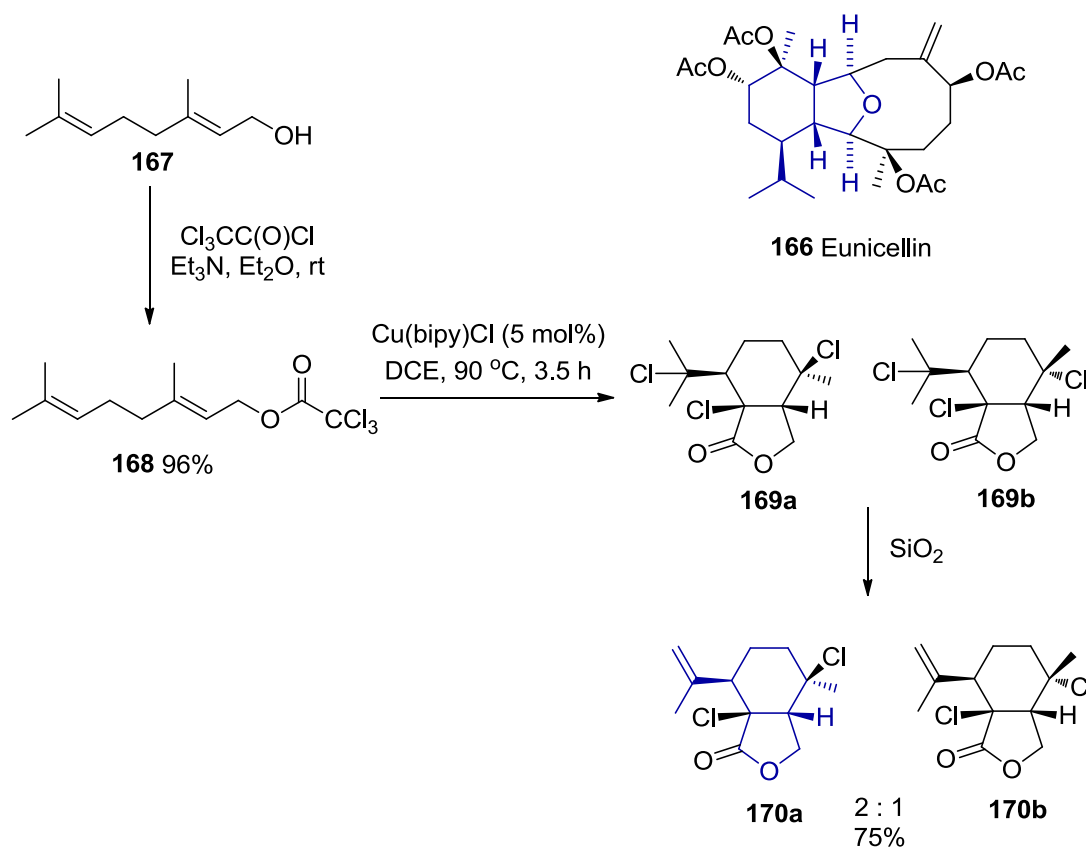
As an alternative to the radical protocols mediated by organostannane and organosilane reagents, copper-catalysed ATRC has also found application in synthesis of biologically interesting natural products. Felluga *et al.* have applied a Cu(bipy)Cl catalyst system to the chemoenzymatic synthesis of Quercus lactones (**164** and **165**),¹⁰⁶ naturally found in different types of wood and responsible for the sensory characteristics of wine and other alcoholic beverages. Starting from racemic 1-hepten-3-ol **158** and 1-octen-3-ol **159**, the (+)-*trans* whisky lactone **164** and (+)-*trans* cognac lactone **165** were prepared *via* lipase-catalysed kinetic resolution of

dichloroacetates **160** and **161**. This was followed by Cu(bipy)Cl-mediated ATRC to give intermediates **162** and **163**, which were converted to **164** and **165** by reduction (Scheme 1.48).



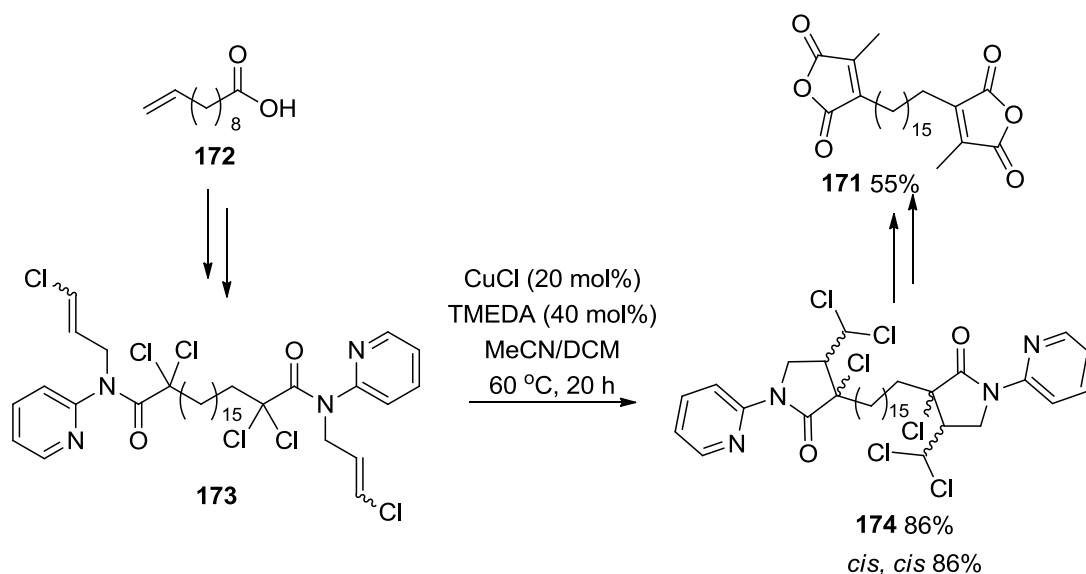
Scheme 1.48: (\pm) *trans* whiskey (**164**) and cognac (**165**) lactones via Cu(Bipy)Cl-Mediated ATRC

The same catalyst complex (Cu(bipy)Cl) has also been applied to tandem ATRC reactions providing rapid access to 2-oxabicyclo-[4.3.0]-nonane ring systems that are present biologically in terpenes such as Eunicellin¹⁰⁷ **166**. The cyclisation precursor **168** was obtained by trichloroacetylation of geraniol **167**. Subsequent treatment with Cu(bipy)Cl (5 mol%) gave the desired products **169a/b**, which are key intermediates to the formation 2-oxabicyclo-[4.3.0]-nonane ring systems. However, purification gave alkenes **170a/b** due to elimination of HCl on the chromatography column (Scheme 1.49).

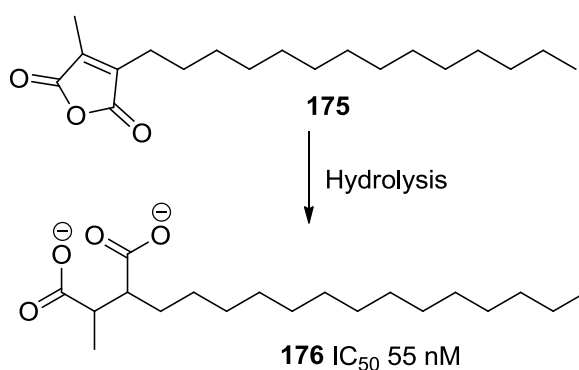


Scheme 1.49: Cu(Bipy)Cl-Mediated ATRC as a Key Step to the Synthesis of Eunicellin

Roncaglia and co-workers have made use of the Cu(TMEDA)Cl complex for a key step in the synthesis of Tyromycin A¹⁰⁸ **171**, which has shown potential as a immunomodulating drug target,¹⁰⁹ and can be obtained from 10-undecanoic acid **172**, a renewable starting material obtained in ample quantities from castor oil. In a key step of the synthesis, Cu(TMEDA)₂Cl (1 : 2 CuCl, TMEDA) was applied for the cyclisation of diamide **173** to give intermediate **174** in 86% yield and good diastereoselectivity (*cis, cis* 86%). The natural product **171** was then obtained *via* 2-step functional rearrangements (Scheme 1.50).



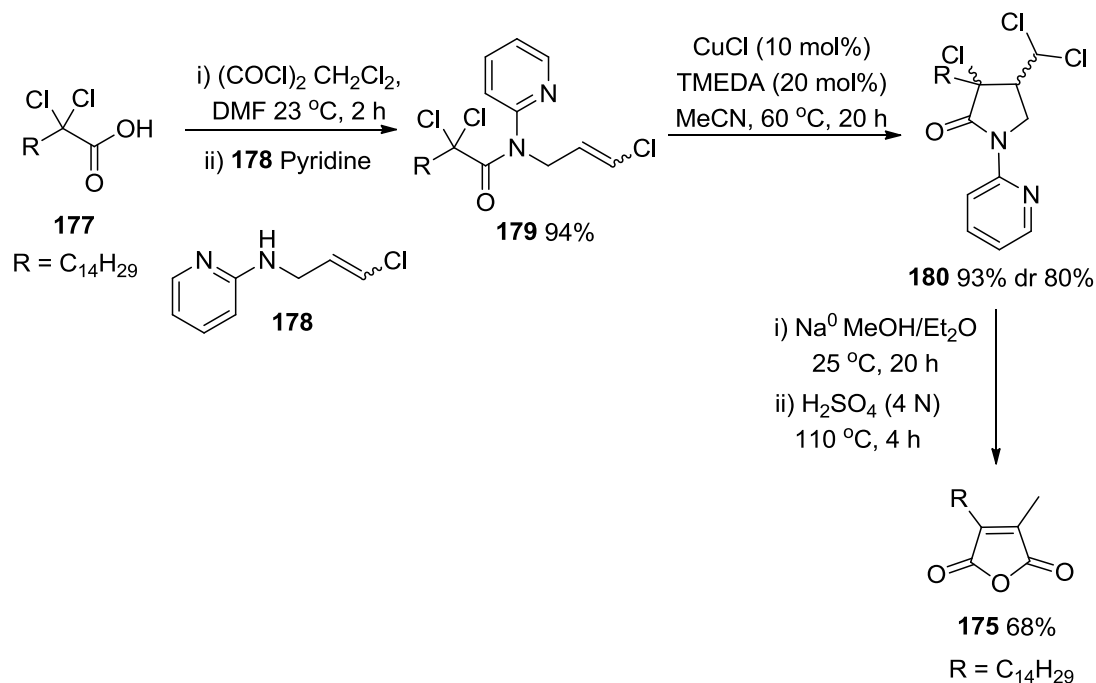
Ghelfi and co-workers have used the same catalyst system for the synthesis of chaetomelic anhydride A¹¹⁰ **175** from 2,2-dichloropalmic acid **177**. The anhydride **175** can be easily hydrolysed to give the diacid **176**¹¹¹ which is known to inhibit recombinant human FTPase with an IC₅₀ value of 55 nM.¹¹²



Scheme 1.51: Biologically Active Chaetomelic Diacid 176 from Chaetomelic Anhydride 175

Again a key step in the synthesis was the copper-catalysed ATRC of intermediate **179** using a 1 : 2 ratio of CuCl (10 mol%) and TMEDA (20 mol%). This furnished the cyclised product **180** in 93% yield as a 9 : 1 ratio of *cis* and *trans*

diastereomers. The synthesis was completed by a 2-step functional rearrangement to give the desired product **175** in 68% overall total yield (Scheme 1.56).



Scheme 1.52: $\text{Cu}(\text{TMEDA})_2\text{Cl}$ -Mediated ATRC as a Key Reaction Towards Chaetomelic Anhydride

1.6 SUMMARY

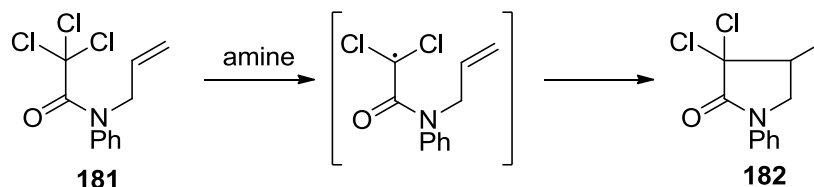
Atom transfer radical cyclisation reactions are attractive due to the catalytic nature of the mediators involved, the ease of work up and preservation of functionality in the cyclised products. This methodology is constantly evolving and efficient lab scale cyclisation is now possible using either solid-supported reagents^{54,55,56,57} or using low catalyst loadings in solution.³³ For industrial application, these two methods require to be combined into a single process for solid-supported ATRC at low catalyst loadings. Herein, we report a contribution to the field of copper-mediated ATRC in which we investigate the effect of the

presence of additives as a move towards reducing catalyst loadings even further, and for mediating radical cyclisations under aerobic conditions.

2.0 Radical Cyclisation Reactions Using 1,4-Dimethylpiperazine

2.1 INTRODUCTION

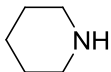
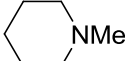
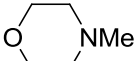
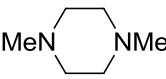
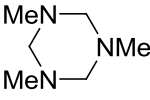
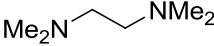
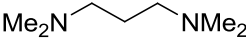
Organic amines are known to act as electron donors in single electron transfer (SET) reactions, and have gained utility as reagents for reductive dehalogenation of α -halo carbonyl compounds.^{113,114,115,116} Common amines used for this process include *N,N*-dimethylaniline, morpholine and 1,8-diazabicyclo[5.4.0]undec-7-ene (DBU). It is believed to occur *via* a radical mechanism, which involves single electron transfer from the nitrogen atom of an amine to the α -halo carbonyl compound. Subsequent loss of a halogen anion to leave a radical which is reductively quenched, furnishes a reduced product. However, until recently the only examples of organic amines being utilised as reagents for radical cyclisations have involved photoirradiation of alkyl bromides in the presence of triethylamine.¹¹⁷ Ishibashi recognised the potential for organic amine mediated radical cyclisation and screened a variety of amines during a study of the cyclisation of *N*-allylic α,α,α -trichloroacetamide **181**.¹¹⁸



Scheme 2.1: Amine-Mediated Radical Cyclisation

Ishibashi's initial experiments involved heating **181** in simple amines with sequentially greater boiling points. In triethylamine (89 °C), no reaction was

observed (Table 2.3, entry 1) but when amines with higher boiling points were used cyclisation was evident. Tripropylamine (156 °C) gave **182** in 2% yield (entry 2) whereas dibutylamine (159 °C) provided **182** in 44% yield (entry 3). Encouraged by these results he decided to focus on reactions in cyclic and acyclic, secondary and tertiary amines with boiling points > 100 °C.

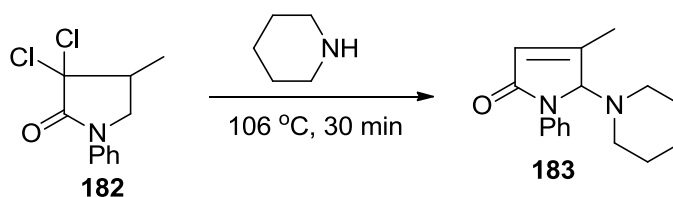
Entry	Amine	Bpt (°C)	Time (min)	Yield X ^a
1	Et ₃ N	89	30	0 (97)
2	Pr ₃ N	156	30	2 (82)
3	Bu ₂ NH	159	30	44 (32)
4		106	20	34^b (0)
5		106	90	18 (77)
6		116	90	46 (33)
7		133	2	75 (0)
		100	15	77 (0)
		65	120	81 (0)
8		162	90	2 (0)
9		122	30	17 (32)
10		145	30	26 (58)

^a Numbers in parentheses correspond to the yield of starting material **181**.

^b Yield of compound **183**.

Table 2.1: Attempted Cyclisations Using a Variety of Amines

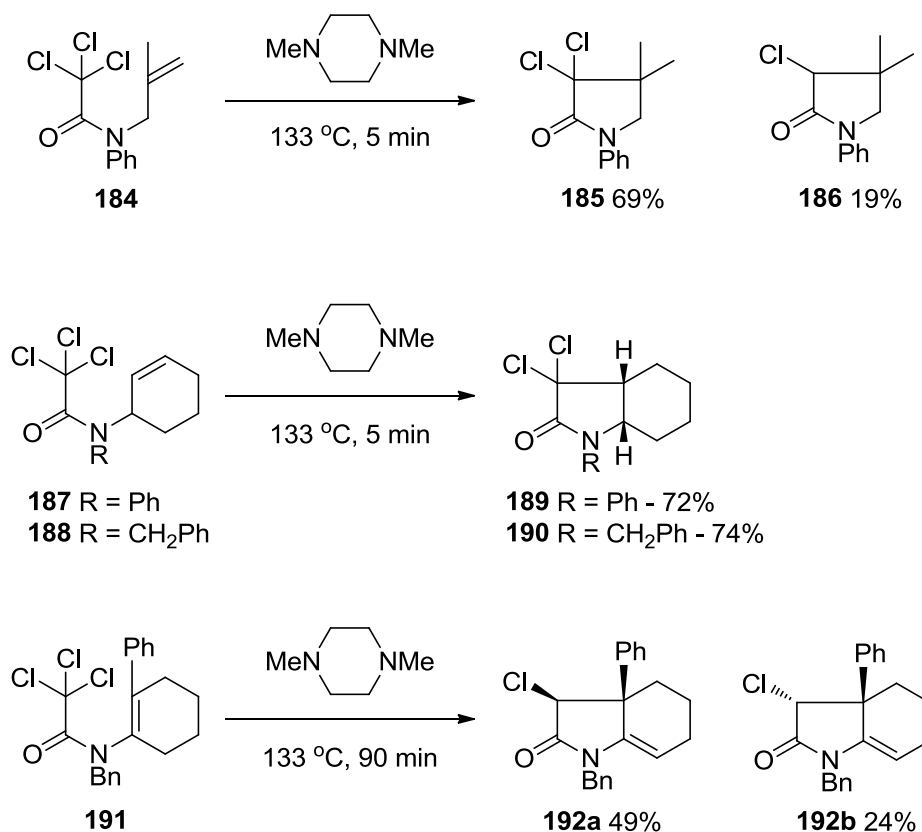
The only cyclic secondary amine investigated was piperidine (entry 4) which provided a 34% yield of the unexpected cyclised product **183** (Scheme 2.2). It was speculated that **183** was actually formed from the compound **182** under the reaction conditions. This was confirmed as **183** was formed in 79% yield when cyclised product **182** was treated with boiling piperidine for 30 minutes.



Scheme 2.2: Cyclised Product Obtained From Piperidine-Mediated Radical Cyclisation

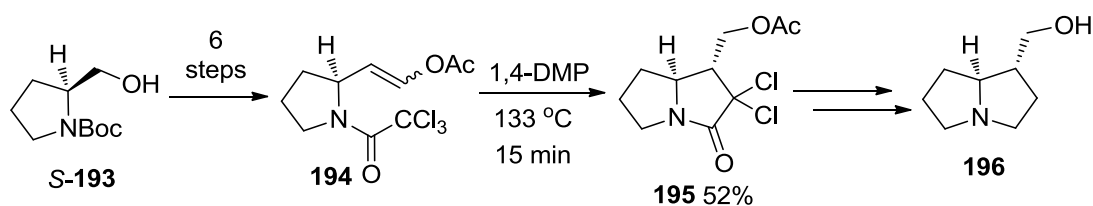
The tertiary cyclic amines (entries 5-8) provided the most promising results. Cyclic tertiary diamine 1,4-dimethylpiperazine (1,4-DMP, entry 7), gave solely the desired cyclised product **182** in 75% yield after only 2 minutes. Acyclic diamines tetramethylethylenediamine (TMEDA, entry 9) and tetramethylpropanediamine (entry 10) did furnish **182** but yields were not as impressive as when 1,4-DMP was used. Given the results obtained for 1,4-DMP, the effect of reaction temperature was examined. It was found that the yield steadily increased as the reaction temperature was reduced to 100 °C (77%) and then 65 °C (81%). The increase in yield was compromised by longer reaction times but the results suggested cyclisation probably took place at lower temperatures than initially thought. Unfortunately, cyclisation was not observed at room temperature.

The scope of the reaction was shown to extend to efficient *5-exo trig* cyclisation of substituted *N*-allylic α,α,α -trichloroacetamide **184**, and *N*-(cyclohex-2-enyl-1-yl)- α,α,α -trichloroacetamides **187** and **188**, and to the disfavoured *5-endo trig* cyclisation of enamide **191** (Scheme 2.3).



Scheme 2.3: 1,4-DMP Mediated Radical Cyclisation

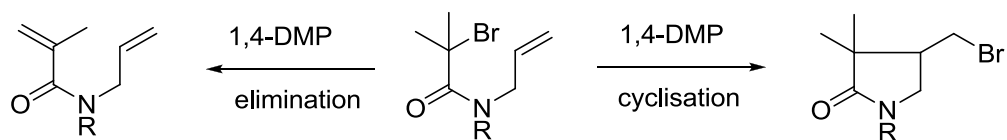
Ishibashi recently applied this methodology to a key cyclisation step in the synthesis of pyrrolizidine alkaloid (-)-trachelanthamide **196**.¹¹⁹ The cyclisation precursor **194** was prepared in 6 steps from (*S*)-(+)-pyrrolidinemethanol **193** and sequential catalytic hydrogenolysis and reduction of the cyclised product **195** furnished (-)-trachelanthamide **196**. The key cyclisation step, mediated by 1,4-DMP, was efficient (15 min, 133 °C) and provided **195** in 52% yield.


 Scheme 2.4: 1,4-DMP Mediated Radical Cyclisation Applied to the Synthesis of Trachelanthamide **196**

There are numerous advantages with the single electron transfer methodology mediated by organic amines. Existing radical cyclisation protocols require either the presence of toxic reagents, such as organostannanes (Bu_3SnH), or transition metal catalysts (ATRC). The presence of such reagents can complicate the purification procedure following cyclisation and add to the cost of running reactions, particularly on scale up. However, in the presence of 1,4-DMP Ishibashi has shown that radical cyclisation can be performed efficiently and cleanly for activated α,α,α -trichloroacetamides, in the absence of other reagents.

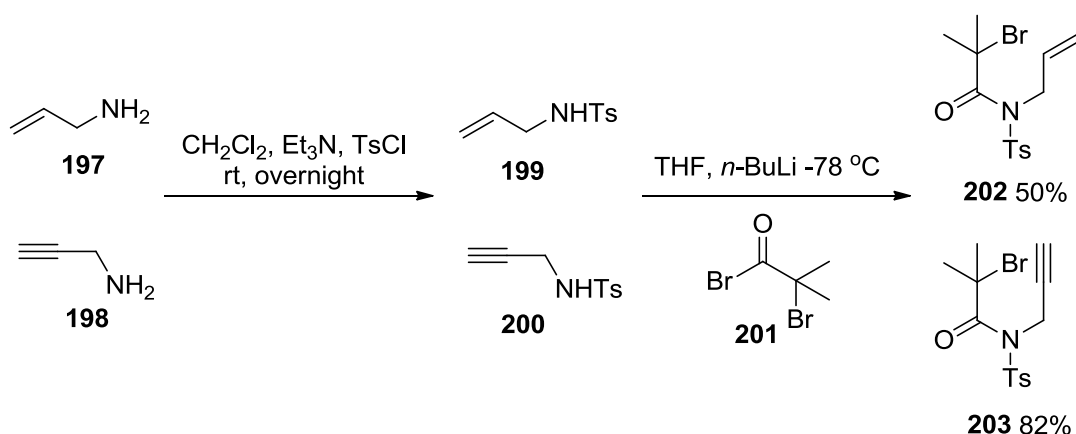
2.2 RESULTS AND DISCUSSION

The work of Ishibashi inspired a brief investigation into the scope of the 1,4-DMP mediated single electron transfer radical cyclisation methodology. It would be interesting to discover whether 1,4-DMP could mediate the cyclisations of less activated acetamides that possessed competing reaction pathways. Monobromoacetamides undergo efficient *5-exo trig* radical cyclisations in the presence of ligand-bound copper complexes.²⁴ However, catalyst loadings are not ideal (30 mol%), so cyclisation in the absence of a catalyst would be an attractive prospect. Additionally, as these acetamides contain tertiary bromides, they would also be susceptible to base-catalysed elimination in the presence of a suitable amine, providing a competitive reaction pathway (Scheme 2.5). The success of the relatively slow *5-endo trig* radical cyclisation (Scheme 2.3) suggested that *5-exo dig* radical cyclisation onto alkynes, which are known to be slower than *5-exo trig* cyclisations, may also be possible using 1,4-DMP.



Scheme 2.5: Possible Reaction Pathways Using 1, 4-DMP

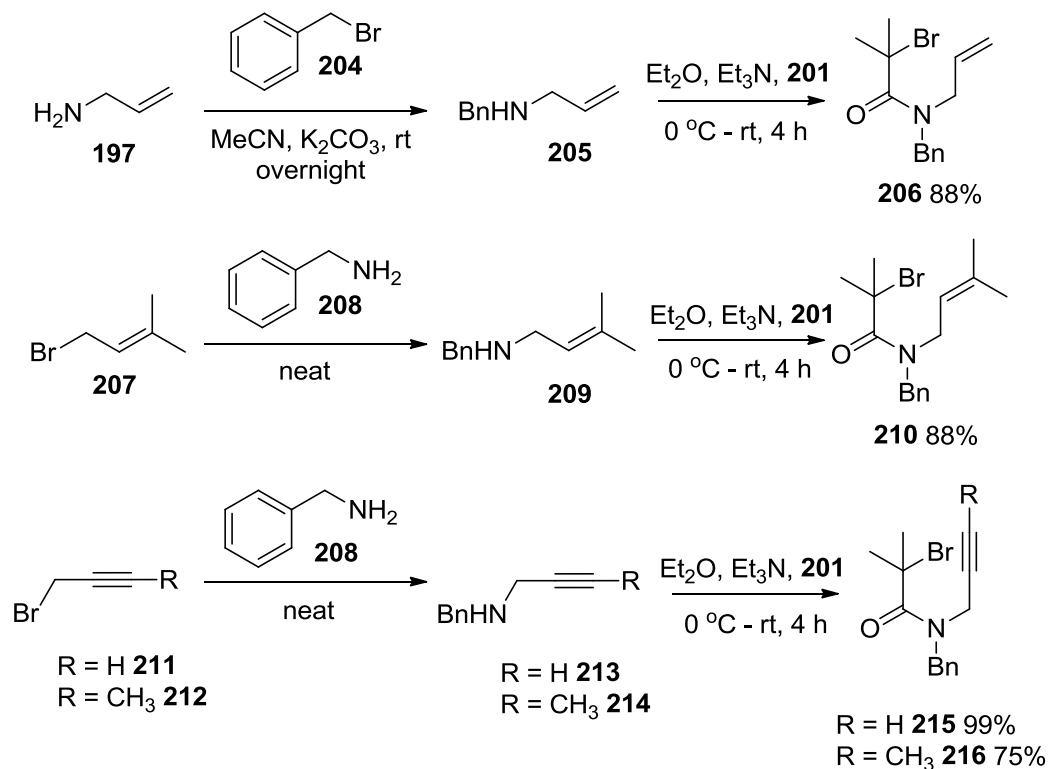
In transition metal-mediated ATRC the nature of the *N*-protecting group is known to have an effect on the efficiency of cyclisation,¹⁸ with larger and electron-withdrawing substituents forming the most efficient substrates. As a result, both *N*-tosyl and *N*-benzyl acetamides were prepared. The *N*-tosyl acetamides **202** and **203** were synthesised from allylamine **197** and propargylamine **198**, with the key step being the acetylation of intermediates **199** and **200** using 2-bromoisobutyryl bromide **201** (Scheme 2.6).



Scheme 2.6: Synthesis of 5-Exo Trig and Dig Substrates for Radical Cyclisation

The *N*-benzyl analogues were synthesised *via* alternative routes. Acetamide **206** was prepared from allylamine **197** and benzyl bromide **204**, and acetamides **210** and **215** were prepared from benzylamine **208** using dimethylallyl bromide **207** and propargyl bromides **211** respectively. Again the key step in these reactions was the acetylation reaction using 2-bromoisobutyryl bromide **201**. To complete the reaction

set of three 5-*exo trig* and three 5-*exo dig* precursors, the internal alkyne **216** was prepared from benzylamine **208**, using 1-bromo-2-butyne **212** (Scheme 2.7).

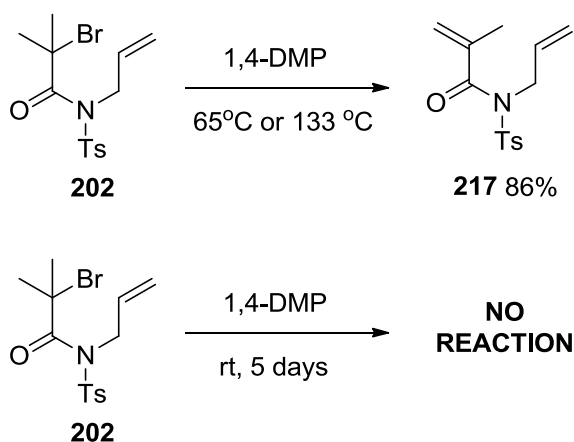


Scheme 2.7: Synthesis of Substrates for 5-*Exo Trig* and *Dig* Radical Cyclisation

2.2.1 1,4-DMP Mediated Radical Cyclisation

Under transition metal catalysed, atom transfer conditions, cyclisation of *N*-tosyl acetamide **202** has been shown to be facile,^{23,32} and as a result initial attempts at 1,4-DMP mediated cyclisation were approached with confidence. Disappointingly, at reflux (133 °C) and at the previously reported optimum temperature (65 °C), cyclisation was not observed. Alternatively, the only product isolated was **217** which arose from the elimination of HBr from the tertiary bromide present in **202**. The formation of **217** was not unexpected as the acetamides chosen for the

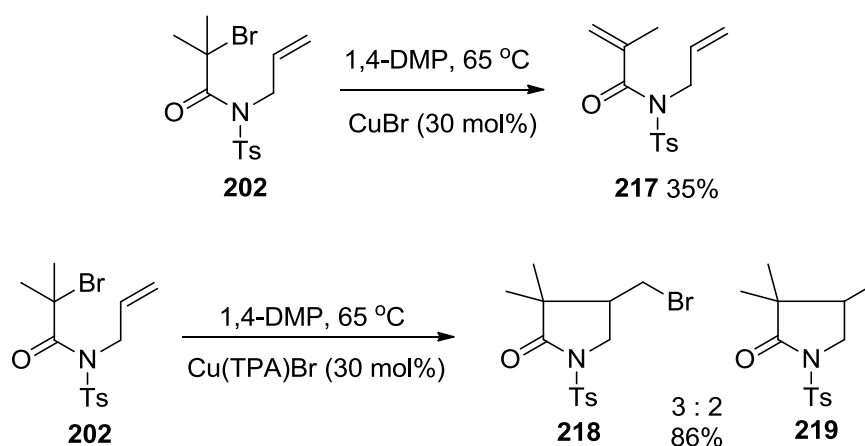
investigation were prepared with the competing elimination pathway in mind. Thus, from the initial results it was concluded that between 65-133 °C, base-mediated elimination occurred faster than the initiation of the radical chain. The reaction was therefore repeated at room temperature in the hope of slowing the rate of elimination. Unfortunately, after 5 days no reaction had occurred (Scheme 2.8).



Scheme 2.8: Initial Attempts at 1,4-DMP Mediated Radical Cyclisation

In order to accelerate the rate of initiation, a copper catalyst was added to the reaction mixture at 65 °C. To ensure that the reaction could proceed in 1,4-DMP, the solvent remained the same and the effect of copper bromide (CuBr, 30 mol%) addition was examined. Tertiary amines can chelate copper salts and form active copper complexes for ATRC by assisting in the dissolution of the CuX salt and stabilizing the low oxidation state (Chapter 1). However, this was not observed for 1,4-DMP as the solubility of CuBr was poor and the eliminated product **217** prevailed (Scheme 2.9). Tetradentate nitrogen ligand TPA **53**, is known to form one of the most active copper complexes (Cu(TPA)Br) for ATRC,³³ and upon addition of this complex (Cu(TPA)Br, 30 mol%) to the *N*-tosyl acetamide **202** in 1,4-DMP, cyclisation was achieved. Under conventional ATRC conditions (DCM, rt), atom

transfer product **218** is obtained exclusively in almost quantitative yields (98%), though this was not the case in 1,4-DMP at 65 °C. Atom transfer product **218** was obtained along with a second cyclised product that was characterized as reduced cyclic product **219**. Crude NMR identified the two products as a 3 : 2 (**218** : **219**) mixture which was purified to give a combined yield of 86% (Scheme 2.9).

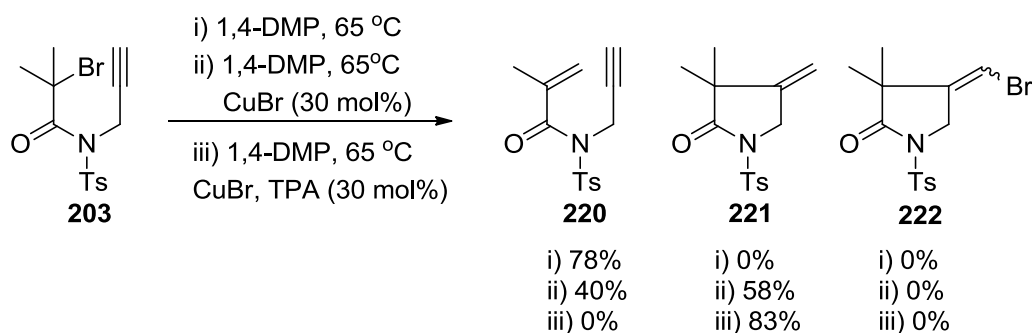


Scheme 2.9: 1,4-DMP Mediated 5-Exo Trig Radical Cyclisation in the Presence of Cu(TPA)Br

Addition of the catalyst (Cu(TPA)Br) is unlikely to enhance the rate of single electron transfer from 1,4-DMP to the substrate. It is more probable that cyclisation is mediated by the copper complex and that the rate of ATRC is faster than the rate of elimination. Furthermore, the reduced product **219** can arise from the competitive reduction of the reactive primary radical formed upon cyclisation by the 1,4-DMP solvent.

The sequence of reactions performed to accomplish the 5-*exo trig* radical cyclisation of *N*-tosyl acetamide **202** was repeated, using *N*-tosyl acetamide **203** (alkyne), to determine the likelihood of 5-*exo dig* radical cyclisation in 1,4-DMP. Unsurprisingly, attempted cyclisation in 1,4-DMP at 65 °C was unsuccessful with elimination occurring to form **220** (78%). However, in the presence of CuBr and

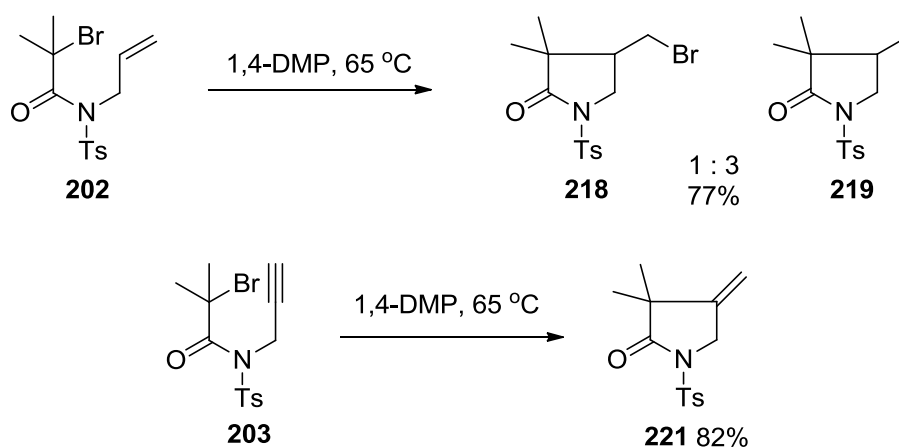
1,4-DMP, cyclisation was observed in reasonable yield (58%), and this was improved in the presence of the complex Cu(TPA)Br (83%). The 5-*exo dig* cyclised product was not the expected atom transfer compound **222**, but the reduced compound **221** and no atom transfer was detected at all. The vinyl radicals formed during 5-*exo dig* radical cyclisation, are more reactive than the primary radicals formed during 5-*exo trig* cyclisation, and presumably are reduced by 1,4-DMP at a much faster rate than potential atom transfer (Scheme 2.12).



Scheme 2.10: 1,4-DMP Mediated 5-Exo Dig Radical Cyclisation

Despite being satisfied with observing 5-*exo trig* and *dig* cyclisations in 1,4-DMP, the need for a catalyst to initiate cyclisation was disappointing, as this had previously been avoided by Ishibashi.¹¹⁸ However, the initial results of this study indicated that the rate of elimination of HBr from the starting material was greater than the rate of single electron transfer radical chain initiation. This conclusion was drawn from reactions performed using 1,4-DMP that was 6-12 months old and open to the atmosphere. Therefore it was highly likely that the reagent had collected a degree of moisture which could have facilitated the elimination reaction. Consequently the decision was taken to purchase a fresh batch of 1,4-DMP, dry it over molecular sieves (4 Å), degas it through the freeze-pump-thaw technique and store it under nitrogen to eliminate any moisture present.

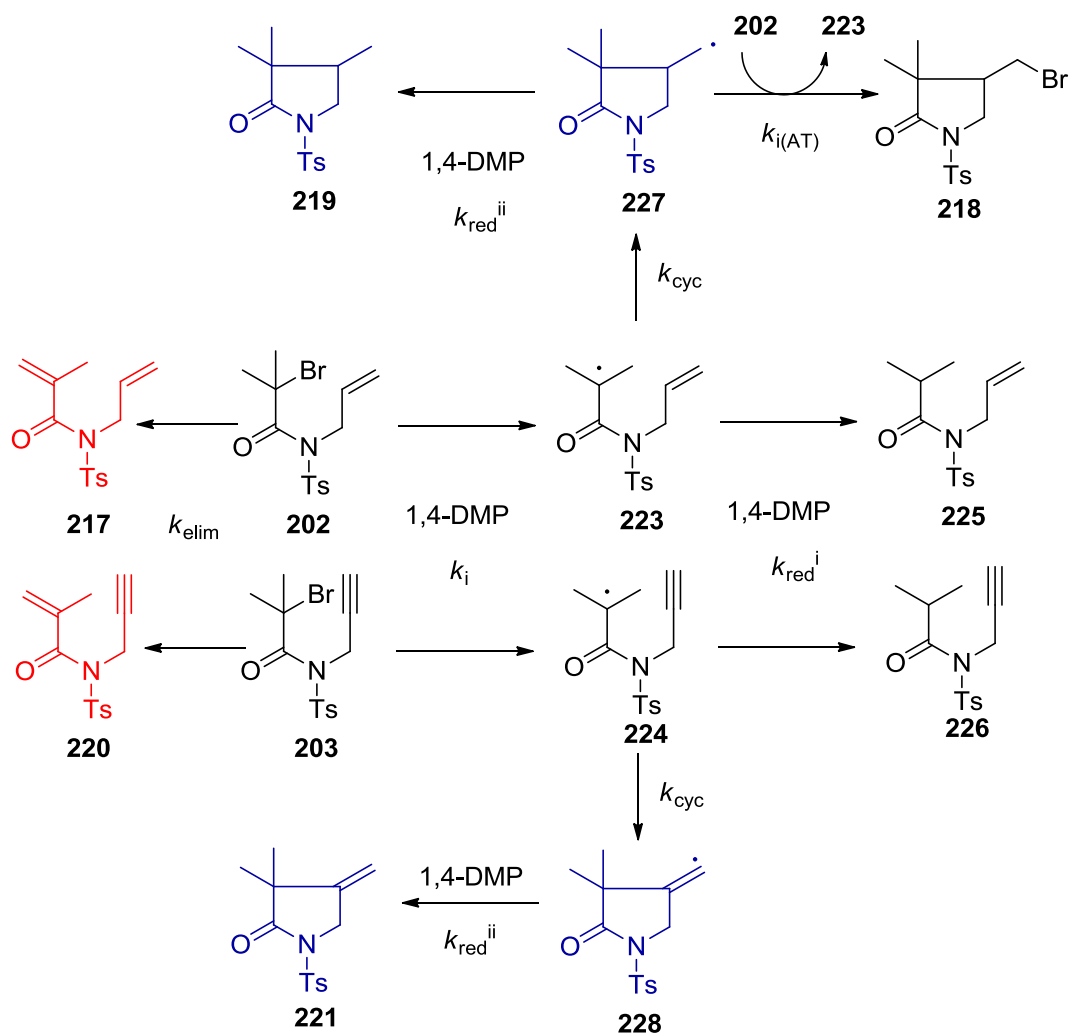
The 5-*exo trig* cyclisation of **202** and 5-*exo dig* cyclisation of **203** was then attempted using the dried 1,4-DMP at 65 °C, and under inert conditions cyclisation was observed. For 5-*exo trig* cyclisation of **202** the major product was identified as the reduced compound **219**, as a 3 : 1 mixture with the atom transfer compound **218**, giving a combined yield of 77%. A single product was isolated for the 5-*exo dig* cyclisation of alkyne **203**, and it was characterised as the reduced compound **221** (82%).



Scheme 2.11: 1,4-DMP Mediated 5-*Exo Trig* and *Dig* Radical Cyclisation in the Absence of Cu(TPA)Br

These results suggest that, in the absence of moisture, the rate of single electron transfer from 1,4-DMP to **202** and **203** is faster than the rate of elimination ($k_i > k_{\text{elim}}$). At this point the exact mechanism of 1,4-DMP mediated cyclisation is unknown and requires investigation. Ishibashi has suggested that initiation is likely to occur *via* single electron transfer¹¹⁸ to the substrates from the nitrogen of 1,4-DMP, followed by elimination of a bromine anion. This would furnish the familiar radical intermediates **223** and **224** (Scheme 2.12), which could undergo cyclisation to give radicals **227** and **228**. At this point, the results obtained suggest that the vinyl radical **228** is reductively quenched by 1,4-DMP to give **221** ($k_{\text{red}}^{\text{ii}} \gg \gg k_{i(\text{AT})}$), whereas

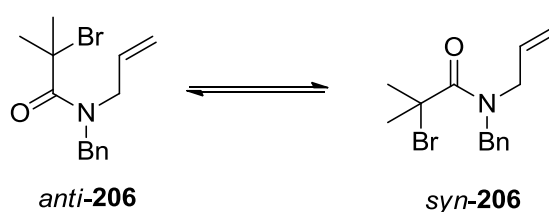
although primary radical **227** is preferentially reductively quenched by 1,4-DMP (**219**), some atom transfer to give **218** does occur, presumably by abstraction of a bromine radical from the substrate **202** to reinitiate the radical chain ($k_{\text{red}}^{\text{ii}} > k_{\text{i(AT)}}$). As reductions of cyclised radicals **227** and **228** are observed, potential reductions of radicals **223** and **224** are also possible. However, the isolation of cyclised products strongly implies that cyclisation is the much faster process for these substrates ($k_{\text{cyc}} \gg k_{\text{red}}^{\text{i}}$) (Scheme 2.12).



Scheme 2.12: Possible Reaction Pathways Followed 1,4-DMP Mediated Radical Formation

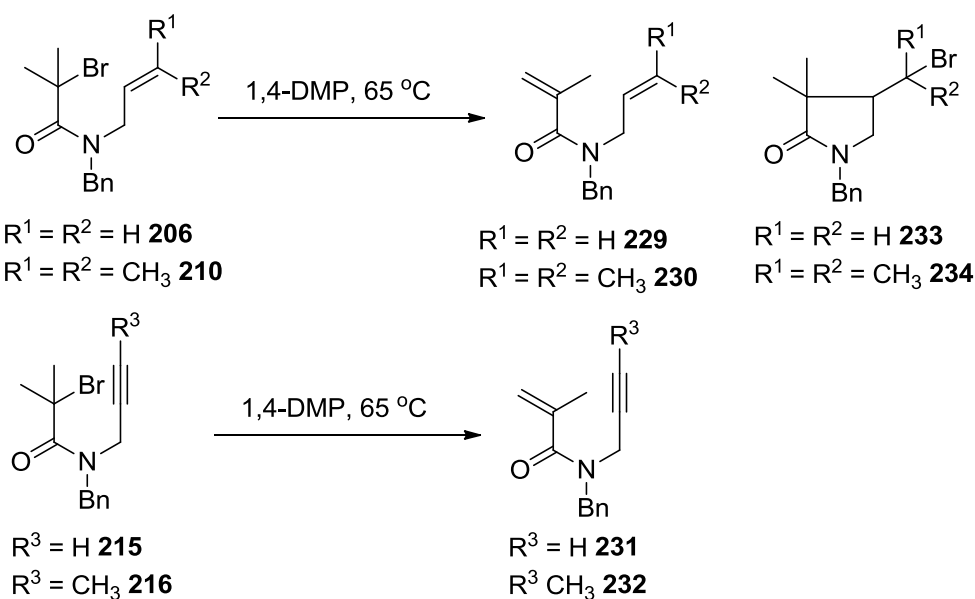
change in the product ratio (entry 5). At 70 °C, the preference for the reduced product **219** decreased when CuBr was added (entry 8). Finally, addition of the ATRC complex (Cu(TPA)Br) provided cyclisation at all temperatures, generally favouring the atom transfer product **218** (entries 3, 6, 9). Cyclisation in the presence of the copper complex (Cu(TPA)Br) at 50 °C implied that the rate of initiation of the ATRC reaction, was greater than the rate of single electron transfer (k_i , Scheme 2.12). At all temperatures 1,4-DMP was found to contribute to the quenching of the reaction leading to the formation of **219**.

The most favorable results for 1,4-DMP mediated cyclisation occurred at a temperature of 65 °C (entries 10, 11, 12). Consequently, the *N*-benzyl acetamides that are known to be harder to cyclise than the *N*-tosyl analogues were next considered under these conditions. These substrates were expected to have a slower rate of cyclisation (k_{cyc}), as in the ground state an unfavourable population of the *syn*-amide rotamer exists which cannot cyclise upon initiation, due to the radical being held too far away from the acceptor (Scheme 2.13).¹⁴



Scheme 2.13: Amide Rotomers of Monobromide Acetamide **206**

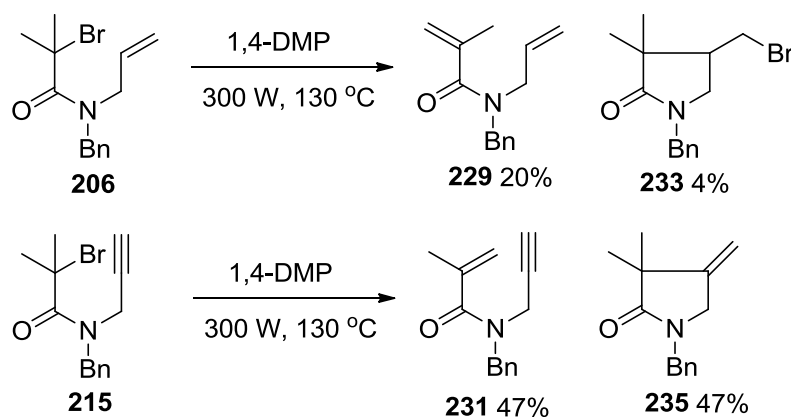
Cyclisations of *N*-benzyl acetamides **206**, **210**, **215** and **216** in 1,4-DMP at 65°C were unsuccessful. Conversions were low, even after 72 hours, and in the event of any conversion, the eliminated products **229-232** were exclusively obtained, except in the case of the 5-*exo trig* cyclisation of **206** which furnished atom transfer product **233** in a meager 1% yield (Table 2.3).



Entry	Solvent	Temp °C	Products	Yield
1 (206)	1,4-DMP	65	206 (SM)	73%
			229	6%
			233	1%
2 (210)	1,4-DMP	65	210 (SM)	63%
			230	13%
3 (215)	1,4-DMP	65	231	69%
4 (216)	1,4-DMP	65	232	70%

Table 2.3: Reaction Products of Attempted 1,4-DMP Mediated 5-Exo Trig and Dig Radical Cyclisations

The results suggested that cyclisation was indeed much slower than the *N*-tosyl acetamides **202** and **203**, but evidence of atom transfer product **233** indicated that formation of cyclised products was possible. Consequently, the reactions of **206** and **215** were repeated in a microwave (Scheme 2.14) to determine whether the rate of cyclisation could become comparable to those observed for related *N*-tosyl acetamides **202** and **203**.



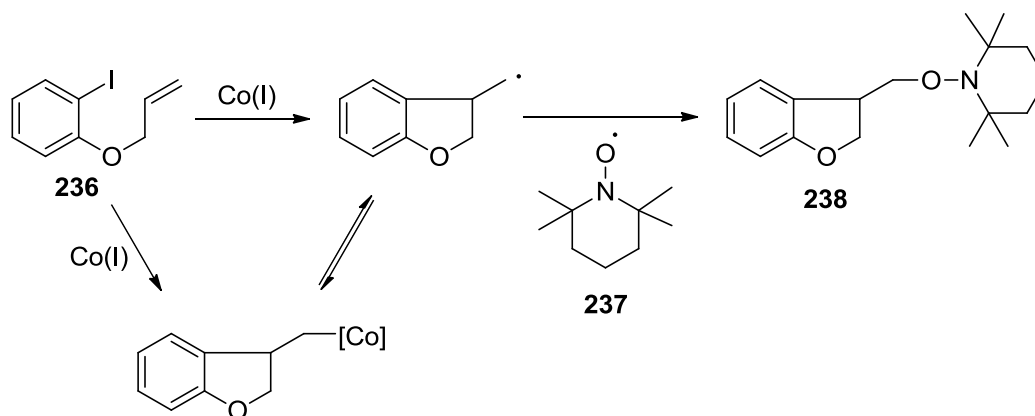
Scheme 2.14: Microwave Assisted 1,4-DMP Mediated 5-Exo Trig and Dig Radical Cyclisation

For both substrates the reaction time was set at 1 hr with a temperature of 130 °C, just below the boiling point of 1,4-DMP. Compound **215** gave significantly improved results providing a 1 : 1 mixture of the eliminated **231** and cyclised **235** products in a combined yield of 94%, while **206** gave a four-fold increase in conversion improving the yield of **229** to 20% and **233** to 4%. Thus, use of microwave heating improved the situation markedly, but the overall transformation was still not synthetically useful for *N*-benzyl acetamides. Consequently, 1,4-DMP mediated radical cyclisation (at the present time) is limited to activated trichloro-precursors with fast rates of cyclisation.

2.2.2 Radical Trapping

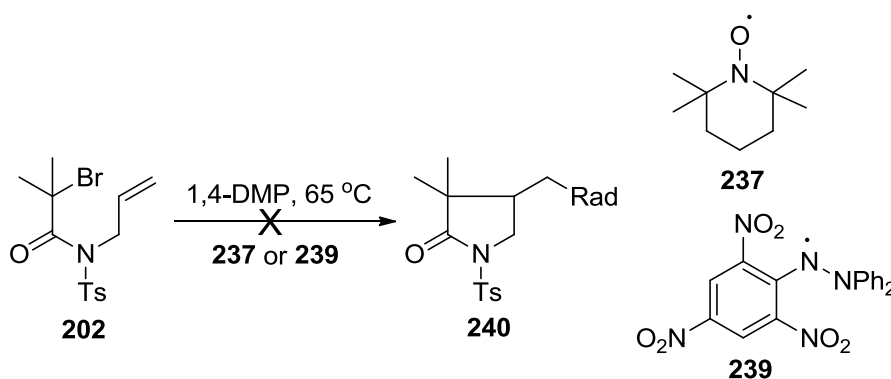
In the late 1980's/early 1990's Pattenden at Nottingham was using alkylcobalt complexes in the formation of carbo- and heterocyclic compounds.^{80,120} During this time, Pattenden proposed the combination of transition metal mediated radical cyclisation and radical trapping methodologies.⁸⁰ The result of this amalgamation was a synthetic route to heterocycles, through intramolecular carbon-to-carbon bond formation, followed by immediate trapping of the radical

intermediate to introduce new functionality (Scheme 2.15). For example, cobalt(I) mediated cyclisation of the allyl ether **236** followed by radical trapping using TEMPO ¹²¹ **237**, furnished **238** which on reaction with zinc and acetic acid underwent reductive cleavage to yield a primary alcohol.



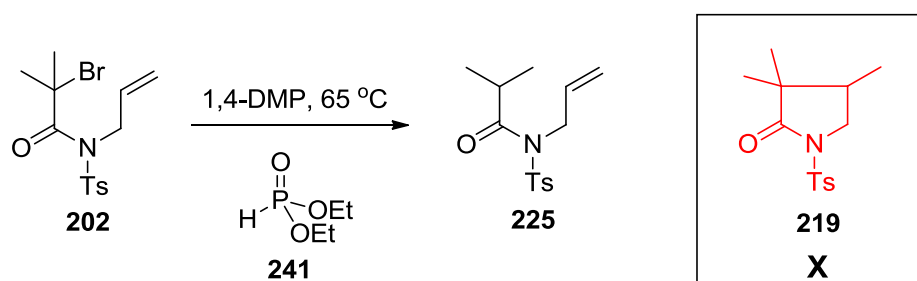
Scheme 2.15: Cobalt Mediated Radical Cyclisation

The cyclisation of *N*-tosyl acetamide **202** in 1,4-DMP led to the formation of an atom transfer **218** and reduced **219** products, the ratios of which were shown to be temperature-dependent (Table 2.2). The possibility of trapping the radical intermediate (**227**, Scheme 2.12) was briefly considered as this would furnish products with new functional groups where further chemistry could take place. The concept of radical trapping has found considerable application in synthetic chemistry, and consequently a number of radical traps exist.^{122,123,124,125,126} In this investigation, stable radicals TEMPO **237**, and diphenylpicryl hydrazyl radical **239** were considered, as reductive cleavage of the trapped intermediates would yield the respective primary alcohol and amine.

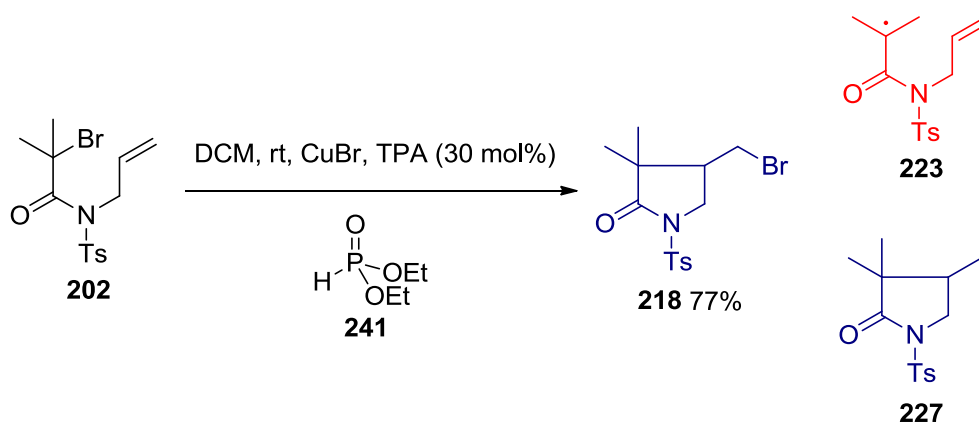


Scheme 2.16: Attempted Radical Trapping During 1,4-DMP Mediated Radical Cyclisation

Unfortunately, under the reaction conditions (1,4-DMP, 65 °C), addition of the radical traps did not furnish any trapped product **240**, and their inclusion retarded that rate of cyclisation as only starting material **202** was recovered after 24 hours (Scheme 2.16). The functionalized trapping of intermediate **227** was abandoned at this point and an attempt to exclusively obtain the reduced cyclised compound **219** was pursued. Cyclisation of **202** was repeated (1,4-DMP, 65 °C) with addition of an excess of diethyl phosphite **241** (with its labile P-H bond), which was expected to yield an increased proportion of **219** by trapping the primary radical **227** with a hydrogen atom. However, the lability of the P-H bond was exploited prior to cyclisation by the radical intermediate **223**, to give **225** in 41 % yield (Scheme 2.17).

Scheme 2.17: Attempted 1,4-DMP Mediated Radical Cyclisation in the Presence of Hydrogen Donor Diethyl Phosphite as a route to **219**

This implied that the rate of cyclisation (k_{cyc}) of **202** was now slower than the rate of reduction (k_{red}^i) in the presence of diethyl phosphite. For comparison, the cyclisation of **202** was attempted under conventional transition metal-mediated ATRC conditions (30 mol%, rt), in the presence of the same excess of diethyl phosphite **241**. Reduction of the intermediate **223** was not observed, alternatively cyclisation followed by atom transfer to intermediate **227** produced cyclised product **218** (Scheme 2.18). Increasing the concentration of diethyl phosphite to 10 equivalents had little effect and ATRC was able to proceed to furnish **218**.



Scheme 2.18: Copper-Mediated ATRC in the Presence of Hydrogen Donor Diethyl Phosphite

Significantly, this implies a superior rate of cyclisation (k_{cyc}) for the ATRC mechanism compared to the single electron transfer mechanism. Thus, this could mean that the mechanism and intermediates involved in the two pathways are not identical as first thought. To fully comprehend the results presented in this chapter a more definite idea of the mechanism for 1,4-DMP and Cu(TPA)Br mediated radical cyclisation is required.

2.2.3 Conclusion

A novel method for radical cyclisation, utilizing tertiary amine 1,4-DMP, has been applied to the radical cyclisations of *N*-tosyl acetamides **202** and **203**. Acetamides possessing the tertiary bromide acyl group can also undergo base-mediated elimination. However, under anhydrous and anaerobic conditions, the rate of cyclisation (k_{cyc}) was found to be greater than the rate of elimination (k_{elim}). Conversely, for less reactive *N*-benzyl intermediates, k_{cyc} was found to be slower than k_{elim} , and cyclisation was not observed in synthetically useful yields. Cyclisation of acetamide **202** furnished two products (**218** and **219**) with yields that were tentatively shown to be temperature-dependent. Attempts to trap cyclised radical **227** to furnish functionalized products were unsuccessful and addition of diethyl phosphite, with a labile P-H bond, led to trapping of the intermediate radical **223** prior to cyclisation ($k_{\text{red}}^{\text{i}} > k_{\text{cyc}}$). However, the extent of the lability of the P-H bond was not sufficient enough to trap the same intermediate under ATRC (30 mol% Cu(TPA)Br) conditions. In order to fully understand these results a comprehensive mechanistic investigation is required.

3.0 Copper-Mediated Atom Transfer Radical Cyclisation Using AIBN and Other Additives

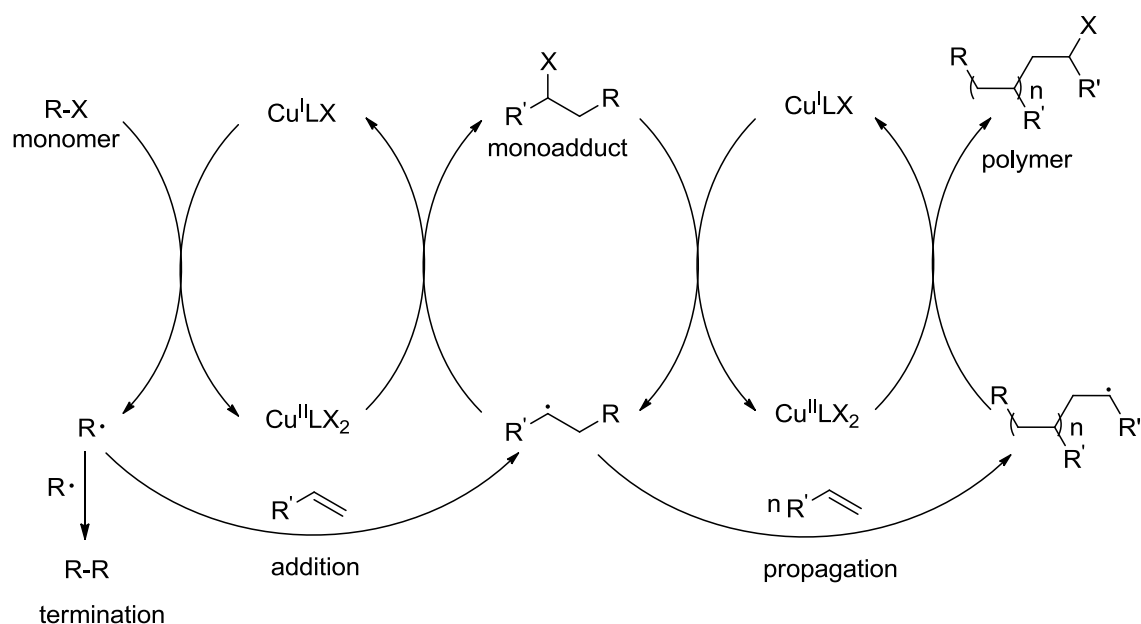
3.1 INTRODUCTION

3.1.1 The Use of Additives in Atom Transfer Radical Addition and Polymerisation

Transition metal-catalysed radical additions and cyclisations have been well studied and have proved to be useful synthetic tools (Chapter 1). However, a common drawback for these reactions was the need for high catalyst loadings (up to 30 mol%) to achieve the desired products, often causing difficulties in product separation and purification, and in catalyst regeneration. Taken together these obstacles made these processes, although very useful, environmentally unfriendly and expensive. Consequently, recent academic research has focused on reducing catalyst loadings to make these processes more attractive.

In the 1990's atom transfer radical polymerisation (ATRP)⁷³ was born out of the fundamental concepts of atom transfer radical addition (ATRA)⁷³ and cyclisation (ATRC),¹⁸ opening a new field of research led by the groups of Matyjaszewski,⁶² Sawamoto⁶³ and Haddleton.^{127,128} The mechanism of ATRP^{129,130,131} is thought to be similar to that of ATRA,^{6,7,8,73} differing only due to the reaction conditions applied, to favour single or multiple additions forming monoadducts (ATRA) or polymers (ATRP) (Scheme 3.1). In order to selectively obtain a monoadduct, initial radical concentrations (from an alkyl halide, R-X) should be low (to avoid termination reactions R-R), activation of the monoadduct should be avoided and the rate of

propagation (polymer formation) should be suppressed. Conversely, to observe polymerisation the reactivity of the initial radical (from R-X) and radical formed from addition should be similar and the rate of propagation should not be suppressed. If this is the case the activation-addition-deactivation cycle can continue until all of the monomer has been completely consumed, forming a polymer product.

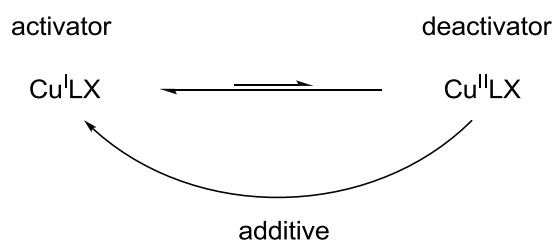


Scheme 3.1: Mechanisms of ATRA and ATRP

A number of transition metals have been shown to catalyse both the addition (Cu, Fe, Ru, Ni)^{73,82,132,133} and polymerisation (Ti, Mo, Re, Fr, Ru, Os, Rh, Co, Ni, Pd, Cu)¹²⁹ reactions. However, particularly for the polymerisation reaction, copper complexes have been found to be the most efficient, allowing a range of monomers to be polymerised under a variety of conditions depending on the nature of the complex ($\text{Cu}^{\text{I}}\text{LX}$).

It was in the field of ATRP that the origin of a solution to high catalyst loadings was developed.⁷³ High monomer conversions relied on an equilibrium between the activator ($\text{Cu}^{\text{I}}\text{LX}$) and deactivator ($\text{Cu}^{\text{II}}\text{LX}_2$), in favour of the activator

(Scheme 3.2). The deactivator ($\text{Cu}^{\text{II}}\text{LX}_2$) tends to accumulate during these reactions due to unavoidable termination reactions (forming R-R, Scheme 3.1) which results in slower polymerisation rates and lower monomer conversions. This is known as the persistent radical effect.^{134,135,136} Although high catalyst loadings alleviated this problem, it also caused leaching of the catalyst into the polymer product, complicating the purification process, particularly when scaled up. Consequently, a method was developed in which the activator for polymerisation ($\text{Cu}^{\text{I}}\text{LX}$) was continuously regenerated from the deactivator ($\text{Cu}^{\text{II}}\text{LX}_2$) by additives (Scheme 3.2) such as phenols,⁶⁴ monosaccharides,^{65,66} ascorbic acid,^{67,68} hydrazine,⁶⁵ tertiary amines^{137,138} and diazo compounds such as AIBN.⁶⁵

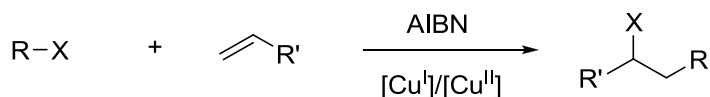


Scheme 3.2: Proposed Activator Regeneration of Copper(I) Complexes

This method is commonly known as ‘activators regenerated by electron transfer’ atom transfer radical polymerisation (ARGET-ATRP). The method can also be applied to polymerisations in which there is no activator ($\text{Cu}^{\text{I}}\text{LX}$) present to begin with and the deactivator ($\text{Cu}^{\text{II}}\text{LX}_2$) is reduced *in situ* to give the active complex ($\text{Cu}^{\text{I}}\text{LX}$). This is known as ‘activators generated by electron transfer’ (AGET-ATRP). Indeed these new methods have allowed for efficient, well controlled polymerisations of *n*-butyl acrylate, methyl methacrylate and styrene (amongst others) with catalyst concentrations as low as 50 ppm.^{66,139,140} Furthermore, the

antioxidant nature of the additives (phenols, glucose, ascorbic acid) allowed the reactions to be performed in the presence of air.¹⁴¹

If the reaction conditions are such that formation of a monoadduct is favoured (ATRA), the mechanism still relies on the equilibrium between activator ($\text{Cu}^{\text{I}}\text{LX}$) and deactivator ($\text{Cu}^{\text{II}}\text{LX}_2$), and under the same rationale the unavoidable accumulation of ($\text{Cu}^{\text{II}}\text{LX}_2$) has an adverse effect upon conversion. Recently, copper catalysed ATRA has focussed on the complex formed from tetradentate nitrogen ligand TPA (**53**) as both $\text{Cu}^{\text{I}}\text{X}$ and $\text{Cu}^{\text{II}}\text{X}_2$ complexes are highly active.^{70,71} Using these catalysts, Pintauer has shown that polychlorinated and polybrominated substrates can add to simple alkenes, such as 1-hexene and 1-octene, and more complex alkenes, styrene and methyl acrylate (MA) to selectively form monoadduct products (Table 3.1).



Entry	Alkene	R-Cl	[Alk]:[Cu ^I]	Yield	R-Br	[Alk]:[Cu ^I]	Yield
1	1-Hexene	CCl ₄	5000:1	98%	-	-	-
2	1-Octene	CCl ₄	5000:1	87%	-	-	-
3	Styrene	CCl ₄	250:1	85%	CBr ₄	200000:1	95%
4	MA	CCl ₄	1000:1	60%	CBr ₄	200000:1	81%
5	1-Hexene	CHCl ₃	1000:1	56%	CHBr ₃	10000:1	61%
6	1-Octene	CHCl ₃	500:1	49%	CHBr ₃	10000:1	69%
7	Styrene	CHCl ₃	1000:1	58%	CHBr ₃	10000:1	70%
8	MA	CHCl ₃	1000:1	63%	CHBr ₃	1000:1	57%

Table 3.1: Copper-Mediated ATRA in the Presence of AIBN

Using AIBN as an additive, and the Cu(TPA)Cl complex as catalyst, allowed for excellent conversions to the monoadduct when 1-hexene (Table 3.1, entry 1) and 1-octene (entry 2) were used with only 200 ppm catalyst (Cu(TPA)Cl). Experiments conducted using the Cu(TPA)Cl₂ complex as catalyst also yielded similar results in

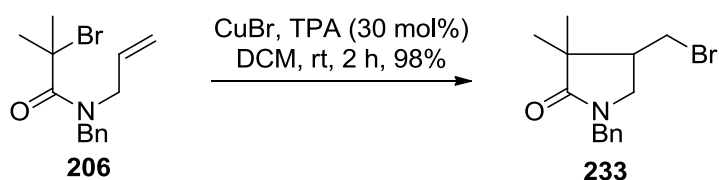
the presence of AIBN suggesting the additive was capable of generating and regenerating the active complex. The results for the polybrominated substrates were achieved using only the Cu(TPA)Br₂ complex which would require *in situ* activation. Remarkably, excellent yields of monoadduct products were obtained for previously difficult alkenes, such as styrene (entry 3) and methyl acrylate (MA) (entry 4) with as little as 5 ppm catalyst. The improved efficiency, compared to the polychlorinated results, was not unexpected as C-Br and Cu-Br bonds are much weaker than the corresponding chloride analogues. However, the extent of the improvement was significant, indicating that the addition of AIBN vastly improved the efficiency of additions of polybrominated compounds, including less active bromoform compounds (entries 5-8) using as little as 5-100 ppm catalyst.

The mechanism for ATRC (Chapter 1, Scheme 1.6) has been identified as an intramolecular version of ATRA, where the radical initiator (halogenated group) and radical sink (alkene) are within the same compound and in close proximity. Consequently, it was recognised that catalyst loadings could possibly be reduced by the introduction of additives with the purpose of activator regeneration. The principal advantages of activator regeneration for the cyclisation methodology would be reduced catalyst loadings and the ability to perform reactions under aerobic conditions, which up to now has not been possible for copper-catalysed ATRC due to the deactivation of the catalyst by adventitious oxygen present in reaction mixtures.

3.2 RESULTS AND DISCUSSION

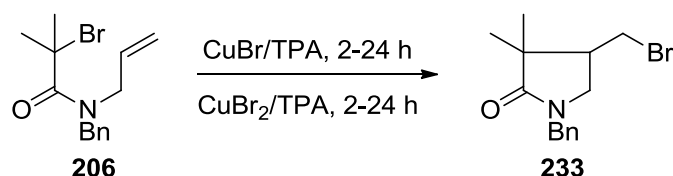
3.2.1 Screening Potential Additives for Copper Mediated ATRC

The applicability of activator regeneration in ATRC was assessed by the investigation of the 5-*exo trig* radical cyclisation of tertiary bromide **206** (Scheme 3.3). Under conventional ATRC conditions (30 mol% Cu(TPA)Br, DCM) a 98% yield of cyclised product **233** is obtained within 2 hours.



Scheme 3.3: Established Conditions for Copper-Mediated 5-Exo Trig ATRC

Given the results obtained by Pintauer for copper-catalysed ATRA using AIBN,^{70,71} attention was turned to reducing the catalyst loading for ATRC using the same additive. A 30-fold decrease in catalyst (1 mol%, Table 3.2, entry 2) afforded only 5% conversion, in the absence of AIBN, in 24 hours at room temperature. Repeating the reaction at reflux caused the conversion to increase but only to 14% (entry 3). At such low catalyst loadings, conversions are likely to be limited due to the equilibrium of activator and deactivator (Scheme 3.2) favouring the deactivator, which limits the C-Br bond homolysis required to initiate cyclisation.

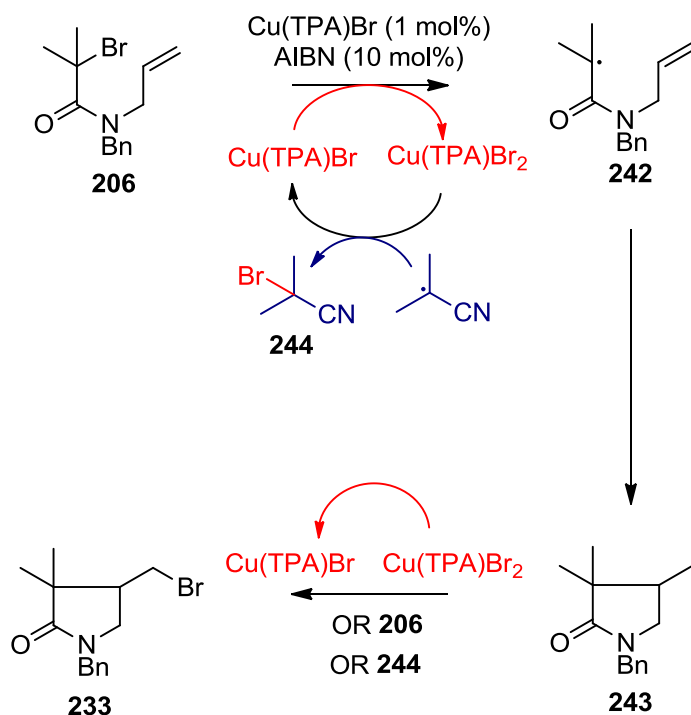


Entry	Time	Temp °C	Solvent	AIBN	CuBr/TPA	Conv	MB
1	2	RT	CH ₂ Cl ₂	-	30 mol%	100%	98%
2	24	RT	CH ₂ Cl ₂	-	1 mol%	5%	98%
3	24	50	CH ₂ Cl ₂	-	1 mol%	14%	99%
4	24	50	CH ₂ Cl ₂	10 mol%	1 mol%	100%	84%
5	24	50	CH ₂ Cl ₂	10 mol%	-	-	98%
6	24	50	CH ₂ Cl ₂	5 mol%	1 mol%	95%	99%
7	24	50	CH ₂ Cl ₂	10 mol%	0.1 mol%	40%	89%
8	24	110	toluene	10 mol%	1 mol%	100%	87%
9	24	50	CH ₂ Cl ₂	10 mol%	1 mol%	100%	97%

Table 3.2: Establishing AIBN as a Useful Additive for Copper-Mediated ATRC

Upon addition of 10 mol% AIBN (entry 4), complete conversion was observed and after work-up the cyclised product **233** was isolated in 84% yield. The reaction was also found to proceed in toluene at reflux (110 °C, entry 8). To ensure that AIBN was not homolysing the C-Br bond and initiating the radical chain itself the reaction was repeated in the absence of the catalyst Cu(TPA)Br (entry 5). Under these conditions no conversion to **233** was observed which indicated that AIBN was acting to regenerate Cu(TPA)Br, and not mediating the reaction. The amount of AIBN added could be reduced (5 mol%) with little effect on conversion, to afford **233** in 94% yield (entry 6). However, when the copper catalyst loading was reduced further (0.1 mol%) conversions and yields decreased (entry 7) even in the presence of AIBN. Finally, in *situ* generation of the activator (Cu(TPA)Br) from the deactivator (Cu(TPA)Br₂) (AGET-ATRC) was investigated by changing the oxidation state of the copper catalyst (Cu(TPA)Br₂), which afforded cyclised product **233** in the greatest yield (97%, entry 9). Addition of AIBN to the reaction mixture was therefore shown to facilitate the regeneration and generation of the activator

(Cu(TPA)Br) from (Cu(TPA)Br₂). Purification techniques were not complicated by the addition of AIBN as the proposed by-products would be volatile and facilitate work-up. A revised mechanism is shown in Scheme 3.4, showing the expected redox mechanism (red) and the proposed role of AIBN (blue).

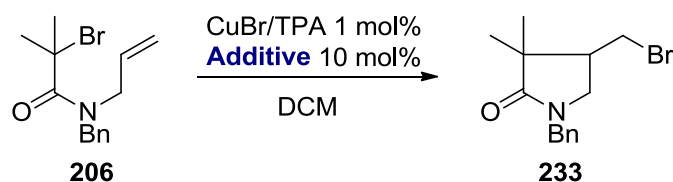


Scheme 3.4: Proposed Mechanism for Copper-Mediated ATRC in the Presence of AIBN

Traditionally the mechanism for ATRC is believed to be initiated and terminated *via* a copper(I)-copper(II) redox process that continually regenerates the copper(I) catalyst (Chapter 1, Scheme 1.6). However, the catalyst efficiency can be compromised by accumulation of non-catalytic copper(II) which is possible if radicals such as **243** are quenched by radical precursors such as **206**. This limits the amount of copper(I) available to re-initiate the reaction when catalyst loadings are reduced. In our reaction (Scheme 3.4) it is proposed that the addition of AIBN reduces non-catalytic Cu(TPA)Br₂ back to Cu(TPA)Br for further initiation of **206**. Furthermore the likely pathways for quenching radical **243** include the traditional

route (red), by $\text{Cu}(\text{TPA})\text{Br}_2$, which is unlikely given its constant reduction to $\text{Cu}(\text{TPA})\text{Br}$, as well as quenching *via* the precursor **206** and cyano-intermediate **244** which are both consumed during the reaction and/or the work-up processes.

In light of the results obtained using AIBN as an additive, a number of other compounds were investigated based upon their application in ARGET-ATRP as activator regenerators.^{65,66,67,68} To compare the efficiencies of these additives with AIBN, the AIBN reaction was repeated at a reaction time of 5 hours at reflux (Table 3.3, entry 1). Pleasingly, complete conversion was obtained to provide **233** in 87% yield. AIBN requires elevated temperatures in order to split into its radical constituents, required to regenerate the activator ($\text{Cu}(\text{TPA})\text{Br}$). However, this is not necessarily the case for other additives, so as well as being carried out at reflux, reactions were also carried out at room temperature for 24 hours (Table 3.3). Initially, a range of phenols were investigated including electron-withdrawing and donating phenols.



Entry	Time	Temp °C	Additive	Conv	MB
1	5 h	50	AIBN	100%	87%
2	24 h	RT	AIBN	5%	98%
3	5 h	50	Phenol	91%	91%
4	24 h	RT	Phenol	-	97%
5	5 h	50	4-Methoxyphenol	18%	87%
6	24 h	RT	4-Methoxyphenol	-	99%
7	5 h	50	4-Nitrophenol	13%	45%
8	24 h	RT	4-Nitrophenol	-	99%
9	5 h	50	4-Trifluoromethylphenol	100%	51%
10	24 h	RT	4-Trifluoromethylphenol	trace	99%

Table 3.3: Effect of AIBN and Other Additives on Copper-Mediated ATRC

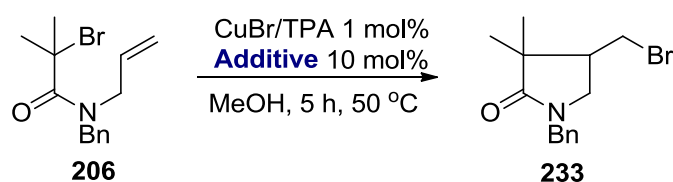
At reflux, phenol (entry 3) and 4-trifluoromethylphenol (entry 9) provided cyclised product **233** in 91% and 100% conversion with yields of 83% and 51% respectively. When 4-methoxyphenol was used as an additive (entry 5) no improvement on conversion, relative to the reaction in the absence of an additive (Table 3.2, entry 3), was observed. The reaction using a second electron-withdrawing phenol, 4-nitrophenol (entry 5), also offered no improvement. Experiments at room temperature offered only disappointing results. Unsurprisingly, at room temperature only 5% conversion was achieved in the presence of AIBN after 24 hours (entry 2). As the half-life of AIBN decomposition^{142,143,144,145,146} is 10 hours at 65 °C access to its radical constituents required to regenerate Cu(TPA)Br would be limited at room temperature. Unfortunately, only little, or no conversion at all was observed at room temperature after 24 hours with the phenol derivatives (entries 4, 6, 8, 10).

Next, due to their antioxidant nature, *L*-ascorbic acid and *D*-glucose were investigated, and to complete the investigation hydrazine, which has been used in ARGET-ATRP,⁶⁵ was also considered (Table 3.4). The reactions were again carried out at both reflux and room temperature for 5 hours and 24 hours respectively for direct comparison with the AIBN results.

Entry	Time	Temp °C	Additive	Conv	MB
1	5 h	50	<i>D</i> -Glucose	27%	38%
2	24 h	RT	<i>D</i> -Glucose	-	96%
3	5 h	50	<i>L</i> -Ascorbic Acid	55%	16%
4	24 h	RT	<i>L</i> -Ascorbic Acid	-	94%
5	5 h	50	Hydrazine	54%	10%
6	24 h	RT	Hydrazine	-	86%

Table 3.4: Effect of Additives on Copper-Mediated ATRC

At room temperature no conversion to **233** was observed in either case (Table 3.4, entries 2, 4, 6). At reflux, *d*-glucose furnished 27% conversion but when the mass balance was considered this only equated to a 10% yield (entry 1). Similarly, despite *L*-ascorbic acid and hydrazine leading to 55% (entry 3) and 54% (entry 5) conversions, when the mass balances were taken into account this translated to disappointing yields of 9% and 5% respectively. It was recognized that *d*-glucose and *L*-ascorbic acid were only sparingly soluble in DCM under the reaction conditions, so the experiments for all additives, including AIBN, were repeated in methanol at 50 °C (Table 3.5).



Entry	Additive	Conv [*]	MB
1	AIBN	50% (100)	87%
2	Phenol	10% (91)	99%
3	4-Methoxyphenol	5% (18)	75%
4	4-Nitrophenol	3% (13)	89%
5	4-Trifluoromethylphenol	19% (100)	99%
6	<i>D</i> -Glucose	23% (27)	73%
7	<i>L</i> -Ascorbic Acid	95% (55)	86%
8	Hydrazine	14% (54)	82%

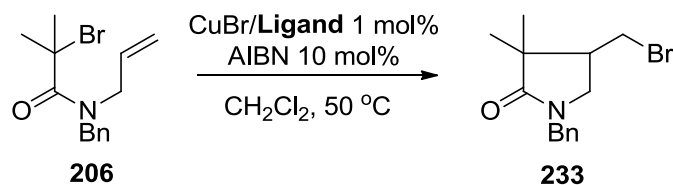
*Numbers in parentheses are yields obtained in DCM at 50 °C after 5 h.

Table 3.5: Effect of Additives on Copper-Mediated ATRC in Methanol

Interestingly, AIBN was not as efficient when methanol was used as solvent (Table 3.5, entry 1). Likewise, the phenols examined also lost efficiency in methanol (entries 2-5). With respect to the yield of **233** obtained, *D*-glucose (17%), *L*-ascorbic acid (82%) and hydrazine (11%) all performed better in methanol (entries 6-8). The improvement observed for *l*-ascorbic acid was significant as simply

changing the solvent saw the yield of **233** rise from 9% to 82%. The performance of *L*-ascorbic acid in methanol was a promising result, but in terms of reproducibility, reliability and the ease of work up, it was obvious from this investigation that AIBN would be the ideal additive for reactions carried out in DCM.

Under the conventional reaction conditions (30 mol% catalyst) it has been shown that different ligand complexes can mediate the same cyclisation reaction with differing efficiencies. The cyclisation of tertiary bromide **206** proceeds with 30 mol% CuBr and ligands in the following order, TPA (**42**) > Me₆-Tren (**41**) > PMDETA (**40**) > Bipy (**30**).^{21,24,25,32} In order to determine whether this reactivity order would be translated to the reaction carried out at lower loadings in the presence of AIBN (Table 3.2, entry 4), the substrate **206** was heated at reflux in the presence of each complex (Table 3.6).



Entry	Ligand	Time	Conv
1	TPA (42)	24 h	100%
2	Me ₆ -Tren (41)	24 h	100%
3	PMDETA (40)	24 h	85%
4	Bipy (30)	24 h	5%
5	TPA (42)	6 h	100%
6	Me ₆ -Tren (41)	6 h	100%
7	TPA (42)	2 h	15%
8	Me ₆ -Tren (41)	2 h	5%

Table 3.6: The Effect of Ligand on Complex Efficiency for Copper-Mediated ATRC in the Presence of AIBN

When the reaction was allowed to run for 24 hours it became evident the TPA (**42**) and Me₆-Tren (**52**) (Table 3.6, entries 1 and 2) were more efficient than

PMDETA (**40**) (entry 3), which in turn was more efficient than Bipy (**30**) (entry 4). In order to distinguish between TPA (**41**) and Me₆-Tren (**42**) the reaction time was reduced to 6 hours. Again complete conversion was observed for both complexes (entries 5 and 6), so both reactions were repeated and stopped after 2 hours. After this time TPA (**42**) was found to provide 15% conversion (entry 7) whilst Me₆-Tren (**41**) could only provide 5% conversion. Consequently, the order of reactivity (Figure 3.1) was not compromised by the reduction in the catalyst loading and the addition of AIBN.

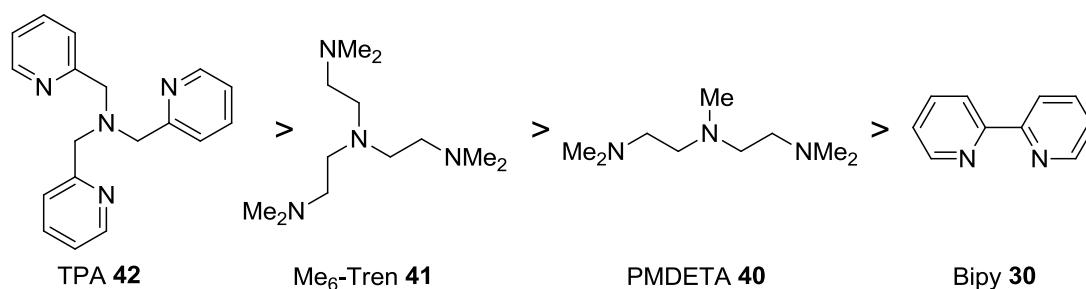


Figure 3.1: Reactivity Scheme for Complexes Formed From Chelating Ligands

3.2.2 Scope of Copper-Mediated ATRC Using AIBN

To investigate the scope and limitation of the reaction conditions developed in section 3.2.1 (1 mol% Cu(TPA)Br, 10 mol% AIBN, DCM, reflux) a number of 5-*exo trig* and *dig* substrates were prepared. The preparation of substrates **202**, **203**, **210** and **215** was detailed in chapter 2. The remaining substrates **249-251** were all prepared by a similar route in which allylic halides **245-247** were reacted with tosylsulfonamide **248** then acetylated using 2-bromoisobutyryl bromide **201** (Scheme 3.5).

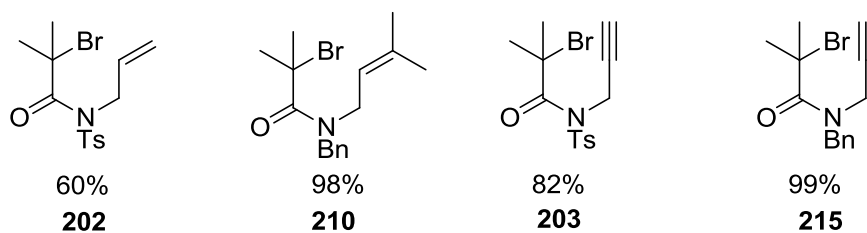
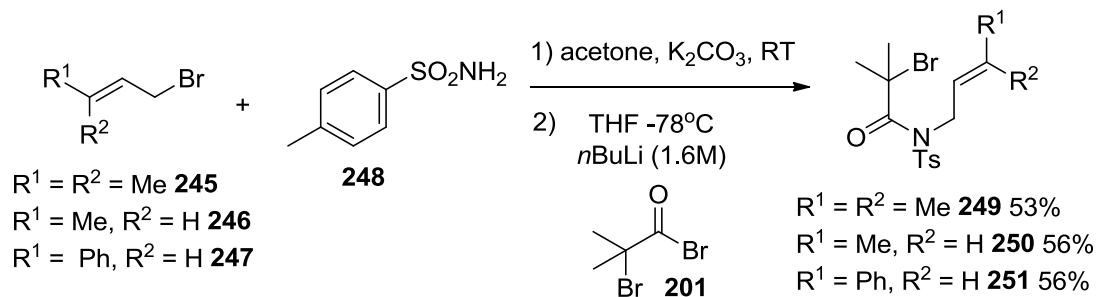
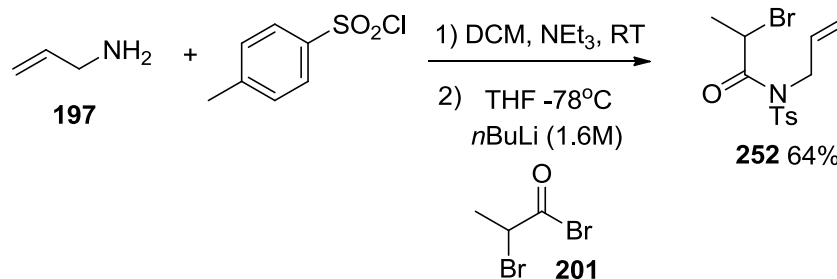


Figure 3.2: Substrates Selected to Demonstrate the Scope of Copper Mediated ATRC in the Presence of AIBN



Scheme 3.5: Synthesis of 5-Exo Trig ATRC Substrates

Finally, a secondary bromide **252** was also prepared to see if the reaction conditions could extend to facilitate more difficult 5-*exo trig* cyclisations.

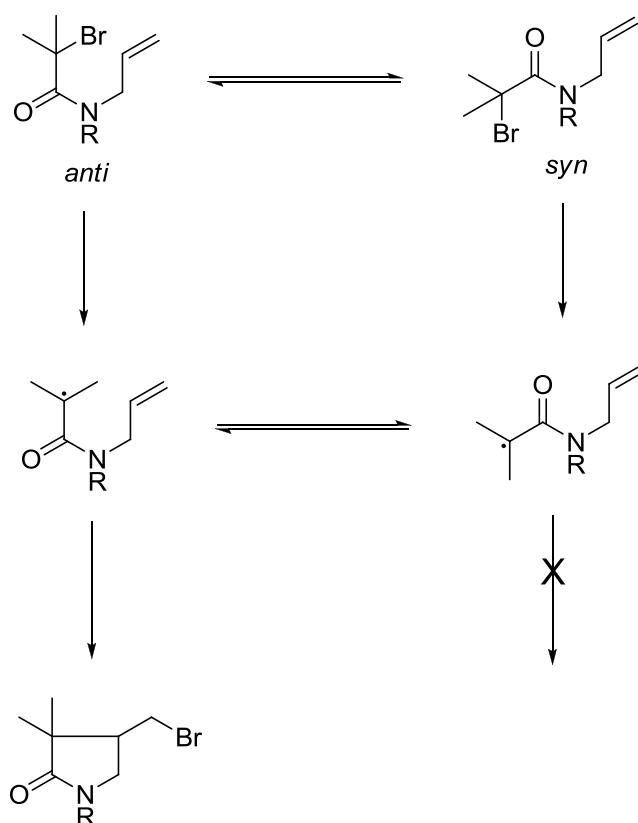


Scheme 3.6: Synthesis of Secondary Bromide Acetamide for 5-Exo Trig ATRC

3.2.2.1 5-*exo trig* ARGET-ATRAC

Substrates **202** and **249-251**, were investigated first. The cyclisation of **202** would offer a direct comparison with the *N*-benzyl acetamide **206**, extensively studied in sections 3.2.1 and 3.2.2. It has been reported that the *N*-protecting group

can have a significant effect on the efficiency of cyclisations of acetamides such as **206** by dictating the amide conformation. Acetamides can exist as two possible amide rotamers and only the *anti* rotamer is predisposed for cyclisation (Scheme 3.7). It is known that increasing the size of the *N*-protecting group, or making the group electron-withdrawing favours the *anti* rotamer.¹⁴ Conveniently, the sulfur atom (*N*-tosyl) bound to the amide nitrogen can make an extra contribution to bonding through its empty, low level *d*-orbitals, which would also favour the *anti* rotamer and consequently, changing from an *N*-benzyl to *N*-tosyl protected nitrogen was expected to result in more efficient cyclisations.



Scheme 3.7: Allowed and Disallowed Conformations for ATRC

As expected, following the reactions of the *N*-tosyl acetamides (**202** and **249-251**) by TLC revealed that these reactions were complete within 1 hour furnishing

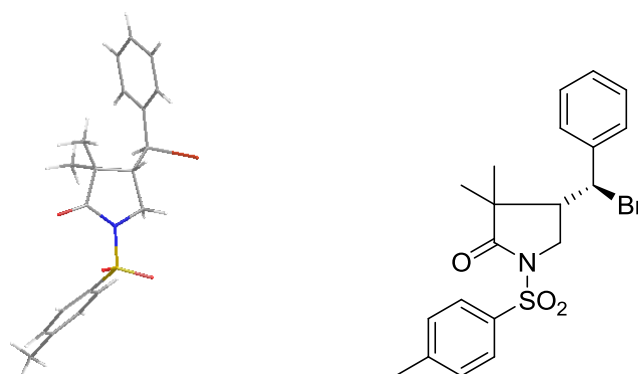
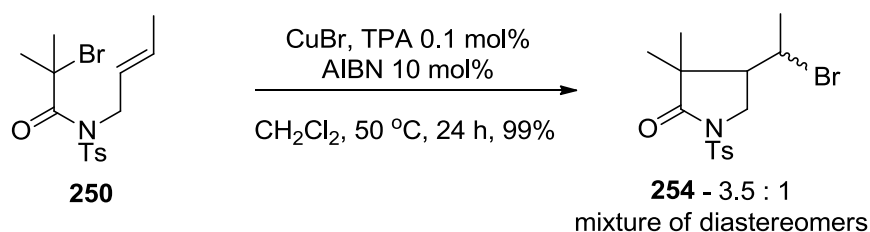
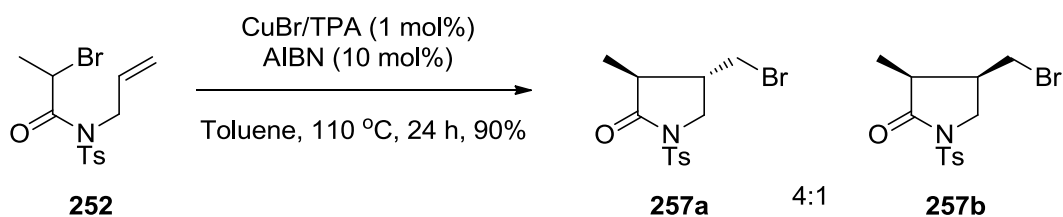


Figure 3.3: Crystal Structure of Cyclised Product 254



Scheme 3.8: 5-Exo Trig ATRC of Crotyl Acetamide 250

The reaction of the *N*-benzyl acetamide **210** was expected to be accompanied by a reduction in reaction efficiency relative to its *N*-tosyl analogue **249**. Indeed, even after 24 hours at 50 °C in DCM only 14% conversion was obtained (Table 3.8, entry 1), and changing the copper source (Cu(TPA)Br₂) did little to improve the rate of cyclisation (entry 3). During the initial investigation into using AIBN as an additive for these reactions, the cyclisation of **206** was shown to proceed in toluene at 110 °C (Table 3.2, entry 8), as well as in DCM at 50 °C (Table 3.2, entry 4). Consequently, the cyclisation of acetamide **210** was repeated at 110 °C in toluene in the hope of obtaining an acceptable rate of cyclisation (Table 3.8, entries 2 and 4).

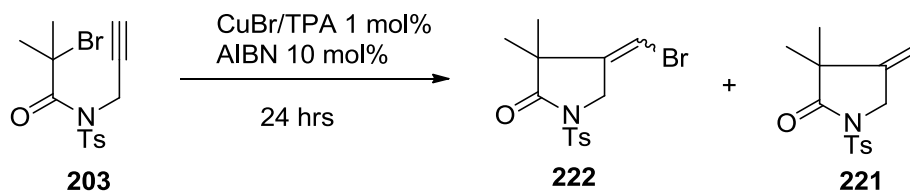


Scheme 3.9: Copper-Mediated 5-Exo Trig ATRC of Secondary Bromide 252 in the Presence of AIBN

3.2.2.2 5-exo dig ARGET-ATRC

Cyclisations onto alkynes have been studied previously,¹⁵ and under conventional conditions (30 mol%, DCM, rt) they have been found to be up to 100 times slower than 5-exo trig cyclisations, and the products obtained are solvent-, ligand- and *N*-protecting group-dependent. For instance, terminal alkynes are known to undergo facile oxidative dimerisations in the presence of copper halide/pyridine complexes (Chapter 1, Scheme 1.13). It is also known that the nature of the *N*-substituent has an effect on the cyclisation efficiency.¹⁴ Nagashima and co-workers have reported that substrates with bulky or electron-withdrawing groups, such as *N*-tosyl and *N*-Boc, cyclise more efficiently than the *N*-benzyl substrates (Chapter 1).

Given the success of the 5-exo trig reactions in the presence of AIBN discussed earlier in this chapter, the extent to which this could apply to 5-exo dig cyclisations was investigated using previously studied *N*-tosyl acetamide **203** and less activated *N*-benzyl acetamide **215**.



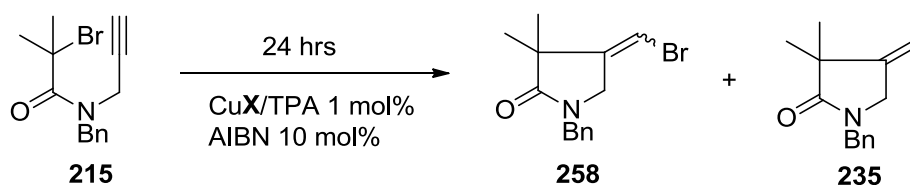
Entry	Temp °C	Solvent	R	CuX	Ratio 222 : 221	Conv	MB
1	50	CH ₂ Cl ₂	Ts	CuBr	1 : 2	33%	99%
2	50	CH ₂ Cl ₂	Ts	CuBr ₂	2 : 3	10%	95%
3	110	toluene	Ts	CuBr	1 : 1	67%	99%
4	110	toluene	Ts	CuBr ₂	1 : 1	80%	99%

Table 3.10: Copper-Mediated 5-Exo Dig ATRC of 203 in the Presence of AIBN

Firstly, *N*-tosyl acetamide **203** was investigated, and the reaction conditions previously applied to 5-*exo trig* cyclisations of tertiary bromides (1 mol% catalyst, 10 mol% AIBN, DCM, 50 °C), were found to be inadequate in the presence of either Cu(TPA)Br or Cu(TPA)Br₂. Conversions were limited to 33% (Table 3.10, entry 1) and 10% (entry 2) respectively. In the hope of obtaining a more acceptable rate of 5-*exo dig* cyclisation, the reactions were repeated using Cu(TPA)Br and Cu(TPA)Br₂ in toluene at 110 °C. Pleasingly, under these reaction conditions, more acceptable conversions were obtained. Cu(TPA)Br (1 mol%) afforded a 67% conversion to a 1 : 1 mixture of atom transfer **222** and reduced **221** products (entry 3), and when Cu(TPA)Br₂ was used as catalyst this increased to 80% conversion to the same products (entry 4). Under the conventional conditions (30 mol%, rt, DCM, 48 h) the atom transfer product **222** was preferentially formed (25 : 1), but this bias was not observed during these reactions as the reduced product **221** was the major product in DCM, and a 1 : 1 mixture was observed in toluene.

As the *N*-benzyl acetamide **215** was thought to be less efficient than the *N*-tosyl acetamide **203**, it came as no surprise that attempts to perform the 5-*exo dig* cyclisation using the 5-*exo trig* conditions (1 mol% catalyst, 10 mol% AIBN, DCM,

50 °C), were again unsuccessful (Table 3.11). Both Cu(TPA)Br (Table 3.11, entry 1) and Cu(TPA)Br₂ (entry 3) gave 33% conversion to the atom transfer **258** and reduced **235** products in a 3 : 2 and 1 : 1 ratio respectively. Repeating the reaction using Cu(TPA)Br and heating it at reflux for 72 hours provided 74% conversion to **258** and **235** in a 2 : 1 ratio (entry 2), suggesting the rate of 5-*exo dig* cyclisation was particularly slow and would require harsher reaction conditions to observe an acceptable rate.



Entry	Temp °C	Solvent	R	CuX	Ratio 258 : 235	Conv	MB
1	50	CH ₂ Cl ₂	Bn	CuBr	3 : 2	33%	90%
2	50 ^a	CH ₂ Cl ₂	Bn	CuBr	2 : 1	74%	90%
3	50	CH ₂ Cl ₂	Bn	CuBr ₂	1 : 1	33%	86%
4	110	toluene	Bn	CuBr	1 : 1	75%	68%
5	110	toluene	Bn	CuBr ₂	2 : 1	82%	76%
6	110	toluene	Bn	CuBr ₂ ^b	1 : 1	84%	74%
7	110	toluene	Bn	CuBr ₂ ^c	1 : 1	100%	70%
8	75	THF	Bn	CuBr	1 : 10	30%	98%

^a 72 hour reflux

^b 2.5 mol% Cu(TPA)Br₂

^c 5.0 mol% Cu(TPA)Br₂

Table 3.11: Effects of Solvent and Temperature on Copper-Mediated 5-*Exo Dig* ATRC of **215 in the Presence of AIBN**

The reactions of **215** using Cu(TPA)Br and Cu(TPA)Br₂ were repeated using toluene at 110 °C. After 24 hours the results obtained were comparable with those obtained for the *N*-tosyl acetamide **203**. Cu(TPA)Br afforded 75% conversion to **258** and **235** in a 1 : 1 ratio (entry 4), whilst Cu(TPA)Br₂ gave 82% conversion to **258** and **235** in a 2 : 1 ratio (entry 5). As Cu(TPA)Br₂ provided better conversions than Cu(TPA)Br for both the *N*-tosyl **203** and *N*-benzyl **215** acetamides, the loading

of Cu(TPA)Br₂ was increased in the hope of achieving complete conversion of the *N*-benzyl acetamide **215**. Increasing the loading to 2.5 mol% (entry 6) had little effect, furnishing an 84% conversion to **258** and **235** in a 1 : 1 ratio. However, when the loading was increased further to 5 mol% Cu(TPA)Br₂ complete conversion was obtained within 24 hours to afford **258** and reduced **235** products in a 1 : 1 ratio. In comparison with the *N*-tosyl acetamide **203** the bias for the atom transfer product, observed when reactions were carried out under conventional conditions (30 mol%), was not observed for the *N*-benzyl acetamide **215**. However, when the 5-*exo dig* cyclisation of **215** was attempted using Cu(TPA)Br in THF at reflux, the reduced product **235** was preferentially formed (**258** : **235**, 1 : 10), though conversions were low (entry 8). Interestingly, in all cases where the atom transfer products **222** or **258** were observed, the *E* : *Z* ratio was constant (1 : 9), with the *Z* isomer formed in favour of the *E* isomer. The isomers were assigned by comparison with authentic samples prepared during previous research.^{15,21}

3.2.3 Conclusion

It was possible to mediate a range of relatively slow 5-*exo trig* and 5-*exo dig* atom transfer radical cyclisations of tertiary and secondary bromoacetamides using Cu(TPA)Br at a reduced catalyst loading of 1 mol% in the presence of AIBN (10 mol%). Compared to the conventional conditions for ATRC (30 mol%), this equates to a 30 fold reduction in the amount of catalyst required to mediate such reactions. It is proposed that AIBN acts to regenerate the activator (Cu(TPA)Br), reducing the potential build up of deactivator (Cu(TPA)Br₂), which is known to hinder ATRC and related reactions (ATRA, ATRP). It was also possible to perform the cyclisation

reactions in the absence of the activator (Cu(TPA)Br), as the AIBN can generate it from the oxidatively stable deactivator (Cu(TPA)Br₂) *in situ*, which allowed the reactions to be carried out under aerobic conditions (AGET-ATRC). The cyclisation of more reactive *N*-tosyl acetamides were mediated at a catalyst loading of 0.1 mol% in the presence of AIBN (10 mol%). This suggests that if the substrate and catalyst reactivity can be adequately tuned, applying the AIBN protocol in conjunction with solid supported catalyst systems, could lead to an industrially attractive ATRC methodology.

4.0 Copper-Mediated Radical Cyclisation in the Presence of Borohydrides

4.1 INTRODUCTION

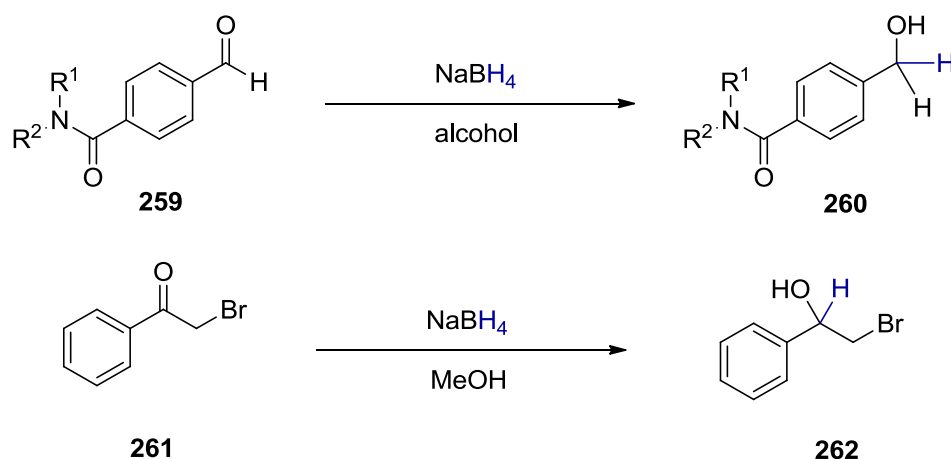
Chapters 1-3 have discussed the origins, and recent developments of radical cyclisation reactions, in particular copper-mediated atom transfer radical cyclisations, and their synthetic utility in the formation of lactone and lactam products, which are prevalent in natural products and synthetic drug candidates. Initially, the high temperatures (50-110 °C) and high catalyst loadings (30 mol%) required to drive these reactions made them industrially unattractive. Chapter 3 discusses how this can be alleviated by the addition of additives, notably AIBN, which allows the catalyst loading to be reduced up to 300 fold for reactive substrates and 30 fold for less reactive substrates.³³ However these cyclisation reactions require temperatures above room temperature (50-110°C), and some are sluggish offering moderate yields after 24 hrs.

The inspiration for the work in this chapter came from literature scrutinised during research for Chapter 3, and from numerous discussions with both the project supervisor and Dr David Fox, a fellow academic within the department. The literature for radical cyclisations, specifically copper-mediated radical cyclisations is sparse concerning the use of additives to reduce catalyst loadings. However, the literature for related ATRP and ATRA offers numerous publications, reviewed in 2008 by Matyjaszewski and Pintauer,⁷³ detailing the use of additives to reduce catalyst loadings for desirable polymerisation and addition reactions. These additives tend to be reductive or anti-oxidant in nature, and their principal role is to

reduce Cu(L)Br_2 , which can build-up under the reaction conditions and in the presence of adventitious oxygen, to the active Cu(L)Br . To our knowledge there is no such evidence for the use of borohydrides of any kind, to facilitate ATRC, ATRA or ATRP.

Herein we report an investigation designed to improve the reaction conditions of copper mediated radical cyclisations, focussing on reducing catalyst loadings further, and the potential to perform reactions under aerobic conditions, making the methodology more industrially amenable.

4.1.1 Classical Borohydride Chemistry¹⁴⁷

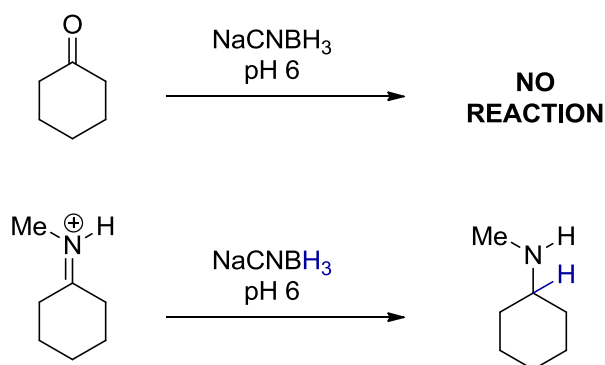


Scheme 4.1: Carbonyl Reductions Using Sodium Borohydride

In classical organic chemistry, the borohydride anion, usually present as a Na^+BH_4^- salt, is used for selective reductions of carbonyl compounds. Borohydrides act as a nucleophilic source of hydrogen reducing aldehydes and ketones selectively *via* a ‘hydride transfer.’ Although there is no detectable hydride ion (H^-) present during the reaction, reduction is achieved by a hydrogen atom and an attached pair of electrons. Reactive carbonyls such as aldehydes and ketones can be reduced to the

corresponding alcohols, whereas less active carbonyls such as esters and amides are inert (Scheme 4.1). A variety of other functional groups are also tolerant to reaction conditions, including nitro groups and, significantly, alkyl halides such as **261**.

The reactivity of borohydrides can be tuned by inclusion of electron-withdrawing anions such as cyano groups to give sodium cyanoborohydride (NaCNBH_3), and acetates to give sodium triacetoxyborohydride ($\text{NaB}(\text{OAc})_3\text{H}$). In both these cases the reactivity of the borohydride is reduced as the electron-withdrawing substituents decrease the ease in which hydrogen, and a pair of electrons, can be transferred. Consequently, at pH 6 unprotonated ketones are not reduced by these reagents, but the analogous reaction of imines, which are protonated and fully polarized at pH 6 is successfully. As a result these reagents find application in a number of reductive amination methods (Scheme 4.2).



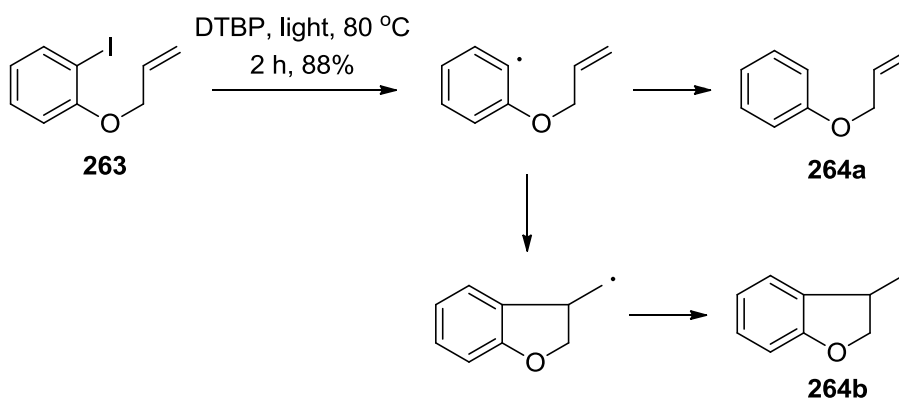
Scheme 4.2: Organic Reductions Using Less Reactive Borohydride Reagents

4.1.2 Radical Reactions Involving Sodium Borohydride

Perhaps a less common, but extremely relevant application of sodium borohydride is its participation in radical chain mechanisms leading to reductive

dehalogenation or radical cyclisation, depending on the nature of the substrates and conditions used.

Having demonstrated that lithium aluminium hydride, in the presence of di-*tert*-butyl peroxide (DTBP)^{148,149} could facilitate reductive dehalogenation of aryl halides, Beckwith investigated the use of sodium borohydride (NaBH₄), which had previously been shown to reduce a variety of alkyl halides in polar aprotic solvents, in such reactions.



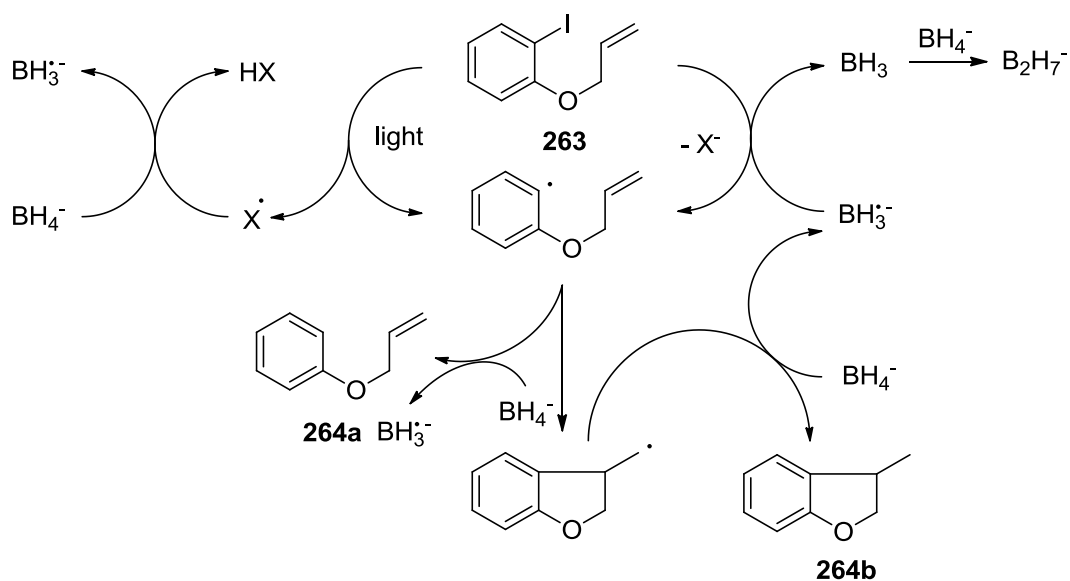
Scheme 4.3: NaBH₄ Mediated Reductive Dehalogenation and Cyclisation

The NaBH₄ mediated process relied on photolytic homolysis of the C(aryl)-X bond, induced by a medium pressure Hg lamp ($\lambda = 254$ nm), and was efficient for a range of aryl iodides and reactive bromides, such as 1-bromonaphthalene.¹⁵⁰ The radical nature of the reaction was confirmed by the diagnostic ring-closure of *o*-allyloxyiodobenzene **263** which was transformed to reduced and cyclised products **264a** and **264b** depending on the reaction conditions (Scheme 4.3).^{150,151,152}

More recently, Liu and Yu were able to selectively produce the cyclic product **264b** from *o*-allyloxyiodobenzene *via* a photo-induced radical cyclisation using NaBH₄.¹⁵³ It was found the inclusion of DTBP was unnecessary if the

substrates were directly excited by UV radiation in the presence of excess NaBH_4 . Efficient 5-*exo trig* and *dig* cyclisations were achieved and a degree of 6-*endo trig* cyclisation was observed from *o*-but-3-enyloxy-halobenzenes substrates. However, due to the slow progress of the 6-*endo* cyclisations competitive dehalogenation was also observed.

Considering NaBH_4 mediated reductive dehalogenation had previously been attributed to a radical chain process,^{154,155} Liu and Yu proposed a similar mechanism for their cyclisation reactions (Scheme 4.4). The mechanism is initiated by UV light (Hg lamp 254 nm) and the key propagating species is thought to be the borane radical anion ($\text{BH}_3^{\cdot-}$).



Scheme 4.4: Proposed Mechanism for NaBH_4 Mediated Radical Cyclisation

4.1.3 Copper Borohydride (CuBH_4)

The chemistry of borohydrides has been widely researched leading to many sophisticated methods of reduction. Of particular interest to the Clark group was

evidence in the literature in which borohydrides were shown to be compatible with copper complexes, in particular those stabilised by nitrogen containing ligands.

Copper(I) borohydride (CuBH_4) was first reported by Wiberg and Henle in 1952¹⁵⁶ as a thermally unstable compound arising from the reaction of ethereal LiBH_4 at $-20\text{ }^\circ\text{C}$ with CuCl suspended in THF. However, as the temperature approached $0\text{ }^\circ\text{C}$ decomposition was observed to copper hydride (CuH) and diborane. This was supported by the work of Klingen who reported the precipitation of thermally unstable CuBH_4 from a mixture of LiBH_4 and CuCl in ether at $-45\text{ }^\circ\text{C}$, supporting his observations with reliable analytic data.¹⁵⁷ The stoichiometries of the reactions between LiBH_4 and CuCl at room temperature and $-45\text{ }^\circ\text{C}$, as determined by Klingen are shown in schemes 4.5 and 4.6.

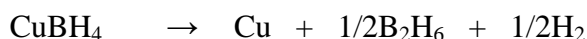


Scheme 4.5



Scheme 4.6

Where decomposition was previously reported at $0\text{ }^\circ\text{C}$, the CuBH_4 prepared by Klingen decomposed at $-12\text{ }^\circ\text{C}$ to give copper(0), diborane and hydrogen as shown in scheme 4.7.



Scheme 4.7

Recently, in order to understand and apply copper borohydrides, thermally stable complexes containing phosphine ligands such as bis(triphenylphosphine)-copper(I) borohydride ((Ph₃P)₂CuBH₄) **265** have been developed (Figure 4.1).¹⁵⁸ This complex is commercially available through Aldrich for the selective reduction of carbonyl compounds.¹⁵⁹ Additionally, it has been reported to form adducts with aldehydes and ketones though the nature of these structures is not clear.¹⁶⁰ Another ligand associated with copper borohydride complexes is the substituted phenanthroline ligand. This closely resembles the complexes of pyridyl and pyridyl-imine ligands with copper(I), used previously for ATRC reactions (chapter 1) and has been used to form a stable CuBH₄ complex **266** (Figure 4.1),¹⁶¹

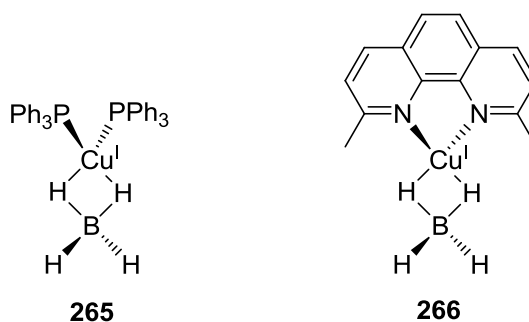


Figure 4.1: Copper Borohydride Stabilised by Phosphine **265** and Phenanthroline **266** Ligands

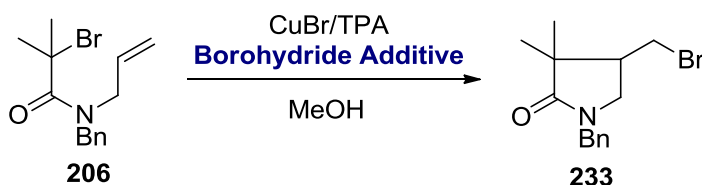
Typically, phosphine complexes of CuBH₄, such as **265** are much more stable than their imine/pyridine counterparts, but given its similarity to ATRC copper complexes, the 2,9-dimethyl-1,10-phenanthroline complex **266** was of particular interest. Research has shown that not only can free and coordinated borohydride act as a versatile reductant, but it can also take part in charge transfer reactions. For example, Volger and co-workers have demonstrated the formation of donor-acceptor adducts between phosphine complex **265** and phenanthroquinone *via* an outer-sphere charge transfer (OSCT).¹⁶² Interestingly, the borohydride

coordinated to this adduct can then reduce the quinone to a hydroquinone *via* charge transfer. Consequently, the same group proposed that the ligand-to-ligand charge transfer from CuBH_4 to the phenanthroline ligand (stabilised by steric hindrance due to the 2,9-dimethyl arrangement) would allow formation of complex **266**. This was the case as indicated by long wavelength absorption at λ_{max} 465 nm which was assigned as the $\text{BH}_4^- \rightarrow$ phenanthroline charge transfer transition.

4.2 RESULTS AND DISCUSSION

4.2.1 The Effect of Borohydride Addition

The reaction chosen to investigate the effects of borohydride addition was the 5-*exo trig* cyclisation of **206** (Scheme 4.8). The monobromide substrate was identical to that used in Chapter 3, and crucially the amide carbonyl would be inert to reduction by the borohydrides used. All conversions were determined by ^1H NMR of the crude reaction mixture, and in instances where only partial conversion was observed, the only other product present in the crude NMR was the starting material.

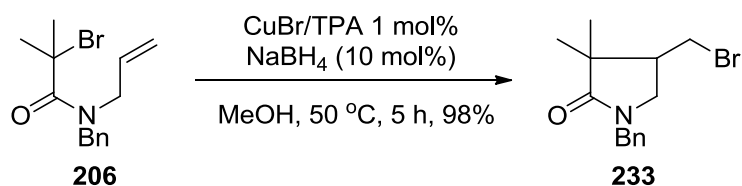


Scheme 4.8: General Reaction Scheme for Investigating the Effect of Borohydride Addition on ATRC in Methanol

In Chapter 3, optimum results for the cyclisation of **206** were observed using AIBN as an additive, in DCM at $50\text{ }^\circ\text{C}$.³³ Immediately it was recognised that, rather

than simply changing a single variable, namely the additive, the insolubility of borohydride salts in DCM enforced a change of solvent too. Selecting an alternative solvent was not a difficult choice. Generally organic reductions using borohydride salts are carried out in methanol or ethanol, and in the literature there are examples of methanol being employed as a solvent for radical polymerisations.¹⁶³ The use of methanol allowed full dissolution of substrate, catalyst and borohydride salt.

The first reaction performed in methanol used sodium borohydride (NaBH₄) as an additive, with the same catalyst, loadings, time and temperature used in Chapter 3. Pleasingly this provided the desired cyclised product **233** in 98% yield in 5 hrs at 50 °C (Scheme 4.9).



Scheme 4.9: Copper Catalysed ATRC in the Presence of Sodium Borohydride

When AIBN was employed as an additive, the primary reason for using elevated temperatures, even for reactive substrates, was to facilitate the decomposition of AIBN into its radical constituents. As this was not necessary for NaBH₄, the reaction shown in scheme 4.7 was repeated at room temperature. To our delight after 1 hour at room temperature, 100% conversion was observed (Table 4.1, entry 1). Additional experiments (Table 4.1) under these conditions ensured that the combination of Cu(TPA)Br and NaBH₄ was in fact having an effect on the reaction, and dispelled any thoughts that NaBH₄ may be catalysing the reaction on its own. This is truly remarkable because previously the *N*-benzyl derivative had required high temperatures to undergo efficient cyclisation in order to obtain the correct

rotamer populations. Consequently, the success of this room temperature reaction may suggest an alternative reaction mechanism, possibly through a CuBH_4 species.



Entry	Time	Temp °C	Solvent	CuBr/TPA	Additive (10 mol%)	Conv	MB
1	1 h	RT	MeOH	1 mol%	NaBH_4	100%	82%
2	1 h	RT	MeOH	1 mol%	-	Trace	90%
3	1 h	RT	MeOH	-	NaBH_4	-	82%

Table 4.1: Establishing NaBH_4 as a Useful Addition for Copper Catalysed ATRC of 206

Under the conditions described above, 100% conversion is observed furnishing **233** in 82% yield (Table 4.1, entry 1). However when the additive or the catalyst was removed only trace amounts of **233** were observed at best (entry 2, 3), confirming the synergistic role of both NaBH_4 and $\text{Cu}(\text{TPA})\text{Br}$.

Having shown that NaBH_4 could mediate this transformation, attention was turned to screening a range of commercially available borohydrides (Table 4.2).

Entry	Time	Temp °C	Solvent	CuBr/ TPA	Additive (10 mol%)	Conv	MB
1	1 h	RT	MeOH	1 mol%	LiBH_4	24%	73%
2	10 min	RT	MeOH	1 mol%	NaBH_4	100%	89%
3	10 min	RT	MeOH	1 mol%	KBH_4	100%	68%
4	10 min	RT	MeOH	1 mol%	$\text{NaB}(\text{OAc})_3\text{H}$	100%	84%

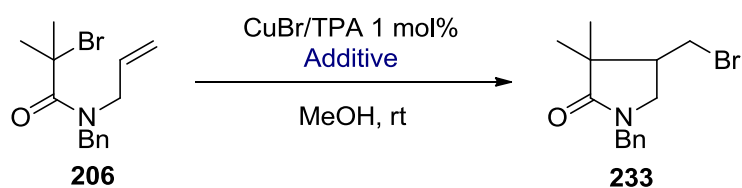
Table 4.2: Effect of Commercially Available Borohydrides on Copper Catalysed ATRC of 206

When the conditions outlined above were used with lithium borohydride (LiBH_4 , Table 4.2, entry 1), only 24% conversion was achieved. When the mass balance was taken into account, a disappointing yield of 18% was the result. With

Chapter 4: Copper-Mediated Radical Cyclisation in the Presence of Borohydrides

sodium borohydride (NaBH₄), potassium borohydride (KBH₄) and sodium triacetoxyborohydride (NaB(OAc)₃H), complete conversion to the cyclised product was achieved within 10 mins (entries 2-4). The general procedure involved dissolving the substrate **206** in dry MeOH at room temperature at a concentration of 0.12 M. When fully dissolved, the desired amount of Cu(TPA)Br as the complex in a solution of MeOH (0.01 M) was added. This produced a faint blue solution, indicative of Cu^{II}. Finally the borohydride was added, and the reaction was allowed to stir at room temperature. Within the time of the reaction (10 min), the colour of the reaction medium changed from blue, to brown (almost immediately upon addition of borohydride), then finally over time changed again to a faint green colour. These colour changes were indicative of the reaction's progress, as once all colour changes ceased the reaction was invariably complete, and in the case of **206** this was always within 10 mins. If the borohydride was added before the catalyst complex, conversions did not always reach 100%.

To distinguish between the reactive borohydrides (entries 2 and 3), the reactions were repeated at lower loadings (Table 4.3).



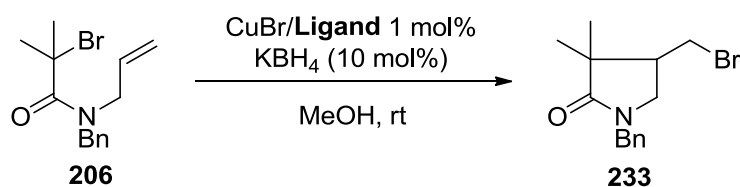
Entry	Time	Additive	Conv	MB
1	10 min	NaBH ₄ (5 mol%)	67%	67%
2	10 min	KBH ₄ (5 mol%)	100%	74%
3	10 min	NaB(OAc) ₃ H (5 mol%)	100%	72%
4	10 min	KBH ₄ (2.5 mol%)	50%	82%
5	10 min	NaB(OAc) ₃ H (2.5 mol%)	-	78%

Table 4.3: Establishing the Most Efficient Borohydride Additive

When the loading was reduced to 5 mol% it became clear that KBH_4 and $\text{NaB(OAc)}_3\text{H}$ were better additives than NaBH_4 . Thus, while KBH_4 and $\text{NaB(OAc)}_3\text{H}$ gave complete conversion to **233** (Table 4.3, entries 1-2), 5 mol% NaBH_4 only provided 67% conversion furnishing **233** in 45% yield (entry 3). Decreasing the loading further to 2.5 mol% led to the conclusion that KBH_4 was the optimum reagent providing a 50% conversion to **233** in 41% yield (entry 4), whereas $\text{NaB(OAc)}_3\text{H}$ gave no conversion at all. Considering this, for all future reactions KBH_4 was the reagent of choice.

4.2.2 The Effects of the Copper Salt and Ligand

As stated in chapter 3 there is a general order of reactivity in ATRC observed for copper complexes formed using different nitrogen-containing ligands, and for 5-*exo* cyclisations the order of reactivity for these ligands is TPA (**42**) > $\text{Me}_6\text{-Tren}$ (**41**) > PMDETA (**40**) > Bipy (**30**).^{21,24,25,32,33} A set of reactions was performed using substrate **206** to determine if this order of reactivity was also observed in the presence of KBH_4 (Table 4.4).



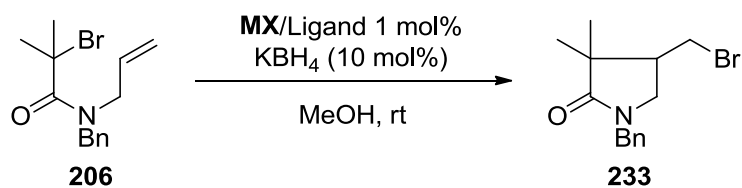
Entry	Ligand	Time	Conv
1	Bipy (30)	10 min	-
2	PMDETA (40)	10 min	-
3	$\text{Me}_6\text{-Tren}$ (41)	10 min	77%
4	TPA (42)	10 min	100%

Table 4.4: The Ligand Reactivity Series as Observed for Copper Catalysed ATRC of **206** in the Presence of KBH_4

Chapter 4: Copper-Mediated Radical Cyclisation in the Presence of Borohydrides

Unsurprisingly, the efficiencies of the complexes formed mirrored those reported previously, and under these reaction conditions, for this substrate, it was ascertained that TPA > Me₆-Tren > PMDETA > Bipy. Consequently, TPA was the ligand of choice for all future reactions, along with KBH₄ chosen as the reagent of choice. The final variable that would require investigation was the identity of the copper salt. Up to this point all reactions had been carried out using CuBr, but a number of copper salts and other transition metal salts, were identified as potential alternative sources of catalyst.

To identify whether any of the alternative sources of catalyst were more efficient than CuBr, all other variables, including time and temperature were kept constant. Initially a range of transition metal salts were investigated (Table 4.5).

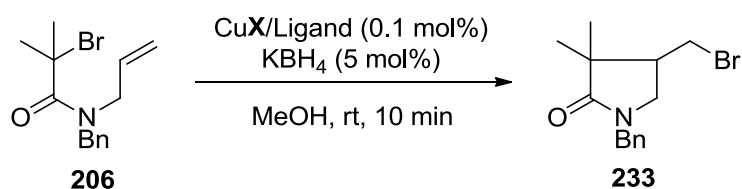


Entry	Time	MX	Conv
1	10 min	CuBr	100%
2	10 min	CuBr ₂	100%
3	10 min	FeBr ₂	-
4	10 min	NiBr ₂ .H ₂ O	5%
5	10 min	CrBr ₃ .6H ₂ O	-
6	10 min	AgBr	7%
7	10 min	CoBr ₂ .H ₂ O	7%

Table 4.5: The Effect of Alternative Transition Metal Salts

Complete conversion was observed with CuBr, and CuBr₂ (Table 4.5, entries 1-2), however, when the investigation was extended into the d-block, results were less impressive. Complexes formed containing Fe(II) (entry 3) and Cr(III) (entry 5) gave no conversion at all. A degree of conversion was observed, however, for

complexes containing Ni(II) (entry 4), Ag(I) (entry 6) and Co(II) (entry 7), but unfortunately yields were low, 5-7%. Consequently the decision was made to persist with copper catalysts, and in order to optimise the reaction conditions a number of different Cu(I) and Cu(II) salts were investigated. To compare the degree of conversion for each copper salt the catalyst loading was further reduced to 0.1 mol%, and the KBH_4 loading was reduced to 5 mol%, under the assumption the conversions would not reach 100%. The results are displayed in Table 4.6.



Entry	X	Conv	MB
1	Br	23%	94%
2	Br ₂	Trace	89%
3	OAc	16%	79%
4	(OAc) ₂ ·H ₂ O	16%	88%
5	OC(O)CF ₃ ·H ₂ O	Trace	92%
6	(acac) ₂	100%	83%
7	(trifluoro acac) ₂	43%	76%
8	(OTf) ₂	100%	85%
9	OTf	92%	90%
10	(OCC(CH ₃) ₃ CHCOCF ₂ CF ₂ CF ₃) ₂	100%	97%
11	SO ₄ ·5H ₂ O	100%	97%
12	(ClO ₄) ₂ ·6H ₂ O	100%	85%
13	(NO ₃) ₂ ·H ₂ O	32%	85%

Table 4.6: An Investigation into the Effect of Copper Salt

Initially, reducing the catalyst and KBH_4 loading revealed that CuBr , was a better source of catalyst than CuBr_2 (Table 4.6, entries 1-2), providing 23% conversion to **233** in 22% yield. This result was also better than those observed for the acetate salts of copper, which gave only between 1-14% yields (entry 3-5). The other Cu(II) salts investigated offered significantly improved results. Even at the

Chapter 4: Copper-Mediated Radical Cyclisation in the Presence of Borohydrides

reduced loadings of catalyst (0.1 mol%) and KBH_4 (5 mol%), in a number of cases 100% conversion was observed (entries 6, 8, 10-12) with excellent yields (83-97%). In order to distinguish between the reactivity of these copper salts the loading of catalyst (0.05 mol%) and KBH_4 (2.5 mol%) was reduced further (Table 4.7).

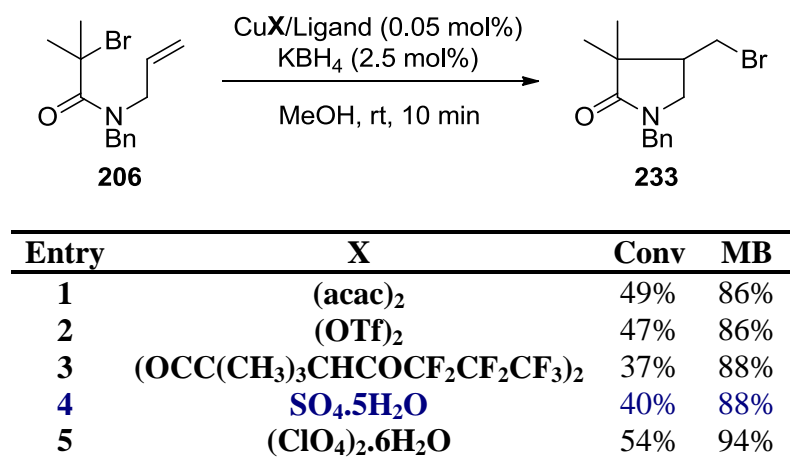


Table 4.7: Investigating the Effect of Copper Salt

Even at these considerably lower loadings, conversions between 37-54% were observed in 10 mins at RT, and yields also ranged between 33-50%. The most satisfying result of this investigation was achieved using CuSO_4 (Table 4.7, entry 4). Although the overall conversion and yield in this instance was not the highest, when considering the cost $\text{CuSO}_4 \cdot 5\text{H}_2\text{O}$, which can be bought on the kilo scale for £20-30, possible scale up of this reaction would be attractive, certainly cost-wise, in industry. Consequently for the remaining attempted cyclisations, CuSO_4 was selected as the copper salt of choice.

4.2.3 UV Experiments

In all the experiments discussed in this section, the colour change alluded to in section 4.2.1., was observed. When alternative copper salts and ligands were used the colour and/or the intensity was variable, but the standard blue, brown, green shift was observed within the reaction time. Accordingly, a number of reactions were followed by UV-*vis* spectroscopy in the hope of gaining an insight into the mechanism and identity of the species involved. Firstly CuBr, CuBr₂ and CuSO₄ were all dissolved in methanol and their absorbance was measured (Figure 4.2)

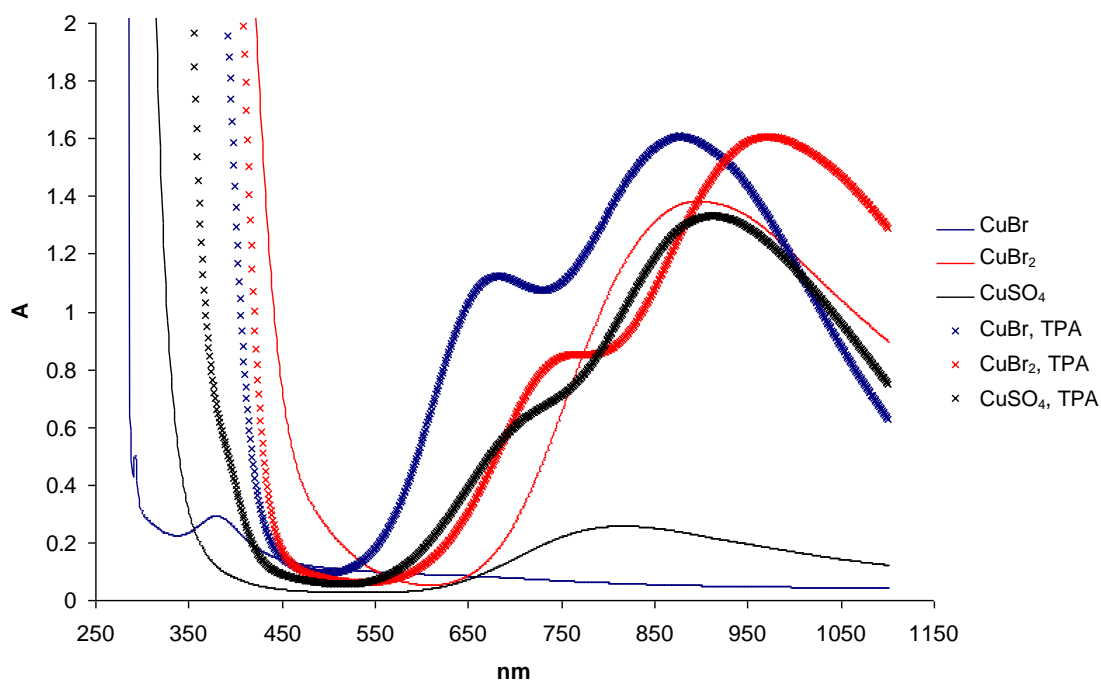


Figure 4.2: UV Traces of Selected Copper Salts and Complexes

Then TPA was added (Figure 4.2) to determine the effect of complex formation. A characteristic absorbance for Cu^{II}(TPA)X was observed at 900-950 nm for all three copper sources.^{163, 164} Cu(TPA)Br is known to undergo

disproportionation forming Cu(0) metal and Cu(TPA)Br₂ in polar solvents such as methanol and DMSO, and this is what is observed in this case.^{165,166,167} In polymer chemistry this dissociation mechanism leads to reaction *via* a single electron transfer living radical polymerisation (SET-LRP) where the actual catalytic species is Cu(0).¹⁶⁸ Thus, this potential alternative mechanism involving a Cu(0) species initiating the cyclisation reaction with CuBr/TPA in methanol is possible. However, under these reaction conditions (Cu(TPA)Br 1.0 mol%) only trace amounts of conversion of **206** to **233** were observed in the absence of KBH₄. As a result the effect of KBH₄ addition was examined for one of the copper salts, namely Cu(TPA)SO₄ (Figure 4.3).

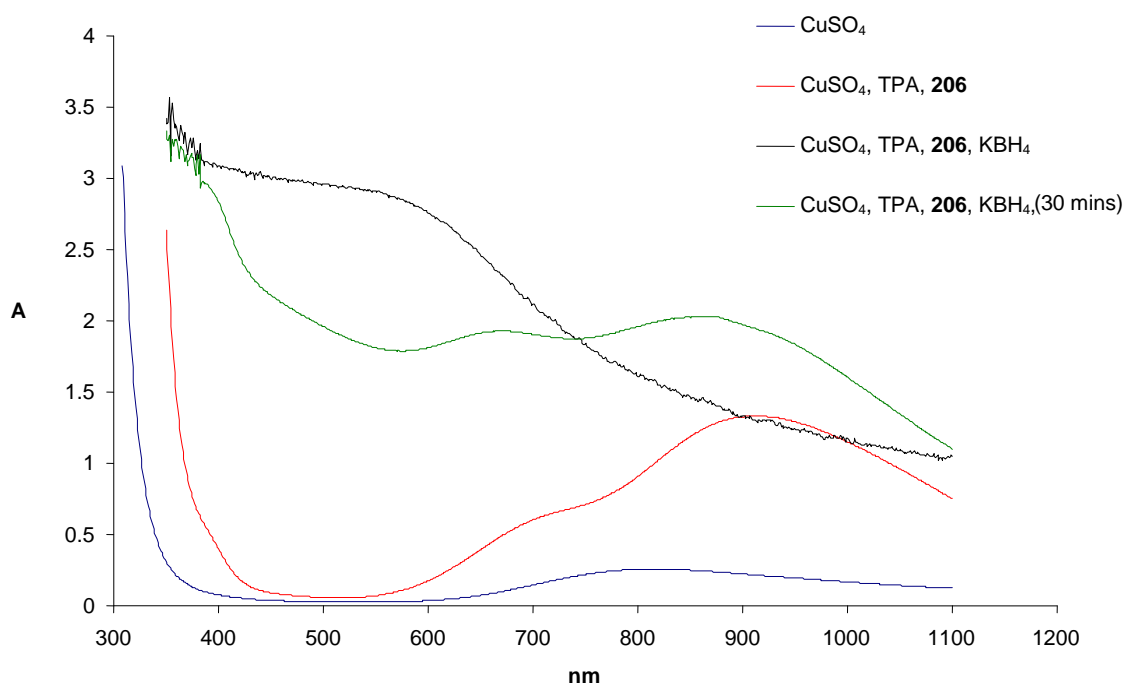


Figure 4.3: UV Traces Following the Progress of the Reaction

Addition of KBH₄ to the reaction mixture had a profound effect on the absorption profile. The characteristic Cu^{II}(TPA)X absorbance between 900-950 nm was replaced by an absorbance at approximately 450 nm. However, after 30 mins

the $\text{Cu}^{\text{II}}(\text{TPA})\text{X}$ peak was seen to return. In order to monitor the change in absorbance for the reaction, against time, a second sample was prepared containing $\text{Cu}(\text{TPA})\text{SO}_4$ and substrate, and the effect of KBH_4 addition was monitored at 2.5 minute intervals (Figure 4.4).

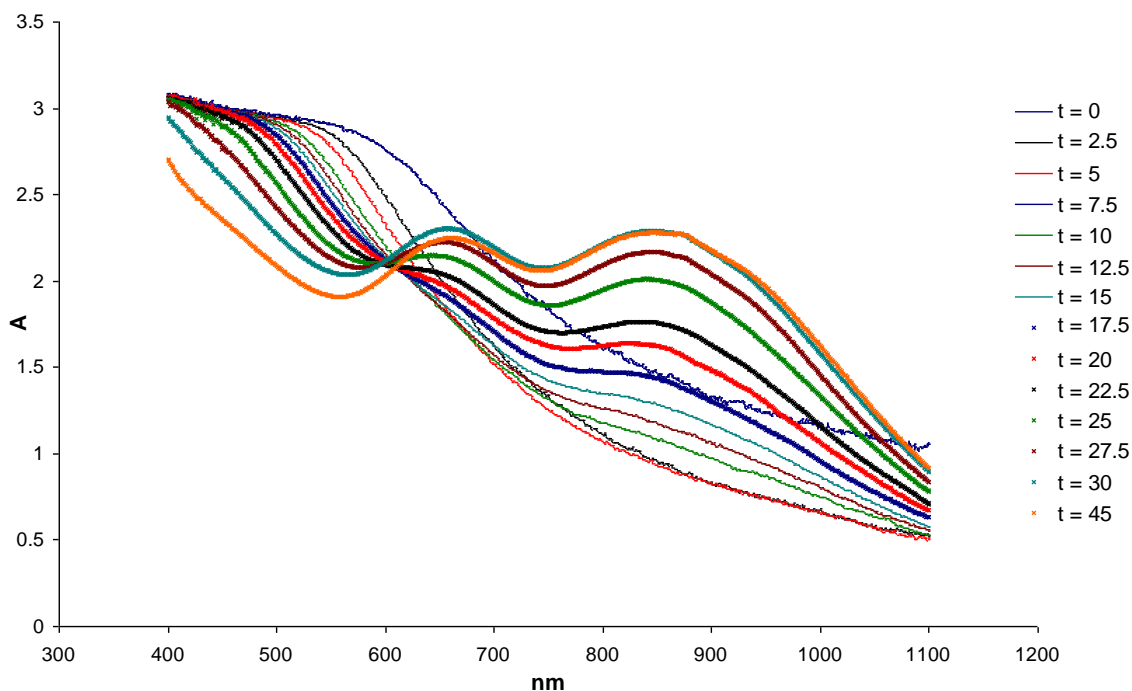


Figure 4.4: UV Traces Tracking the Progress of CuSO_4 Mediated ATRC

As seen in figure 4.3, the scan at $t = 0$ lacked an absorbance peak at 900-950 nm, (indicative of $\text{Cu}^{\text{II}}(\text{TPA})\text{X}$) but contained the alternative peak, reaching maximum at approximately 450 nm. This absorbance profile was consistent up to 10 minutes after which time the $\text{Cu}^{\text{II}}(\text{TPA})\text{X}$ peak began to return and the peak at 450 nm was found to gradually decrease. The scans between 10-45 minutes show an increase in absorbance at 900 nm, providing evidence for the accumulation of $\text{Cu}^{\text{II}}(\text{TPA})\text{X}$, and further decrease in the 450 nm absorbance.

As previously alluded to (section 4.1.3) Kunkely and Volger^{161,162} have been able to prepare CuBH₄ complexes stabilised by phosphine **265** and phenanthroline **266** ligands (Figure 4.5), and through UV-*vis* spectroscopy identify charge transfer processes between coordinated ligands. Significantly, one of these processes was a ligand-to-ligand charge transfer (LLCT) between coordinated borohydride and phenanthroline ligands in complex **266**. This process gave a UV absorbance at λ_{max} 465 nm, which is not too dissimilar to the absorbance we observed when tracing our reaction (~ 450 nm). Given the structural similarities of the ligands (phenanthroline **267**, TPA **53**, Figure 4.5) it would not be unreasonable to tentatively assign the observed absorbance to a borohydride-TPA ligand-to-ligand charge transfer. For the conversion of **206** to **233** it was observed that the reaction was complete within 10 minutes. Consequently from figure 4.3 the catalytic species that is involved in this process is predicted to be that responsible for the absorbance at ~ 450 nm, which is not a Cu^{II}(TPA)X species, but could in fact be a CuBH₄ complex, proceeding *via* an as yet unknown mechanism.

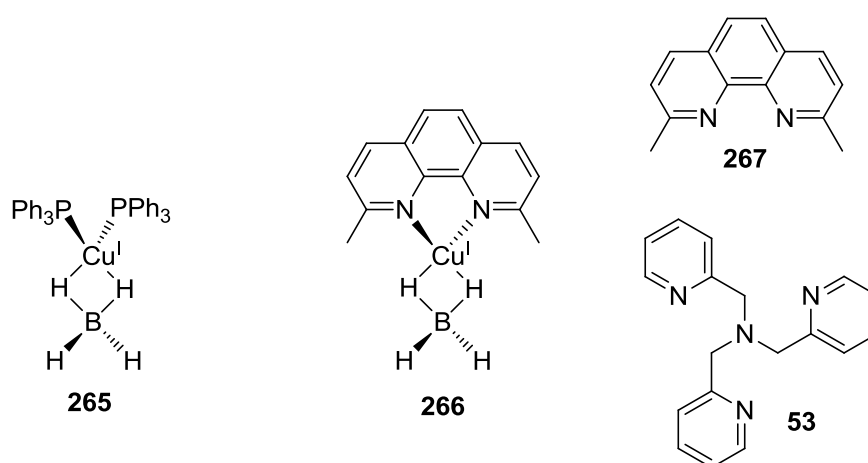


Figure 4.5: Known Borohydride Complexes and Nitrogen Containing Ligands Phenanthroline **267** and TPA **53**

To investigate the catalytic species in the absence of substrate a second time experiment was performed (Figure 4.6). As predicted, upon addition of KBH_4 , at $t = 0$ there is no evidence of $\text{Cu}^{\text{II}}(\text{TPA})\text{X}$ species and the peak at ~ 450 nm prevails. Over time, as observed previously, this peak diminishes and the $\text{Cu}^{\text{II}}(\text{TPA})\text{X}$ absorbance at 900 nm returns. This suggested that the catalytic species itself is highly reactive as even in the absence of substrate its lifetime suggested by UV-*vis* is of the order of minutes.

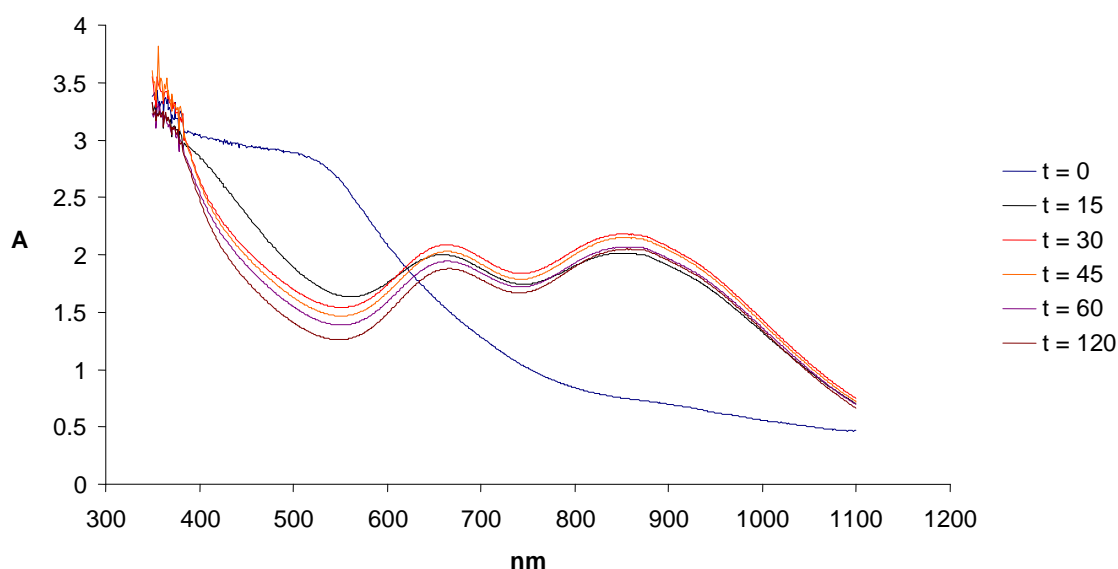
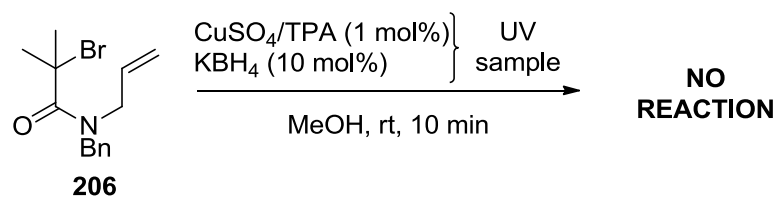


Figure 4.6: UV Traces in the Absence of Substrate

This observation was supported by the result of an attempted cyclisation of **206** using the aged UV sample ($t = 45$ min) as the source of catalyst. Hence, reaction of **206** with the aged UV sample provided no reaction with only starting material being recovered (Scheme 4.10).



Scheme 4.10: Attempted Cyclisation of 206 Using an Aged Catalyst Solution

4.3 SCOPE AND LIMITATION of Cu(TPA)SO₄/KBH₄ MEDIATED CYCLISATION

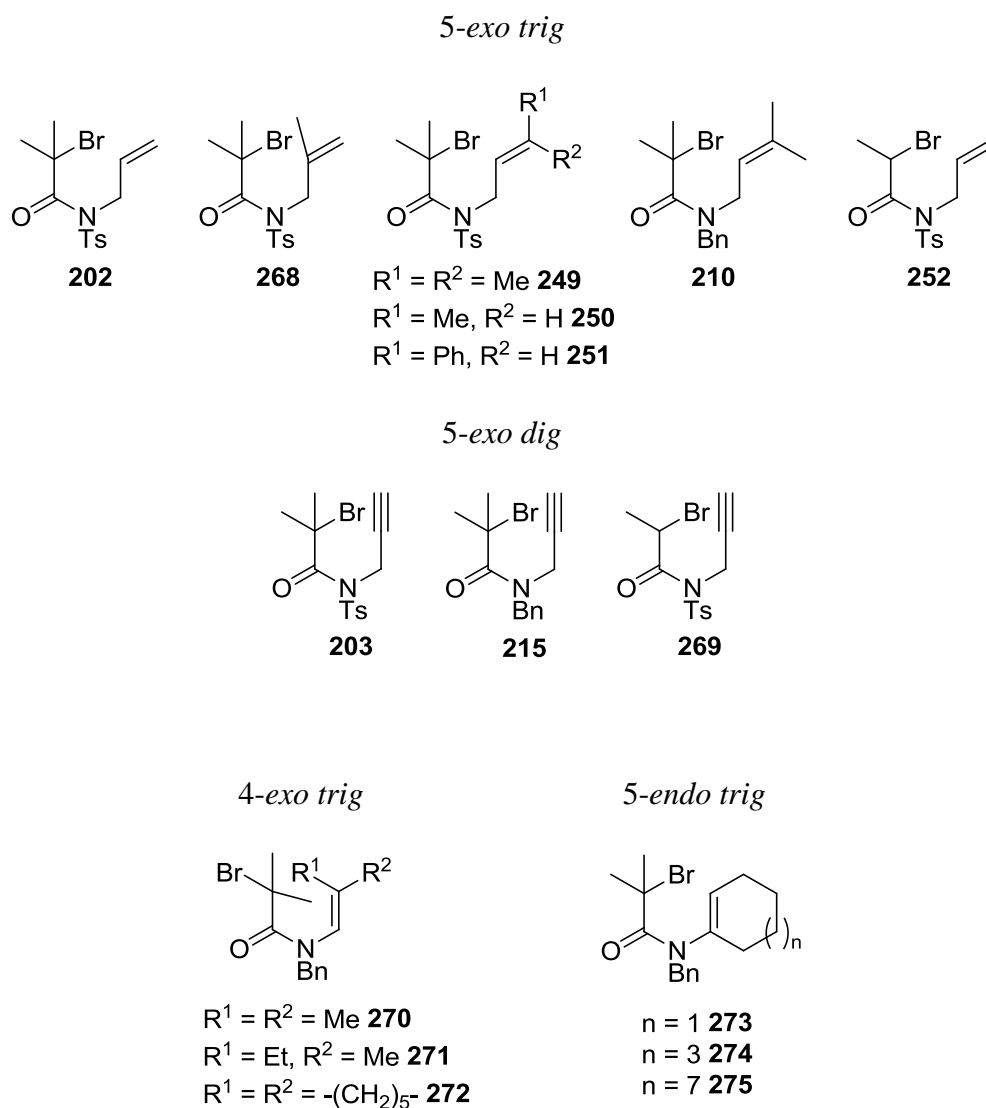
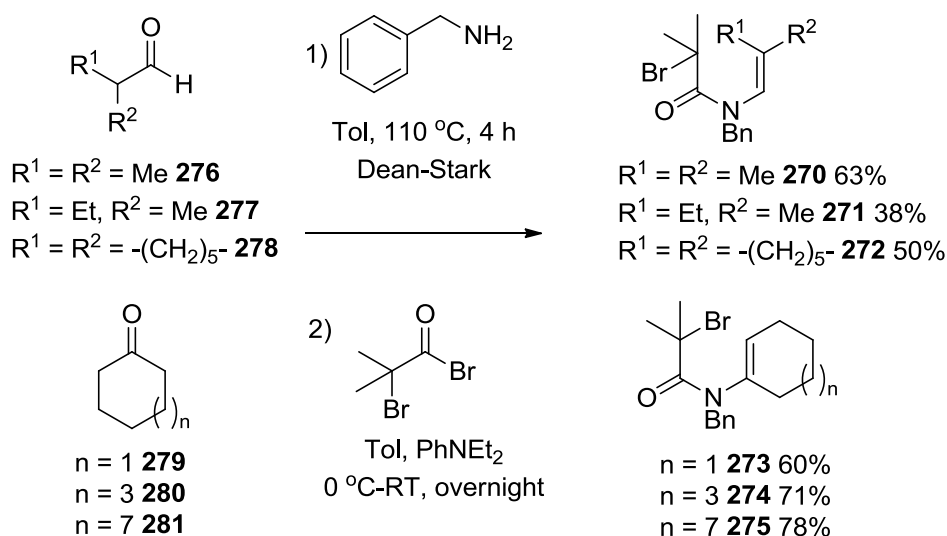


Figure 4.7: Substrates Selected to Investigate the Scope of Copper Catalysed ATRC in the Presence of KBH₄

Having determined model conditions for the conversion **206** to **233** in methanol (Cu(TPA)SO₄, 0.1 mol %, KBH₄ 10 mol %), the scope of the cyclisation methodology was investigated. A number of *5-exo trig* and *dig* substrates were investigated for comparison with previously reported methods, and more recent methods reported in chapter 3.³³ In addition, *4-exo* and *5-endo trig* cyclisations, which are ‘disfavoured’, were investigated to determine if the scope of the reaction could extend to more difficult cyclisations.

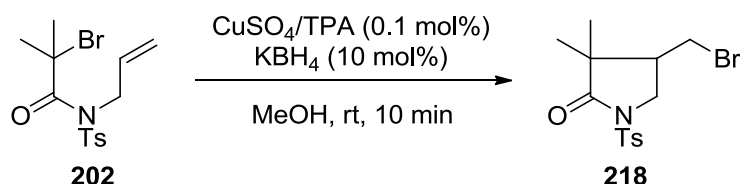
The synthesis of *5-exo trig* and *dig* substrates was discussed in chapters 2 and 3. However, the *4-exo* **270-272** and *5-endo* **273-275** substrates were prepared differently. They were prepared by acetylating the corresponding imines, prepared *in situ*, from the corresponding aldehydes (**276-278**) and ketones (**279-281**) (Scheme 4.11).



Scheme 4.11: Preparation of 4-Exo and 5-Endo Trig Radical Cyclisation

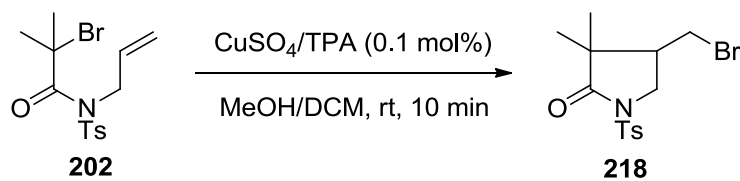
4.3.1 5-Exo trig AGET-ATRC

Initially the cyclisation of tertiary bromide **202** with Cu(TPA)SO₄ (0.1 mol%) and KBH₄ (10 mol%) was attempted.



Scheme 4.12: Copper Mediated 5-Exo Trig ATRC of Activated *N*-Tosyl Acetamide **202**

Under these conditions conversions were much lower than anticipated (33%) considering the results obtained in chapter 3, where the *N*-tosyl substrates were shown to be more reactive than their *N*-benzyl counterparts. It was observed that **202** was only sparingly soluble in methanol, which could have caused the conversion rates and yields to decrease. Two solutions were identified to overcome this problem. While the sulfonamide was found to be soluble in methanol at elevated temperatures, this had previously been avoided, so alternatively a few drops of DCM were added as a co-solvent to assist dissolution of **202** (Table 4.8).



Entry	Time	KBH ₄	Conv	MB
1	10 min	10 mol%	33%	84%
2	10 min	20 mol%	57%	87%
3	10 min	50 mol%	94%	79%
4	10 min	100 mol%	100%	90%

Table 4.8: Effect of Increasing KBH₄ Loading on the Conversion of **202** to **218**

Addition of DCM as a co-solvent did result in full dissolution of **202** but had little effect on the conversion when 10 mol% KBH_4 was used (Table 4.8, entry 1). Consequently, rather than increasing the catalyst loading (0.1 mol%), the amount of KBH_4 was gradually increased. At 20 mol% the conversion was still disappointing (54%, 50 % yield), so the loading was increased further to 50 mol%. Conversions were more acceptable at this loading (94%, 74% yield) but it was not until the loading was increased to 100 mol% (1 equivalent) that complete conversion (100%, 90% yield) was obtained on a reliable, reproducible basis.

For the remaining sulfonamide substrates 1 equivalent of KBH_4 was used along with $\text{Cu}(\text{TPA})\text{SO}_4$ (0.1 mol%) in methanol, spiked with a few drops of DCM (Table 4.9).



Entry	Substrate	Time	CuSO_4/TPA	R^1	R^2	R^3	R^4	Conv	MB
1	268	10 min	0.1 mol%	Ts	Me	H	H	100%	84% ^a
2	249	10 min	0.1 mol%	Ts	H	Me	Me	100%	76%
3	250	10 min	0.1 mol%	Ts	H	Me	H	100% ^b	90%
4	251	10 min	0.1 mol%	Ts	H	Ph	H	100% ^c	81%
5	210	20 min	1.0 mol%	Bn	H	Me	Me	100% ^d	72%

^a Cyclised product **282** was isolated in 80% yield.

^b 3.8 : 1.0 mixture of diastereomers.

^c 5.0 : 1.0 mixture of diastereomers.

^d Isolated as a 10 : 1 mixture of **256a** : **256b**, in a combined yield of 98%.

Table 4.9: CuSO_4 Mediated 5-Exo Trig ATRC

In the case of substrates **249-251** (Table 4.9, entries 2-4) only the 5-*exo trig* cyclised products were produced. However, for substrate **268**, 4% of non-cyclised compounds were also produced. Although not fully characterised (due to the

inability to isolate compounds during chromatography), tentative structures were assigned as **283a** and **283b**.

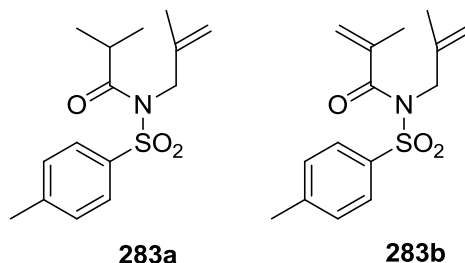


Figure 4.8: Minor Products Obtained From the Cyclisation of **268** as Identified by ^1H NMR

Evidence for these structures was seen in the crude NMR. A septet (1H) at δ 2.98 ppm, coupling to doublet (6H) at δ 1.02 ppm was indicative of **283a** whilst additional terminal alkene protons at δ 5.27 ppm and δ 5.15 ppm coupling to an additional methyl group at δ 1.91 ppm indicated the presence of the eliminated product compound **283b**.

Substrates **250** and **251** underwent complete conversion to the cyclised products **254** and **255** in 90% and 81% yield respectively. Cyclic product **254** was isolated as a 3.8 : 1.0 mixture of diastereomers, whilst **255** was isolated as a 5.0 : 1.0 mixture. In previous work, using AIBN mediation (chapter 3), **254** and **255** were isolated as 3.5 : 1.0 and 6.0 : 1.0 mixtures of diastereomers respectively.³³

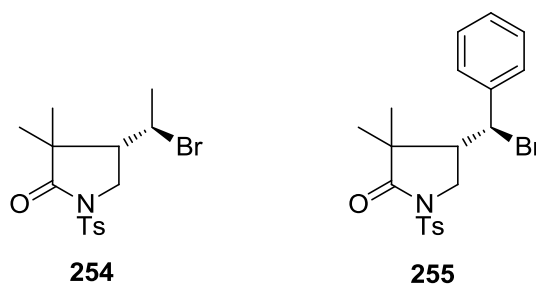


Figure 4.9: Products of CuSO_4 Mediated 5-*Exo Trig* ATRC of Crotyl **250** and Cinnamyl **251** Substrates

For reactions involving AIBN mediation (chapter 3), substrate **210** (entry 6) required significantly longer reaction times and temperatures (24 h, 110 °C) than its sulfonamide counterparts to achieve comparable yields. Thus, the reaction of **210** using Cu(TPA)SO₄ (0.1 mol%) and KBH₄ (10 mol%) produced only a trace amount of cyclisation. However, when the catalyst loading was comparable to those used in chapter 3 (1.0 mol%), in the presence of 1 equivalent KBH₄, complete conversion was achieved within 20 minutes at room temperature to give a 15 : 14 : 1 mixture of atom transfer product **284** and alkene regioisomers **256a/b** in a combined yield of 98% (Figure 4.10). Purification by column chromatography led to the elimination of HBr from the tertiary bromide **284**, and a subsequent 10 : 1 mixture of alkene regioisomers **256a/b** was isolated. The ratio of alkene regioisomers obtained was significantly different to that reported when AIBN was used in chapter 3 (1 : 2).

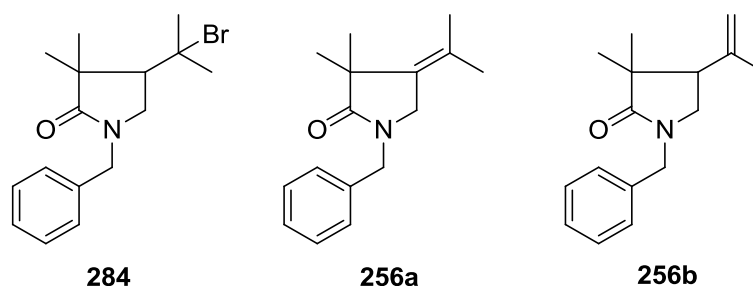
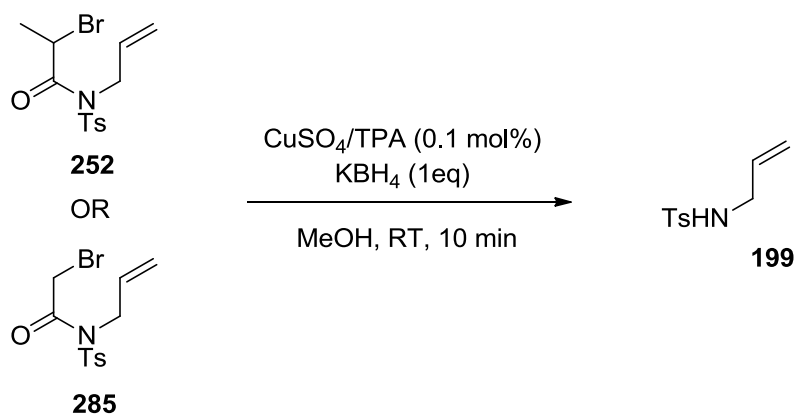


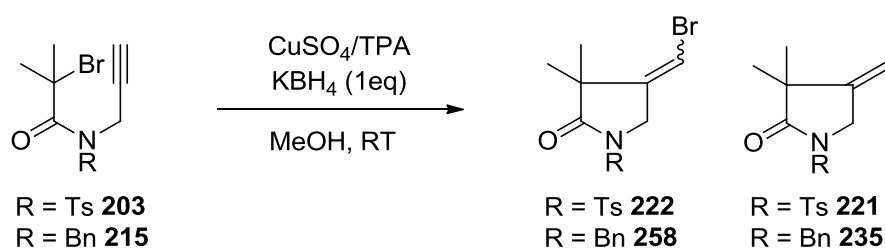
Figure 4.10: Atom-Transfer and Subsequent Elimination Products Formed Under the Reaction Conditions

Unfortunately, when more challenging *5-exo trig* cyclisations of secondary and primary bromides were attempted under these conditions only hydrolysed or reduced products were obtained. The rates of these cyclisations are slower than those of tertiary bromides, and this allows unwanted side reactions, potentially hydrolysis or reduction of the sulfonamides to produce **199** (Scheme 4.13).

Scheme 4.13: Failed Attempted Cyclisations of Secondary **252** and Primary **285** Bromides

4.3.2 5-Exo dig AGET-ATRC

In chapter 3, 5-*exo dig* cyclisations onto alkynes were more difficult to mediate than related 5-*exo trig* cyclisations. For this investigation, initial attempts at the cyclisation of substrates **203** and **215** employed $\text{Cu}(\text{TPA})\text{SO}_4$ (0.1 mol%) and KBH_4 (1 equivalent) in methanol (Table 4.10).



Entry	Substrate	Time	CuSO_4/TPA	R	Ratio	Conv	MB
1	203	10 min	0.1 mol%	Ts ^a	1.0 : 2.8 (222 : 221)	100%	70% ^b
2	215	10 min	1.0 mol%	Bn	1 : 2 (258 : 235)	100%	67% ^c

^a A few drops of DCM were added to help dissolve the sulphonamide fully.

^b Yield of **222**, 18% (as a 1 : 12 mixture of *E*:*Z* isomers). Yield of **221**, 66%.

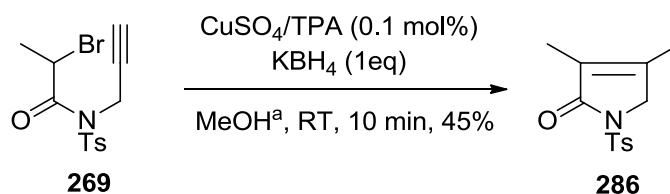
^c Yield of **258**, 22% (as a 8 : 1 mixture of *E*:*Z* isomers). Yield of **235**, 61%.

Table 4.10: CuSO_4 Mediated 5-*Exo Dig* ATRC in the Presence of KBH_4

Complete conversion of the sulfonamide substrate **203** (Table 4.10, entry 1) was afforded in 10 minutes at room temperature using 0.1 mol% catalyst and 1 equivalent KBH_4 to give a 1.0 : 2.8 ratio of **222** and **221**, with **222** obtained as a 1 : 12 mixture of *E* : *Z* regioisomers, in a combined yield 84%. Alkyne **215** required a greater catalyst loading to observe comparable conversions (entry 2). Using $\text{Cu}(\text{TPA})\text{SO}_4$ (1.0 mol%) and KBH_4 a 1 : 2 ratio of **258** and **235** was obtained, with **258** isolated as a 8 : 1 mixture of *E* : *Z* regioisomers, in 83% total yield.

The ratio of atom transfer to reduced products has been shown to be solvent- and ligand-dependent (Chapter 1), and in the presence of methanol a higher proportion of the reduced products (**221** and **235**) was obtained. These results present a significant improvement in the efficiency of 5-*exo dig* cyclisation even compared to the results presented in chapter 3. Conversions comparable to those of 5-*exo trig* cyclisations are possible without the need for more severe reaction conditions.

Despite the lack of success in attempting to perform a 5-*exo trig* cyclisation using a secondary bromide, partial success was observed for the secondary bromide **269** undergoing 5-*exo dig* cyclisation to give **286** in 45% yield (Scheme 4.14).



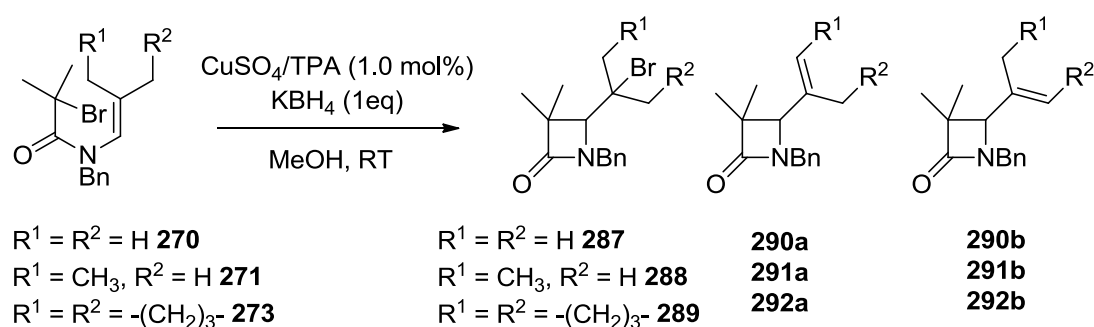
^a A few drops of DCM were added to help dissolve the sulphonamide fully.

Scheme 4.14: CuSO_4 Mediated 5-*Exo Dig* ATRC of Secondary Bromide **269**

4.3.3 4-Exo trig AGET-ATRC

The 4-*exo trig* substrates were examined to determine whether the Cu(TPA)SO₄/KBH₄ procedure could be applied to β -lactam synthesis. Previously, efficient synthesis of β -lactams was achieved using catalytic CuBr (30 mol%) and TPA (**53**) (30 mol%) at room temperature in 1 hr.³⁵ Using the new conditions, the aim was achieve comparable results with a 30-fold reduction in catalyst (1.0 mol% Cu(TPA)SO₄) within 10 minutes.

Examination of the crude NMR spectra obtained during this investigation indicated the atom-transfer products **287-289** were the major products for all 3 substrates **270-272**. However, during chromatography elimination of HBr from the tertiary bromide functional groups partially occurred, which led to the isolation of alkene regioisomers **290a/b-291a/b** in addition to the atom transfer products **287-289** (Table 4.11).



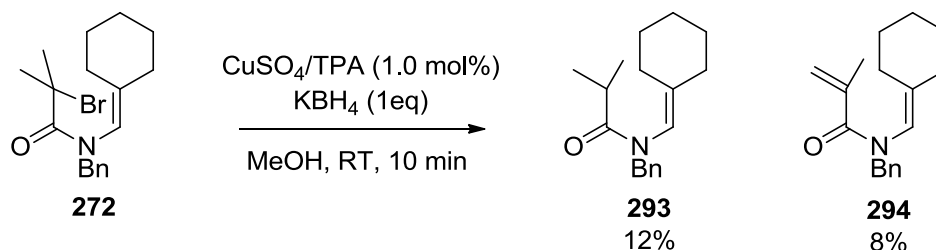
Entry	Substrate	Time	R ¹	R ²	Ratio ^a	Conv	Yield
1	270	10 min	H	H	3 : 1 : 0 (287 : 290a : 290b)	100%	81%
2	271	10 min	CH ₃	H	1.7 : 3.7 : 1.0 (288 : 291a : 291b)	100%	89%
3	272	10 min	-(CH ₂) ₃ -	-(CH ₂) ₃ -	1 : 1 : 0 (289 : 292a : 292b)	100%	80% ^b

^a Ratio for cyclised products after purification.

^b Compounds **293** and **294** were also isolated in 12% and 8% yields respectively.

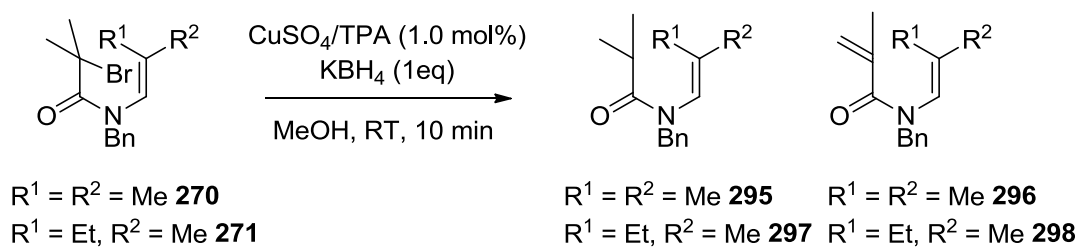
Table 4.11: CuSO₄ Mediated 4-Exo Trig ATRC in the Presence of KBH₄

Reaction of **272** proceeded to give two further, isolable, compounds formed from direct reduction of **272** to give **293**, and elimination of HBr from **272** to give **294**, in 12% and 8% yield respectively (Scheme 4.15).



Scheme 4.15: Minor Byproducts Obtained From the Cyclisation of 272 as Identified by ¹H NMR

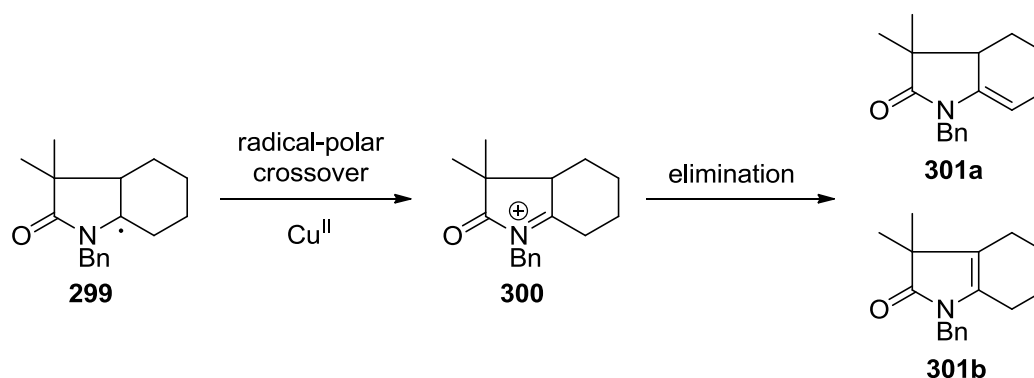
The yields obtained for substrates **270** and **271** were comparable. Substrate **270** provided a 3.0 : 1.0 ratio in favour of the atom transfer product, with a total yield of 81% (Table 4.11, entry 1) whereas **271** gave a 1.7 : 3.7 : 1.0 ratio in favour of the alkene regioisomers, with a total yield of 89% (entry 2). The atom transfer product **288** was obtained as a 3.0 : 1.0 mixture of diastereomers, and the major alkene regioisomer was the internal alkene **291a** which was obtained as a 3.0 : 1.0 mixture of *E* and *Z* isomers. Again, the reactions of **270** and **271** proceeded to give two further compounds (Scheme 4.16). Although it was not possible to purify these minor components, they were tentatively assigned as **295-298** from crude NMR. Evidence for **295** and **297** was present in the form of enamide protons at δ 5.72 and 5.81 ppm respectively, along with septets at δ 2.76 and 2.78 ppm respectively. Eliminated substrates **296** and **298** also displayed enamide protons at δ 5.69 (**296**) and 5.68 ppm (**298**), as well as terminal alkene protons at δ 5.18 (**296**) and 5.15 ppm (**298**).



Scheme 4.16: Minor Byproducts Obtained From the Cyclisation of 270 and 271 as Identified by ^1H NMR

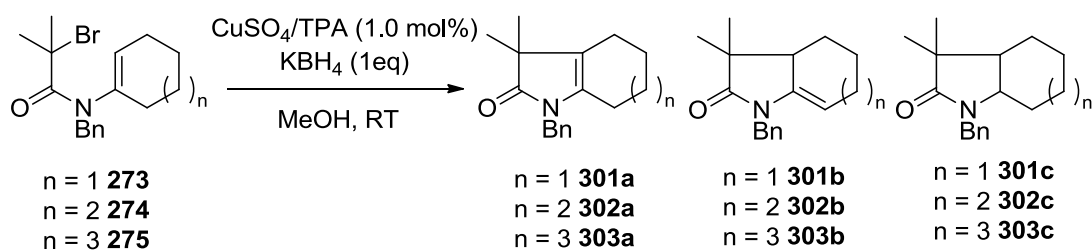
4.3.4 5-Endo trig Radical Cyclisations

Having shown it was possible to mediate 4-*exo trig* cyclisation, the 5-*endo trig* cyclisations of **273-275** were investigated. As discussed previously, the mechanism of CuBr/TPA mediated 5-*endo* radical cyclisation of enamides differs to that of the related 5-*exo* ATRC, proceeding through a radical-polar crossover mechanism *via* an *N*-acyliminium ion **300** (Scheme 4.17).²⁵



Scheme 4.17: Pathway to the Alkene Regioisomeric Products Obtained From 5-Endo Trig Radical Cyclisation

This *N*-acyliminium ion (**300**) can undergo elimination of a proton to furnish two alkene regioisomers **301a/b**. Using Cu(TPA)SO₄ (1.0 mol%) and KBH₄ (1.0 equivalent) in methanol, further evidence for the intermediacy of an *N*-acyliminium ion was investigated under these reductive conditions (Table 4.12).



Substrate	Time	n	Ratio	Conv	Yield
273	30 min	1	2 : 4 : 1 ^a	100%	83%
			a : b : c		
274	30 min	3	1 : 12 : 2 ^b	100%	86%
			a : b : c		
275	30 min	7	0 : 1 : 0 ^c	100%	55%
			a : b : c		

^a Corresponding yields are 24%:47%:12%.

^b Corresponding yields are 6%:69%:11%.

^c Only trace, unisolable amounts of **303a** and **303c** observed in crude NMR.

Table 4.12: CuSO₄ Mediated 5-Endo Trig Radical Cyclisation in the Presence of KBH₄

The reaction of substrate **275** yielded only cyclised product **303b** in 55%. However, reaction of **273** and **274** with Cu(TPA)SO₄ (1.0 mol%) and KBH₄ (1.0 equivalent) led not only to the alkene regioisomers (**301/302 a** and **b**), but also to reduced products (**301c/302c**). Due to the presence of an equivalent of KBH₄ in the reaction mixture it is likely that the *N*-acyliminium ion intermediates (**300**) were reduced to furnish these products. It was a surprise that, due to the reaction conditions and nucleophilic nature of the solvent (methanol), compound **304** was not isolated.^{169,170}

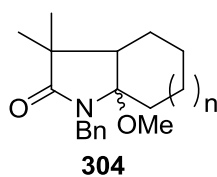


Figure 4.11: Product Anticipated From 5-Endo trig Radical Cyclisation Followed by Nucleophilic Substitution

4.3.5 Tetralone Enamides

At this point it was decided to investigate the cyclisations of two tetralone enamides **305** and **306**. These were synthesised using the method outlined in section 4.3 from α -tetralone and β -tetralone in 58% and 84% yield respectively.

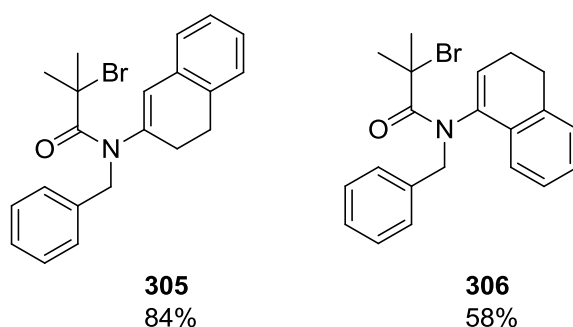
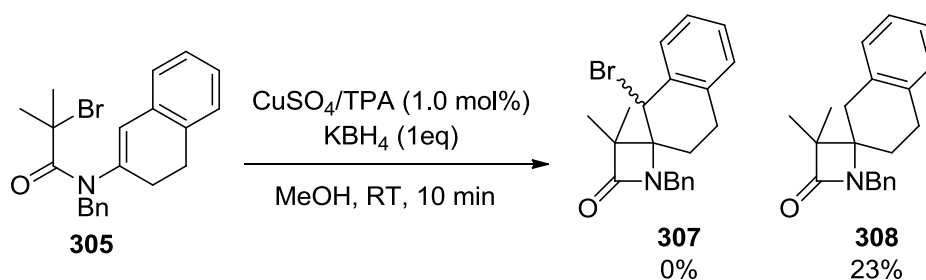
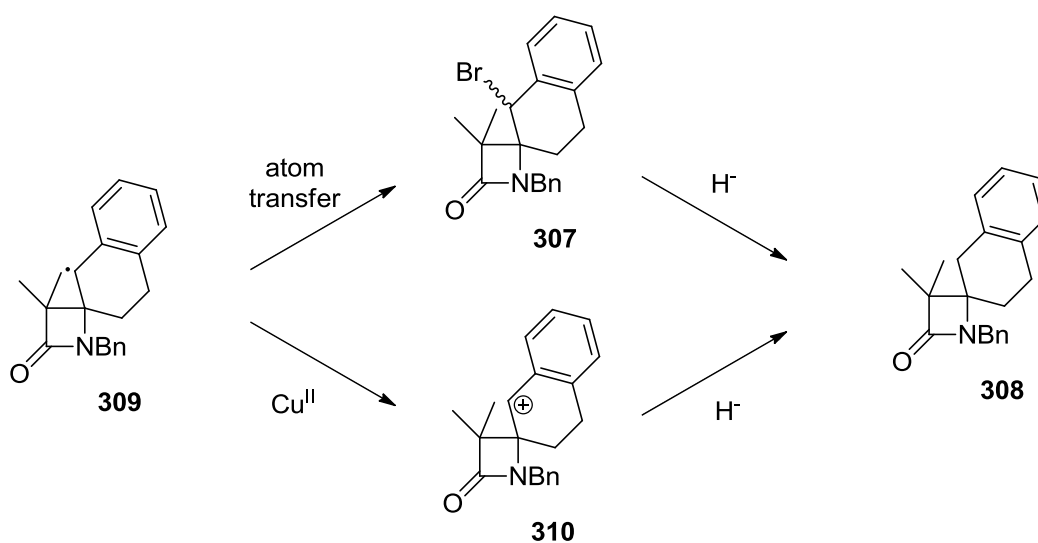
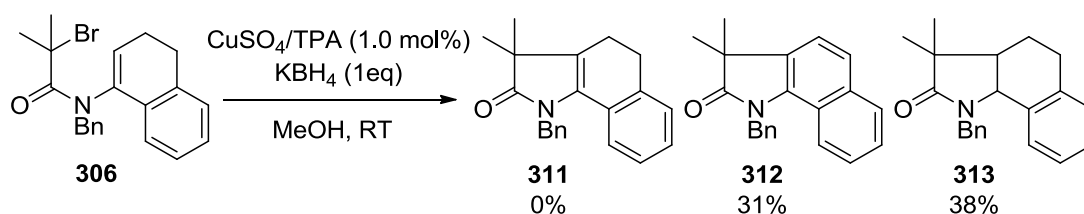


Figure 4.12: β -Tetralone **305** and α -Tetralone **306**

The reaction of the β -tetralone enamide **305** using Cu(TPA)SO₄ (1.0 mol%) and KBH₄ (1.0 equivalent), was expected to furnish the 4-*exo trig* atom transfer product **307**.²⁵ However this product was not observed, instead the only product identified was **308** in a disappointing 23% yield (Scheme 4.18). It could be possible to arrive at **308** *via* two pathways. Firstly, hydride (H) reduction of the reactive atom transfer product **307**, could yield **308**. Secondly, due to the stability of the benzylic radical **309** formed, an oxidation by Cu(II), could yield a cation **310** that could also undergo hydride reduction to yield **308** (Scheme 4.19).

Scheme 4.18: CuSO_4 Mediated 4-Exo Trig ATRC of β -Tetralone **305**Scheme 4.19: Possible Reaction Pathways to Reduced Product **308**

The cyclisation of α -tetralone enamide **306** using $\text{Cu}(\text{TPA})\text{SO}_4$ (1.0 mol%) and KBH_4 (1.0 equivalent) was expected to yield **311**.²⁵ However this was not observed, instead, naphthalene **312** and reduced product **313** were observed in a combined yield of 69% (Scheme 4.20).

Scheme 4.20: CuSO_4 Mediated Radical Cyclisation of α -Tetralone **306**

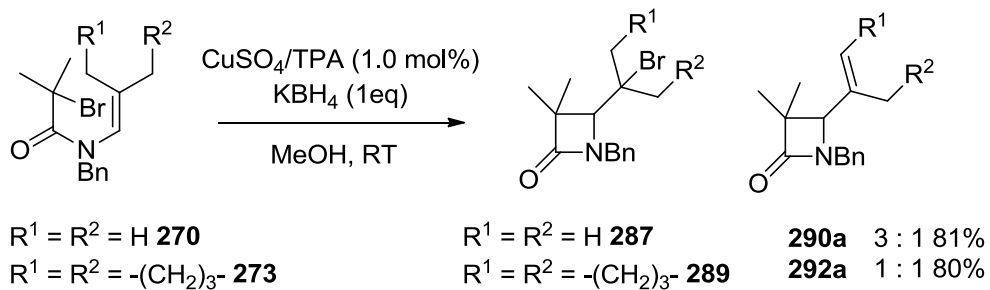
Product **313** arises from the reduction of *N*-acyliminium ion, whilst **312** presumably arises from the oxidation of **311** to form the fully conjugated naphthalene derivative. Oxidations of tetralone derivatives are not uncommon in the literature, but it is not known how **312** is formed under these reductive reaction conditions. Due to the similarities in the yields obtained for **312** and **313** one possible explanation could involve a radical disproportionation from **311**, which would also explain why **311** is not isolated from the reaction mixture.

4.4 CONCLUSIONS

It has been shown that efficient copper mediated *5-exo trig* and *dig* as well as *4-exo* and *5-endo trig* radical cyclisation of tertiary bromides can be achieved at room temperature, in methanol, by CuSO₄/TPA (0.1-1.0 mol%), in the presence of KBH₄ (10-100 mol%) in 10-30 minutes. This corresponds to a significant improvement in the catalytic efficiency of these reactions, and moreover the use of Cu^{II} salts negates the previous need for an inert atmosphere. Additionally UV-*vis* analysis of this reaction has discounted the possibility of the mechanism being similar to that of SET-LRP in polar solvents, and indicates that the catalytic species is a Cu^I species, the true identity of which unfortunately remains unknown at this time. A drawback identified when using these conditions was identified when investigating the *4-exo* and *5-endo trig* radical cyclisations. Although, in the main, conversions and yields were comparable to those reported previously, there was very little control over product distributions. For example, where under conventional ATRC conditions (30 mol%), enamides **270** and **273** gave exclusively atom transfer

Chapter 4: Copper-Mediated Radical Cyclisation in the Presence of Borohydrides

products **287** and **289**, the revised conditions (Cu(TPA)SO_4 1mol%, KBH_4 1 eq) gave a mixture of atom transfer **287** and **289**, and eliminated products **290a** and **292a**.



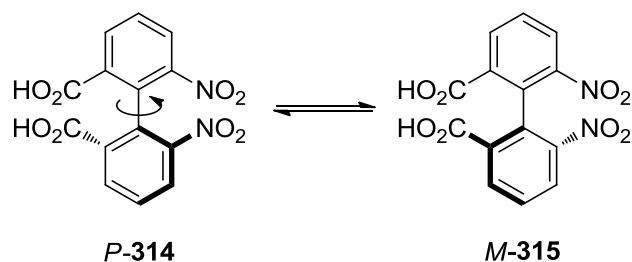
5.0 Atropisomeric Enamides. A Route to Asymmetric 5-Endo Radical Cyclisation?

5.1 INTRODUCTION

5.1.1 Early Evidence of Atropisomerism

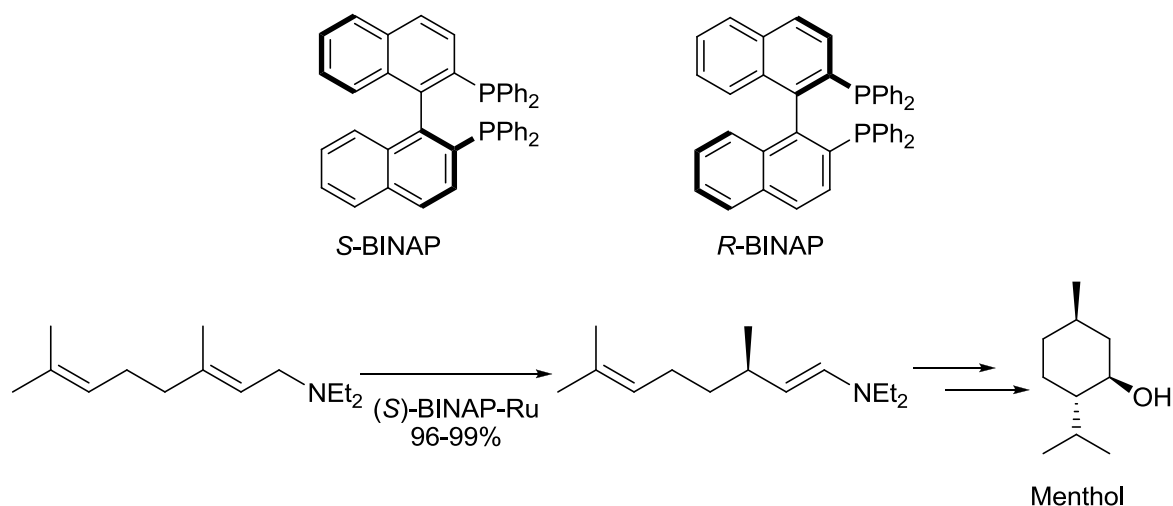
There are qualitative and quantitative definitions for atropisomerism. Qualitatively it is defined as ‘*the phenomenon of chirality as a result of restricted rotation about a single bond.*’ Quantitatively this was translated by Ōki who defined an atropisomer as a conformer which can retain its axial chirality with a half life for racemisation of $t_{1/2} \geq 1000$ seconds.¹⁷¹

Unlike stereoisomers, atropisomers do not necessarily contain a stereogenic centre, however chirality arises from two possible spatial arrangements about a given axis, an axis of chirality, giving rise to enantiomers. It is these ‘spatial enantiomers’ that are commonly known as atropisomers. Consequently, atropisomers are also identified using the Cahn-Ingold-Prelog notation, but unlike *R* and *S*, used for stereoisomers, atropisomers are identified using *M* and *P*.¹⁷² Considering the definitions of an atropisomer, another point of interest is that, as chirality arises through restricted rotation about a single bond, racemisation occurs thermally, rather than chemically. Therefore rather than performing a chemical reaction, breaking and forming bonds, the energy required for racemisation is simply the energy needed to overcome the barrier to rotation for a single bond to rotate 180°.



Scheme 5.1: First Isolated Atropisomers Isolated by Christie and Kenner

The first stable atropisomer was isolated in 1922 by Christie and Kenner.¹⁷³ The 6,6'-dinitro-2,2'-diphenic acid was resolved by co-crystallisation with a chiral amine. Subsequent research has shown that biaryl structures with *ortho* substitution tend to exhibit axial chirality about the single bond between the two aryl rings.



Scheme 5.2: BINAP Catalysed Synthesis of Menthol

As the understanding of axial chirality has expanded it has become a major area of synthetic research. Perhaps the most notable example of the synthetic utility of axial chirality and atropisomers has come in the field of ligand design for transition metal catalysed asymmetric synthesis. The impact of such research has not gone unrecognized and in 2001, Noyori shared the Nobel Prize in Chemistry for his work on asymmetric catalysis, with the use of axial chiral ligands, having

contributed significantly to his unquestionable success. The industrial impact of his work has been far reaching. For example, axially chiral diphosphine ligand BINAP is industrially applied for the production of menthol (Scheme 5.2). Specifically, (*S*)-BINAP is used as the ligand for a ruthenium-catalysed olefin isomerisation to produce a crucial intermediate during the synthesis of menthol in 96-99% *ee* on a multi-ton scale.¹⁷⁴

Axial chirality and atropisomerism are not phenomena confined to synthetic chemistry. A number of natural products contain biaryl systems and as a result have been shown to possess axial chirality. These include the potent, gram positive antibiotic vancomycin,¹⁷⁵ and the protein kinase inhibitor michellamine B,¹⁷⁶ the structures and chiral axes of which are shown in (Figure 5.1).

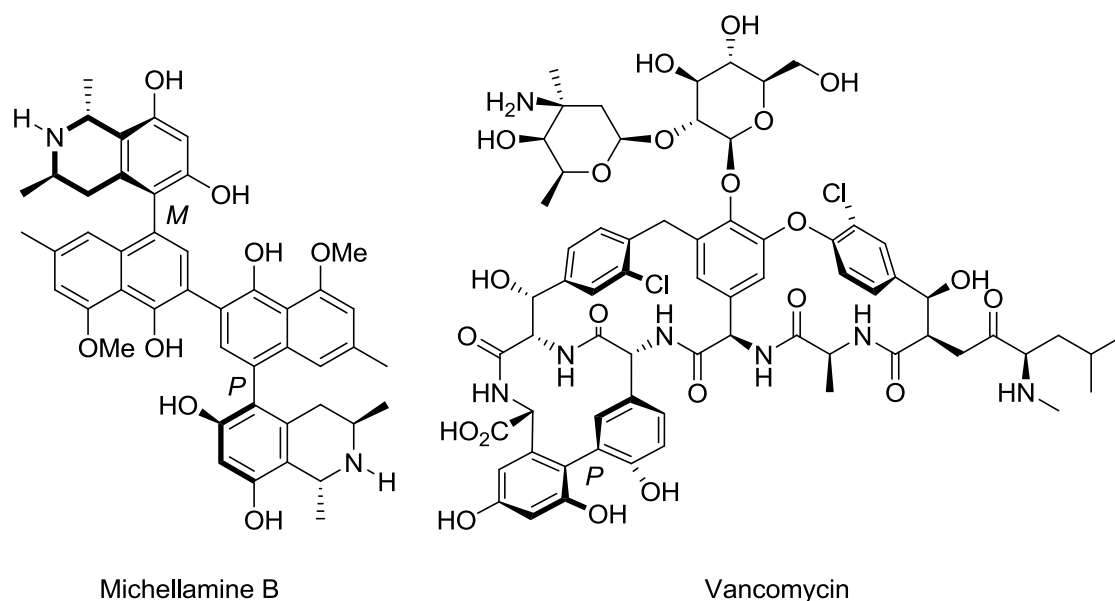


Figure 5.1: Natural Products Containing Axes of Chirality

In more recent years, research into axial chirality has expanded to include alternative synthetic systems. Work by Prof Dennis Curran in Pittsburgh, has shown that axial chirality is also prevalent in the chemistry of acetanilides,^{177,178,179,180,181}

and even enamides,¹⁸² which have been used previously in the Clark group for 5-*endo trig* radical cyclisation.²⁵

Conformational studies^{183,184,185,186,187,188,189,190,191,192} on a number of related substrates containing amide bonds have been conducted by Johnathan Clayden at Manchester. Particular interest has been focused on the stereodynamics of bond rotations in tertiary aromatic amides, such as *ortho* substituted benzamides^{184,187,189,193,194} **316** that tend to exhibit atropisomerism through slow rotation about the Ar-CO bond (Figure 5.2). Related structures include anilides^{195,196} **317** and benzanilides¹⁹¹ **318**. These are also often *ortho* substituted at the aryl groups and exhibit atropisomerism through slow *N*-aryl bond rotation. Benzanilides **316** have an added degree of complexity with possible atropisomerism through slow rotation of the Ar-CO bond. However, the stereogenic amide axes have been shown to exhibit a degree of conformational communication and conformational control in solution.¹⁹¹

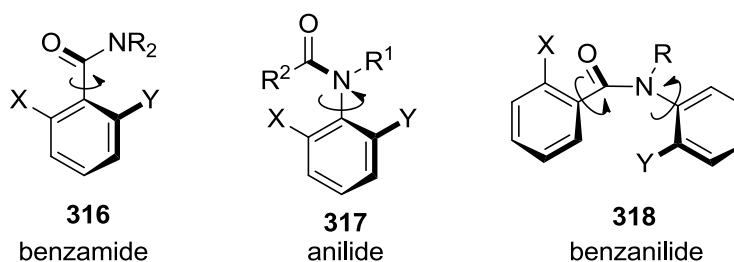
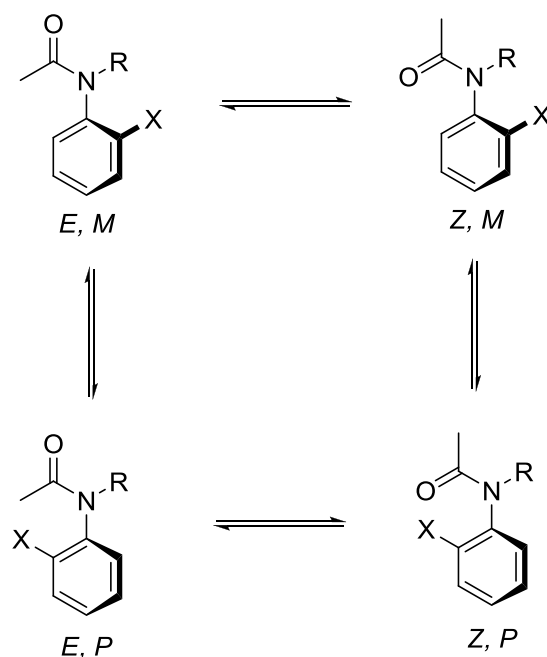


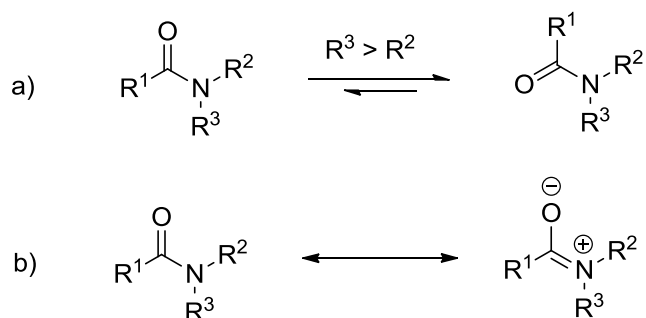
Figure 5.2: Synthetic Compounds Containing Axes of Chirality

In the case of acetanilides and enamides there are two rotational elements that require consideration. Amide rotation about the N-CO bond gives rise to *E* and *Z* amide rotomers,^{196,197} while restricted rotation about an *N*-aryl bond (anilides) can give rise to atropisomerism (Scheme 5.3). In the case of acetanilides *ortho* substitution of the aryl ring is a pre-requisite for atropisomerism.^{178,179,180,198}



Scheme 5.3: Rotational Processes Present in Anilides

Rotational barriers for both processes must be considered. Amide rotation has been well studied and is well understood.¹⁹⁶ Unsymmetrical *N,N*-disubstituted amides can interconvert between *E* and *Z* rotamers by a single rotation of the N-CO bond, and in the case of tertiary amides the *Z* rotamer is preferred at equilibrium placing bulkier groups *cis* to the carbonyl (Scheme 5.4a).¹⁹⁶



Scheme 5.4: a) Amide Bond Rotation b) Amide Bond Resonance

Generally *N,N*-disubstituted amides have rotational barriers between 15-20 kcal mol⁻¹.¹⁹⁷ The precise values are dictated by steric and electronic effects of the substituents.^{199,200} In the ground state the N-CO bond exhibits partial double bond character (Scheme 5.4b). As a result neighbouring substituents are co-planar and the greatest steric interactions occur between them. Increasing the steric bulk of R² and R³ has a destabilizing effect on the partial double-bond character causing the barrier of rotation to decrease.^{199,200} Conversely, if R¹ is electron-withdrawing, for example if there is multiple α -halogen substitution, then the barrier is raised due to electron density being withdrawn from the carbonyl group, stabilizing the ground state.¹⁹⁹

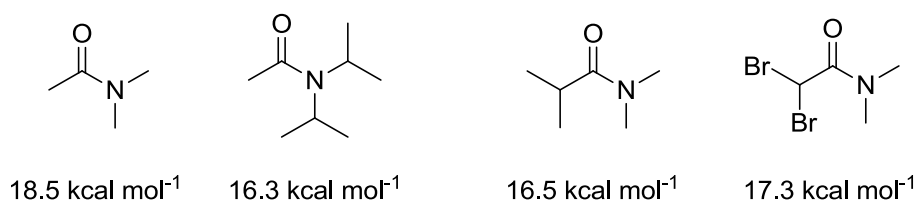
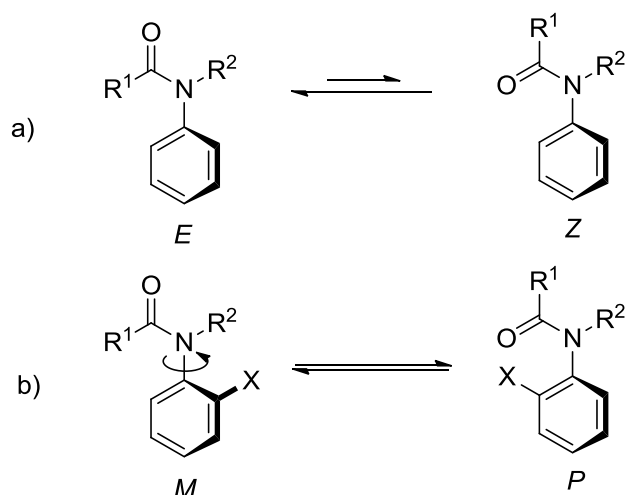
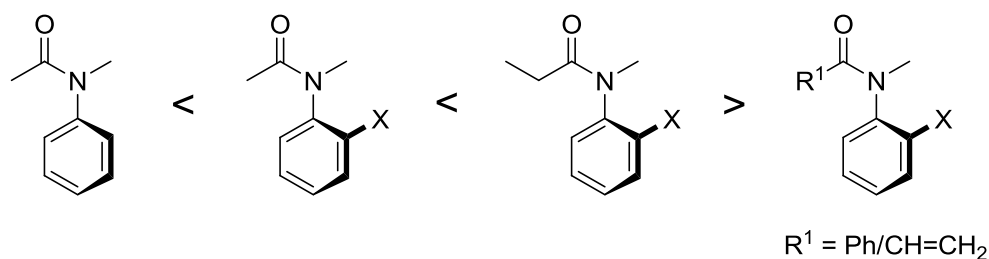


Figure 5.3: The Steric and Electronic Effects on the Barrier to Amide Rotation

The second, more subtle rotation present in acetanilides is the rotation about the *N*-aryl bond. Aryl groups bonded to the amide nitrogen tend to break the planarity observed in tertiary amides by twisting into an almost orthogonal plane relative to the amide plane.²⁰¹ This minimizes steric interactions with neighbouring groups and consequently, in contrast to tertiary amides, tertiary anilides prefer the *E*-configuration in solution.¹⁷⁸ Atropisomerism occurs in tertiary anilides when the aryl group is *ortho* substituted, leading to a barrier to rotation great enough to install an axis of chirality about the *N*-aryl bond (Scheme 5.5b).^{178,179,180,198}

Scheme 5.5: a) Amide Bond Rotation b) *N*-Aryl Bond Rotation (Atropisomerism)

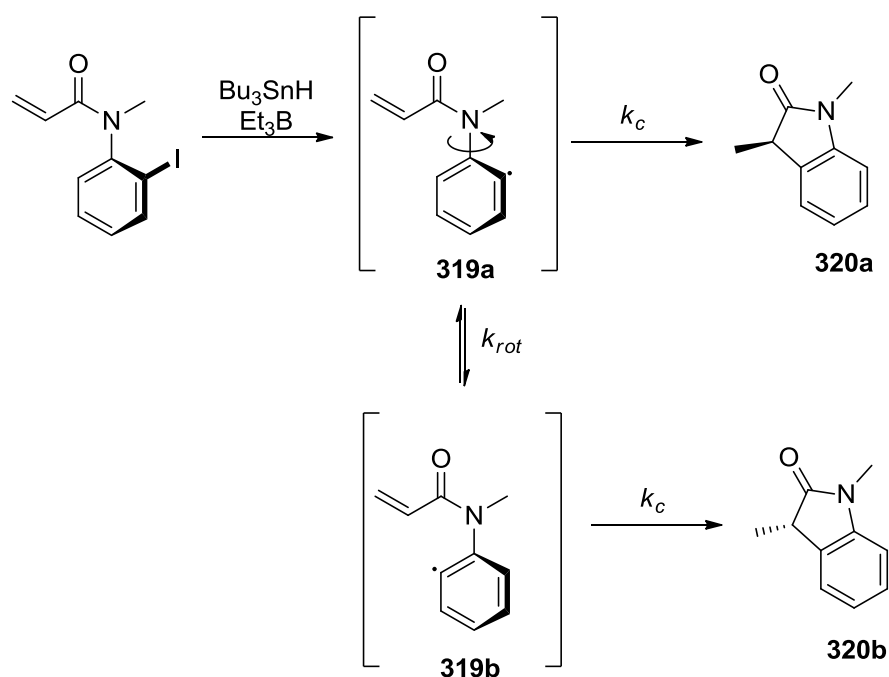
If the substituent X is sufficiently bulky, the atropisomers can be resolved by laboratory means, such as chiral HPLC.^{178,179,180,181,198,202,203} The magnitude of the rotational barrier is dependent upon the degree of substitution present in the anilide. Increasing the degree of substitution around the aryl ring, the bulk of either the X substituent or the bulk at the α -position of the carbonyl (R^1), increases the barrier to rotation (Figure 5.4). However the barrier to rotation decreases for both benzoyl and acrylanilides, where R^1 is an aryl ring and vinyl group respectively. This is because, unlike simple alkyl groups, these conjugated groups can twist out of planarity with the carbonyl group, minimizing steric clashes with the substituted *N*-aryl group in the rotation transition state.¹⁷⁸

Figure 5.4: Effects of Substitution on Barrier to *N*-Aryl Bond Rotation

A barrier to rotation large enough for resolution at room temperature is afforded when $X = I$, and Curran *et al.* have shown that acrylanilides can be manipulated to perform 5-*exo trig* radical cyclisation reactions with impressive chirality transfer (Section 5.1.2).

5.1.2 Chiral Induction in Radical Cyclisation

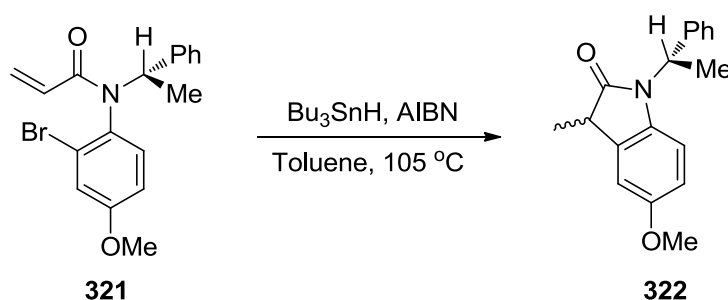
Transfer of chirality requires an element of chirality present in the starting material to be preserved throughout a reaction, to yield a chiral product with the same stereochemistry.^{204,205,206} Acrylanilides, designed for 5-*exo trig* radical cyclisation, have an axis of chirality about the *N*-aryl bond.¹⁹⁸ However the barrier to rotation of the starting materials, which are *ortho* substituted, are much greater than configurationally labile radical intermediates **319a-b**.



Scheme 5.6: If $k_c > k_{rot}$ Acrylanilide Chiral Induction is Possible

Consequently, in order for the stereochemistry of the starting atropisomer to be transferred to the cyclised product (**319a** → **320a**) the rate of cyclisation k_c must be greater than the rate of rotation k_{rot} (**319a** → **319b**) of the radical intermediate (Scheme 5.6).²⁰³ Furthermore the cyclisation must proceed with facial selectivity to avoid racemisation.

Prior to the identification of atropisomerism in acrylanilides, chirality transfer in rapid 5-*exo trig* cyclisations was investigated using chiral inducing groups incorporated into the substrates producing acrylanilides such as **321**. However under the reaction conditions applied a 1 : 1 mixture of diastereomers was obtained with no selectivity (Scheme 5.7).²⁰⁷



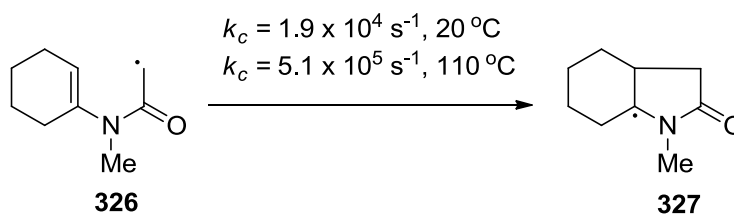
Scheme 5.7: Unsuccessful Attempted Chirality Transfer Using a Chiral Inducing Group

It was unclear at the time why this was the case. Curran then recognized that due to slow rotation about the *N*-aryl bond an axis of chirality was present in **321**, as well as the chiral inducing group. Consequently the starting material **321** was a mixture of diastereomers, and despite a fast rate of cyclisation ($\sim 10^8\text{ s}^{-1}$) a mixture of diastereomers was obtained due to the formation of diastereomeric radical intermediates. Curran then predicted that resolution of diastereomers of the related iodide **323** would lead to chiral induction.²⁰³

cyclisations of this sort (Scheme 5.9) suggest that this is the case. The rates of cyclisation for radicals formed from **324** have been measured and are in the order of $3 \times 10^9 \text{ s}^{-1}$.¹⁷⁹

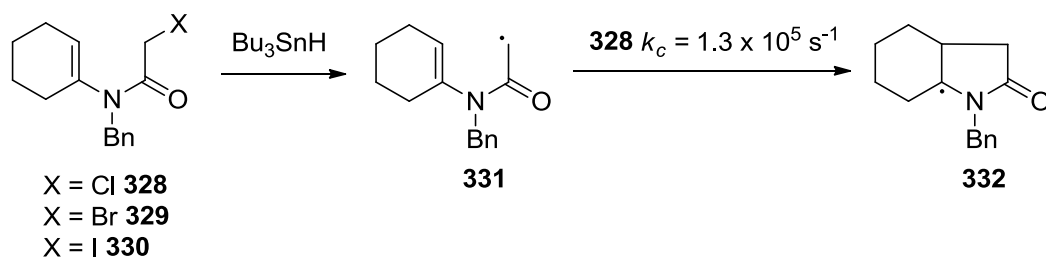
5.1.3 Atropisomerism in Enamides

Enamides are related to anilides through a N-C(alkenyl) bond. A common reaction of enamides is the tin-mediated 5-*endo trig* radical cyclisation of α -haloenamides.^{25,34,209,210,211,212,213} Only the *E*-rotamer of enamide radicals such as **326** can undergo cyclisation, as in the *Z*-rotamer, the radical formed is too far away from the alkene to attack. Comprehensive mechanistic studies^{212,214} have led to the determination of rates of cyclisation (k_c) and Chatgililoglu was able to experimentally determine k_c for the cyclisation of α -amide radical of enamide **326** (Scheme 5.10).

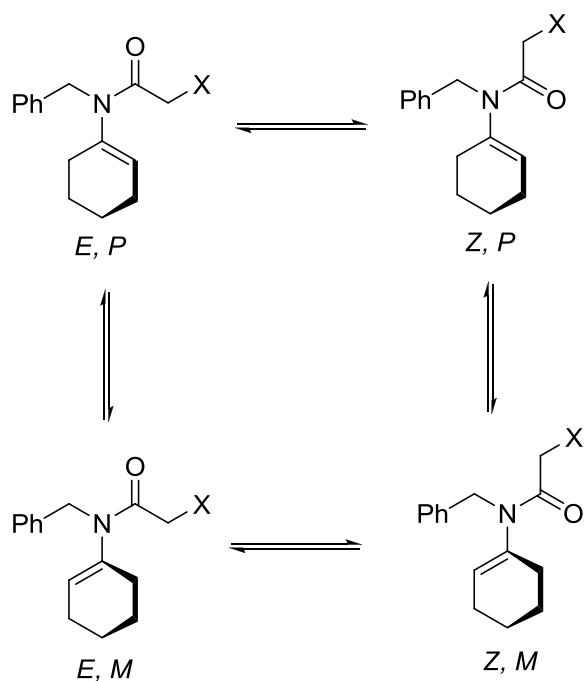


Scheme 5.10: Representative Rates of Rotation and Cyclisation for Acyl Radicals

Subsequently, Curran performed kinetic investigations to calculate k_c for *N*-benzyl α -haloenamides **328-330**²¹³ and his results were in good agreement with Chatgililoglu's experimental findings for the *N*-methyl enamide **326** at 110 °C regardless of the nature of the halogen. For example, α -chloroenamide **328** was found to have a rate of cyclisation of $1.3 \times 10^5 \text{ s}^{-1}$.

Scheme 5.11: Rate Cyclisation Acyl Radicals Derived From α -Haloenamides

These values are of the order of 10^4 slower than those reported for the aryl 5-*exo trig* radical cyclisations for acrylanilides (**324**, $3 \times 10^9 \text{ s}^{-1}$).¹⁷⁹ Consequently chirality transfer in 5-*endo trig* cyclisations is expected to be more difficult to achieve than the related 5-*exo trig* cyclisations. To determine whether chirality transfer could be possible for 5-*endo trig* cyclisations of enamides, a greater conformational understanding of these substrates is required (Scheme 5.12).



Scheme 5.12: Rotational Processes Present in Enamides

The most recent conformational analysis of α -haloenamides **328** and **330**, performed by Curran and co-workers was designed in order to establish the *syn/anti* amide geometry of these substrates, using ^1H NMR techniques.²¹³ Variable temperature NMR showed a single peak for both the benzyl and α -protons at room temperature. It was concluded that this was indicative of either the existence of a single rotamer²¹⁵ in solution or an unusually low barrier to rotation about the N-CO amide bond giving rise to sharp, coalesced rotamer signals (Figure 5.5).^{216,217}

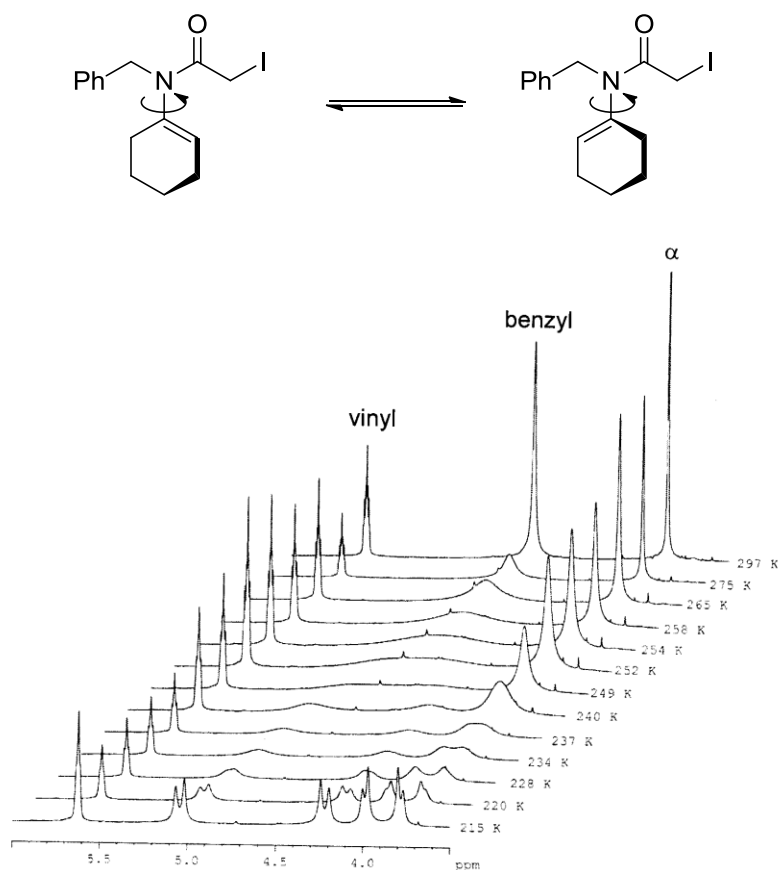
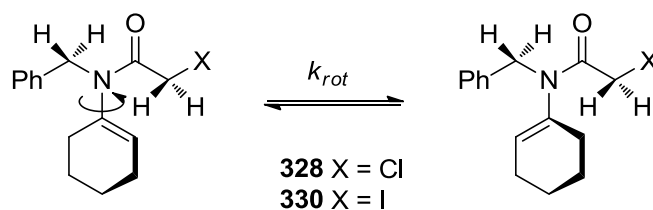


Figure 5.5²¹⁷: Room Temperature NMR of α -Iodoenamide **330**

As the sample was cooled the benzyl and α -proton singlets decoalesced into mutually coupled doublets. Spectroscopically this behaviour was not thought to be the result of slowing down and locking out the *E/Z* amide rotamers²¹⁸ as this would

have resulted in the doubling up of all signals near the amide bond. Additionally, as there was no element of chirality present in **330** the benzyl- and α -protons were expected to be homotopic, but at lower temperatures they were found to be diastereotopic (Figure 5.5).



Scheme 5.13: Diastereotopic benzyl- and α -Haloenamides Used as a Handle for VTNMR

The diastereotopicity of the benzyl and α -protons suggested that at low temperatures an element of asymmetry was present in substrates of this structure. It was proposed that this was due to the slowing down of rotation about the N-C(cycloalkenyl) bond, to produce an axis of chirality, analogous to the one present in acetanilides,¹⁹⁸ visible on the NMR timescale. It had been shown previously, by Mannschreck and coworkers,²¹⁹ that the barriers to rotation for enamides could be determined spectroscopically from the coalescence temperature of diastereotopic protons.²²⁰ Consequently, Curran and coworkers set about determining the rate of rotation (k_{rot}) and the barrier to rotation (ΔG^\ddagger) for their α -haloenamides. Line shape analysis of variable temperature NMR spectra^{221,222} allowed values for k_{rot} to be determined at each temperature, which factored into the Arrhenius equation (Equation 5.1), allowed determination of ΔG^\ddagger at each temperature.

$$\Delta G = -RT \ln \left(\frac{k \cdot h}{k_B T} \right)$$

Equation 5.1

Equation 5.2 was used to produce an Eyring plot, allowing access to important kinetic and thermodynamic parameters for the N-C(cycloalkenyl) bond rotations.

$$\ln\left(\frac{k}{T}\right) = \left(\frac{-\Delta H^\ddagger}{R}\right)\left(\frac{1}{T}\right) + \frac{\Delta S^\ddagger}{R} + \ln\left(\frac{k_B}{h}\right)$$

Equation 5.2

$$k_{298} = 298K \cdot e^{\left(\frac{\text{slope}}{298K} + \text{int.}\right)}$$

Equation 5.3

$$\Delta G_{298}^\ddagger = -R \cdot 298K \cdot \ln\left(\frac{k_{298} \cdot h}{k_B \cdot 298K}\right)$$

Equation 5.4

Curran and coworkers determined that *N*-cycloalkenyl bond rotations in **328** and **330** had k_{rot} values of 8.49×10^3 and $1.12 \times 10^4 \text{ s}^{-1}$ at 298 K (Equation 5.3) and when these values were factored into equation 5.1 to give equation 5.4, ΔG_{298}^\ddagger was found to be $12.1 \text{ kcal mol}^{-1}$ and $11.9 \text{ kcal mol}^{-1}$ respectively.¹⁸² These values are lower than those reported for related amide bond rotations ($15\text{-}17 \text{ kcal mol}^{-1}$). Additionally in an overlay, the Eyring plots for **328** and **330** were shown to almost coincide (Figure 5.6)²¹⁷ which suggested the dynamics in each substrate were similar.

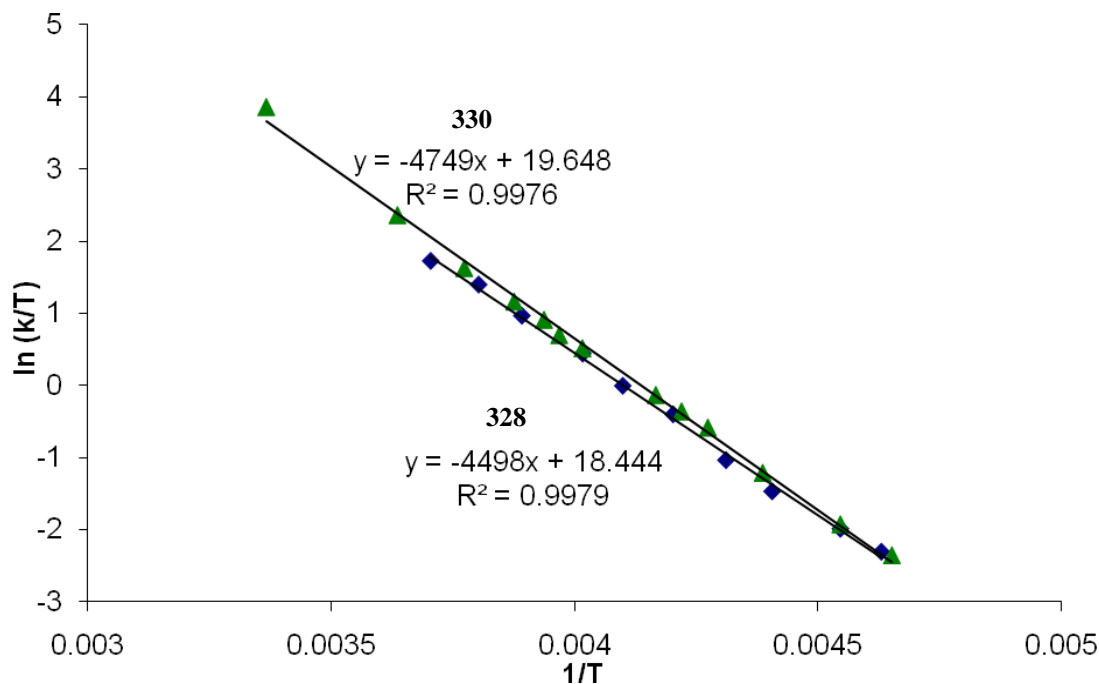


Figure 5.6: Coinciding Eyring Plots of α -Chloroenamide **328** and α -Iodoenamide **330**

Overall the spectroscopic analysis of **328** and **330** strongly suggested that the α -haloenamides exist as single rotamers in solution and that the N-C(cycloalkenyl) bond rotation was the major conformational process occurring in these compounds. Further evidence for this was elucidated from the X-ray crystal structure obtained for **328** (Figure 5.7).²¹⁷

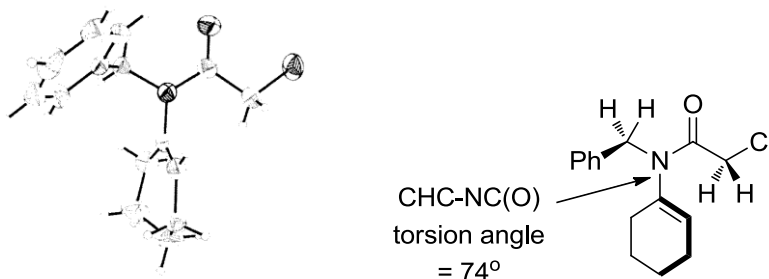


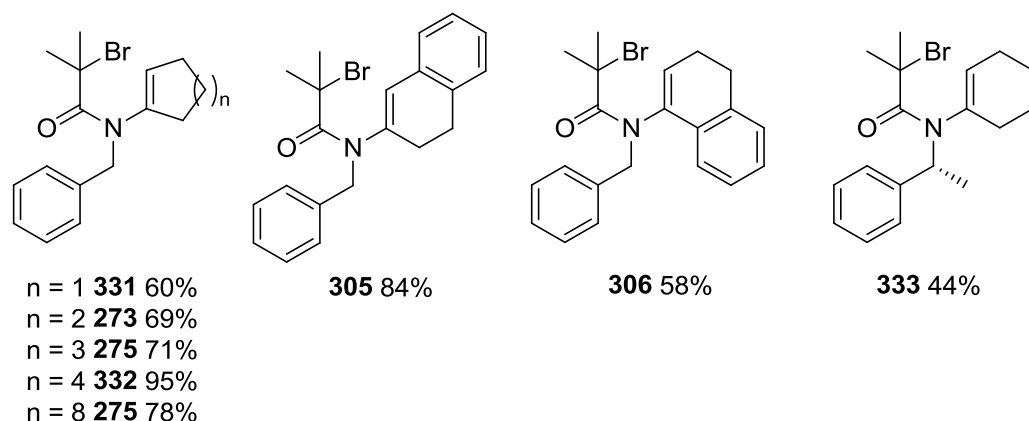
Figure 5.7²¹⁷: X-Ray Crystal Structure of α -Chloroenamide **328**

This showed the *N*-cyclohexenyl bond preferred to lie orthogonal to the plane of the N-CO amide bond and that the torsional angle was 74°. Finally the amide bond was shown to possess the *E*-conformation and to exhibit the anticipated sp² character in the ground state, and the sum of the bond angles around the nitrogen was found to be 359.9° dismissing any suspicion of pyramidalisation.

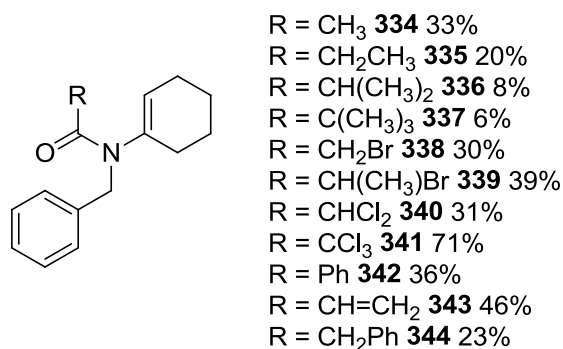
Given the conformation of enamides such as **328** and **330**, and the rate of cyclisation ($\sim 10^4 \text{ s}^{-1}$),²¹² it has been postulated that transfer of chirality could be observed during 5-*endo trig* cyclisations providing cyclisation occurs faster than *N*-cycloalkenyl bond rotation. In order to better contemplate the prospects of chirality transfer during these reactions, a basic investigation of the rotational dynamics of a number of enamides has been performed using variable temperature NMR. Albrecht and co-workers reported on the rotational dynamics of acyclic enamides and related compounds in 1979.²²⁰ In our work, the effect of the cycloalkenyl group¹⁸² and substitution in the α -position of the carbonyl have been examined. Furthermore tetrasubstituted enamides have been synthesised, towards the preparation of enamides with $k_c > k_{rot}$.

5.2 RESULTS AND DISCUSSION

The cycloalkenyl enamides discussed in sections 5.2.1 and 5.2.2 were all synthesised by the same technique outlined in section 4.2.2. Acetylation of the imines formed from the corresponding ketones, *in situ*, produced enamides **273-275**, **305-306** and **331-333** (Figure 5.8).

Figure 5.8: Enamides Selected to Investigate *N*-Cycloalkenyl Bond Rotation

In order to investigate the effect of α -substitution at the carbonyl group on the rate of rotation, the acetylating group (acid halide) was also changed to produce cyclohexenyl enamides **334-344** (Figure 5.9).

Figure 5.9: Enamides Selected to Investigate *N*-Cyclohexenyl Bond Rotation

5.2.1 Barriers to Rotation for Cycloalkenyl Enamides – Effect of α -Halogen

In the last section we reported the work initiated by Curran and co-workers who performed a conformational analysis on α -chloro- and α -iodoenamides **328** and **330** (section 5.1.2). For completion, we synthesised the α -bromoamide **338** and analysed it by variable temperature NMR. Bromide **338** was dissolved in CDCl_3 ,

containing tetramethylsilane for use as a line width and internal standard. ^1H NMR was recorded at temperature intervals in the range of 213-298 K. Portions of these spectra are displayed in (Figure 5.9, x marks an impurity).

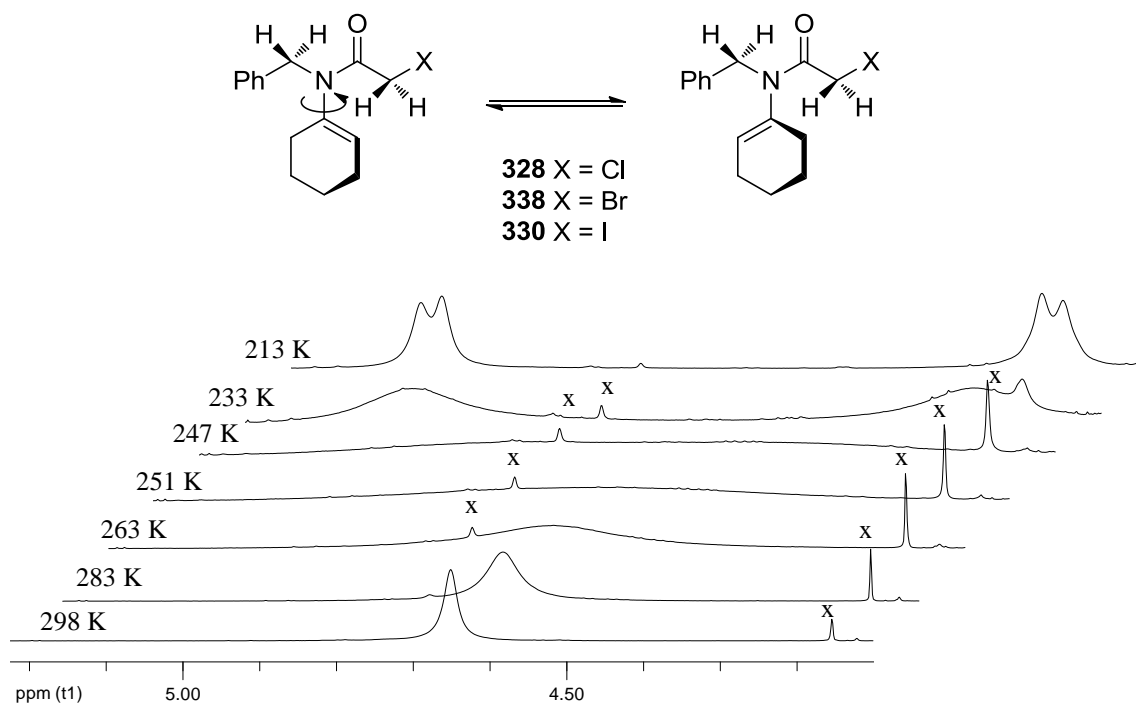


Figure 5.9: Stack Plot of α -Bromoamide **338**

The results were consistent with those expected from the analysis of **328** and **330**, suggesting that **338** existed in solution as mainly the *E*-amide rotamer. At 298 K two singlets were observed for the benzyl and α -protons and upon cooling both decoalesced to give mutually coupled doublets (213 K). As discussed previously (section 5.1.2) this is not consistent with N-CO bond rotation as this would lead to a doubling up of all peaks and would not result in the emergence of diastereotopic geminal protons. Consequently, the major rotational process was assigned as the *N*-cyclohexenyl rotation, which was slow enough at lower temperatures to generate a chiral axis. This was confirmed by overlaying the Eyring plot of **338** with those

determined previously by Curran and co-workers to produce Figure 5.11 which suggested the rotational dynamics of the α -haloenamides were all similar.

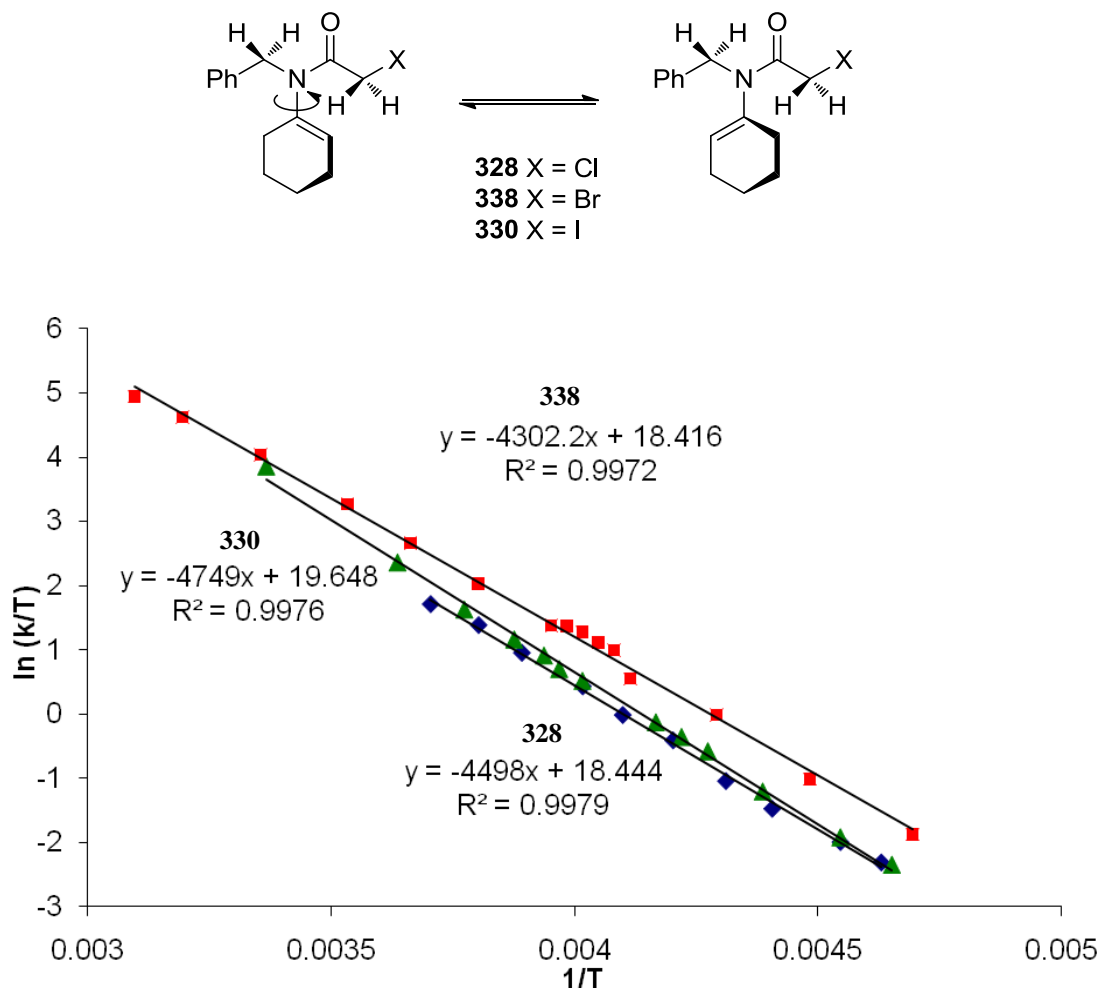
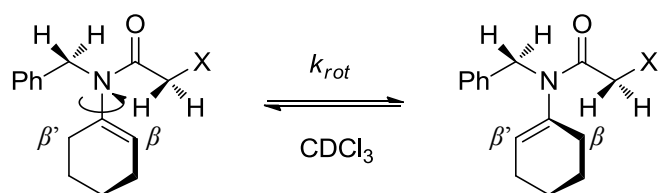


Figure 5.11: Coinciding Eyring Plots of α -Haloenamides

Using the program WINDNMR²²¹ the k_{rot} for α -bromoamide **338** was determined at each temperature. From this plot it was possible to calculate the rate of rotation about the *N*-cylcohexenyl bond at 298 K (k_{298}) using equation 5.3, which could then be factored into the Arrhenius equation (equation 5.1) to determine the barrier to rotation at 298 K (ΔG_{298}^\ddagger).



Substrate	X	k_{298}	ΔG_{298}^\ddagger
328	Cl	$8.49 \times 10^3 \text{ s}^{-1}$	$12.1 \text{ kcal mol}^{-1}$
338	Br	$1.59 \times 10^4 \text{ s}^{-1}$	$11.7 \text{ kcal mol}^{-1}$
330	I	$1.12 \times 10^4 \text{ s}^{-1}$	$11.9 \text{ kcal mol}^{-1}$

Table 5.1: Rates and Barriers to Rotation for α -Haloenamides Determined by VTNMR

The coincidence of the Eyring plots is replicated in the values obtained for k_{298} and ΔG_{298}^\ddagger (Table 5.1). Using the Eyring plots, it was also possible to determine the entropy and enthalpy for the *N*-cyclohexenyl bond rotation using equations 5.5 and 5.6. These figures have been omitted from table 5.1 but can be seen later in table 5.2.

$$\Delta H^{\ddagger} = -R \cdot \text{slope}$$

Equation 5.5

$$\Delta S^{\ddagger} = R \cdot \left(\text{int.} - \ln \left(\frac{k_B}{h} \right) \right)$$

Equation 5.6

5.2.2 General Appearance of ^1H NMR of Enamide Substrates

The study was then extended to a series of α -bromoisobutyryl enamides¹⁸² that could undergo either 5-*endo trig* or 4-*exo trig* radical cyclisations. The ^1H NMR spectra of α -haloenamides (**328**, **330**, **338**) were relatively simple at room temperature and peak broadening and decoalescence was only observed upon

cooling. However, the ^1H NMR of the α -bromoisobutyryl enamides **273-275**, **305-306**, **331-333** at room temperature, exhibited a range of behaviours depending on the nature of the cycloalkenyl group. For the cyclopentenyl enamide **331**, the benzyl protons were a sharp singlet at room temperature (Figure 5.12), and as a result, like α -haloenamides (**328**, **338**, **330**), only cooling of the sample would be required to observe decoalescence in order to determine k_{298} and ΔG^\ddagger_{298} . Conversely, for the α -tetralone-derived enamide **306** the benzyl protons were resolved, mutually coupled doublets at room temperature (Figure 5.13), and consequently heating of the sample would be required.

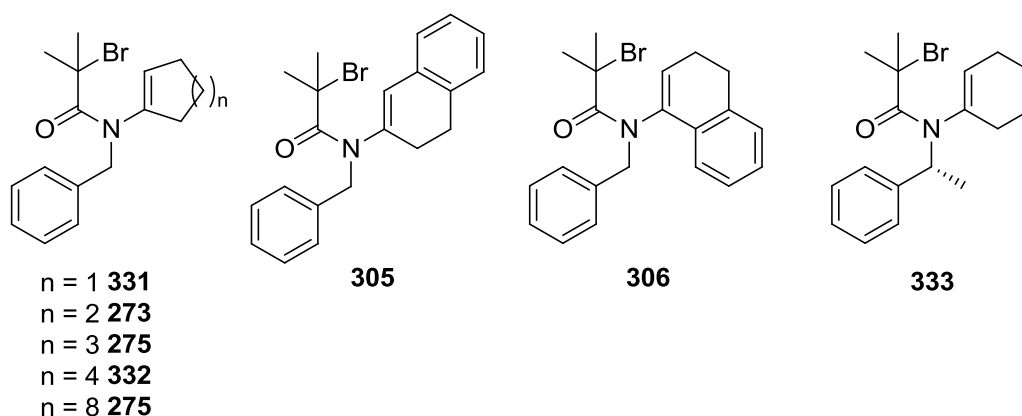


Figure 5.12: α -Bromoisobutyryl Enamides for NMR Analysis

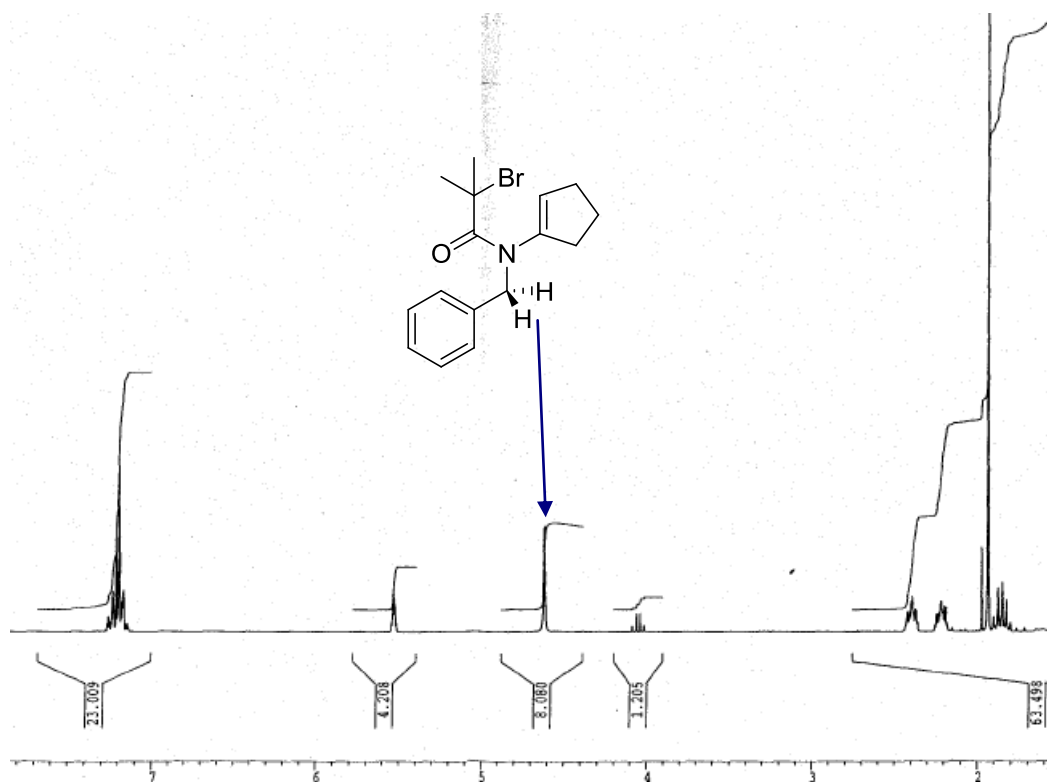


Figure 5.13a: Room Temperature NMR of Cyclopenteny Enamide 331 Showing a Sharp Signal for Benzyl Protons

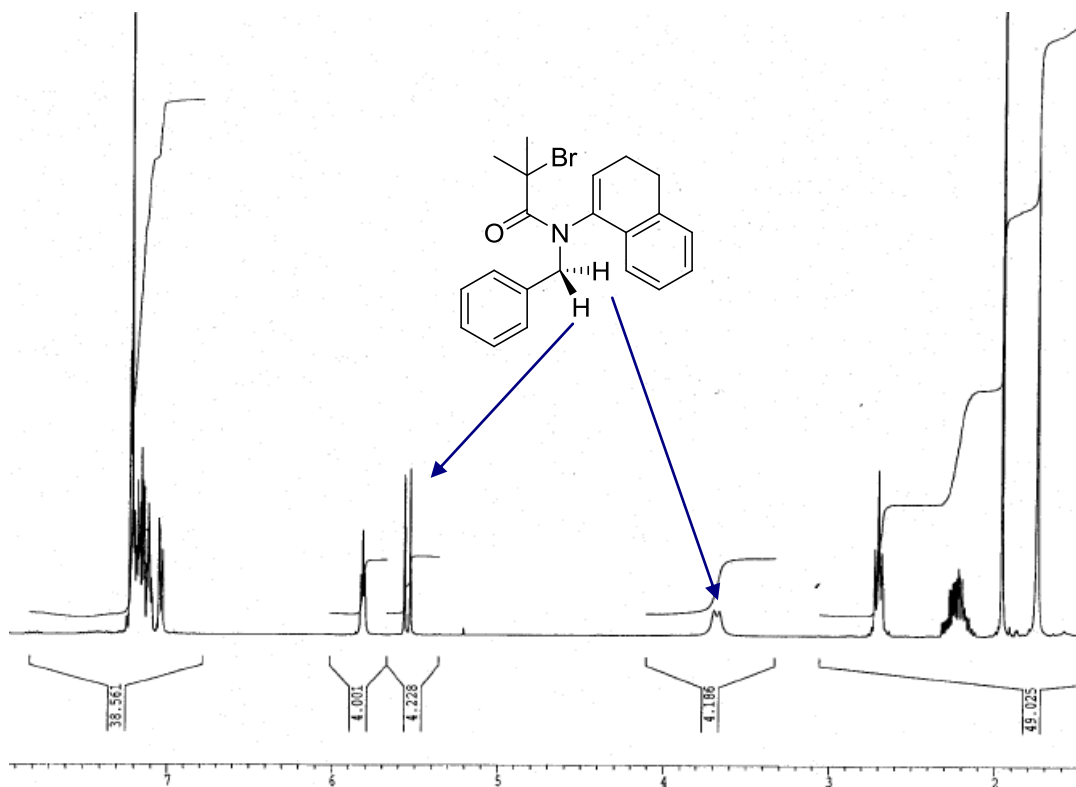


Figure 5.13b: Room Temperature NMR of α -Tetralone Enamide 306 Showing Diastereotopic Benzyl Protons

5.2.3 Effect of Ring Size

Figures 5.13a and 5.13b display the two extremes observed and the remaining α -bromoisobutyryl enamides exhibited behaviour between them, often displaying broad resonances. In the case of **275** and **332** the resonances were so broad that they disappeared in to the baseline. Accordingly, these samples were both heated and cooled in order to determine k_{298} and $\Delta G^{\ddagger}_{298}$. As the need to heat the samples during variable temperature NMR was now apparent, δ_8 -toluene was selected as the solvent for this set of experiments to extend the range for data collection (183-373 K).

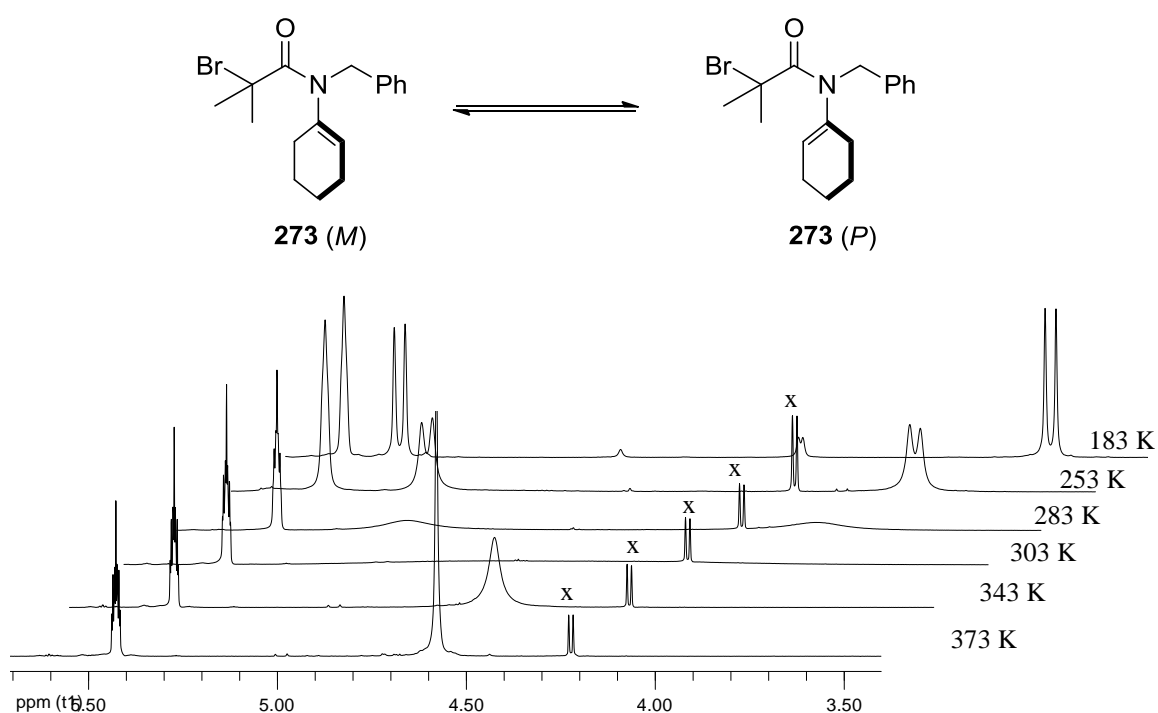


Figure 5.14: Stack Plot of α -Bromoisobutenamide **273**

As the α -position of the carbonyl was now substituted, and the appearance of benzyl protons was well resolved in every case, the benzyl protons were made the focal points of the line shape analyses.^{221,222} Figure 5.14 shows a portion of the

variable temperature NMR spectra obtained for α -bromoisobutyryl enamide **273**. An impurity arising from the reaction of the acid bromide with unreacted benzylamine has been marked x.

At low temperature (183 K) mutually coupled doublets were observed, due to slow *N*-cyclohexenyl bond rotation. Increasing the temperature increased the rate of rotation, causing the doublets to broaden (283 K), and eventually complete coalescence was observed (303 K). At high temperatures (373 K) rotation about the *N*-cyclohexenyl bond was so rapid, a sharp singlet was observed. Line shape analysis of **273** found a rate of *N*-cyclohexenyl bond rotation of 1.06×10^3 and a barrier to rotation of $13.3 \text{ kcal mol}^{-1}$ (Table 5.2), calculated from the Eyring plot (Figure 5.15).

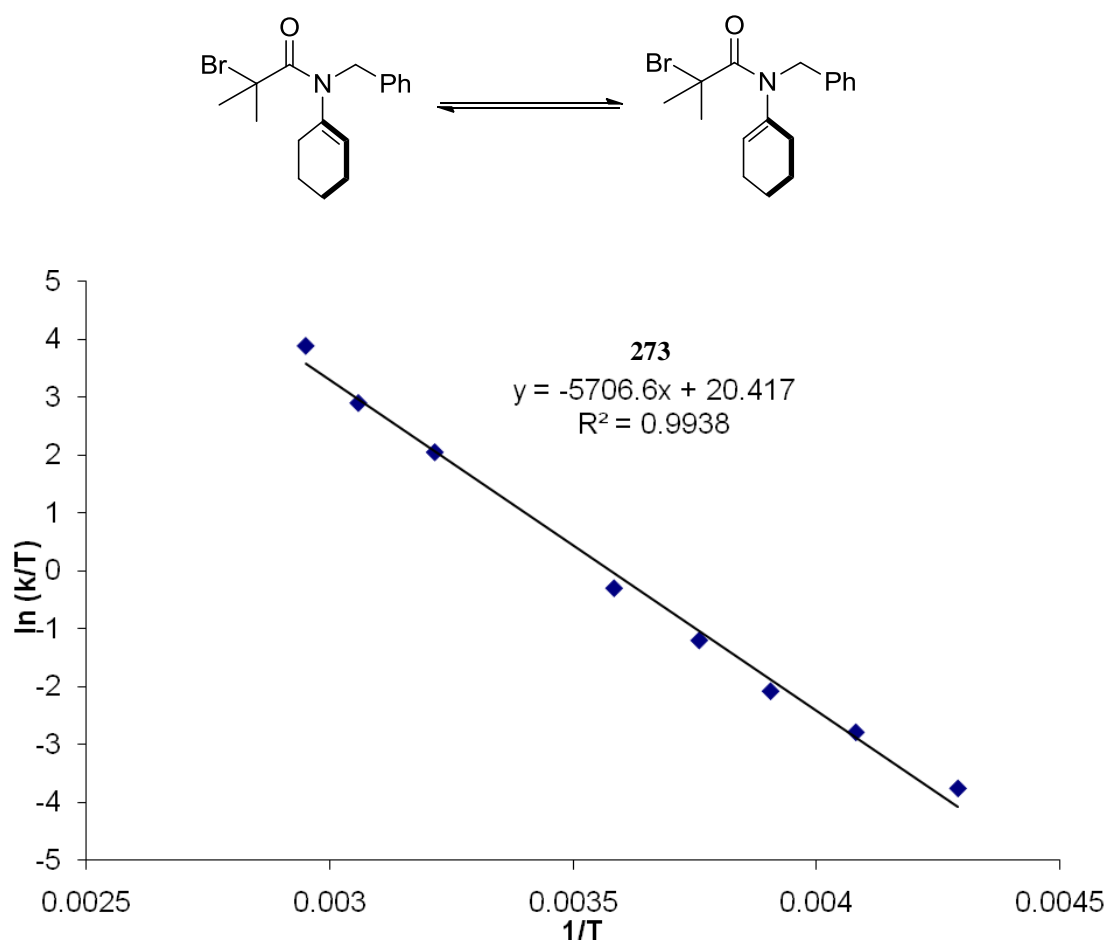


Figure 5.15: Eyring Plot for *N*-Cyclohexenyl Bond Rotation of α -Bromoisobutyryl enamide **273**

This analysis was performed on all the α -bromoisobutyryl enamides (Eyring plots can be found in appendix A) and the resulting rate constants (k_{298}) and activation parameters are displayed in table 5.2.

Entry	Substrate	Temp Range (K)	k_{298} (s ⁻¹)	ΔH^\ddagger (kcal mol ⁻¹)	ΔS^\ddagger (cal mol ⁻¹ K ⁻¹)	ΔG^\ddagger_{298} (kcal mol ⁻¹)
1	328 ^a	297-215	8.49 x 10 ³	8.9	-10.6	12.1
2	338 ^a	323-213	1.58 x 10 ⁴	8.5	-10.6	11.7
3	330 ^a	270-216	1.12 x 10 ⁴	9.2	-9.0	11.9
4	338	323-193	4.54 x 10 ⁴	8.1	-10.0	11.1
5	331	290-186	3.11 x 10 ⁵	8.0	-6.6	10.0
6	273	311-233	1.06 x 10 ³	11.3	-6.6	13.3
7	332	350-250	7.35 x 10 ²	11.8	-5.7	13.5
8	275	341-230	3.09 x 10 ³	11.4	-4.3	12.7
9	275	341-230	4.88 x 10 ³	11.4	-3.5	12.4
10	305	313-203	1.77 x 10 ⁴	9.8	-6.3	11.7
11	306	379-341	4.08 x 10 ⁻¹	11.9	-20.4	18.0
12	333 ^b	350-271	1.83 x 10 ²	12.7	-5.4	14.4
			3.64 x 10 ²	12.7	-4.0	14.0

^a CDCl₃ was the solvent.

^b Additional stereocentre gives rise to diastereomers with an equilibrium constant of 2.

Table 5.2: Kinetic and Thermodynamic Parameters for α -Bromoisobutenamides Derived From VTNMR

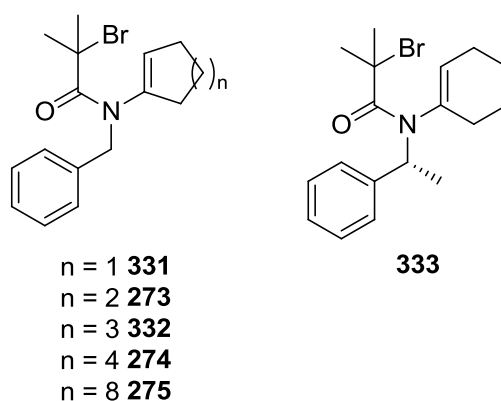


Figure 5.16: α -Bromoisobutenamides Used to Investigate Barriers to Rotation

For comparison, the results obtained for the α -haloenamides (**328**, **338**, **330**) have been included and **338** was resubmitted for analysis in δ_8 -toluene. The presence of quaternary carbon on the acyl group furnishes a barrier to rotation of

13.3 kcal mol⁻¹ for enamide **273** (Table 5.2, entry 6). This was over 1 kcal mol⁻¹ greater than the barrier observed for α -haloenamides **328**, **338**, **330** (entries 1-3) in CDCl₃, and when **338** was analysed in δ_8 -toluene (entry 4) the rotational barrier of **273** was found to be ~ 2 kcal mol⁻¹ greater. Varying the ring size of the cycloalkenyl group (entries 6-9) had little effect on the barrier to rotation (12.4-13.3 kcal mol⁻¹) except when the ring size was small for cyclopentenamide **331** (entry 5) which had a barrier to rotation of 10.0 kcal mol⁻¹.

Enamide **333** has an additional stereocentre and, as a result, slow rotation about the *N*-cyclohexenyl bond gives rise to diastereomers, not enantiomers. Upon cooling the diastereomers were resolved as a 2 : 1 mixture, but no attempt to identify the major diastereomer was made. As the rotamers were diastereomers, forward and reverse rates were measured (entry 12), and the presence of the phenethyl group increased to the barrier to rotation by ~ 1 kcal mol⁻¹.

5.2.4 Tetralone Enamides

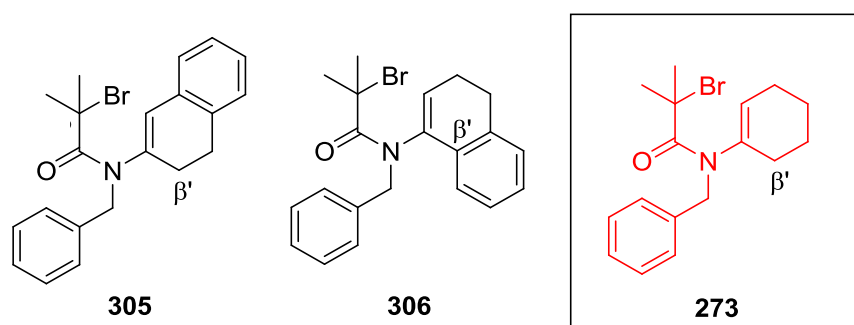


Figure 5.17: α -Tetralone and β -Tetralone Enamides

The tetralone enamides **305** and **306** have different β' (Figure 5.17) substitutions and as a result give remarkably different results. β -Tetralone enamide **305**, is unsubstituted at the β' position, which is a sp³ hybridised CH₂ group. In that

respect it was expected to resemble the cyclohexenamide **273**. However, the barrier to rotation was calculated at $11.7 \text{ kcal mol}^{-1}$ (entry 10) which was $1.6 \text{ kcal mol}^{-1}$ lower than **273** (entry 6). In contrast, the α -tetralone enamide **306** is sp^2 hybridised at β' due to the aromatic portion of the tetralone unit. Consequently, **306** better resembles an anilide than cyclohexenamide **273**, and this is reflected in the barrier to rotation which was found to be $18.0 \text{ kcal mol}^{-1}$ (entry 11). Even at the highest possible temperatures for the solvent in question (δ_8 -toluene) only the beginnings of coalescence was observed for **306** and as a result values obtained may not be as accurate as the others.

A crystal of **305** was grown in the hope of gaining an indication as to why a lower than expected barrier to rotation was observed (Figure 5.18).

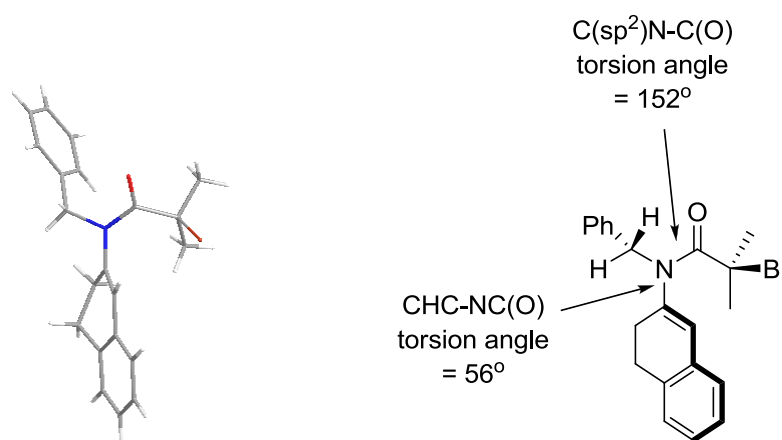


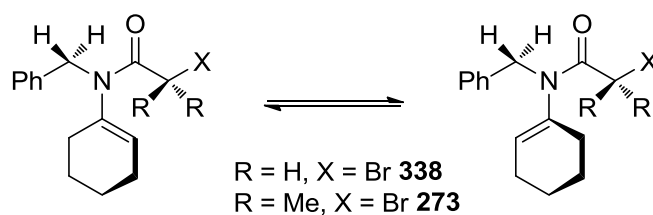
Figure 5.18: X-ray Crystal Structure of β -Tetralone Enamide **305**

The *N*-alkenyl bond torsional angle was found to be 56° which was lower than that previously found for related anilides (70 - 90°), and α -haloenamide **328** (74°).^{213,217} It is possible that additional overlap of the nitrogen lone pair through the alkene to the phenyl ring reduces the twist angle and subsequently the rotation barrier compared to anilides and α -haloenamides. Furthermore the sum of the angles

around nitrogen was found to be 356.9° indicating a deviation away from planarity²²³ (360°) and the torsion angle for N-CO amide bond, relative to the cycloalkene was found to be 152° and not 180° as expected for an sp^2 hybridised nitrogen. Consequently these values suggest a partial rehybridisation of the amide nitrogen from sp^2 to sp^3 , which could also reduce the barrier to rotation.

5.2.5 Effect of Solvent

The effect of solvent^{224,225} on rate constants and rotational barriers was briefly explored for α -haloenamide **338** and α -bromoisobutyryl enamide **273** (Table 5.3). 5-Endo trig cyclisations of enamides can be mediated by organostannane reagents and with copper complexes under ATRC conditions. The former tend to be carried out in non-polar solvents such as toluene, while for ATRC, more polar solvents are required (DCM, methanol). Generally, it was found that more polar solvents decreased the rate of rotation and increased the rotation barrier, although the difference was not significant ($0.5\text{-}0.9 \text{ kcal mol}^{-1} \pm 0.2 \text{ kcal mol}^{-1}$). Unfortunately, there did not seem to be an obvious correlation between the rotation barrier and dielectric constant (ϵ), dipole moment (μ) or the viscosity (η) of the solvents studied. The solvents used for organostannane (toluene) and ATRC (chlorinated, methanol) reactions exhibited identical trends with the ΔG^\ddagger_{298} increasing for the more polar solvents (toluene < methanol ~ CDCl_3), for both **273** and **338** which also corresponds to a decrease in the rate of *N*-cyclohexenyl bond rotation.



Substrate	Solvent	k_{298}	$\Delta G^{\ddagger}_{298}$
338	δ_8 -toluene	4.54×10^3	$11.1 \text{ kcal mol}^{-1}$
338	δ_4 -methanol	1.96×10^3	$11.6 \text{ kcal mol}^{-1}$
338	CDCl_3	1.58×10^3	$11.7 \text{ kcal mol}^{-1}$
273	δ_8 -toluene	$1.06 \times 10^3 \text{ s}^{-1}$	$13.3 \text{ kcal mol}^{-1}$
273	CD_3CN	371.4	$13.9 \text{ kcal mol}^{-1}$
273	δ_4 -methanol	326.1 s^{-1}	$14.0 \text{ kcal mol}^{-1}$
273	CDCl_3	251.4 s^{-1}	$14.2 \text{ kcal mol}^{-1}$
273	CD_3NO_2	245.3 s^{-1}	$13.9 \text{ kcal mol}^{-1}$

Table 5.3: Effect of Solvent on the Rate and Barrier to Rotation

None of the enamides in this investigation had *N*-cycloalkenyl rotation barriers high enough for atropisomer resolution at room temperature. However, when taken with previous results, enamides show a number of parallels with the related anilides which have been well studied. From enamide **306** (Table 5.2, entry 11) it was recognised that substitution at β and β' positions could lead to resolvable enamides at room temperature. Precedence for this in the literature has been reported by Albrecht and co-workers²²⁰ who have shown that it is possible to partially resolve tetrasubstituted enamide **345**, and its rotational barrier has been measured ($\sim 25 \text{ kcal mol}^{-1}$). Tetrasubstituted enamides will be discussed in section 5.2.3.

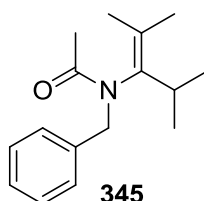
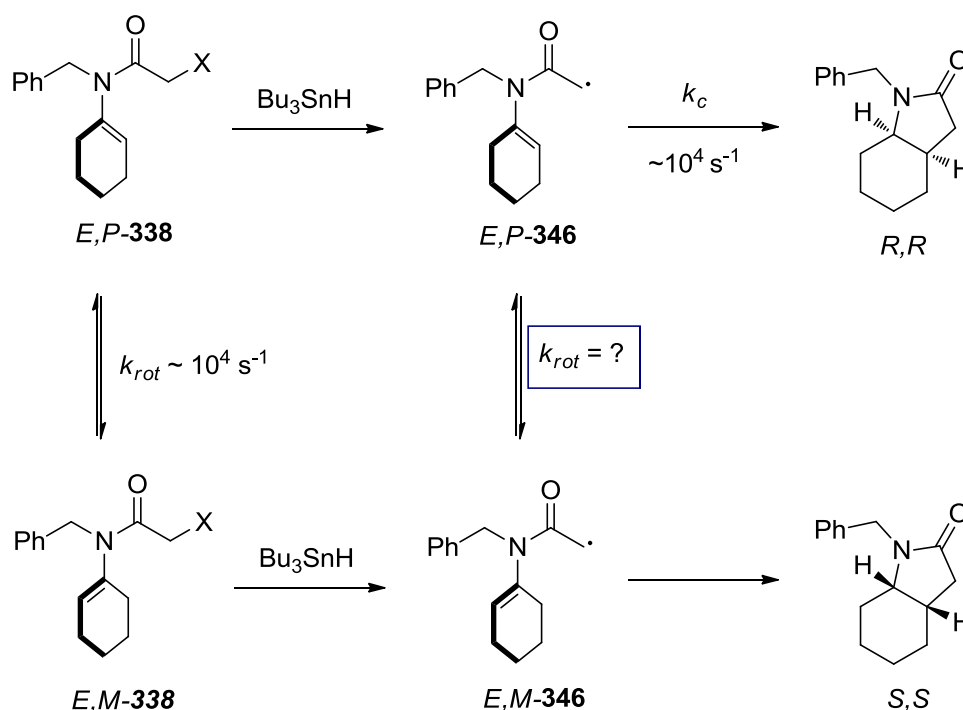


Figure 5.19: Tetrasubstituted Enamide

5.2.6 Barriers to Rotation for Cyclohexenyl Enamides, Varying the Acyl Group and Modelling the Barrier to Rotation in Related Radicals

Transfer of chirality requires the rate of cyclisation (k_c) of the radical enamide (e.g. *E,P*-**346**) to be greater than the rate of *N*-alkenyl bond rotation (k_{rot}) (e.g. *E,P*-**346** \rightarrow *E,M*-**346**) (Scheme 5.20). For α -haloenamides the k_c has been determined ($\sim 10^4 \text{ s}^{-1}$),²¹² and is approximately equal to the k_{rot} for the enamides **328**, **330**, **338** ($\sim 10^4 \text{ s}^{-1}$).²¹³ The rate and barrier to rotation for α -bromoisobutyryl enamides (**273-275**, **305-306**, **331-333**) have also been determined¹⁸² (Table 5.2, section 5.2.1), but up to now little is known of the rotation of the radical intermediates (e.g. *E,P*-**346** \rightarrow *E,M*-**346**).



Scheme 5.20: Potential Chirality Transfer in Enamides

To better contemplate the prospects of chirality transfer in the 5-endo trig cyclisations of enamides, and to complement previous work, a series of *N*-

cyclohexenyl enamides **334-344**, in which the size of the acyl group is varied, have been investigated. These experiments were designed to better estimate the barrier to rotation for the reactive radicals (**346-349**) produced by replacing the halogen (Br) with a hydrogen atom (**334-337**). Aryl and vinyl groups (**342** and **343**), furnishing a sp^2 hybridised acyl substituent have also been considered.

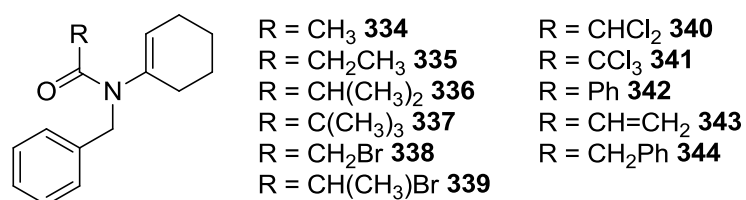


Figure 5.20: Enamides For Study

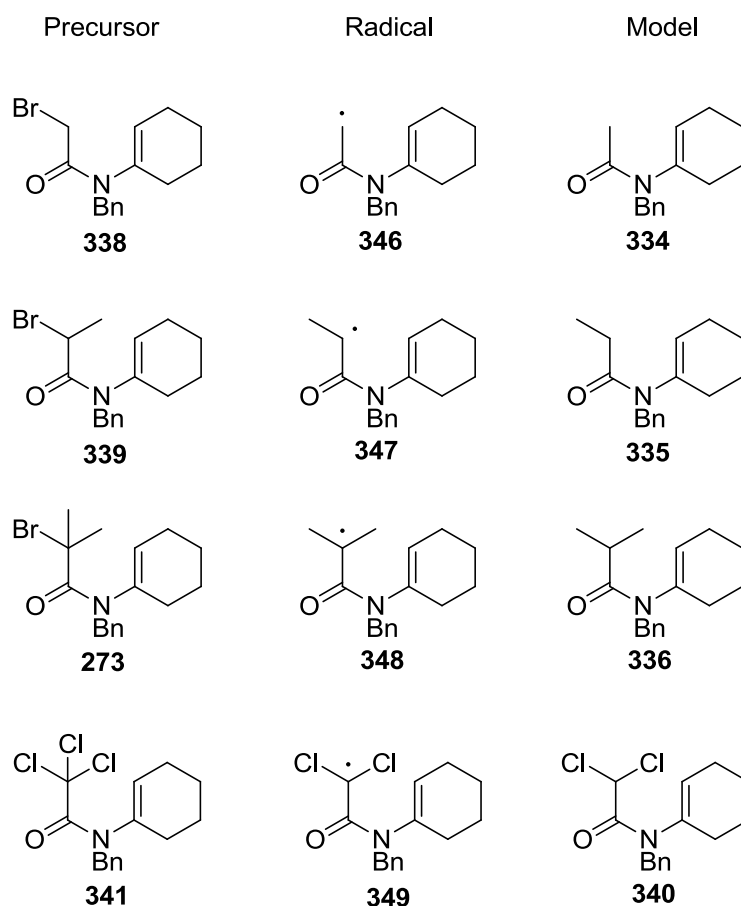
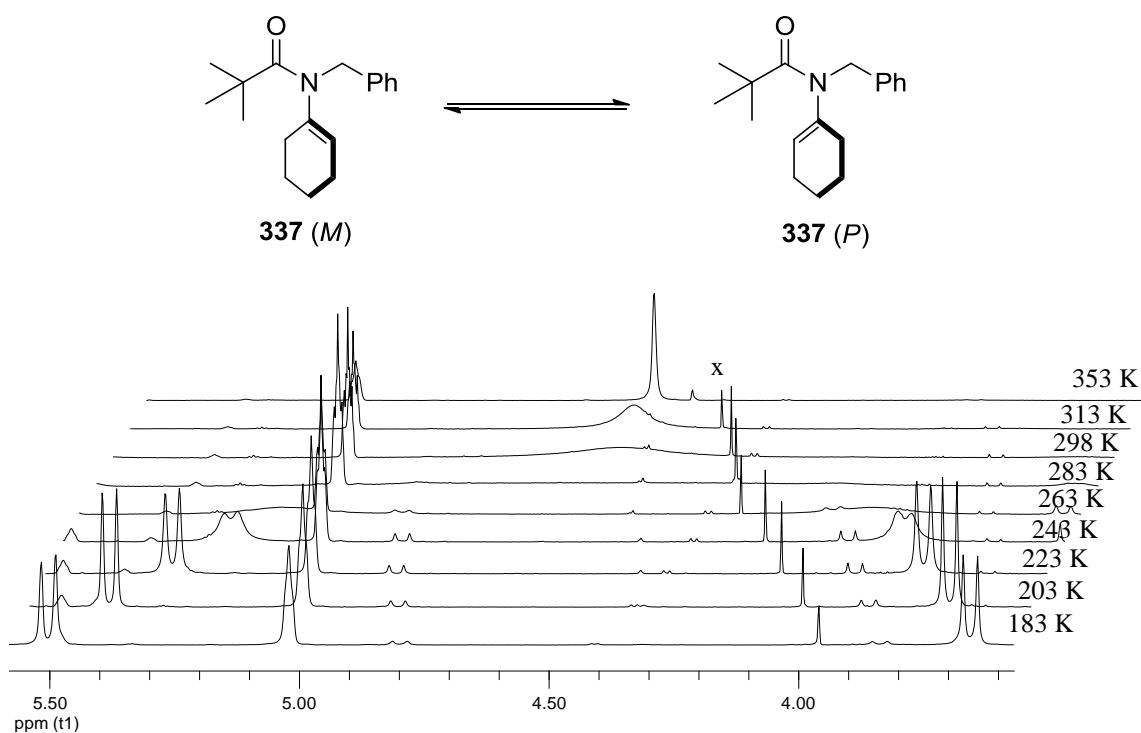


Figure 5.21: Designing Substrates as Models for Radical Intermediates Present During Cyclisation

The experiments were initiated by the preparation of **339**, completing the bromoenamide series **338** → **339** → **273**, to determine the effect of sequential replacement of hydrogen atoms with methyl groups. Additionally enamides **334-336** were also prepared to determine the same effect in instances where the bromine had been replaced by a hydrogen atom to provide potential models for the reactive radicals **346-348**. The di- and trichloro enamides **340** and **341** were also prepared as these have also be shown to undergo 5-endo trig cyclisations, with the additional halogens facilitating reaction. Conveniently, **340** could also act as a model for the radical **349**.

For analysis all samples were dissolved in d_8 -toluene, spiked with tetramethylsilane for use as an internal and line width standard and NMR were recorded at temperature intervals in the range of 183-373 K. For enamide **337** a portion of these spectra is shown in figure 5.22 (x marks an impurity).

Figure 5.22: Stack Plot of Enamide **337**

Consistent with previous observations, as the samples were cooled decoalescence of the benzyl protons was observed to afford mutually coupled, geminal, doublets, indicative of largely a single *E*-rotamer in solution and slowing down of the *N*-cyclohexenyl bond rotation. Enamide **339** has an additional stereocentre so, like **333** in section 5.2.1, its rotamers are diastereomers. During this experiment, the equilibrium constant for the two diastereomers was measured at low temperature and found to be 1. Rotational rate constants (k_{rot}) were determined at each temperature and activation parameters and k_{298} were determined (Table 5.4) from the subsequent Eyring plots (appendix A). Standard Eyring plots for the enamide **334** (radical model) and fully substituted enamide **337** are shown in figure 5.23.

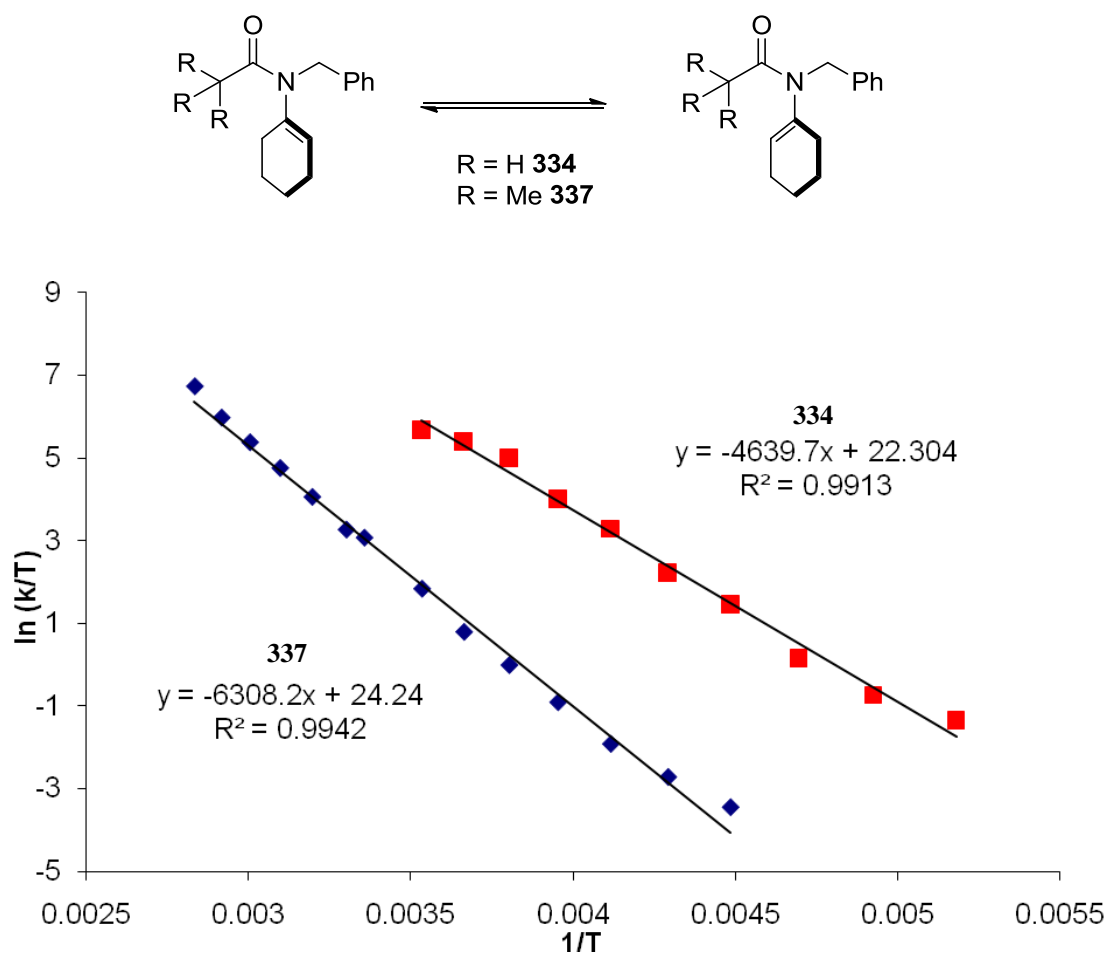


Figure 5.23: Eyring Plots of Unsubstituted and Fully Substituted Enamides **334** and **337**

Entry (Substrate)	R	k_{rot} 298 K (s ⁻¹)	ΔH^\ddagger (kcal mol ⁻¹)	ΔS^\ddagger (cal mol ⁻¹ K ⁻¹)	ΔG^\ddagger_{298} (kcal mol ⁻¹)
1 (338)	CH ₂ Br	4.54 x 10 ⁴	8.1	-10.0	11.1
2 (339)^a	CH(CH ₃)Br	9.00 x 10 ³	7.9	-13.8	12.0
		9.00 x 10 ³	7.9	-13.8	12.0
3 (273)	C(CH ₃) ₂ Br	1.06 x 10 ³	11.3	-6.6	13.3
4 (341)	CCl ₃	2.53 x 10 ²	14.8	2.0	14.2
5 (334)	Me	2.51 x 10 ⁵	9.2	-2.9	10.1
6 (335)	Et	7.46 x 10 ⁴	6.4	-14.7	10.9
7 (336)	ⁱ Pr	1.80 x 10 ⁴	9.3	-7.7	11.7
8 (340)	CCl ₂	6.66 x 10 ³	10.0	-7.4	12.2
9 (337)	^t Bu	6.43 x 10 ³	12.5	0.9	12.3
10 (343)	CH=CH ₂	7.45 x 10 ⁴	7.5	-11.1	10.8
11 (342)	C ₆ H ₅	4.88 x 10 ⁵	6.0	-12.2	9.7
12 (344)	CH ₂ Ph	2.29 x 10 ⁴	7.8	-12.4	11.5

^a Addition stereocentre gives rise to diastereomers with an equilibrium constant of 1.

Table 5.4: Kinetic and Thermodynamic Parameters Obtained for *N*-Cyclohexenyl Enamides

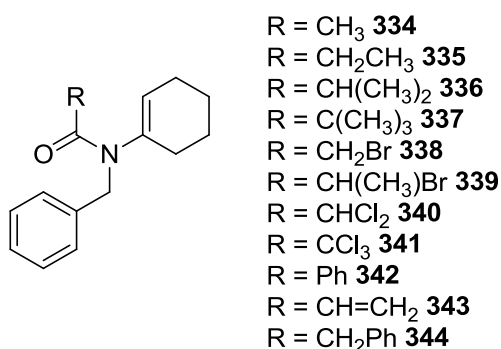
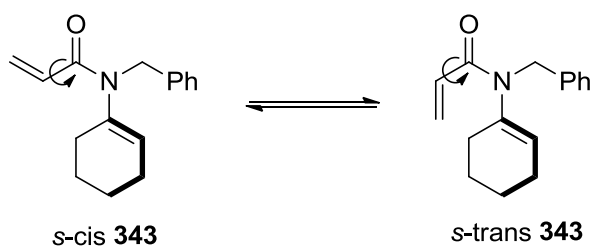


Figure 5.24: *N*-Cyclohexenyl Enamides Selected to Investigate Barriers to Rotation

Sequential addition of methyl groups was unsurprisingly found to steadily increase the rotation barrier. Adding a methyl group to transform **334** → **335** was seen to increase the barrier 0.8 kcal mol⁻¹ (Table 5.4, entry 5 → 6) and this increase was repeated upon addition of second methyl, converting **335** → **336** (entry 6 → 7). A third addition afforded **336** → **337** and fit the pattern increasing the ΔG^\ddagger_{298} by 0.6 kcal mol⁻¹ (entry 7 → 9). This steady increase in ΔG^\ddagger_{298} was also observed upon substitution of bromoenamide **338**. Sequential addition of methyl groups to **338** → **339** → **273** increase the barrier by 0.9 kcal mol⁻¹ (entry 2) and 1.3 kcal mol⁻¹ (entry

3) respectively. A more significant comparison is between the radical precursors (**338**, **339**, **273**) and their ‘radical models’ (**334-336**), where the bromine atoms have been replaced by hydrogen atoms. Substituting bromine for hydrogen was found to decrease $\Delta G_{298}^{\ddagger}$ by 1-1.6 kcal mol⁻¹ (entries 1, 2, 3 → 5, 6, 7). An even greater decrease of 2.0 kcal mol⁻¹ (entry 4 → 9) was observed between the trichloroenamide **341** and its dichloroenamide ‘radical model’ **340**. Thus, $\Delta G_{298}^{\ddagger}$ was found to decrease between 1.0-2.0 kcal mol⁻¹ for the radical precursors and their ‘radical models’ and this constitutes to a 5-26 fold increase in rate (k_{298}) for *N*-cycloalkenyl rotation in the radical models.

As the reactive radicals (**346-348**) would be sp² hybridised in the α -acyl position, aryl **342** and vinyl **343** substituted enamides were thought to be more appropriate ‘radical models.’ For radical **347** the sp² and sp³ ‘models’ are in reasonable agreement (10.8, 10.9 kcal mol⁻¹ respectively). However, the same cannot be said for the sp² and sp³ ‘models’ of radical **348**, where the sp² ‘model’ barrier (**342**, entry 11) was found to be significantly lower (2 kcal mol⁻¹) than the sp³ ‘model’ (**335**, entry 6). This trend is consistent with observations made for benzoyl anilides and occurs due to the aryl ring twisting out of the plane of the *N*-cyclohexenyl rotation.²⁰¹ Acrylanilides analogous to **342** tend to manifest a similar decrease which was not observed here. Presumably this is because, compared to acrylanilides, the enamide **343** exhibits a degree of both the *s-cis* **343** and *s-trans* **343** conformers,²²⁶ and the *s-trans* conformer, can lie in the plane of the *N*-cyclohexenyl bond rotation (Scheme 5.21).

Scheme 5.21: Rotation of the Acrylate Bond giving Rise to *s*-cis and *s*-trans Isomers

Finally the benzylic derivative (**344**, entry 12) was analysed and gave a barrier of $11.5 \text{ kcal mol}^{-1}$, which was greater than the primary bromide (**338**, entry 1), but similar to the isopropyl enamide (**336**, entry 7).

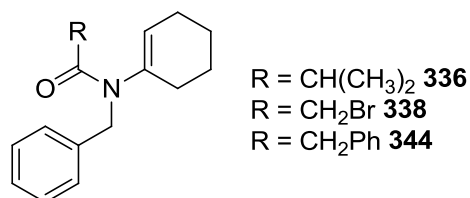


Figure 5.25: Enamides Representing the Radical Precursor and Models

The structure of one of the diastereomers of **339** was solved by X-ray crystallography (Figure 5.26), and resembled the previously solved anilides, and α -haloenamide **328**.^{213,217} The torsion angle of the *N*-alkenyl bond was found to be 84° , and unlike the tetralone enamide (**305**, figure 5.18) there was little evidence to suggest partial rehybridisation of the nitrogen to sp^3 . The sum of the angles around nitrogen was found to be 359.9° (356.9° for **305**), and the torsion angle of the N-CO amide bond was found to be 179.1° (152.0° for **305**), which is indicative of sp^2 hybridisation.

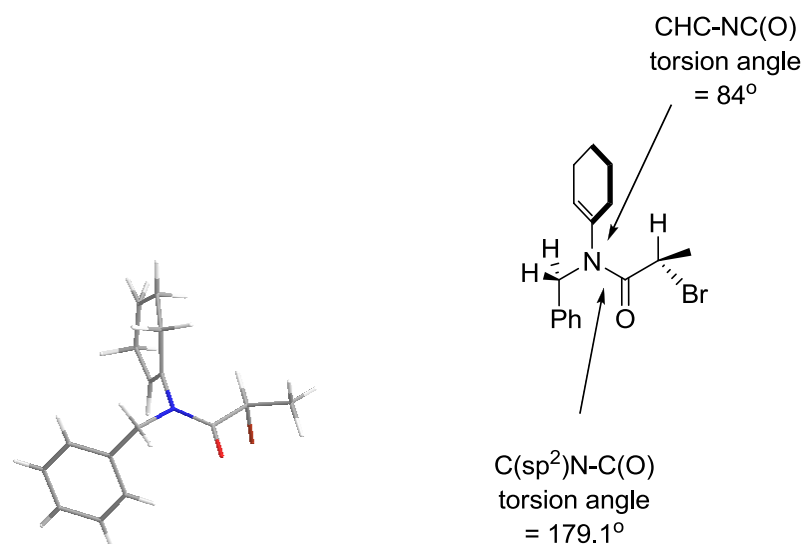


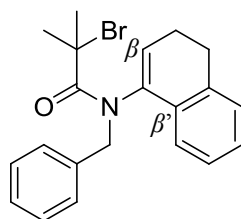
Figure 5.26: X-Ray Crystal Structure of Cyclohexenamamide 339

The analysis of enamides in which the acyl group has been varied has allowed an estimation of possible rates of rotation about the *N*-alkenyl and for reactive radical species involved in 5-*endo trig* radical cyclisation reactions. It was estimated that the rate of rotation would increase by 5-26 times for reactive radicals compared to their radical precursors. Unfortunately, considering the rates of rotation and cyclisation, this makes chiral transfer unlikely for enamides **273-275**, **305-306**, **331-333**. However taken with the results from section 5.2.1 it has become evident that the rates of rotation need to be decreased and that this may be possible by changing the substitution pattern of the enamides. Consequently a number of tetrasubstituted enamides were prepared to determine if they could offer a route to chiral transfer in 5-*endo trig* radical cyclisations.

5.2.7 Tetrasubstituted Enamides

In section 5.2.1 it was recognised that α -tetralone enamide **306**, substituted in the β' position, gave rise to the greatest barrier to rotation about the *N*-alkenyl

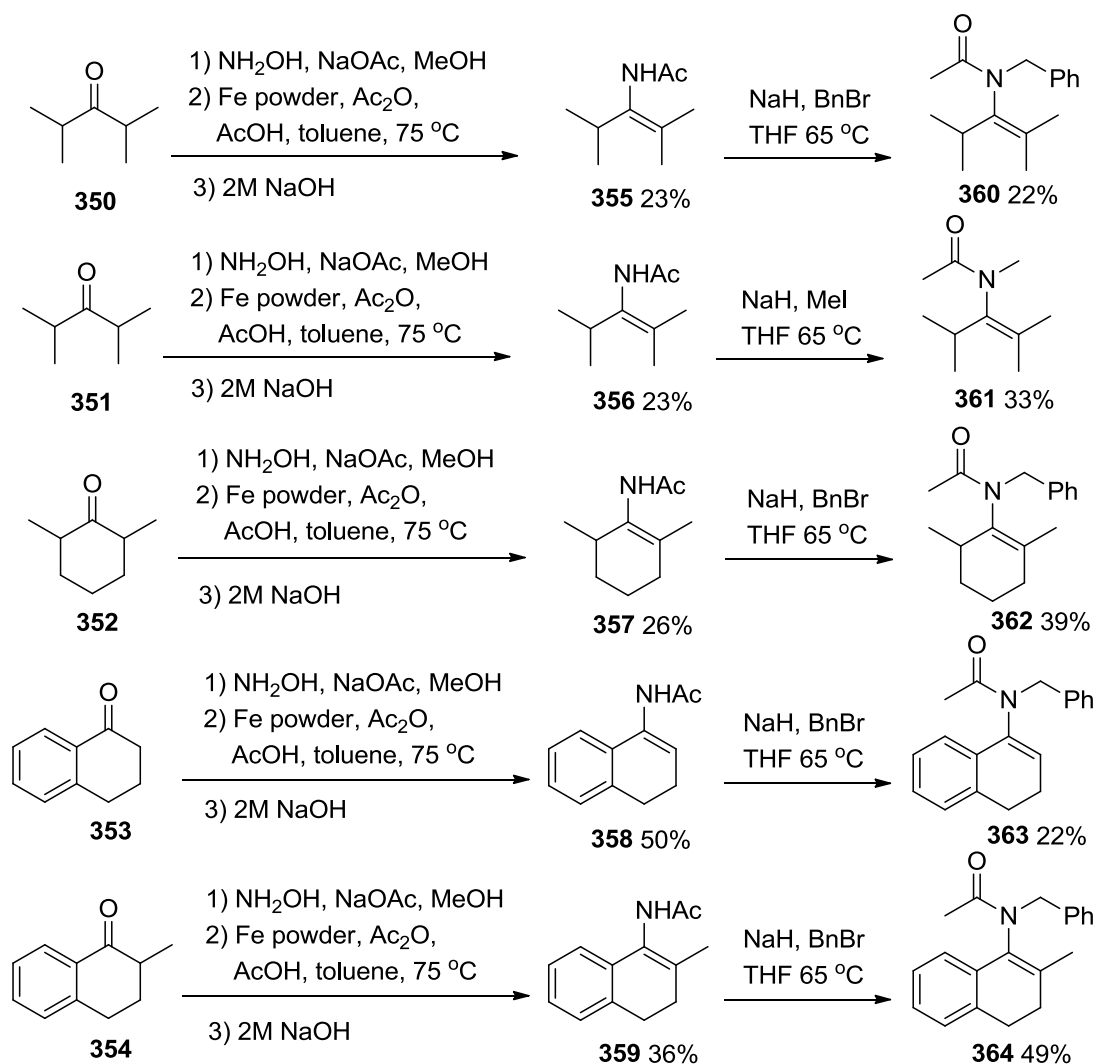
bond.¹⁸² Consequently, a range of enamides, with both β and β' substitution were pursued in order to determine the magnitude of their rotation barriers and assess their potential utility as substrates able to undergo chiral transfer during 5-endo trig radical cyclisation.



306 ~ 18 kcal mol⁻¹

Figure 5.27: Trisubstituted α -Tetralone Enamide 306

Attempts to synthesise tetrasubstituted enamides using the existing synthetic route, involving acetylation of corresponding imines was unsuccessful. As a result, an alternative synthesis of enamides^{227,228,229,230,231} from the corresponding ketones *via* oxime intermediates was pursued. Hence oxime formation, followed by iron-mediated rearrangement then alkylation²³² gave the *N*-benzyl enamides **360-364** (Scheme 5.22).



Scheme 5.22: Synthesis of Tetrasubstituted Enamides

Although the yields obtained were not impressive, they were ample for the purpose of the investigation. α -Tetralone enamide **363** was analysed by variable temperature NMR (appendix A) and a barrier (ΔG_{298}^\ddagger) of 17.7 kcal mol⁻¹ was determined which equated to a rate of rotation of the *N*-alkenyl bond (k_{rot}) of 0.7 s⁻¹. This was not as low as would have been predicted given the results obtained for α -tetralone **306** in section 5.2.1, and the effect of acyl substitution as determined in section 5.2.2. The tetrasubstituted enamides were all thought to have rotation barriers significantly larger than α -tetralone enamide **306** (18.0 kcal mol⁻¹), and consequently were not analysed by variable temperature NMR. Instead they were

sent to Pittsburgh for HPLC analysis and separation by Prof Dennis Curran co-workers.

Pleasingly, separation of enamides **360-362** and **364** was possible by chiral HPLC using a Whelk-O[®] column. A degree of separation was observed for **361** (appendix B), but given that the other substrates were benzylated and provided much better separation, this was not analysed any further, or considered for possible chiral transfer in this investigation. Substrates **360** (Figure 5.28) and **364** (Figure 5.29) gave particularly good separation. Their atropisomers were resolved and their barriers to rotation were determined. Enamide **360** had been partially resolved previously and its barrier to rotation had been measured ($\sim 24 \text{ kcal mol}^{-1}$).²²⁰ For this study, in which the barrier was determined from the rate of racemisation using chiral HPLC, it was calculated as $25.7 \text{ kcal mol}^{-1}$. Likewise the barrier for **364** was found to be $27.5 \text{ kcal mol}^{-1}$.

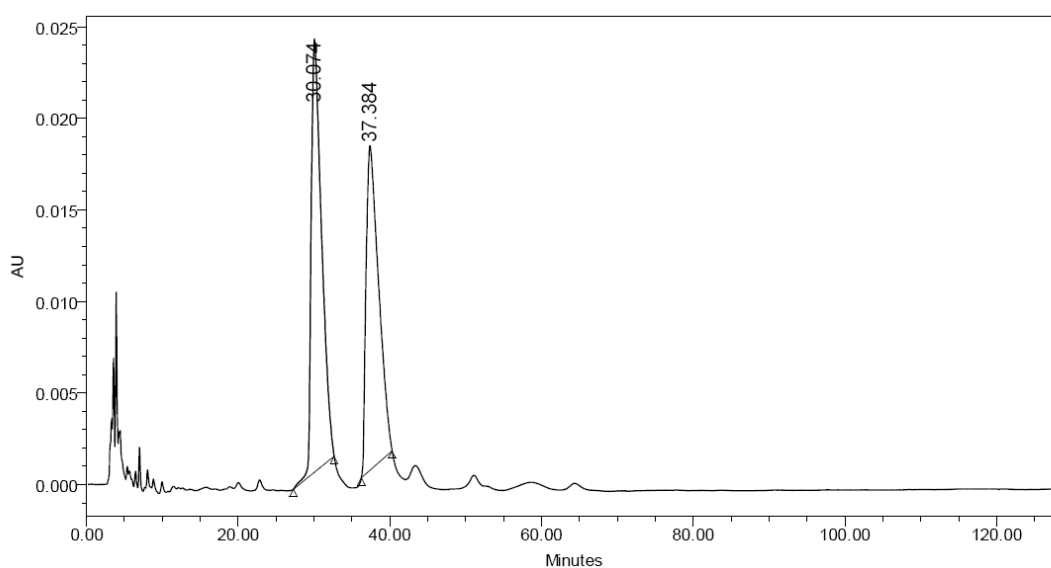
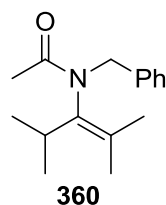


Figure 5.28: HPLC Trace of Tetrasubstituted Enamide **360** Showing Two Atropisomers

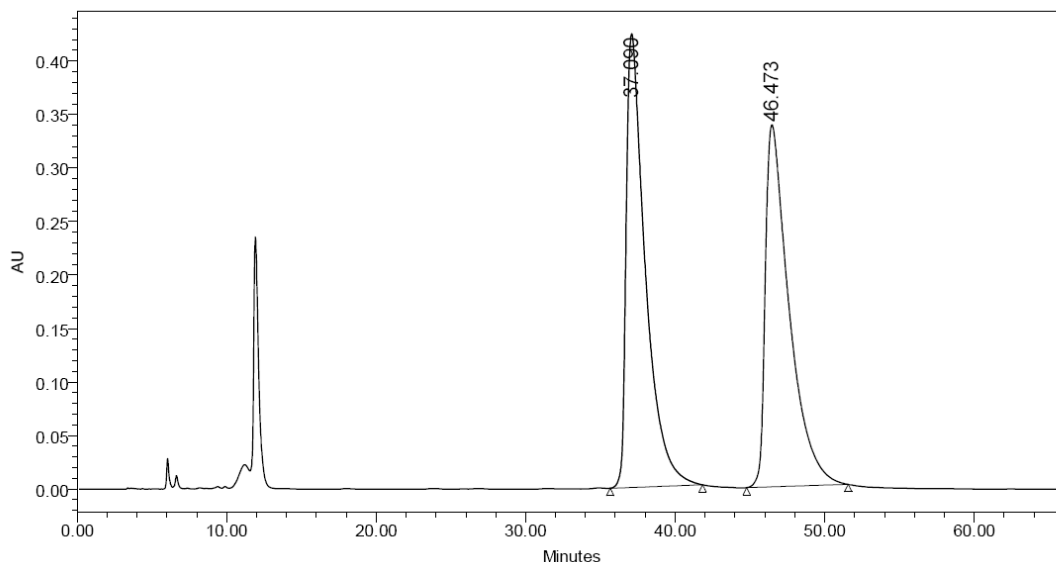
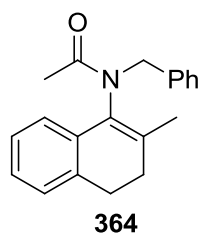


Figure 5.29: HPLC Trace of Tetrasubstituted Enamide 364 Showing Two Atropisomers

The barrier for **362** (appendix B) was not determined, but due to the structural similarity with **360** it is presumably ~ 25 kcal mol⁻¹. A crystal structure of **364** was solved (Figure 5.30), and it resembled the anilide structure rather than that observed for the β -tetralone **305**. The *N*-alkenyl bond torsion angle was found to be 74.3° , the *N*-CO angle was 175.1° and finally the sum of the angle around nitrogen was 359.9 , suggesting the nitrogen was sp^2 hybridised.

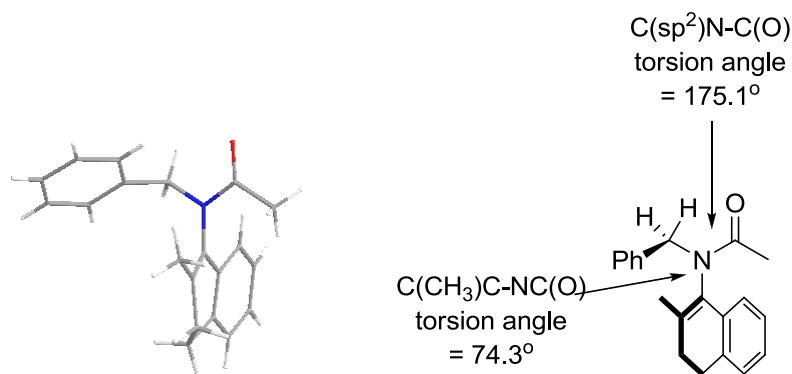
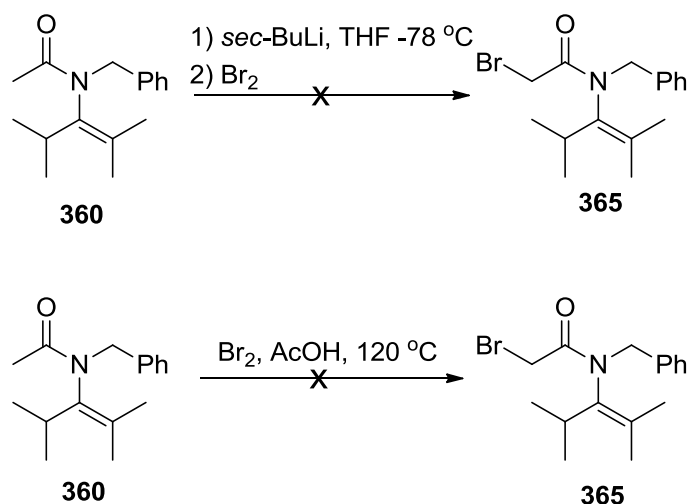


Figure 5.30: X-Ray Crystal Structure of Tetrasubstituted Enamide 364

Unfortunately, despite the tetrasubstituted enamides being resolvable by chiral HPLC, there was no radical source (halogen) present to initiate cyclisation by either organostannane- or copper-mediated processes. Therefore, bromination at the α -carbon of the acyl group of **360** was attempted. Given the results obtained in section 5.2.2 these α -bromoenamides would be expected to have barriers > 25.7 kcalmol⁻¹ and therefore would also be resolvable.

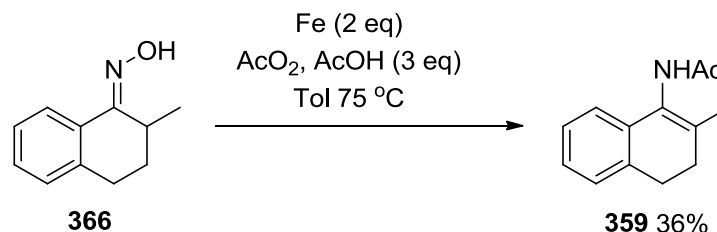
Two methods of bromination were attempted^{233,234} Acid-catalysed bromination using Br₂ in acetic acid was unsuccessful, as was base-mediated bromination, using *sec*-BuLi and Br₂ (Scheme 5.23). For base-mediated bromination, both normal and inverse addition of the anion formed was unsuccessful. The acid catalysed reaction led to the isolation of only starting material **360** even after prolonged periods of heating (3 days), whereas the base-catalysed reaction led to hydrolysis of the amide bond, presumably due to the acceleration of the haloform reaction.



Scheme 5.23: Unsuccessful Attempts at Bromination of Tetrasubstituted Enamide 360

Alternative approaches to halogen introduction were attempted. The Fe mediated rearrangement²³¹ of oximes (Scheme 5.24) to give enamides (**366** \rightarrow **359**)

has been only been reported using simple anhydrides (acetic anhydride) as acylating agents.



Scheme 5.24: Fe Mediated Synthesis of Tetrasubstituted Enamides

The ability to use trichloroacetyl chloride and chloroacetyl chloride in place of acetic anhydride in this reaction has not been investigated previously. These acetylating agents were applied to the rearrangement reaction and although the reactions were unoptimised, halogen-containing enamides **367-371** (Figure 5.31) were prepared. In addition **359** was alkylated using *o*-bromobenzyl bromide to give **372** as an alternative radical cyclisation substrate.

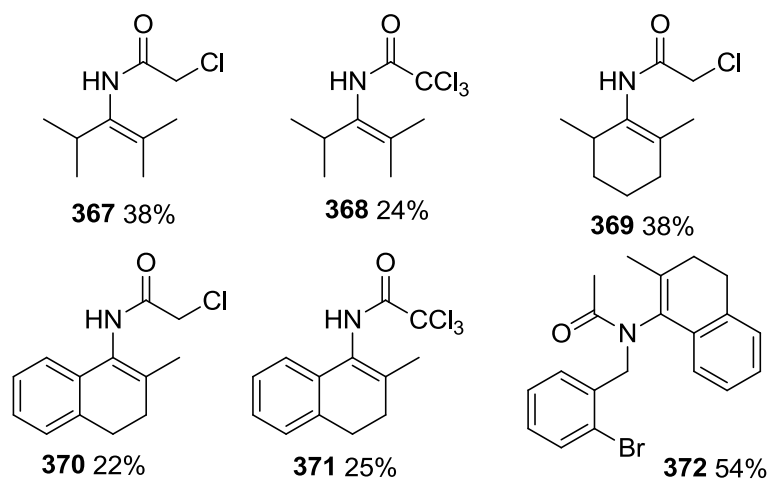
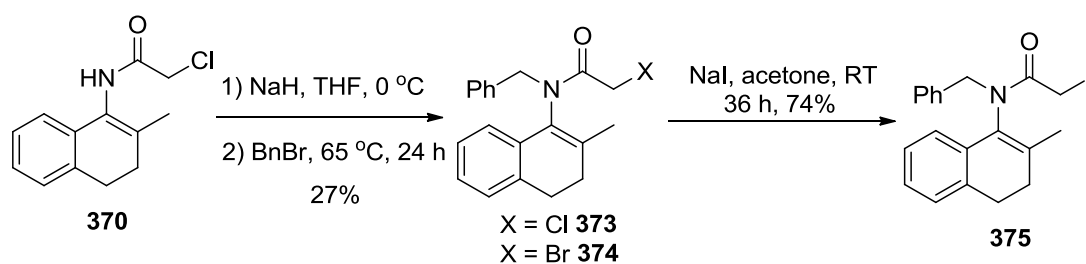


Figure 5.31: Tetrasubstituted Enamides Synthesised by Iron Mediated Acetylation

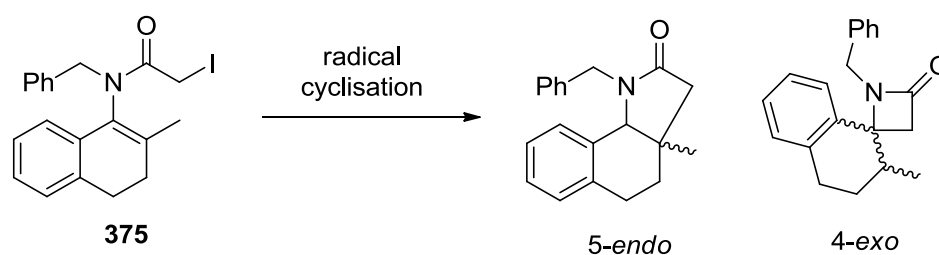
At this stage attentions were focused to the attempted (racemic) cyclisation of **375** formed from the benzylation of enamide **370** with benzyl bromide. As the product of this benzylation reaction was a 5 : 1 mixture of α -chloro and α -bromo enamides **373** and **374**, a literature procedure²⁰⁹ of the Finkelstein reaction using sodium iodide (NaI) in acetone was performed to convert the mixture to the α -iodoenamide **375**.



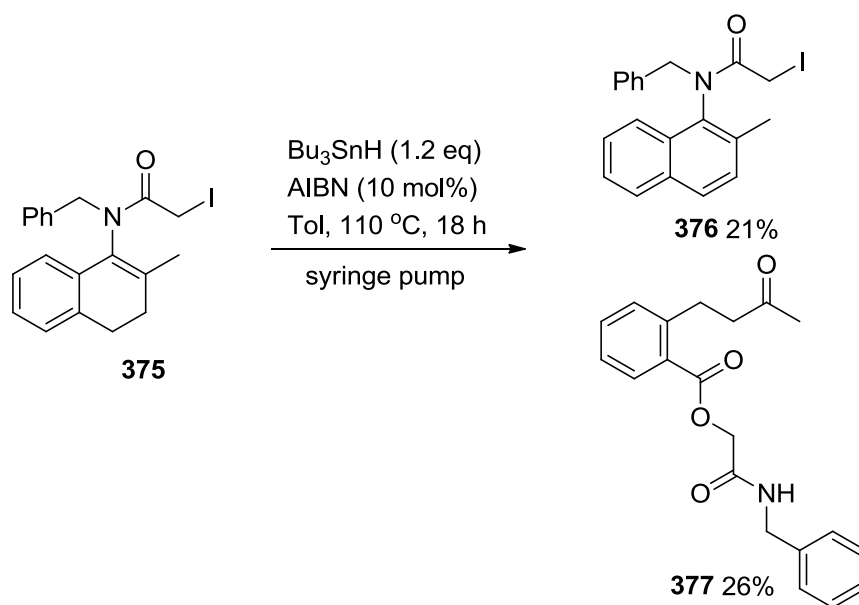
Scheme 5.25: Procedure for the Alkylation of Tetrasubstituted Enamides

Mechanistic studies of the cyclisations of α -haloenamides performed by Curran and co-workers have shown that the rate for cyclisation (k_c) depends on the nature of the halogen present in the radical precursor, despite the reactions going through identical intermediates.²¹³ Unfortunately, it was determined in their studies that α -iodoenamides were the poorest cyclisation substrates, leading to the highest proportion of direct halogen reduction. Cyclisation was observed at low tin concentrations, but diminished as the concentration was increased. Consequently it was hoped that some cyclisation of **375** would be observed at low tin concentrations.

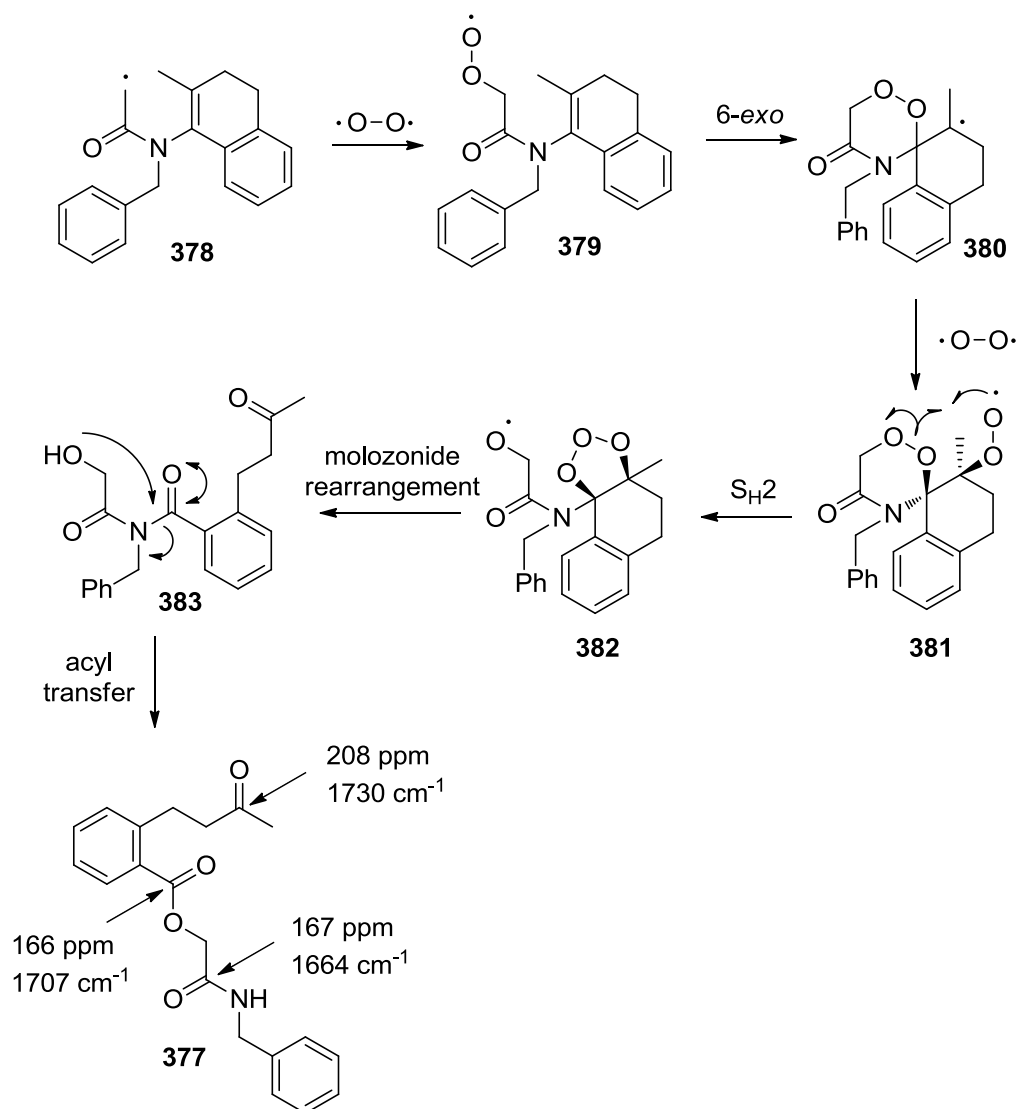
Enamide **375** was chosen for cyclisation due to its significantly larger barrier to rotation ($>27.5 \text{ kcal mol}^{-1}$). Considering the substitution pattern of the alkenyl bonds it was difficult to predict whether 4-*exo* or 5-*endo trig* cyclisation would predominate (Scheme 5.26). However, either outcome would result in an asymmetric centre to which chiral information could be transferred from **375**.

Scheme 5.26: Possible Products From the Cyclisation of **375**.

Copper mediated cyclisations are generally unsuccessful for primary α -halo precursors, and consequently the standard tin reaction was attempted using AIBN, in toluene at reflux, using a syringe pump to maintain the tin concentration at ~ 10 mM. To ensure the absence of moisture and air, both the reaction and reagent mixtures (in toluene) were thoroughly degassed prior to the reaction. Despite this, no cyclisation was observed and a mixture of interesting, seemingly oxidized, products **376** and **377** were obtained (Scheme 5.27).

Scheme 5.27: Attempted Tin-Mediated Radical Cyclisation of Tetrasubstituted Enamide **375**

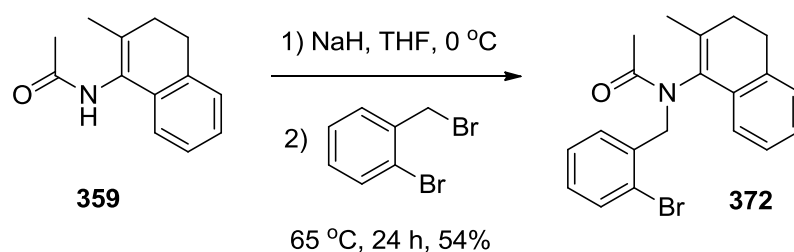
It was initially unclear how these oxidized products could be formed under reductive conditions. A second sample of **375** was heated in toluene with AIBN (1 equivalent), in the absence of Bu₃SnH and open to the atmosphere. Under these conditions the naphthalene **376** was obtained in 53% yield along with unreacted starting material. This indicated that the AIBN mediated rate of the oxidation, to form the naphthalene, was likely to have been quicker than initiation of the radical chain leading to the homolysis of the C-I bond. The greatest confusion came from the formation of **377**, which could only be identified after HRMS, IR and exhaustive NMR analysis. Standard ¹³C NMR (75 MHz) indicated the existence of three carbonyl groups (208.2, 167.3, 166.1 ppm), and this was confirmed by three distinguishable bands in the IR (1731, 1701, 1665 cm⁻¹). The HRMS revealed a molecular formula of C₂₀H₂₁NNaO₄, which indicated that there must have been adventitious oxygen (at least 2 molecules) present in the reaction mixture. Mechanistically it is unclear how **377** was formed but we can speculate that cleavage of the enamide bond may have taken place after the addition of oxygen to the radical intermediate **378** (Scheme 5.28).

Scheme 5.28: Proposed Mechanism for the Formation of **377**

Hence, 6-*exo* cyclisation of the peroxy radical **379**, followed by trapping with another molecule of oxygen would furnish **381** which, after a ' $\text{S}_{\text{H}2}$ '-like reaction and molozonide rearrangement would furnish imide **383**. Given this rationale, it was initially thought that the compound isolated could have been intermediate **383**. However the actual structure **377** was confirmed after a HMBC experiment was performed. This showed the amide C=O (167 ppm) coupling with both the adjacent CH_2 and the benzyl CH_2 (through the amide bond). Additionally it confirmed the position of the ester functional group as its C=O (166 ppm) was seen to couple with

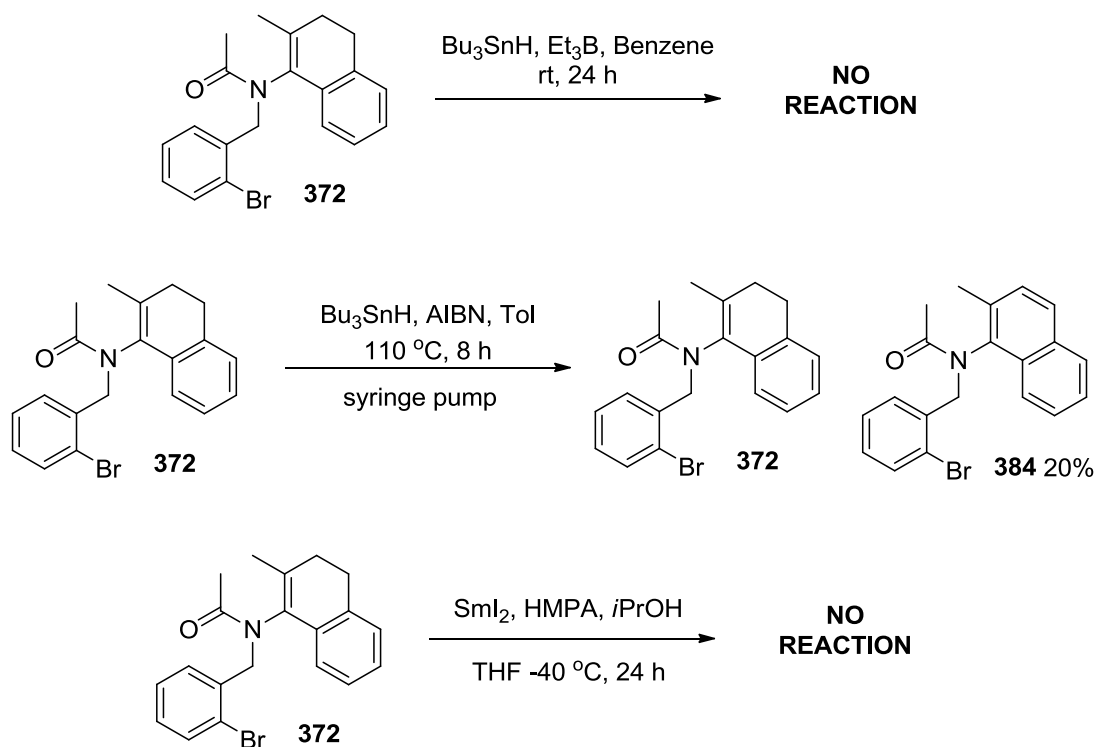
both the aryl ring and the CH₂ adjacent to the ester bond. Thus, if this mechanistic pathway was followed intermediate **383** must have undergone a further acyl transfer during the course of the reaction. The failure to isolate a racemic cyclised product was disappointing. The production of **377** was particularly intriguing and confirmation of the ‘pseudo-ozonolysis’ mechanism would require a number of reactions designed to trap out the radical intermediates for characterization and was beyond the scope of this investigation.

Finally, in the hope of observing a cyclisation reaction for the tetrasubstituted enamides, an aryl bromide analogue of **364** was synthesized using *o*-bromobenzyl bromide as the alkylating agent to produce **372**.



Scheme 5.29: Synthesis of an Alternative Precursor for Tetrasubstituted Enamide Radical Cyclisation

It was predicted that cyclisation may be more favourable for the aryl bromide **372** as the reactive aryl radical could undergo *5-exo trig* cyclisation attacking the α -carbon of the enamide. Support for this hypothesis comes from the rates of cyclisation obtained for the *5-exo trig* cyclisation of aryl radicals formed from acrylanilides.¹⁷⁹ Indeed the first reaction attempted borrowed the conditions from such reactions utilising Et₃B as an initiator at room temperature, open to the atmosphere. Unfortunately, after 24 hours only starting material was recovered (Scheme 5.30).

Scheme 5.30: Unsuccessful Protocols Attempted to Observe Cyclisation of **372**

Repeating the reaction using the standard tin conditions was equally disappointing. Again no cyclisation was observed and, similar to the reaction of α -iodoamide **375**, a naphthalene derivative **384** was obtained, as indicated by additional aromatic doublets at 7.81 and 7.75 ppm in the crude NMR, suggesting an oxidation was taking place under reductive reaction conditions. Subsequently, a 2 : 1 mixture of **372** and **384** was heated at reflux in the presence of AIBN and absence of Bu_3SnH . This caused the ratio of the naphthalene to increase and a 1 : 2 ratio of **372** and **384** was re-isolated, suggesting that, like the α -iodoamide **375**, the AIBN was responsible for the oxidation. A third and final attempt was made to cyclise **372**, using the samarium iodide (SmI_2),²³⁵ hexamethylphosphoramide (HMPA) technique. This too was unsuccessful, leading to the recovery of only starting material.

It was surprising that, given that no cyclisation was observed, no directly reduced product (**364**) was obtained. The structure of **372** was solved by x-ray

crystallography in order to determine how hindered the aryl bromide was (Figure 5.32).

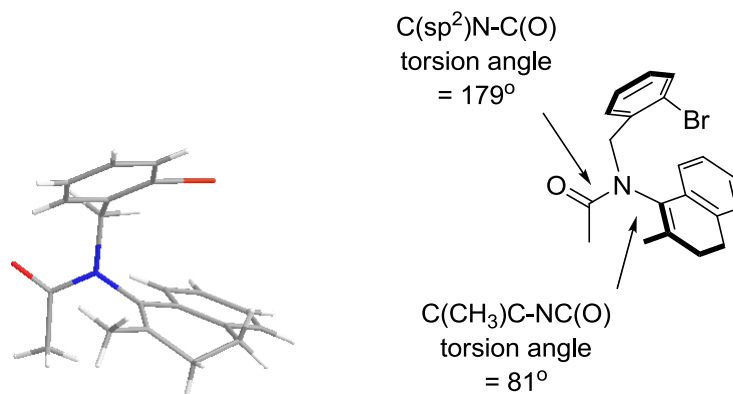


Figure 5.32: X-Ray Crystal Structure of Tetrasubstituted Cyclisation Precursor 372

The structure was comparable to the previously solved structures (**339** and **364**) and with anilides, and the relevant torsion angles were found to be 81° (*N*-alkenyl bond) and 179° (*N*-CO bond). Furthermore the sum of the bond angles around nitrogen was found to be 359.6° indicative of sp² hybridisation. The bromine did not appear to be particularly hindered but there was a degree of disorder associated with a rotation around the C-C(aryl) bond, which placed the bromine away from the alkenyl bond in the minor rotamer. On closer examination it was clear that cyclisation would be difficult for either rotamer as the aryl radicals produced would not be in close proximity to the alkenyl group for 5-*exo trig* cyclisation.

5.2.8 Conclusions

A number of enamides have been prepared in order to gain an insight into their potential as possible reagents for chiral transfer in 4-*exo* and 5-*endo trig* radical

cyclisation reactions. Variable temperature NMR was used to determine the rate of rotation and barrier to rotation about the *N*-alkenyl bond. The size of the cycloalkenyl group had little effect on the barrier to rotation. However, when the enamide is substituted at the β '-position, particularly if it is sp^2 hybridised (resembling an anilide) then the barrier was seen to significantly increase (**306**, 18.0 kcal mol⁻¹). Substitution at the acyl group also allowed for a crude estimation of the rotation barrier for the reactive radicals, which up to now have been unknown, but are crucial in establishing the potential for chiral transfer. Using sp^3 and sp^2 hybridised 'radical models' the barrier to rotation was found to decrease by 1-2 kcal mol⁻¹ compared to the radical precursors, which equates to a 5-26 fold increase in rate of rotation about the *N*-alkenyl bond. Finally, tetrasubstituted enamides have been prepared, substituted at the β and β '-positions. These have been resolved by chiral HPLC and the barriers for two examples (**360** and **364**) have been found to be significantly higher (25.7-27.5 kcal mol⁻¹) than any other enamide synthesised during this investigation. Halogens were incorporated to prepare an enamide suitable for cyclisation. The barrier to rotation was not measured for this enamide but it is safe to assume that it would be >27.5 kcal mol⁻¹, and therefore resolvable and suitable for chiral transfer. However, attempts to racemically cyclise the tetrasubstituted enamides **375** and **372** were unsuccessful.

5.3 FUTURE WORK

It was possible to prepare resolvable enamides, however, attempts to cyclise them were unsuccessful. A common problem associated with the cyclisations of tetralone derived enamides **372** and **375** was AIBN initiated aromatisation, forming a

naphthalene product. To alleviate this problem a number of alternative substrates could be prepared. Indanone enamides **385-387**, would have a lower barrier to rotation than the tetralone enamide (up to 3.3 kcal mol⁻¹ lower based on the comparison between cyclopentenyl and cyclohexenyl enamides in section 5.2.1), but aromatisation would not be possible. Furthermore, the potential 5-*exo trig* cyclisation of these enamides could be investigated using more flexible groups **386**.

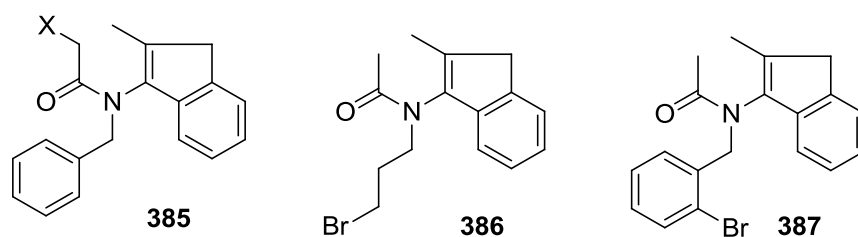
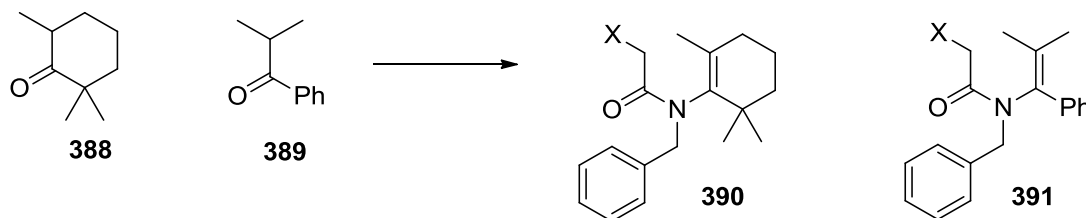


Figure 5.33: Alternative Tetrasubstituted Enamides

Other commercially available ketones such as **388** and **389** could also provide access to enamides **390** and **391** that may have barriers to rotation great enough to be resolved by chiral HPLC (based on results for other tetrasubstituted enamides **360-364**) and would also avoid the problem of possible aromatisation.



Scheme 5.31: Alternative Tetrasubstituted Enamides

6.0 Experimental

6.1 GENERAL INFORMATION AND PROCEDURES

All reactions were performed using oven dried glassware and heat transfer was achieved using either an oil bath (chapter 2) or drysyn[®] apparatus. All reactions were performed using commercially available anhydrous solvents, and exhaustive deoxygenation was not required except for the case of 1,4-DMP which required thorough degassing and an inert atmosphere. Degassing was achieved using the freeze-pump-thaw technique and reactions were performed on a Schlenk line under a nitrogen atmosphere. With the exception of 1,4-DMP, all chemicals were used as received without any further purification.

Reactions were followed by TLC, performed on silica coated aluminium plates (Merck Kieselgel 60F₂₅₄ 230-400 mesh) developed either from UV fluorescence (254 nm) or potassium permanganate. Flash chromatography was carried out using Merck 9385 Kieselgel 60 SiO₂ (230-400 mesh).

IR was achieved using a Perkin-Elmer 1720X Fourier transform spectrometer. Solids were compressed into a thin tablet and oils/non-volatile liquids were analysed as films over a diamond sensor.

¹H and ¹³C NMR spectroscopy was performed on Bruker DPX300 and DPX400 machines at either 300 or 400 MHz and 75 or 100 MHz respectively. Chemical shifts are quoted in ppm relative to the internal standard tetramethylsilane ($\delta = 0$) and reference to the residual solvent. All coupling constants are quoted in hertz (Hz). For variable temperature NMR samples were submitted to the NMR service and analysis on a Bruker DPX500 spectrometer. Spectra obtained were

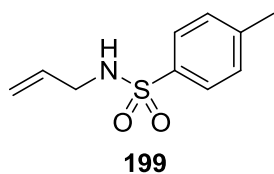
analysed using Mestrec[®] and NUTS[®] software prior to lineshape analysis using WINDNMR.²²¹

Mass Spectroscopy was achieved using either electron, chemical or electrospray ionisation techniques. The bulk of low resolution analyses were performed on a Bruker Esquire 200 machine. Accurate mass spectroscopy was available through the in house mass spec service using either Bruker HCT or Bruker HCT Ultra machines to perform accurate mass ESI analysis. Elemental analysis was performed by Warwick Analytical Service using a CE440 Elemental Analyser.

Analytical chiral HPLC was performed by the Curran group in Pittsburgh and was conducted using either an (*S,S*)-Whelk-O 1 column (Pirkle, 250 mm x 4.6 mm ID) or a Chiralcel OD column (Daicel, 250 mm x 4.6 mm ID).

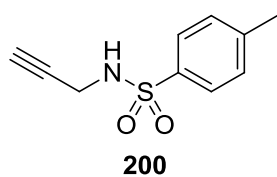
6.2 GENERAL PROCEDURES

6.2.1 General Procedure for Substrates Synthesised in Chapter 2

6.2.1.1 *N*-Allyl-4-methyl-benzenesulfonamide **199**²³⁶

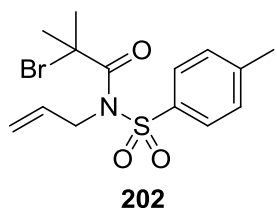
Allylamine (4.50 ml, 60.0 mmol) was dissolved in dichloromethane (70 cm³) and cooled to 0°C. Triethylamine (8.36 ml, 60.0 mmol) was added followed by *p*-toluenesulfonyl chloride (11.40 g, 60.0 mmol) in dichloromethane (70 cm³), which was added via a dropping funnel over 5 minutes. The reaction was allowed to reach room temperature overnight. After 18 hrs the reaction was quenched with 1 M HCl (150 cm³) and the aqueous layer was extracted using dichloromethane (3 x 150 cm³). The combined organic extracts were washed with brine (150 cm³), dried using MgSO₄, filtered and concentrated in *vacuo* to yield **199** as a pale yellow solid (11.72 g, 55.5 mmol, 93%); *R_f* (3:1 petrol:EtOAc) 0.56; mpt 64-65 °C, lit²³⁶ 64-65 °C; ν_{\max} (cm⁻¹) 3245, 2852, 1595, 1493, 1422, 1317, 1289, 1156, 1061, 810; δ_{H} (300 MHz, CDCl₃) 7.75 (2H, d, J_{HH} 8.1, Ar), 7.31 (2H, d, J_{HH} 8.1, Ar), 5.71 (1H, ddt, J_{HH} 17.1, 10.2, 5.7 Hz, $\text{CH}=\text{CH}_2$), 5.19 (1H, dd, J_{HH} 17.1, 1.5 Hz, $\text{CH}=\text{CH}_2$), 5.10 (1H, dd, J_{HH} 10.2, 1.5 Hz, $\text{CH}=\text{CH}_2$), 4.70 (1H, br t, J_{HH} 6 Hz, NH), 3.57 (2H, ddd, J_{HH} 6.0, 5.7, 1.5 Hz, $\text{N}-\text{CH}_2$), 2.42 (3H, s, CH_3); δ_{C} (75.5 MHz, CDCl₃) 142.9 (Ar quaternary), 136.3 (Ar quaternary), 132.4 ($\text{CH}=\text{CH}_2$), 129.1, 126.5 (Ar), 117.1 ($\text{CH}=\text{CH}_2$), 45.2 ($\text{N}-\text{CH}_2$), 20.9 (CH_3); *m/z* (EI) 211 [M]⁺; [Found: C, 56.7; H, 6.2; N, 6.6; C₁₀H₁₃NO₂S requires: C, 56.9; H, 6.3; N, 6.6].

6.2.1.2 4-Methyl-N-prop-2-ynyl-benzenesulfonamide **200**²³⁷



Using the same procedure as 6.2.1.1, propargylamine (1.00 g, 18.2 mmol), triethylamine (5.60 ml, 40.0 mmol) and *p*-toluenesulfonyl chloride (3.47 g, 18.2 mmol) in dichloromethane (30 cm³) yielded **200** as an off-white solid (3.43 g, 16.4 mmol, 90%). *R_f* (3:1 petrol:EtOAc) 0.31; mpt 77-78 °C, lit²³⁷ 77-78 °C; ν_{\max} (cm⁻¹) 3267, 2858, 2596, 1436, 1320, 1156, 1091, 1066, 869, 813, 698; δ_{H} (300 MHz, CDCl₃) 7.71 (2H, d, J_{HH} 8.1 Hz, Ar), 7.24 (2H, d, J_{HH} 8.1 Hz, Ar), 4.74 (1H, br t, J_{HH} 5.7, NH), 3.76 (2H, dd, J_{HH} 5.7, 2.4 Hz, N-CH₂), 2.36 (3H, s, CH₃), 2.04 (1H, t, J_{HH} 2.4 Hz, CH); δ_{C} (75.5 MHz, CDCl₃) 143.9 (Ar quaternary), 136.5 (Ar quaternary), 129.7, 127.4 (Ar), 73.0 (CH), 32.9 (N-CH₂), 21.6 (CH₃); *m/z* (EI) 209 [M]⁺; [Found: C, 57.1; H, 5.3; N, 6.6; C₁₀H₁₁NO₂S requires: C, 57.4; H, 5.3; N, 6.7].

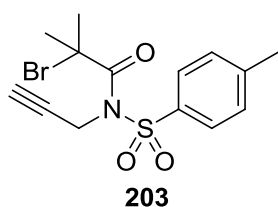
6.2.1.3 *N*-Allyl-*N*-(2-bromo-2-methyl-propionyl)-4-methyl-benzenesulfonamide **202**²³⁸



N-Allyl-4-methyl-benzenesulfonamide (2.11 g, 10.0 mmol) was dissolved in dry THF (100 cm³) and cooled to -78°C at which point *n*-BuLi (2.5 M in hexanes, 4.40 ml, 11.0 mmol) was added dropwise via syringe. The reaction was allowed to proceed for 30 mins, 2-bromoisobutyryl bromide (1.48 ml, 12.0 mmol) was added and the reaction was allowed to reach room temperature overnight. The reaction was quenched with NH₄Cl (10 cm³) and partitioned between NaHCO₃ (200 cm³) and dichloromethane (200 cm³). The aqueous layer was extracted using dichloromethane (2 x 200 cm³).

The combined organic extracts were washed with brine (200 cm³), dried with MgSO₄, filtered and concentrated in *vacuo* to yield a crude yellow oil as product. Purification was achieved *via* flash chromatography, eluting with 5:1 pet ether:EtOAc, monitored by TLC eluting with 3:1 hexane:EtOAc, to afford **202** as a pale yellow solid (1.80 g, 5.0 mmol, 50%); *R_f* (3:1 petrol:EtOAc) 0.73; mpt 82-84 °C, lit²³⁸ 83-84 °C; ν_{\max} (cm⁻¹) 2961, 2935, 2873, 1672, 1593, 1458, 1350, 1315, 1287, 1187, 1117, 1086, 925, 717; δ_{H} (300 MHz, CDCl₃) 7.86 (2H, d, *J*_{HH} 8.1 Hz, Ar), 7.30 (2H, d, *J*_{HH} 8.1 Hz, Ar), 5.98 (1H, ddt, *J*_{HH} 17.1, 10.5, 4.8 Hz, CH=CH₂), 5.39 (1H, br d, *J*_{HH} 17.1 Hz, CH=CH₂), 5.38 (1H, br d, *J*_{HH} 10.5 Hz, CH=CH₂), 4.95 (2H, dt, *J*_{HH} 4.8, 1.8 Hz, N-CH₂), 2.43 (3H, s, CH₃), 1.88 (6H, s, C(CH₃)₂); δ_{C} (75.5 MHz, CDCl₃) 170.4 (C=O), 144.7 (Ar quaternary), 136.1 (Ar quaternary), 133.6 (CH=CH₂), 129.2, 128.9 (Ar), 118.2 (CH=CH₂), 57.0 (C(CH₃)₂), 50.6 (N-CH₂), 32.0 (C(CH₃)₂), 21.7 (Ar-CH₃); *m/z* (ESI) 361 ([M]⁺H); [Found: C, 46.8; H, 5.0; N, 3.9; C₁₄H₁₈BrNO₃S requires: C, 46.6; H, 5.0; N, 3.9].

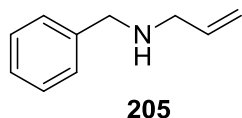
6.2.1.4 *N*-(2-bromo-2-methyl-propionyl)-4-methyl-*N*-prop-2-ynyl-benzenesulfonamide **203**²³⁸



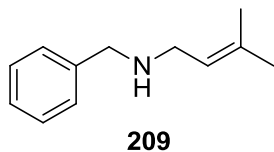
Using the same procedure as 6.2.1.3 4-methyl-*N*-prop-2-ynyl-benzenesulfonamide (1.05 g, 5 mmol) dissolved in dry THF (50 cm³), *n*-BuLi (2.5M in hexanes, 2.20 ml, 5.5 mmol), and 2-bromoisobutyryl bromide (0.75 ml, 6.0 mmol) yielded a crude pale yellow oil. Purification was achieved *via* flash chromatography eluting with 5:1 pet ether:EtOAc, monitored by TLC eluting with 3:1 hexane:EtOAc, to afford **203** as a white solid (1.47 g, 4.1 mmol, 82%); *R_f* (3:1 petrol:EtOAc) 0.7; mpt 90-92 °C, lit²³⁸ 92-93

$^{\circ}\text{C}$; ν_{max} (cm^{-1}) 3293, 2934, 1678, 1594, 1457, 1350, 1170, 1084, 820; δ_{H} (300 MHz, CDCl_3) 7.97 (2H, d, J_{HH} 8.1 Hz, Ar), 7.31 (2H, d, J_{HH} 8.1 Hz, Ar), 5.13 (2H, d, J_{HH} 2.4 Hz, N- $\underline{\text{CH}}_2$), 2.46 (1H, t, J_{HH} 2.4 Hz, $\underline{\text{CH}}$), 2.43 (3H, s, Ar- $\underline{\text{CH}}_3$), 1.94 (6H, s, C($\underline{\text{CH}}_3$) $_2$); δ_{C} (75.5 MHz, CDCl_3) 169.7 ($\underline{\text{C}}=\text{O}$), 145.0 (Ar quaternary), 135.6 (Ar quaternary), 129.3, 129.1 (Ar), 78.8 ($\underline{\text{C}}\text{CH}$), 74.0 ($\underline{\text{C}}\text{H}$), 56.7 ($\underline{\text{C}}(\text{CH}_3)_2$), 37.8 (N- $\underline{\text{C}}\text{H}_2$), 31.7 (C($\underline{\text{C}}\text{H}_3$) $_2$), 21.7 (Ar- $\underline{\text{C}}\text{H}_3$); m/z (EI) 359 ($[\text{M}]^+\text{H}$); [Found: C, 47.2; H, 4.5; N, 3.9; $\text{C}_{14}\text{H}_{16}\text{BrNO}_3\text{S}$ requires: C, 46.9; H, 4.5; N, 3.9].

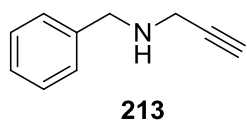
6.2.1.5 *N*-Allyl-*N*-benzylamine **205**²³⁹



Benzyl bromide (2.00 ml, 16.5 mmol) was added dropwise to a mixture of allylamine (6.18 ml, 80.7 mmol) and K_2CO_3 (2.70 g, 19.4 mmol) forming a yellow suspension. Reaction was allowed to proceed overnight. The reaction mixture was filtered through a silica plug and washed with DCM (2 x 50 cm^3), and the resulting organic filtrate was concentrated in *vacuo*. The crude orange liquid was purified by gradient chromatography, eluting in 0-10% EtOAc in pet ether to yield **205** as a yellow liquid (1.00 g, 6.79 mmol, 41%). R_f (50% EtOAc/petrol) 0.92; ν_{max} (cm^{-1}) 3254, 3027, 2809, 1495, 1453, 1359, 1105, 1028, 993, 915, 732; δ_{H} (300 MHz, CDCl_3) 7.35-7.28 (5H, m, Ar), 5.96 (1H, ddt, J_{HH} 17.1, 10.2, 6.0 Hz, $\underline{\text{C}}\text{H}=\text{CH}_2$), 5.22 (1H, ddt, J_{HH} 17.1, 1.5, 1.2 Hz, $\text{CH}=\underline{\text{C}}\text{H}_2$), 5.14 (1H, ddt, J_{HH} 10.2, 1.5, 1.2 Hz, $\text{CH}\underline{\text{C}}\text{H}_2$), 3.82, (2H, s, Ar $\underline{\text{C}}\text{H}_2$), 3.31 (2H, dt, J_{HH} 6.0, 6.0, 1.2 Hz, N- $\underline{\text{C}}\text{H}_2$), 1.46 (1H, br s, $\underline{\text{N}}\text{H}$); δ_{C} (75 MHz, CDCl_3) 139.7 (quaternary), 136.0 ($\underline{\text{C}}\text{H}=\text{CH}_2$) 128.8, 128.2, 126.9 (Ar), 117.4 ($\text{CH}=\underline{\text{C}}\text{H}_2$), 57.8 (N- $\underline{\text{C}}\text{H}_2$), 56.4 (Ar- $\underline{\text{C}}\text{H}_2$); m/z (EI) 147 [M^+]; [Found: [M^+] 147.1052; $\text{C}_{10}\text{H}_{13}\text{N}$ requires 147.1048].

6.2.1.6 *N*-(3-methyl-2-butenyl)-*N*-benzylamine **209**²⁴⁰

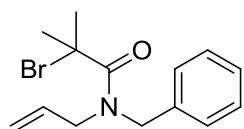
3,3-Dimethylallyl bromide (1.56 ml, 12.1 mmol) was added dropwise, via syringe, to stirring benzylamine (8.0 ml, 72.5 mmol) at room temperature. After 44 hrs the reaction mixture was diluted with water (50 cm³) and ether (50 cm³). The resulting aqueous layer was extracted using ether (2 x 50 cm³) and the combined organic layers were washed with brine (50 cm³), dried over MgSO₄, filtered and concentrated in *vacuo*. The crude liquid was purified via gradient chromatography eluting with 0-10% EtOAc in petrol to yield **209** as a pale yellow liquid (1.35 g, 7.8 mmol, 64%). *R_f* (50% EtOAc/petrol) 0.23; ν_{\max} (cm⁻¹) 3293, 2981, 1495, 1461, 1411, 1247, 1166, 1108, 710, 696; δ_{H} (300 MHz, CDCl₃) 7.34-7.27 (5H, m, Ar), 5.32 (1H, m, CH), 3.81 (2H, s, ArCH₂) 3.25 (2H, d, *J*_{HH} 6.9 Hz, N-CH₂), 1.75 (3H, s, C(CH₃)), 1.64 (3H, s, C(CH₃)), 1.37 (1H, br s, NH); δ_{C} (75 MHz, CDCl₃) 140.5 (Ar quaternary), 134.5 (C(CH₃)₂), 128.4, 128.4, 126.9 (Ar), 123.0 (CH), 60.4 (N-CH₂), 53.5 (Ar-CH₂), 25.8 (C(CH₃)₂), 21.1 (C(CH₃)₂); *m/z* (ESI) 176 ([M]⁺H); [Found: C, 81.7; H, 9.9; N, 7.4; C₁₂H₁₇N requires: C, 82.2; H, 9.8; N, 7.9].

6.2.1.7 *N*-Benzyl-2-propynylamine **213**²⁴¹

Using the same procedure as 6.2.1.5, propargyl bromide (3.75 cm³, 33.6 mmol) and benzylamine (22.0 cm³, 201.3 mmol) furnished the crude product. Gradient chromatography eluting with 0-10% EtOAc in pet ether was performed to yield **213** as a yellow liquid (3.01 g, 20.7 mmol, 62%).

R_f (50% EtOAc/petrol) 0.52; ν_{\max} (cm^{-1}) 3291, 3063, 3030, 2923, 2817, 1495, 1453, 1328, 1117, 740; δ_{H} (300 MHz, CDCl_3) 7.27 (5H, m, Ar), 3.80 (2H, s, Ar- CH_2), 3.35 (2H, d, J_{HH} 2.4 Hz, N- CH_2), 2.18 (1H, t, J_{HH} 2.4 Hz, CH), 1.46 (1H, br s, NH); δ_{C} (75 MHz, CDCl_3) 139.4 (Ar quaternary), 128.5 128.4 127.2 (Ar), 82.1 (CH_2CCH), 71.6 (CH_2CCH), 52.3 (Ar- CH_2), 37.3 (N- CH_2); m/z (EI) 146.1 ($[\text{M}]^+\text{H}$); [Found: 146.0966; $\text{C}_{10}\text{H}_{12}\text{N}$ requires: 146.0970].

6.2.1.8 *N*-Allyl-*N*-benzyl-*N*-2-bromo-2-methyl-propanamide **206**

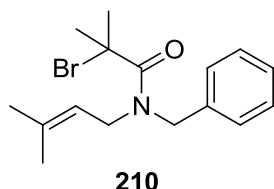


206

N-Allyl-*N*-benzylamine (0.43 g, 2.9 mmol) was dissolved in Et_2O (25 cm^3) and cooled to 0°C at which point Et_3N (0.70 cm^3 , 5.0 mmol) was added. After 20 mins 2-bromoisobutyryl bromide (0.36 cm^3 , 2.9 mmol) was added and the reaction mixture was allowed to reach room temperature. After 4 hours the reaction was quenched with sat. NH_4Cl (10 cm^3) and partitioned between sat. NaHCO_3 (50 cm^3) and Et_2O (50 cm^3). The organic layer was collected and the aqueous layer was extracted using Et_2O (2 x 50 cm^3). The combined organic extracts were dried over MgSO_4 , filtered and concentrated in *vacuo* to yield **206** as a colourless oil (0.72 g, 2.4 mmol, 84%). R_f (50% EtOAc/petrol) 0.84; ν_{\max} (cm^{-1}) 2980, 2932, 1633, 1495, 1463, 1410, 1169, 1106, 925, 727, 696; δ_{H} (300 MHz, CDCl_3) 7.35 (5H, m, Ar), 5.83 (1H, br, CH) 5.25 (1H, dd, J_{HH} 10.3, 1.4 Hz, $\text{CH}=\text{CH}_2$), 5.16 (1H, br d, J_{HH} 17.9 Hz, $\text{CH}=\text{CH}_2$), 4.92 (2H, br, Ar- CH_2), 4.24 (2H, br, N- CH_2), 2.08 (6H, s, $(\text{CH}_3)_2$); δ_{C} (75.5, CDCl_3) 170.0 ($\text{C}=\text{O}$), 136.3 (Ar, quaternary), 132.3 ($\text{CH}=\text{CH}_2$), 128.1, 127.8, 126.7 (Ar), 115.6 ($\text{CH}=\text{CH}_2$), 65.2 ($\text{C}(\text{CH}_3)_2\text{Br}$), 56.6 (N- CH_2), 48.3 (Ar- CH_2), 32.0 (CH_3), 31.8

($\underline{\text{C}}\text{H}_3$); m/z (ESI) 318 ($[\text{M}]^+\text{Na}$) (^{79}Br), 320 ($[\text{M}]^+\text{Na}$) (^{81}Br); [Found: 318.0465; $\text{C}_{14}\text{H}_{18}^{79}\text{BrNNaO}$ requires: 318.0469].

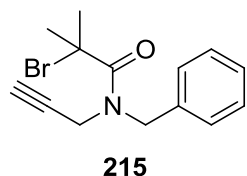
6.2.1.9 2-Bromo-2-methyl-*N*-benzyl-*N*-2-prenyl-propanamide



Using the same procedure as 6.2.1.8 *N*-(3-methyl-2-butenyl)-*N*-benzylamine (0.51 g, 2.9 mmol), Et_3N (0.70 cm^3 , 5.0 mmol) and 2-bromoisobutyryl bromide (0.36 cm^3 , 2.9 mmol) in Et_2O (25 cm^3) produced a crude product which was purified by flash chromatography, eluting with 9:1 petrol-EtOAc to yield **210** as a pale yellow oil (0.83 g, 2.56 mmol, 88%). R_f (50% EtOAc/petrol) 0.67; ν_{max} (cm^{-1}) 2974, 2931, 1631, 1495, 1462, 1436, 1415, 1249, 1162, 1108, 726, 696; δ_{H} (300 MHz, d_8 -Tol) 7.23-7.15 (5H, m, Ar), 5.20 (1H, br, $\underline{\text{C}}\text{H}$), 4.70 (2H, br, Ar- $\underline{\text{C}}\text{H}_2$), 4.14 (2H, br, N- $\underline{\text{C}}\text{H}_2$), 1.88 (6H, s, $\text{C}(\underline{\text{C}}\text{H}_3)_2\text{Br}$), 1.59 (3H, s, $\text{C}(\underline{\text{C}}\text{H}_3)_2$), 1.31 (3H, s, $\text{C}(\underline{\text{C}}\text{H}_3)_2$); δ_{C} (75.5, CDCl_3) 169.8 ($\underline{\text{C}}=\text{O}$), 136.8 (Ar, quaternary) 136.2 ($\underline{\text{C}}(\text{CH}_3)_2$), 128.2, 128.0, 126.9 (Ar), 119.3 ($\underline{\text{C}}\text{H}$), 56.6 ($\underline{\text{C}}(\text{CH}_3)_2\text{Br}$), 47.9 (Ar- $\underline{\text{C}}\text{H}_2$), 45.7 (N- $\underline{\text{C}}\text{H}_2$), 33.6 ($\text{C}(\underline{\text{C}}\text{H}_3)_2\text{Br}$), 33.4 ($\text{C}(\underline{\text{C}}\text{H}_3)_2\text{Br}$), 26.7 ($\text{C}(\underline{\text{C}}\text{H}_3)_2$), 19.8 ($\text{C}(\underline{\text{C}}\text{H}_3)_2$); m/z (ESI) 346 ($[\text{M}]^+\text{Na}$), 323 $[\text{M}]^+$; [Found: C, 58.9; H, 6.8; N, 4.3; $\text{C}_{16}\text{H}_{22}\text{BrNO}$ requires: C, 59.3; H, 6.8; N, 4.3].

6.2.1.10 2-Bromo-2-methyl-*N*-(phenylmethyl)-*N*-2-propynyl-propanamide

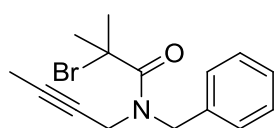
215



Using the same procedure as 6.2.1.8 *N*-benzyl-2-propynylamine (0.53 g, 3.65 mmol), Et_3N (0.70 cm^3 , 5.0 mmol) and 2-

bromoisobutyryl bromide (0.45 cm³, 3.65 mmol) in Et₂O (25 cm³) yielded **215** as a pale yellow oil (1.06 g, 3.61 mmol, 99%). *R_f* (50% EtOAc/petrol) 0.91; ν_{max} (cm⁻¹) 3289, 3006, 2980, 2932, 1636, 1495, 1462, 1411, 1246, 1168, 1107, 727; δ_{H} (300 MHz, CDCl₃) 7.30-7.26 (5H, m, Ar), 4.90 (2H, br, Ar-CH₂), 4.30 (2H, br, N-CH₂), 2.04 (6H, s, C(CH₃)₂), 1.96 (1H, s, CH); δ_{C} (75.5 MHz, CDCl₃) 136.1 (Ar, quaternary), 128.8, 128.2, 127.7 (Ar), 78.4, 65.9 (CC), 56.8 (C(CH₃)₂), 43.3 (Ar-CH₂), 32.7 (N-CH₂), 32.2, 32.1 ((CH₃)₂); *m/z* (ESI) 294 ([M]⁺H) (⁷⁹Br), 296 ([M]⁺H) (⁸¹Br); [Found: [M]⁺ 294.0494; C₁₄H₁₇⁷⁹BrNO requires 294.0490].

6.2.1.11 2-Bromo-2-methyl-N-benzyl-2-butynyl-propanamide **216**



216

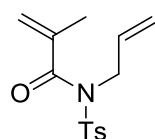
1-Bromo-2-butyne (0.24 ml, 2.7 mmol) was added dropwise via syringe to stirring benzylamine (2.5 ml, 22.9 mmol) at room temperature. Reaction was allowed to proceed for 44 hrs after which time the reaction mixture was quenched with water (25 cm³) and ether (25 cm³). The resulting aqueous layer was extracted using ether (2 x 25 cm³) and the combined organic extracts were washed with brine (25 cm³), dried over MgSO₄, filtered and concentrated in *vacuo*. A portion of the crude product (0.30 g, 1.9 mmol) was dissolved in Et₂O (20 cm³) and cooled to 0°C at which point Et₃N (0.42 cm³, 3.0 mmol). After 20 mins 2-bromoisobutyryl bromide (0.23 cm³, 1.9 mmol) was added and the reaction mixture was allowed to reach room temperature. After 4 hours the reaction was quenched with sat. NH₄Cl (10 cm³) and partitioned between sat. NaHCO₃ (50 cm³) and Et₂O (50 cm³). The organic layer was collected and the aqueous layer was extracted using Et₂O (2 x 50 cm³). The combined organic extracts were dried over MgSO₄, filtered and concentrated in *vacuo* to yield **216** as a

yellow oil (0.44 g, 1.4 mmol, 75%). R_f (50% EtOAc/petrol) 0.86; ν_{\max} (cm^{-1}) 3064, 2981, 2930, 1495, 1450, 1409, 1163, 1118, 696; δ_{H} (300 MHz, CDCl_3) 7.33-7.27 (5H, m, Ar), 4.84 (2H, br, Ar- CH_2), 4.29 (2H, br, N- CH_2), 2.02 (6H, s, (CH_3)₂), 1.82 (3H, t, J_{HH} 2.3 Hz, CCH_3); δ_{C} (75.5 MHz, CDCl_3) 170.2 ($\text{C}=\text{O}$), 136.5 (Ar quaternary) 128.7, 127.6, 127.5 (Ar), 73.6, 73.5 (CC), 57.0 (Ar- CH_2), 50.8 ($\text{C}(\text{CH}_3)_2\text{Br}$), 46.0 (N- CH_2), 32.7, 30.9 ($\text{C}(\text{CH}_3)_2$), 4.9 (CH_3); m/z (ESI) 330 ($[\text{M}]^+\text{Na}$) (^{79}Br), 332 ($[\text{M}]^+\text{Na}$) (^{81}Br); [Found: C, 58.4; H, 5.9; N, 4.7; $\text{C}_{15}\text{H}_{18}\text{BrNO}$ requires: C, 58.5; H, 5.9; N, 4.5].

6.2.2 General Procedure for 1,4-DMP Mediated Radical Cyclisation

The precursor (0.3-0.6 mmol) was dissolved in 1,4-DMP (2 cm^3) at room temperature then heated under reflux at 65°C overnight. The solvent was removed in *vacuo* and the resulting residue was dissolved in DCM (20 cm^3) and washed with 1M HCl (20 cm^3). The aqueous layer was extracted using DCM (2 x 20 cm^3) and the combined organic extracts were washed with water (2 x 20 cm^3), dried over MgSO_4 , filtered and concentrated in *vacuo* to isolate the crude product which was purified by flash chromatography eluting with 5:1/9:1 petrol-EtOAc.

6.2.2.1 2-Methyl-N-[(4-methylphenyl)sulfonyl]-N-2-propenyl-2-propenamide 217

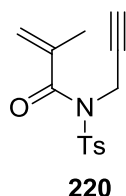


217

N-Allyl-*N*-(2-bromo-2-methyl-propionyl)-4-methylbenzenesulfonamide (200 mg, 0.56 mmol) was subject to the general procedure for 1,4-DMP radical cyclisation (6.2.2). Flash chromatography, eluting

with 5:1 pet ether/EtOAc yielded **217** as a white solid (134 mg, 0.48 mmol, 86%). R_f (3:1 petrol:EtOAc) 0.48; mpt 98-99 °C; ν_{\max} (film)/ cm^{-1} 2986, 2923, 1678, 1595, 1495, 1454, 1422, 1341, 1329, 1158, 1087, 925. 732; δ_{H} 7.82 (2H, d, J_{HH} 8.1 Hz Ar-H), 7.30 (2H, d, J_{HH} 8.1 Hz Ar-H), 5.84 (1H, ddt, J_{HH} 17.2, 10.2, 5.7 Hz, CH=CH₂), 5.24 (1H, dd, J_{HH} 17.2, 1.5 Hz, CH=CH₂) 5.22 (1H, dd, J_{HH} 10.2, 1.5 Hz, CH=CH₂), 5.20 (1H, d, J_{HH} 1.5 Hz C=CH₂), 5.18 (1H, d, J_{HH} 1.5 Hz C=CH₂), 4.44 (2H, dt, J_{HH} 5.7, 1.5 Hz, N-CH₂), 2.42 (3H, s, Ar-CH₃), 1.90 (3H, t, J_{HH} 1.5 Hz, C(CH₃)CH₂); δ_{C} (75.5 MHz, CDCl₃) 171.5 (C=O), 144.4 (C(CH₃)CH₂), 139.7, 135.7 (Ar quaternary), 132.3 (CH=CH₂), 128.9, 127.9 (Ar), 118.4, 117.9 (=CH₂), 46.8 (N-CH₂), 21.0 (Ar-CH₃), 19.9 (CH₃); m/z (EI) 279 [M]⁺; [Found [M]⁺ 279.0931; C₁₄H₁₇NO₃S requires 279.0929].

6.2.2.2 2-Methyl-N-[(4-methylphenyl)sulfonyl]-N-2-propynyl-2-propenamide **220**



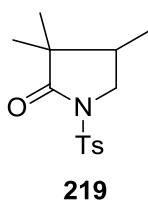
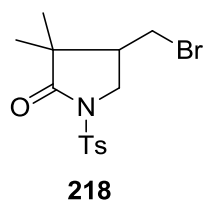
N-(2-bromo-2-methyl-propionyl)-4-methyl-*N*-prop-2-ynyl-benzene-sulfonamide (200 mg, 0.56 mmol) was subject to the general procedure for 1,4-DMP radical cyclisation (6.2.2). Flash chromatography eluting with 5:1 pet ether/EtOAc yielded **220** as a white solid (121 mg, 0.42 mmol, 78%). R_f (3:1 petrol:EtOAc) 0.42; mpt 100-102 °C; ν_{\max} (cm^{-1}) 3294, 2904, 1669, 1595, 1450, 1359, 1187, 1064, 820; δ_{H} 7.85 (2H, d, J_{HH} 8.1 Hz, Ar-H), 7.25 (2H, d, J_{HH} 8.1 Hz, Ar-H), 5.26 (1H, d, J_{HH} 1.5 Hz, C=CH₂), 5.14 (1H, d, J_{HH} 1.5 Hz, C=CH₂), 4.58 (2H, d, J_{HH} 2.4 Hz, N-CH₂), 2.37 (3H, s, Ar-CH₃), 2.25 (1H, t, J_{HH} 2.4 Hz, CH), 1.84 (3H, s, CCH₃); δ_{C} (75.5 MHz, CDCl₃) 164.1 (C=O), 139.9 (C(CH₃)CH₂), 137.3, 136.1 (Ar, quaternary), 129.5, 128.7 (Ar), 79.1, 76.2

(CC), 36.6 (N-CH₂), 21.8, 19.6 (CH₃); *m/z* (ESI) 278 ([M]⁺H); [Found: C, 60.2; H, 5.6; N, 5.0; C₁₄H₁₅NO₃S requires: C, 60.6; H, 5.4; N, 5.1].

6.2.3 General Procedure for 1,4-DMP Mediated Radical Cyclisation Using the Freeze-Pump-Thaw Technique

1,4-DMP was thoroughly degassed using the freeze-pump-thaw and experiments were performed on Schlenk line under a nitrogen atmosphere. The precursor (0.3-0.6 mmol) was dissolved in dry 1,4-DMP (2 cm³) at room temperature then heated under reflux at 65°C overnight. The solvent was removed in *vacuo* and the resulting residue was dissolved in DCM (20 cm³) and washed with 1M HCl (20 cm³). The aqueous layer was extracted using DCM (2 x 20 cm³) and the combined organic extracts were washed with water (2 x 20 cm³), dried over MgSO₄, filtered and concentrated in *vacuo* to isolate the crude product which was purified by flash chromatography eluting with 5:1/9:1 petrol-EtOAc.

6.2.3.1 3,3-Dimethyl-4-bromomethyl-1-(p-toluenesulfonyl)-pyrrolidin-2-one **218**,²³⁸ 3,3-Dimethyl-4-methyl-1-[(4-methylphenyl)sulfonyl]-2-pyrrolidinone **219**²³⁸



N-Allyl-*N*-(2-bromo-2-methyl-propionyl)-4-methyl-benzenesulfonamide (200 mg, 0.56 mmol) was subject to the general procedure for

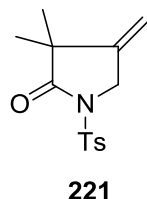
1,4-DMP radical cyclisation under inert conditions (6.2.3). Flash chromatography eluting with 5:1 petrol:EtOAc yielded a 1 : 3 mixture of **218** and **219**. Further

purification by flash chromatography eluting with 9:1 petrol:EtOAc allowed isolation of pure samples of **218** and **219**.

218 isolated as a white solid (39 mg, 0.11 mmol, 20%); mpt 131-132 °C, lit⁵⁵ 132-133 °C; R_f (3:1 petrol:EtOAc) 0.41; ν_{\max} (cm^{-1}) 2972, 1724, 1596, 1480, 1354, 1169, 1118 1090; δ_{H} (300 MHz, CDCl_3) 7.90 (2H, d, J_{HH} 8.1 Hz, Ar), 7.20 (2H, d, J_{HH} 8.1 Hz, Ar), 4.10 (1H, dd, J_{HH} 10.6, 7.2 Hz, N- CH_2), 3.40 (1H, dd, J_{HH} 10.4, 6.9 Hz (CH_2Br), 3.38 (1H, t, J_{HH} 10.4 Hz (CH_2Br), 3.10 (1H, t, J_{HH} 10.6 Hz, N- CH_2), 2.42 (1H, m, CH), 2.40 (3H, s, Ar- CH_3), 1.10 (3H, s, $\text{C}(\text{CH}_3)_2$), 0.80 (3H, s, $\text{C}(\text{CH}_3)_2$); δ_{C} (75.5 MHz, CDCl_3) 176.9 ($\text{C}=\text{O}$), 145.4, 134.8 (Ar, quaternary), 129.8, 128.0 (Ar), 48.8 ($\text{C}(\text{CH}_3)_2$), 45.4 (CH), 45.0 (N- CH_2), 29.9 (CH_2Br), 23.4 (Ar- CH_3), 21.7 (CH_3), 17.8 (CH_3); m/z (ESI) 360.0 ($[\text{M}]^+\text{H}$) (^{79}Br), 362 ($[\text{M}]^+\text{H}$) (^{81}Br); [Found: C, 47.1; H, 5.0; N, 3.8; $\text{C}_{14}\text{H}_{18}\text{BrNO}_3\text{S}$ requires: C, 46.7; H, 5.0; N, 3.9].

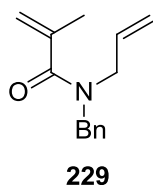
219 isolated as a white solid (115 mg, 0.41 mmol, 57%); mpt 135-136, lit²³⁸ 136-138 °C; R_f (3:1 petrol:EtOAc) 0.59; δ_{H} (300 MHz, CDCl_3) 7.89 (2H, d, J_{HH} 8.1 Hz, Ar- H), 7.32 (2H, d, J_{HH} 8.1 Hz, Ar- H), 3.97 (1H, dd, J_{HH} 10.0, 7.5 Hz, N- CH_2), 3.26 (1H, t, J_{HH} 10.0 Hz, N- CH_2), 2.43 (3H, s, Ar- CH_3), 1.92 (1H, m, CH), 1.05 (3H, s, CH_3), 0.96 (3H, d, J_{HH} 6.9 Hz, CH_3), 0.79 (3H, s, CH_3); δ_{C} (75.5 MHz, CDCl_3) 177.8 ($\text{C}=\text{O}$), 144.4, 134.5 (Ar, quaternary), 129.0, 127.3 (Ar), 50.0 (CH_2), 44.3 ($\text{C}(\text{CH}_3)_2$), 37.0 (CHCH_3), 21.1 ($\text{C}(\text{CH}_3)_2$), 20.7 (Ar- CH_3), 16.7 ($\text{C}(\text{CH}_3)_2$), 11.1 (CH_3); m/z (ESI) (Found 304.1 $[\text{M}+\text{Na}]^+$, requires 281.11 $[\text{M}]^+$); [Found $[\text{M}]^+$ 304.0981; $\text{C}_{14}\text{H}_{19}\text{NNaO}_3\text{S}$ requires 304.0983].

6.2.3.2 3,3-Dimethyl-4-methylene-1-[(4-methylphenyl)sulfonyl]-pyrrolidin-2-one **221**²³⁸



N-(2-bromo-2-methyl-propionyl)-4-methyl-*N*-prop-2-ynyl benzene-sulfonamide (200 mg, 0.56 mmol) was subject to the general procedure for 1,4-DMP radical cyclisation under inert conditions (6.2.3). Flash chromatography eluting with 5:1 pet ether/EtOAc yielded **221** as a white solid (128 mg, 0.46 mmol, 82%); R_f (3:1 petrol:EtOAc) 0.48; mpt 103-105 °C, lit²³⁸ 104-106 °C; ν_{\max} (cm⁻¹) 2970, 1731, 1596, 1494, 1463, 1360, 1340, 1166, 1118, 1090, 813; δ_H (300 MHz, CDCl₃) 7.75 (2H, d, J_{HH} 8.1 Hz, Ar), 7.16 (2H, d, J_{HH} 8.1 Hz, Ar), 4.90 (1H, dt, J_{HH} 1.5, 1.5 Hz, C=CH₂), 4.88 (1H, dt, J_{HH} 1.5, 1.5 Hz, C=CH₂), 4.28 (2H, t, J_{HH} 1.5 Hz, N-CH₂), 2.25 (3H, s, Ar-CH₃), 1.0 (6H, s, C(CH₃)₂); δ_C (75.5 MHz, CDCl₃) 176.9 (C=O), 145.3 (C=CH₂), 145.2, 135.0 (Ar quaternary), 129.7, 128.0 (Ar), 108.5 (C=CH₂), 49.3 (C(CH₃)₂), 46.1 (N-CH₂), 24.4 (Ar-CH₃), 21.7 ((CH₃)₂); m/z (ESI) 302 ([M]⁺Na); [Found: 302.0870, 5.0; C₁₄H₁₇NNaO₃S requires: 302.0873].

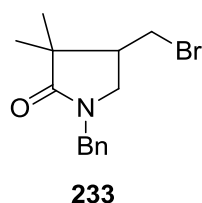
6.2.3.3 2-Methyl-*N*-(phenylmethyl)-*N*-2-propenyl-2-propenamide **229**



N-Allyl-*N*-(phenylmethyl)-*N*-2-bromo-2-methyl propanamide (100 mg, 0.34 mmol) was subject to the general procedure for 1,4-DMP radical cyclisation under inert conditions (6.2.3). Flash chromatography eluting with 9:1 pet ether/ETOAc yielded **229** as a colourless oil (4.0 mg, 20.4 μ mol, 6 %); R_f (3:1 petrol:EtOAc) 0.50; δ_H (300 MHz, CDCl₃) 7.32-7.25 (5H, m, Ar-H), 5.73 (1H, br, CH=CH₂), 5.19 (2H, br, C(CH₃)CH₂), 5.12 (1H,

dd, J_{HH} 14.7, 1.0 Hz, CHCH_2), 5.09 (1H, dd, J_{HH} 7.7, 1.0 Hz, CHCH_2), 4.60 (2H, s, Ar- CH_2), 3.92 (2H, br, CH_2) 1.99 (3H, s, CH_3); δ_{C} (75.5 MHz, CDCl_3) 172.3 ($\text{C}=\text{O}$), 140.0 ($\text{C}(\text{CH}_3)\text{CH}_2$), 132.6 (Ar, quaternary), 128.1, 127.6, 126.8 (Ar), 117.2 ($\text{C}(\text{CH}_3)\text{CH}_2$), 115.1 (CHCH_2), 49.8 (Ar- CH_2), 45.6 (CH_2), 20.2 (CH_3); [Found: 215.1315, $\text{C}_{14}\text{H}_{17}\text{NO}$ requires: 215.1310].

6.2.3.4 3,3-Dimethyl-4-bromomethyl-1-(phenylmethyl)-pyrrolidin-2-one 233



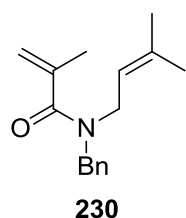
N-Allyl-*N*-(phenylmethyl)-*N*-2-bromo-2-methyl-propanamide

(100 mg, 0.34 mmol) was subject to the general procedure for 1,4-

DMP radical cyclisation under inert conditions (6.2.3). Flash

chromatography eluting with 9:1 pet ether/EtOAc yielded **233** as a colourless oil (1 mg, 0.0034 mmol, 1%). Due to insufficient yields data was collected following reactions in chapter 3 (section 6.2.6.1).

6.2.3.5 2-Methyl-*N*-(phenylmethyl)-*N*-2-prenyl-propenamide 230



2-Bromo-2-methyl-*N*-benzyl-*N*-2-prenyl propanamide (100 mg,

0.31 mmol) was subject to the general procedure for 1,4-DMP

radical cyclisation under inert conditions (6.2.3). Flash

chromatography eluting with 9:1 pet ether/EtOAc afforded **230** as a

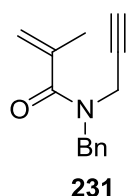
pale yellow oil (10 mg, 0.04 mmol, 13%). R_f (3:1 petrol:EtOAc) 0.50; ν_{max} (cm^{-1})

3029, 2923, 1659, 1495, 1417, 1185, 925, 734; δ_{H} (300 MHz, CDCl_3) 7.33-7.25 (5H,

m, Ar), 5.16 (1H, br, $\text{CH}=\text{C}(\text{CH}_3)_2$), 5.09 (2H, br, $\text{C}(\text{CH}_3)_2\text{CH}_2$), 4.57 (2H, s, Ar- CH_2),

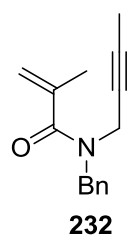
3.92 (2H, br, $\underline{\text{CH}_2}$), 2.00 (3H, s, $\text{C}(\underline{\text{CH}_3})\text{CH}_2$), 1.72 (3H, s, $\underline{\text{CH}_3}$), 1.50 (3H, s, $\underline{\text{CH}_3}$); δ_{C} (75.5 MHz, CDCl_3) 173.5 ($\underline{\text{C}}=\text{O}$) 141.2 ($\underline{\text{C}}(\text{CH}_3)\text{CH}_2$), 139.9 (Ar, quaternary), 133.7 ($\underline{\text{C}}(\text{CH}_3)_2$), 128.6, 128.1, 127.3 (Ar), 115.0 ($\text{C}(\text{CH}_3)\underline{\text{C}}\text{H}_2$), 48.7 (Ar- $\underline{\text{C}}\text{H}_2$), 46.3 ($\underline{\text{C}}\text{H}_2$), 25.8 ($\underline{\text{C}}\text{H}_3$), 20.8, 18.3 ($\text{C}(\underline{\text{C}}\text{H}_3)_2$); m/z (ESI) 244 ($[\text{M}]^+\text{H}$); [Found: ($[\text{M}]^+\text{H}$) 244.1696, $\text{C}_{16}\text{H}_{23}\text{NO}$ requires, 244.1701].

6.2.3.6 2-Methyl-*N*-(phenylmethyl)-*N*-2-propynyl-2-propenamide **231**



2-Bromo-2-methyl-*N*-(phenylmethyl)-*N*-2-propynyl propanamide (100 mg, 0.34) was subject to the general procedure for 1,4-DMP radical cyclisation under inert conditions (6.2.3). Flash chromatography eluting with 9:1 pet ether/EtOAc yielded **231** as a colourless oil (50 mg, 0.23 mmol, 69%). R_f (3:1 petrol:EtOAc) 0.45; ν_{max} (cm^{-1}) 3280, 3031, 2923, 1647, 1495, 1449, 1415, 1252, 1206, 925, 733; δ_{H} (300 MHz, CDCl_3) 7.35-7.28 (5H, m, Ar), 5.25 (2H, br, $\text{C}(\text{CH}_3)\underline{\text{C}}\text{H}_2$), 4.75 (2H, s, Ar- $\underline{\text{C}}\text{H}_2$), 4.06 (2H, br, $\underline{\text{C}}\text{H}_2$), 2.27 (1H, s, $\underline{\text{C}}\text{C}\text{H}$), 2.02 (3H, s, $\underline{\text{C}}\text{H}_3$); δ_{C} (75.5 MHz, CDCl_3) 172.8 ($\underline{\text{C}}=\text{O}$) 140.0 ($\underline{\text{C}}(\text{CH}_3)\text{CH}_2$), 137.5 (Ar, quaternary), 128.8, 127.8, 127.4 (Ar), 116.2 ($\text{C}(\text{CH}_3)\underline{\text{C}}\text{H}_2$), 78.5 ($\underline{\text{C}}\text{C}\text{H}$), 73.2 ($\underline{\text{C}}\text{C}\text{H}$), 49.8 (Ar- $\underline{\text{C}}\text{H}_2$), 32.7 ($\underline{\text{C}}\text{H}_2$), 20.5 ($\underline{\text{C}}\text{H}_3$); m/z (ESI) 214 ($[\text{M}]^+\text{H}$); [Found: ($[\text{M}]^+\text{H}$) 214.1228, $\text{C}_{14}\text{H}_{17}\text{NO}$ requires, 214.1232].

6.2.3.7 2-Methyl-*N*-(phenylmethyl)-2-butynyl-propenamide **232**

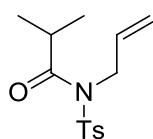


2-Bromo-2-methyl-*N*-benzyl-2-butynyl-propenamide (100 mg, 0.33 mmol) was subject to the general procedure for 1,4-DMP radical cyclisation under inert conditions (6.2.3). Flash chromatography

eluting with 9:1 pet ether/EtOAc yielded **232** as a yellow oil (53 mg, 0.23 mmol, 70%). R_f (3:1 petrol:EtOAc) 0.57; ν_{\max} (cm^{-1}) 3064, 3032, 2920, 1648, 1495, 1452, 1421, 1360, 1191, 698; δ_{H} (300 MHz, CDCl_3) 7.33-7.28 (5H, m, Ar), 5.22 (2H, br, $\text{C}(\text{CH}_3)\underline{\text{C}}\text{H}_2$), 4.73 (2H, s, Ar- $\underline{\text{C}}\text{H}_2$), 4.04 (2H, br, $\underline{\text{C}}\text{H}_2$), 2.01 (3H, s, $\underline{\text{C}}\text{H}_3$), 1.82 (3H, s, $\text{C}\underline{\text{C}}\text{H}_3$); δ_{C} (75.5 MHz, CDCl_3) 174.1 ($\underline{\text{C}}=\text{O}$) 140.2 ($\underline{\text{C}}(\text{CH}_3)\underline{\text{C}}\text{H}_2$), 136.6 (Ar, quaternary), 128.7, 127.6, 127.1 (Ar), 115.9 ($\text{C}(\text{CH}_3)\underline{\text{C}}\text{H}_2$), 72.8 ($\underline{\text{C}}\underline{\text{C}}$), 72.0 ($\underline{\text{C}}\underline{\text{C}}$), 46.7 (Ar- $\underline{\text{C}}\text{H}_2$), 37.9 ($\underline{\text{C}}\text{H}_2$), 20.6 ($\text{C}(\underline{\text{C}}\text{H}_3)\underline{\text{C}}\text{H}_2$), 3.8 ($\underline{\text{C}}\text{H}_3$); m/z (ESI) 250 ($[\text{M}]^+\text{Na}$); [Found: ($[\text{M}]^+\text{Na}$) 250.1203, $\text{C}_{15}\text{H}_{17}\text{NNaO}$ requires 250.1208].

6.2.3.8 *N*-Allyl-*N*-(2-methyl-propionyl)-4-methyl-benzenesulfonamide

225²⁴²



225

N-Allyl-*N*-(2-bromo-2-methyl-propionyl)-4-methyl benzenesulfonamide (100 mg, 0.28 mmol) was subject to the general procedure for 1,4-DMP radical cyclisation under inert condition with the addition of diethyl phosphite (43 μl , 0.34 mmol). Flash chromatography eluting with 9:1 petrol/ETOAc afforded **225** as a white solid (32 mg, 0.11 mmol, 41%). Data match those of previously published work.²⁴²

6.2.4 1,4-DMP Mediated Radical Cyclisation in a Microwave

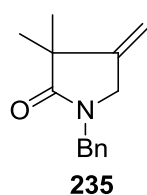
The precursor (0.2-0.2 mmol) was dissolved in degassed and dried 1,4-DMP (1.5 cm^3) at room temperature then heated in a microwave 1 h. The solvent was removed in *vacuo* and the resulting residue was dissolved in DCM (20 cm^3) and washed with 1M HCl (20 cm^3). The aqueous layer was extracted using DCM (2 x 20 cm^3) and

the combined organic extracts were washed with water (2 x 20 cm³), dried over MgSO₄, filtered and concentrated in *vacuo* to isolate the crude product which was purified by flash chromatography eluting with 9:1 pet ether/EtOAc.

1,4-DMP mediated radical cyclisation of *N*-allyl-*N*-(phenylmethyl)-*N*-2-bromo-2-methyl-propanamide (50 mg, 0.17 mmol) in a microwave yielded **229** (7 mg, 0.03 mmol, 20%) and **233** (2 mg, 6.75 μmol, 4%). The data obtained match those reported in 6.2.3.3 and 6.2.3.4 respectively.

1,4-DMP mediated radical cyclisation of 2-bromo-2-methyl-*N*-(phenylmethyl)-*N*-2-propynyl-propanamide (100 mg, 0.25 mmol) in a microwave yielded **231** (26 mg, 0.12 mmol, 47%) and **235**. The data obtained for **231** matched that reported in 6.2.3.6 and the data for **235** is reported in 6.2.4.1.

6.2.4.1 3,3-Dimethyl-4-methylene-1-(phenylmethyl)-2-pyrrolidinone **235**

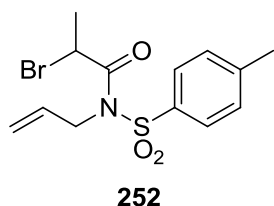


2-Bromo-2-methyl-*N*-(phenylmethyl)-*N*-2-propynyl propanamide (75 mg, 0.34 mmol) was subject to the general procedure for 1,4-DMP radical cyclisation carried out in a microwave. The parameters were set at T = 130 °C, t = 1 hr, power was set to 300 W and the pressure limit was set at 20 bar. Flash chromatography eluting with 9:1 pet ether/EtOAc afforded **235** as a pale yellow oil (35 mg, 0.16 mmol, 47 %). *R_f* (3:1 petrol:EtOAc) 0.59; ν_{\max} (cm⁻¹) 3066, 2966, 2926, 1693, 1495, 1475, 1455, 1425, 1359, 1255, 1166, 698; δ_{H} (300 MHz, CDCl₃) 7.32-7.27 (5H, m, Ar-H), 5.03 (1H, dt, *J*_{HH} 2.4, 1.5 Hz, C=CH₂), 4.96 (1H, dt, *J*_{HH} 2.4, 1.5 Hz, C=CH₂), 4.51 (2H, s, Ar-CH₂), 3.82 (2H, t, *J*_{HH} 1.5 Hz,

$\underline{\text{CH}}_2$), 1.27 (6H, s, ($\underline{\text{CH}}_3$)₂); δ_{C} (75.5 MHz, CDCl_3) 177.5 ($\underline{\text{C}}=\underline{\text{O}}$) 148.8 ($\underline{\text{C}}\underline{\text{CH}}_2$), 136.3 (Ar, quaternary), 128.8, 128.1, 127.6 (Ar), 106.7 ($\underline{\text{C}}=\underline{\text{CH}}_2$), 49.7 ($\underline{\text{C}}$, quaternary), 46.2 (Ar- $\underline{\text{CH}}_2$), 44.5 ($\underline{\text{CH}}_2$), 25.2, 25.0 ($\underline{\text{CH}}_3$); m/z (ESI) 214 ($[\text{M}]^+\text{H}$); [Found: ($[\text{M}]^+\text{H}$) 214.1228, $\text{C}_{14}\text{H}_{17}\text{NO}$ requires, 214.1232].

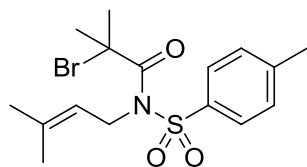
6.2.5 General Procedure for Substrates Synthesised in Chapter 3

6.2.5.1 2-Bromo-*N*-[(4-methylphenyl)sulfonyl]-*N*-2-propenylpropanamide **252**⁵⁵



Using the same procedure as 6.2.1.3, *N*-allyl-4-methylbenzenesulfonamide (2.00 g, 9.5 mmol) in dry THF (75 cm³), *n*-BuLi (1.6 M, 9.40 cm³, 15.0 mmol) and 2-bromopropionyl bromide (1.57 cm³, 15.0 mmol) furnished the crude product which was purified by flash chromatography eluting with 5:1 pet ether/EtOAc to yield **252** as a white solid (1.12 g, 3.2 mmol, 34%); R_f (3:1 petrol:EtOAc) 0.65; mpt 40-41, lit⁵⁵ 39-40; ν_{max} (cm⁻¹) 2931, 2835, 2823, 1652, 1595, 1438, 1348, 1310, 1217, 1157, 1107, 925, 717; δ_{H} (300 MHz, CDCl_3) 7.84 (2H, d, J_{HH} 8.0 Hz, Ar- $\underline{\text{H}}$), 7.32 (2H, d, J_{HH} 8.0 Hz, Ar- $\underline{\text{H}}$), 5.91 (1H, m, $\underline{\text{CH}}$), 5.26 (1H, d, J_{HH} 6.7, 2.4 Hz, $\underline{\text{CH}}=\underline{\text{CH}}_2$), 5.21 (1H, br, $\underline{\text{CH}}=\underline{\text{CH}}_2$), 4.83 (1H, q, J_{HH} 6.6 Hz, $\underline{\text{CH}}(\text{Br})\underline{\text{CH}}_3$), 4.69 (1H, ddt, J_{HH} 17.5, 4.7, 1.8 Hz, N- $\underline{\text{CH}}_2$), 4.40 (1H, ddt, J_{HH} 17.5, 4.7, 1.8 Hz, N- $\underline{\text{CH}}_2$), 2.43 (3H, s, Ar- $\underline{\text{CH}}_3$), 1.72 (3H, d, J_{HH} 6.6 Hz, $\underline{\text{CH}}_3$); δ_{C} (75.5 MHz, CDCl_3) 169.4 ($\underline{\text{C}}=\underline{\text{O}}$), 145.3, 135.6 (Ar quaternary), 132.7 ($\underline{\text{C}}\underline{\text{H}}\underline{\text{C}}\underline{\text{H}}_2$), 129.7, 128.3 (Ar), 118.0 ($\underline{\text{C}}\underline{\text{H}}\underline{\text{C}}\underline{\text{H}}_2$), 48.7 ($\underline{\text{C}}\underline{\text{H}}\underline{\text{C}}\underline{\text{H}}_3\text{Br}$), 39.6 ($\underline{\text{C}}\underline{\text{H}}_2$), 21.2 (Ar- $\underline{\text{C}}\underline{\text{H}}_3$), 20.4 ($\underline{\text{C}}\underline{\text{H}}_3$); m/z (ESI) 368 ($[\text{M}]^+\text{Na}$) (^{79}Br), 370 ($[\text{M}]^+\text{Na}$) (^{81}Br); [Found: ($[\text{M}]^+\text{Na}$) 369.9920; $\text{C}_{13}\text{H}_{16}^{81}\text{BrNNaO}_3\text{S}$ requires 369.9911].

6.2.5.2 2-Bromo-2-methyl-N-[(4-methylphenyl)sulfonyl]-N-2-prenylpropanamide 249

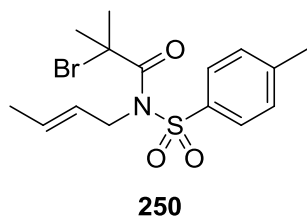


249

p-Toluenesulfonamide (3.40 g, 20.0 mmol) was added to a suspension of K_2CO_3 (2.80 g, 20.0 mmol) in acetone (100 cm^3) at room temperature. The reaction was allowed to proceed for 15 mins, after which time 3,3-dimethylallyl bromide (2.50 g, 16.1 mmol) was added. The reaction was stirred and heated at reflux overnight. The acetone was removed in *vacuo* and the resulting residue was dissolved in an ether/water mixture (50 cm^3 each). The organic layer was collected and the aqueous was extracted using ether (2 x 50 cm^3). The combined organic extracts were dried over $MgSO_4$, filtered and concentrated in *vacuo* to yield the crude product 4-methyl-*N*-(3-methyl-2-buten-1-yl)-benzenesulfonamide, a portion of which (1.27 g, 5.3 mmol) was dissolved in dry THF and taken to $-78\text{ }^\circ C$ at which point *n*-BuLi (1.6 M in hexanes, 3.75 ml, 6.0 mmol) was added. The reaction was allowed to proceed for 30 mins after which time 2-bromoisobutyryl bromide (0.87 ml, 7.0 mmol) was added. The reaction was allowed to reach room temperature overnight. The reaction was quenched with sat. NH_4Cl (10 cm^3) and partitioned between sat. $NaHCO_3$ (100 cm^3) and DCM (100 cm^3). The organic layer was collected and the aqueous layer extracted using DCM (2 x 100 cm^3). The combined organic extracts were washed with brine (100 cm^3), dried over $MgSO_4$, filtered and concentrated in *vacuo* to yield a crude product which was purified by flash chromatography eluting 5:1 pet ether/EtOAc to yield **249** as a white solid (1.07 g, 2.8 mmol, 53 %). R_f (3:1 pet ether:EtOAc) 0.64; mpt $86-88\text{ }^\circ C$; ν_{max} (cm^{-1}) 3000,

2969, 2934, 1676, 1595, 1493, 1462, 1445, 1356, 1292, 1164, 1146, 1076, 823, 706; δ_{H} (300 MHz, CDCl_3) 7.84 (2H, d, J_{HH} 8.1 Hz, Ar-H), 7.28 (2H, d, J_{HH} 8.1 Hz, Ar-H), 5.22 (1H, m, CHC(CH_3)₂), 4.89 (2H, d, J_{HH} 6.0 Hz, N-CH₂), 2.42 (3H, s, Ar-CH₃), 1.90 (6H, s, C(CH₃)₂Br), 1.77 (3H, s, CH₃), 1.75 (3H, s, CH₃); δ_{C} (75.5 MHz, CDCl_3) 170.2 (C=O), 143.9, 135.6 (Ar, quaternary), 135.9 (C(CH_3)₂), 128.5, 128.3 (Ar), 119.9 (CH), 56.2 (C(CH_3)₂Br), 46.8 (N-CH₂), 31.2, 31.1 (C(CH₃)₂Br), 25.0, 17.8 (CH₃)₂), 21.1 (Ar-CH₃); m/z (ESI) 410 ($[\text{M}]^+\text{Na}$) (^{79}Br), 412 ($[\text{M}]^+\text{Na}$) (^{81}Br); [Found: ($[\text{M}]^+\text{Na}$) 410.0396; $\text{C}_{16}\text{H}_{22}^{79}\text{BrNNaO}_3\text{S}$ requires 410.0401].

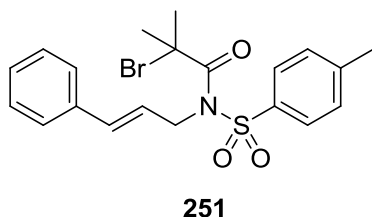
6.2.5.3 2-Bromo-2-methyl-*N*-[(4-methylphenyl)sulfonyl]-*N*-2-crotylpropanamide **250**



Using the same procedure as 6.2.5.2, *p*-toluenesulfonamide (1.37 g, 8.0 mmol), K_2CO_3 (1.38 g, 10.0 mmol) and crotyl bromide (85 %), (1.00 g, 6.3 mmol) in acetone (50 cm^3) at room temperature furnished a crude product 4-methyl-*N*-(3-methyl-2-buten-1-yl)-benzenesulfonamide (0.71 g, 3.2 mmol). This was dissolved in dry THF (50 cm^3) addition of *n*-BuLi (1.6 M in hexanes, 2.5 ml, 4.0 mmol) and 2-bromoisobutyryl bromide (0.5 ml, 4.0 mmol) yielded a crude product which was purified by flash chromatography eluting 5:1 pet ether/EtOAc to **250** as a white solid (0.69 g, 1.8 mmol, 56 %). R_f (3:1 pet ether:EtOAc) 0.64; mpt 80-81 °C; ν_{max} (cm^{-1}) 2938, 1677, 1595, 1494, 1461, 1393, 1349, 1316, 1167, 1118, 1086, 812, 693; δ_{H} (300 MHz, CDCl_3) 7.78 (2H, d, J_{HH} 8.1 Hz, Ar-H), 7.23 (2H, d, J_{HH} 8.1 Hz, Ar-H), 5.78 (1H, m, CHCH₃), 5.52 (1H, m, CHCH₂), 4.79 (2H, d, J_{HH} 5.4 Hz, N-CH₂), 2.36 (3H, s, Ar-CH₃), 1.83 (6H, s, (CH₃)₂), 1.67 (3H, dd, J_{HH} 6.3, 1.2 Hz,

CHCH₃); δ_C (75.5, CDCl₃) 170.0 (C=O), 144.0, 135.7 (Ar, quaternary), 129.6 (CHCH₂), 128.5, 128.3 (Ar), 125.5 (CH₂CH), 49.6 (C(CH₃)₂Br), 45.6 (N-CH₂), 31.4, 31.1 ((CH₃)₂), 21.1 (Ar-CH₃), 17.2 (CHCH₃); m/z (ESI) 396 ([M]⁺Na) (⁷⁹Br), 398 ([M]⁺Na) (⁸¹Br); [Found: ([M]⁺Na) 396.0239; C₁₅H₂₀⁷⁹BrNNaO₃S requires 396.0245].

6.2.5.4 2-Bromo-2-methyl-N-[(4-methylphenyl)sulfonyl]-N-2-cinnamylpropanamide **251**



Using the same procedure as 6.2.5.2, *p*-toluenesulfonamide (1.37 g, 8.0 mmol), K₂CO₃ (1.38 g, 10.0 mmol) and cinnamyl chloride (1.00 g, 6.2 mmol) in acetone (50 cm³) at room temperature furnished the crude product, 4-methyl-*N*-(3-phenyl-2-propenyl) benzenesulfonamide (0.45 g, 1.6 mmol). This was dissolved in dry THF (50 cm³) and addition of *n*-BuLi (1.6 M in hexanes, 1.25 ml, 2.0 mmol) and 2-bromoisobutyryl bromide (0.25 ml, 2.0 mmol) yielded a crude product which was purified by flash chromatography eluting 5:1 pet ether/EtOAc to give **251** as a white solid (0.40 g, 0.9 mmol, 56 %). R_f (3:1 pet ether:EtOAc) 0.62; mpt 101-102 °C; ν_{\max} (cm⁻¹) 2968, 2923, 1676, 1595, 1445, 1392, 1356, 1291, 1164, 1076, 823, 658; δ_H (300 MHz, CDCl₃) 7.88 (2H, d, J_{HH} 8.4 Hz, Ar-H), 7.30 (7H, m, Ar-H), 6.69 (1H, dt, J_{HH} 16.2, 1.2 Hz, CHPh), 6.25 (1H, dt, J_{HH} 16.2, 5.7 Hz, CHCH₂), 5.11 (2H, dd, J_{HH} 5.7, 1.2 Hz, N-CH₂), 2.41 (3H, s, Ar-CH₃), 1.94 (6H, s, (CH₃)₂); δ_C (75.5 MHz, CDCl₃) 170.6 (C=O), 144.7, 136.2, 136.0 (Ar, quaternary), 133.6 (CH₂CH), 129.2, 129.1, 128.7, 128.1, 126.6 (Ar), 124.4 (CHPh), 56.9 (C(CH₃)₂Br), 50.5 (N-CH₂), 32.0 ((CH₃)₂), 21.7 (Ar-CH₃); m/z (ESI)

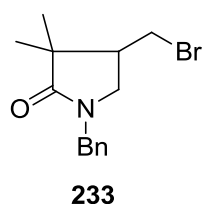
458 ([M]⁺Na) (⁷⁹Br), 460 ([M]⁺Na) (⁸¹Br); [Found: ([M]⁺Na) 458.0396; C₂₀H₂₂⁷⁹BrNNaO₃S requires 458.0401].

6.2.6 General Procedure for Copper Mediated ATRC Using AIBN in Chapter 3

The precursor (0.20-0.31 mmol) was dissolved in DCM (0.12 M) at room temperature. A solution (0.01 M) of CuBr/TPA (1.0 mol%) was added followed by AIBN (10 mol%). The reaction mixture was then heated at reflux for 1-24 h. The mixture was allowed to cool to room temperature and filtered through a silica plug using DCM (50 ml). The filtrate was dried over MgSO₄, filtered and concentrated in *vacuo* to isolate the crude product which was purified by flash chromatography eluting with 5:1/9:1 petrol-EtOAc.

Following the general procedure, precursor **202** (100 mg, 0.28 mmol) was cyclised to give **218** (95 mg, 0.27 mmol, 95%).

6.2.6.1 3,3-Dimethyl-4-bromomethyl-1-(phenylmethyl)-pyrrolidin-2-one **233**

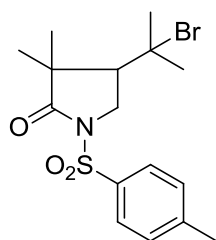


N-Allyl-*N*-(phenylmethyl)-*N*-2-bromo-2-methyl-propanamide (100 mg, 0.34 mmol) was subjected to the general procedure for copper-mediated ATRC using AIBN (6.2.6). Flash chromatography

eluting with 9:1 pet ether/EtOAc yielded **233** as a colourless oil (84 mg, 0.29 mmol, 84%); *R_f* (3:1 petrol:EtOAc) 0.30; ν_{\max} 2964, 2929, 1684, 1427, 1269, 699 cm⁻¹; δ_{H}

(300 MHz, CDCl₃) 7.34-7.27 (5H, m, Ar), 4.52 (1H, d, J_{HH} 14.4 Hz, Ar-CH₂), 4.35 (1H, d, J_{HH} 14.4 Hz, Ar-CH₂), 3.46 (1H, dd, J_{HH} 10.0, 4.8 Hz, CH₂Br), 3.35 (1H, dd, J_{HH} 10.0, 7.5 Hz, N-CH₂), 3.22 (1H, t, J_{HH} 10.0 Hz, CH₂Br), 2.88 (1H, t, J_{HH} 10.0 Hz, N-CH₂), 2.40 (1H, m, CHCH₂Br), 1.24 (3H, s, CH₃), 0.99 (3H, s, CH₃); δ_{C} (75.5 MHz, CDCl₃) 178.5 (C=O), 136.3 (Ar, quaternary), 128.8, 128.1, 127.7 (Ar), 48.9 (C(CH₃)₂), 46.7 (Ar-CH₂), 46.1 (N-CH₂), 44.0 (CH(CH₂Br), 31.5 (CH₂Br), 24.3 (CH₃), 19.6 (CH₃); [Found: 318.0464, C₁₄H₁₈NNaO⁷⁹Br requires: 318.0469].

6.2.6.2 3,3-Dimethyl-4-(2-bromo)isopropyl-1-(p-toluenesulfonyl)-pyrrolidin-2-one **253**

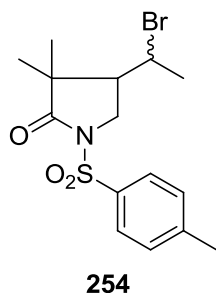


253

2-Bromo-2-methyl-*N*-[(4-methylphenyl)sulfonyl]-*N*-2-prenylpropanamide (100 mg, 0.26 mmol) was subjected to the general procedure for copper-mediated ATRC using AIBN (6.2.6). Flash chromatography eluting with 5:1 pet ether/EtOAc yielded **253** as a white solid (100 mg, 0.26 mmol, 100%); R_f (3:1 pet ether:EtOAc) 0.60; mpt 118-119 °C; ν_{max} (cm⁻¹) 2970, 2922, 1720, 1595, 1485, 1465, 1355, 1257, 1229, 1118, 1090, 817, 759, 668; δ_{H} (300 MHz, CDCl₃) 7.92 (2H, d, J_{HH} 8.2 Hz, Ar-H), 7.34 (2H, d, J_{HH} 8.2 Hz, Ar-H), 4.15 (1H, dd, J_{HH} 10.0, 7.6 Hz, N-CH₂), 3.80 (1H, t, J_{HH} 10.0 Hz, N-CH₂), 2.43 (3H, s, Ar-CH₃), 2.27 (1H, dd, J_{HH} 10.0, 7.6 Hz, CH), 1.86 (3H, s, C(CH₃)₂Br), 1.84 (3H, s, C(CH₃)₂Br), 1.28 (3H, s, C(CH₃)₂), 1.05 (3H, s, C(CH₃)₂); δ_{C} (75.5 MHz, CDCl₃) 177.1 (C=O), 145.3, 134.6 (Ar, quaternary), 129.8, 128.0 (Ar), 65.2 (C(CH₃)₂Br), 54.9 (N-CH₂), 47.7 (CH), 46.7 (C(CH₃)₂), 35.9, 32.9, 26.1, 21.8, 18.9 (CH₃); m/z (ESI) 410 ([M]⁺Na) (⁷⁹Br), 412 ([M]⁺Na) (⁸¹Br); [Found: ([M]⁺Na) 410.0396, C₂₀H₂₂⁷⁹BrNNaO₃S requires

410.0401]; [Found: C, 50.3; H, 5.8; N, 3.5; C₂₀H₂₂BrNNaO₃S requires C, 49.5; H, 5.7; N, 3.6].

6.2.6.3 3,3-Dimethyl-4-(1-bromo)ethyl-1-(*p*-toluenesulfonyl) pyrrolidin-2-one 254

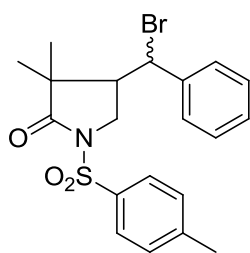


2-Bromo-2-methyl-*N*-[(4-methylphenyl)sulfonyl]-*N*-2-crotylpropanamide (100 mg, 0.27 mmol), was subjected to the general procedure for copper-mediated ATRC using AIBN (6.2.6). Flash chromatography eluting with 5:1 pet ether/EtOAc yielded **254** as a white solid, as a 3.5 : 1.0 mixture of diastereomers (100 mg, 0.25 mmol, 100%).

(±)(*S,S*)-**254**; R_f (3:1 pet ether:EtOAc) 0.59; ν_{\max} (cm⁻¹) 2969, 1723, 1597, 1485, 1464, 1393, 1356, 1168, 1115, 1089, 876, 817, 776, 659; δ_H (300 MHz, CDCl₃) 7.86 (2H, d, J_{HH} 8.1 Hz, Ar-H), 7.26 (2H, d, J_{HH} 8.1 Hz, Ar-H), 4.10 (1H, dd, J_{HH} 10.5, 7.7 Hz, N-CH₂), 4.01 (1H, dq, J_{HH} 8.6, 6.7 Hz CH(CH₃)Br) 3.40 (1H, dd, J_{HH} 10.5, 7.7 Hz, N-CH₂), 2.37 (3H, s, Ar-CH₃), 2.20 (1H, dt, J_{HH} 8.6, 7.7 Hz, CH), 1.71 (3H, d, J_{HH} 6.7 Hz, CH(Br)CH₃), 1.17 (3H, s, C(CH₃)₂), 0.87 (3H, s, C(CH₃)₂); δ_C (75.5 MHz, CDCl₃) 174.2 (C=O) 145.3, 134.9 (Ar, quaternary), 129.7, 128.1 (Ar), 50.5 (CH(Br)CH₃), 48.9 (N-CH₂), 48.8 (CH), 45.4 (C(CH₃)), 25.7 (Ar-CH₃), 25.1 (CH(Br)CH₃), 21.7 (C(CH₃)₂), 17.5 (C(CH₃)₂); m/z (ESI) 396 ([M]⁺Na) (⁷⁹Br), 398 ([M]⁺Na) (⁸¹Br); [Found: ([M]⁺Na) 396.0239, C₂₀H₂₂⁷⁹BrNNaO₃S requires 396.0245].

(±)(*R,S*)-**254**; R_f (3:1 pet ether:EtOAc) 0.59; ν_{\max} (cm^{-1}) 2969, 1723, 1597, 1485, 1464, 1393, 1356, 1168, 1115, 1089, 876, 817, 776, 659; δ_{H} (300 MHz, CDCl_3) 7.86 (2H, d, J_{HH} 8.1 Hz, Ar-H), 7.26 (2H, d, J_{HH} 8.1 Hz, Ar-H), 4.10 (1H, dd, J_{HH} 10.3, 8.6 Hz, N-CH₂), 3.99 (1H, dq, J_{HH} 8.6, 6.7 Hz CH(CH₃)Br) 3.32 (1H, dd, J_{HH} 10.3, 8.6 Hz, N-CH₂), 2.37 (3H, s, Ar-CH₃), 2.20 (1H, dt, J_{HH} 8.6, 7.7 Hz, CH), 1.71 (3H, d, J_{HH} 6.7 Hz, CH(Br)CH₃), 1.17 (3H, s, C(CH₃)₂), 0.87 (3H, s, C(CH₃)₂); δ_{C} (75.5 MHz, CDCl_3) 173.8 (C=O) 145.6, 134.5 (Ar, quaternary), 129.7, 128.1 (Ar), 50.5 (CH(Br)CH₃), 48.9 (N-CH₂), 48.8 (CH), 45.4 (C(CH₃)), 25.7 (Ar-CH₃), 25.1 (CH(Br)CH₃), 21.7 (C(CH₃)₂), 17.5 (C(CH₃)₂); m/z 396 ($[\text{M}]^+\text{Na}$) (^{79}Br), 398 ($[\text{M}]^+\text{Na}$) (^{81}Br); [Found: ($[\text{M}]^+\text{Na}$) 396.0239, $\text{C}_{20}\text{H}_{22}^{79}\text{BrNNaO}_3\text{S}$ requires 396.0245].

6.2.6.4 3,3-Dimethyl-4-(1-bromo)phenylmethyl-1-(*p*-toluenesulfonyl)-pyrrolidin-2-one **255**



255

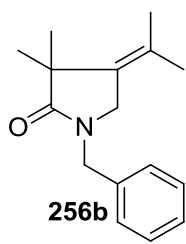
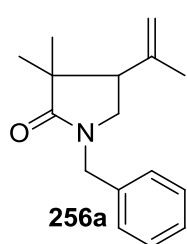
2-Bromo-2-methyl-*N*-[(4-methylphenyl)sulfonyl]-*N*-2-cinnamyl-propanamide (100 mg, 0.23 mmol) was subjected to the general procedure for copper-mediated ATRC using AIBN (6.2.6). Flash chromatography eluting with 5:1 pet ether/EtOAc yielded **255** as a white solid, as a 6.0 : 1.0 mixture of diastereomers (100 mg, 0.23 mmol, 100%).

(±)(*S,S*)-**255**; R_f (3:1 pet ether:EtOAc) 0.57; ν_{\max} (cm^{-1}) 2961, 1728, 1597, 1497, 1461, 1388, 1353, 1261, 1164, 1118, 1091, 1017, 807, 699; δ_{H} (400 MHz, CDCl_3) 7.88 (2H, d, J_{HH} 8.3 Hz, Ar-H), 7.33-7.28 (7H, m, Ar-H), 4.84 (1H, d, J_{HH} 11.3 Hz,

$\underline{\text{CH}}(\text{Br})\text{Ph}$), 4.32 (1H, dd, J_{HH} 10.5, 7.5 Hz, N- $\underline{\text{CH}}_2$), 3.45 (1H, t, J_{HH} 10.5 Hz, N- $\underline{\text{CH}}_2$), 2.89 (1H, m, $\underline{\text{CH}}$), 2.38 (3H, s, Ar- $\underline{\text{CH}}_3$), 0.76 (3H, s, C($\underline{\text{CH}}_3$)₂), 0.45 (3H, s, C($\underline{\text{CH}}_3$)₂); δ_{C} (100 MHz, CDCl_3) 145.3, 139.7, 134.9 (Ar, quaternary), 177.1 ($\underline{\text{C}}=\text{O}$), 129.8, 129.4, 129.0, 128.1, 127.8 (Ar), 50.5 ($\underline{\text{CH}}(\text{Br})\text{Ph}$), 49.9 (N- $\underline{\text{CH}}_2$), 49.6 ($\underline{\text{CH}}$), 45.8 (C($\underline{\text{CH}}_3$)₂), 25.2 (Ar- $\underline{\text{CH}}_3$), 21.7 (C($\underline{\text{CH}}_3$)₂), 17.6 (C($\underline{\text{CH}}_3$)₂); m/z (ESI) 458 ($[\text{M}]^+\text{Na}$) (^{79}Br), 460 ($[\text{M}]^+\text{Na}$) (^{81}Br); [Found: ($[\text{M}]^+\text{Na}$) 458.0396, $\text{C}_{20}\text{H}_{22}^{79}\text{BrNNaO}_3\text{S}$ requires 458.0401].

(\pm)(*R,S*)-**255**; R_f (3:1 pet ether:EtOAc) 0.57; ν_{max} (cm^{-1}) 2961, 1728, 1597, 1497, 1461, 1388, 1353, 1261, 1164, 1118, 1091, 1017, 807, 699; δ_{H} (400 MHz, CDCl_3) 7.77 (2H, d, J_{HH} 8.3 Hz, Ar- $\underline{\text{H}}$), 7.33-7.28 (7H, m, Ar- $\underline{\text{H}}$), 4.66 (1H, d, J_{HH} 10.5 Hz, $\underline{\text{CH}}(\text{Br})\text{Ph}$), 4.32 (1H, dd, J_{HH} 9.5, 7.3 Hz, N- $\underline{\text{CH}}_2$), 3.37 (1H, dd, J_{HH} 9.5, 7.3 Hz, N- $\underline{\text{CH}}_2$), 2.89 (1H, m, $\underline{\text{CH}}$), 2.36 (3H, s, Ar- $\underline{\text{CH}}_3$), 1.43 (3H, s, C($\underline{\text{CH}}_3$)₂), 1.02 (3H, s, C($\underline{\text{CH}}_3$)₂); δ_{C} (100 MHz, CDCl_3) 174.0 ($\underline{\text{C}}=\text{O}$), 145.4, 139.7, 134.9 (Ar, quaternary), 129.8, 129.4, 129.0, 128.1, 127.8 (Ar), 50.5 ($\underline{\text{CH}}(\text{Br})\text{Ph}$), 49.9 (N- $\underline{\text{CH}}_2$), 49.6 ($\underline{\text{CH}}$), 45.8 (C($\underline{\text{CH}}_3$)₂), 25.2 (Ar- $\underline{\text{CH}}_3$), 21.7 (C($\underline{\text{CH}}_3$)₂), 17.6 (C($\underline{\text{CH}}_3$)₂); m/z (ESI) 458 ($[\text{M}]^+\text{Na}$) (^{79}Br), 460 ($[\text{M}]^+\text{Na}$) (^{81}Br); [Found: ($[\text{M}]^+\text{Na}$) 458.0396, $\text{C}_{20}\text{H}_{22}^{79}\text{BrNNaO}_3\text{S}$ requires 458.0401].

6.2.6.5 **3,3-Dimethyl-4-(2-prop-1-ene)-1-(phenylmethyl) pyrrolidin-2-one**
256a, **3,3-Dimethyl-4-enyl-(2-propenyl)-1-(phenylmethyl)**
pyrrolidin-2-one 256b



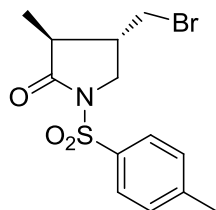
2-Bromo-2-methyl-*N*-benzyl-*N*-2-propenyl-propanamide (100 mg, 0.31 mmol) was

subjected to the general procedure for copper-mediated ATRC using AIBN (6.2.6). Flash chromatography eluting with 9:1 pet ether/EtOAc yielded **256a** and **256b** as a colourless oil, as a 2:1 mixture (75 mg, 0.30 mmol, 99%).

256a; R_f (3:1 pet ether:EtOAc) 0.68; ν_{\max} (cm^{-1}) 2970, 2929, 2869, 1697, 1495, 1430, 1270, 920, 730, 702; δ_{H} (400 MHz CDCl_3) 7.35-7.22 (5H, m, Ar), 4.89 (1H, brs, $\text{C}=\underline{\text{CH}}_2$), 4.68 (1H, brs, $\text{C}=\underline{\text{CH}}_2$), 4.52 (2H, s, Ar- $\underline{\text{CH}}_2$), 3.17 (1H, dd, J_{HH} 9.8, 7.8 Hz, N- $\underline{\text{CH}}_2$), 3.16 (1H, dd, J_{HH} 9.8, 7.8 Hz, N- $\underline{\text{CH}}_2$), 2.59 (1H, t, J_{HH} 7.8 Hz $\underline{\text{CH}}$), 1.71 (3H, s, $\text{C}\underline{\text{CH}}_3$), 1.38 (3H, s, $\text{C}(\underline{\text{CH}}_3)_2$), 1.29 (3H, s, $\text{C}(\underline{\text{CH}}_3)_2$); δ_{C} (100 MHz CDCl_3) 179.6 ($\underline{\text{C}}=\text{O}$), 142.3 (Ar, quaternary), 135.6 ($\underline{\text{C}}=\underline{\text{CH}}_2$), 128.7, 128.2, 127.5 (Ar), 113.2 ($\text{C}=\underline{\text{CH}}_2$), 50.6 ($\underline{\text{CH}}$), 46.8 ($\text{C}(\underline{\text{CH}}_3)_2$), 46.7 (N- $\underline{\text{CH}}_2$), 46.3 (Ar- $\underline{\text{CH}}_2$), 25.3, 25.0 ($\text{C}(\underline{\text{CH}}_3)_2$), 23.0 ($\text{C}\underline{\text{CH}}_3$); m/z (ESI) 266 ($[\text{M}]^+\text{Na}$), 244 ($[\text{M}]^+\text{H}$); [Found: ($[\text{M}]^+\text{H}$) 244.1696, $\text{C}_{16}\text{H}_{22}\text{NO}$ requires 244.1701].

256b; R_f (3:1 pet ether:EtOAc) 0.68; ν_{\max} (cm^{-1}) 2970, 2929, 2869, 1697, 1495, 1430, 1270, 920, 730, 702; δ_{H} (400 MHz CDCl_3) 7.35-7.22 (5H, m, Ar), 4.52 (2H, s, Ar- $\underline{\text{CH}}_2$), 3.73 (2H, s, N- $\underline{\text{CH}}_2$), 1.78 (3H, s, $\text{C}=\text{C}(\underline{\text{CH}}_3)_2$), 1.51 (3H, s, $\text{C}=\text{C}(\underline{\text{CH}}_3)_2$), 1.38 (6H, s, $\text{C}(\underline{\text{CH}}_3)_2$); δ_{C} (100 MHz CDCl_3) 179.6 ($\underline{\text{C}}=\text{O}$), 136.5 (Ar, quaternary), 130.3, 126.0 ($\underline{\text{C}}=\underline{\text{C}}$), 128.4, 128.0, 127.6, (Ar), 49.3 (N- $\underline{\text{CH}}_2$), 46.3 (Ar- $\underline{\text{CH}}_2$), 44.1 ($\text{C}(\underline{\text{CH}}_3)_2$), 24.3 ($\text{C}(\underline{\text{CH}}_3)_2$), 21.3, 20.1 ($\text{C}=\text{C}\underline{\text{CH}}_2$); m/z (ESI) 266 ($[\text{M}]^+\text{Na}$), 244 ($[\text{M}]^+\text{H}$); [Found: ($[\text{M}]^+\text{H}$) 244.1696, $\text{C}_{16}\text{H}_{22}\text{NO}$ requires 244.1701].

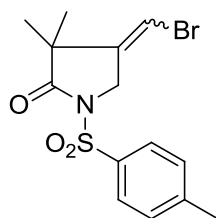
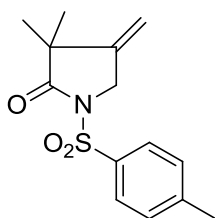
6.2.6.6 **(±)(S,S)-3-Methyl-4-bromomethyl-1-(p-toluenesulfonyl)-pyrrolidin-2-one 257a**⁵⁵

**257a**

2-bromo-*N*-[(4-methylphenyl)sulfonyl]-*N*-2-propenyl propanamide (100 mg, 0.29 mmol) was subjected to the general procedure for copper-mediated ATRC using AIBN (6.2.6). Flash chromatography eluting with 5:1 pet ether/EtOAc yielded **257a** as

a white solid (90 mg, 0.26 mmol, 90%). R_f (3:1 pet ether:EtOAc) 0.52; mpt 122-124 °C, lit⁵⁵ 124-125 °C; ν_{\max} (cm⁻¹) 2917, 1731, 1597, 1482, 1451, 1439, 1362, 1335, 1240, 1181, 1167, 1124, 1076, 708, 661; δ_H (300 MHz, CDCl₃) 7.86 (2H, d, J_{HH} 8.1 Hz, Ar-H), 7.28 (2H, d, J_{HH} 8.1 Hz, Ar-H), 4.04 (1H, dd, J_{HH} 10.2, 7.3 Hz, CH₂Br), 3.46 (1H, m, CH₂Br), 3.45 (1H, m, N-CH₂), 3.29 (1H, dd, J_{HH} 10.7, 7.1 Hz, N-CH₂), 2.37 (3H, s, Ar-CH₃), 2.26 (2H, br, CH), 1.1 (3H, d, J_{HH} 6.6 Hz, CH₃); δ_C (75.5 MHz, CDCl₃) 174.0 (C=O), 145.4, 134.9 (Ar quaternary), 129.8, 128.1 (Ar), 49.6 (CHCH₃), 42.8 (CHCH₂), 41.8 (CH₂Br), 32.8 (N-CH₂), 21.7 (Ar-CH₃), 12.9 (CH₃); m/z (ESI) 368 ([M]⁺Na) (⁷⁹Br), 370 ([M]⁺Na) (⁸¹Br); [Found: ([M]⁺Na) 367.9926, C₁₃H₁₆⁷⁹BrNNaO₃S requires 367.9932]; [Found: C, 44.9; H, 4.7; N, 3.9; C₁₃H₁₆BrNO₃S requires C, 45.1; H, 4.7; N 4.1].

6.2.6.7 **3,3-Dimethyl-4-bromomethylene-1-[(4-methylphenyl)sulfonyl]-pyrrolidin-2-one 222,**²³⁸ **3,3-dimethyl-4-methylene-1-[(4-methylphen-yl)sulfonyl]-pyrrolidin-2-one 221**²³⁸

**222****221**

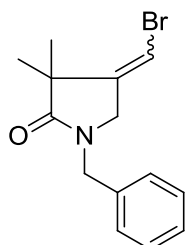
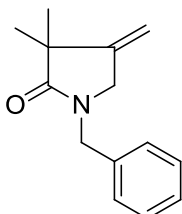
N-(2-bromo-2-methyl-propionyl)-4-methyl-*N*-prop-2-ynyl-benzenesulfonamide

(100 mg, 0.28 mmol) was subjected to the general procedure for copper-mediated ATRC using AIBN (6.2.6). Flash chromatography eluting with 5:1 pet ether/EtOAc yielded **222** and **221** (70 mg, 80%) as a 1:1 mixture of an off-white solid.

221; R_f (3:1 petrol:EtOAc) 0.48; mpt 103-105 °C, lit²³⁸ 104-106 °C; ν_{\max} (cm⁻¹) 2970, 1731, 1596, 1494, 1463, 1360, 1340, 1166, 1118, 1090, 813; δ_H (300 MHz, CDCl₃) 7.84 (2H, d, J_{HH} 8.1 Hz, Ar-H), 7.26 (2H, d, J_{HH} 8.1 Hz, Ar-H), 4.90 (1H, dt, J_{HH} 1.5, 1.5 Hz, C=CH₂), 4.88 (1H, dt, J_{HH} 1.5, 1.5 Hz, C=CH₂), 4.28 (2H, t, J_{HH} 1.5 Hz, N-CH₂), 2.25 (3H, s, Ar-CH₃), 1.0 (6H, s, C(CH₃)₂); δ_C (75.5 MHz, CDCl₃) 176.9 (C=O), 145.3 (C=CH₂), 145.2, 135.0 (Ar quaternary), 129.7, 128.0 (Ar), 108.5 (C=CH₂), 49.3 (C(CH₃)₂), 46.1 (N-CH₂), 24.4 (Ar-CH₃), 21.7 ((CH₃)₂); m/z (ESI) 302 ([M]⁺Na); [Found: 302.0870, 5.0; C₁₄H₁₇NNaO₃S requires: 302.0873].

222; R_f (3:1 petrol:EtOAc) 0.48; mpt 123-125 °C, lit²³⁸ 126-128 °C; ν_{\max} (cm⁻¹) 2970, 1731, 1596, 1494, 1463, 1360, 1340, 1166, 1118, 1090, 813; δ_H (300 MHz, CDCl₃), 7.86 (2H, d, J_{HH} 8.3 Hz, Ar-H), 7.27 ((2H, d, J_{HH} 8.3 Hz, Ar-H)), 6.10 (1H, t, J_{HH} 2.6 Hz, CHBr), 4.37 (2H, m, N-CH₂), 2.37 (3H, s, Ar-CH₃), 1.14 (3H, s, C(CH₃)₂), 1.08 (3H, s, C(CH₃)₂); δ_C (75.5 MHz, CDCl₃); 175.9 (C=O), 145.6, 142.6 (Ar quaternary), 134.7 (CCH₂), 129.8, 128.0 (Ar), 102.4 (CHBr), 50.1 (N-CH₂), 47.7 (C(CH₃)₂), 25.1 (CH₃), 24.4 (CH₃), 21.7 (Ar-CH₃); m/z (ESI); 380 ([M]⁺Na) (⁷⁹Br), 382 ([M]⁺Na) (⁸¹Br), [Found: ([M]⁺Na), 381.9917, C₁₄H₁₆⁸¹BrNNaO₃S requires 381.9911].

6.2.6.8 3,3-Dimethyl-4-bromomethylene-1-(phenylmethyl)-2-pyrrolidinone 258, 3,3-Dimethyl-4-methylene-1-(phenylmethyl)-2-pyrrolidinone 235

**258****235**

2-Bromo-2-methyl-*N*-(phenylmethyl)-*N*-2-propynyl-propanamide (100 mg, 0.34 mmol) was subjected to the general procedure for copper-mediated ATRC using AIBN (6.2.6). Flash chromatography eluting with 9:1 pet ether/EtOAc yielded **258** and **235** (76 mg, 82%) as a 2:1 mixture of a colourless oil.

235; R_f (3:1 petrol:EtOAc) 0.59; ν_{\max} (cm^{-1}) 3066, 2966, 2926, 1693, 1495, 1475, 1455, 1425, 1359, 1255, 1166, 698; δ_{H} (300 MHz, CDCl_3) 7.32-7.13 (5H, m, Ar-H), 5.03 (1H, dt, J_{HH} 2.4, 1.5 Hz, C=CH₂), 4.96 (1H, dt, J_{HH} 2.4, 1.5 Hz, C=CH₂), 4.51 (2H, s, Ar-CH₂), 3.82 (2H, t, J_{HH} 1.5 Hz, CH₂), 1.27 (6H, s, (CH₃)₂); δ_{C} (75.5 MHz, CDCl_3) 177.5 (C=O) 148.8 (CCH₂), 136.3 (Ar, quaternary), 128.8, 128.1, 127.6 (Ar), 106.7 (C=CH₂), 49.7 (C, quaternary), 46.2 (Ar-CH₂), 44.5 (CH₂), 25.2, 25.0 (CH₃); m/z (ESI) 214 ([M]⁺H); [Found: ([M]⁺H) 214.1228, C₁₄H₁₇NO requires, 214.1232].

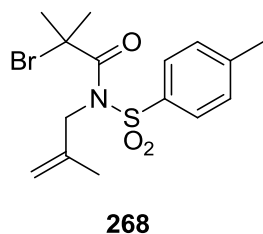
258 as a pale yellow oil; R_f (3:1 pet ether:EtOAc) 0.57; ν_{\max} (cm^{-1}) 3066, 2966, 2926, 1693, 1495, 1475, 1455, 1425, 1359, 1255, 1166, 698; δ_{H} (300 MHz, CDCl_3) 7.32-7.13 (5H, m, Ar), 6.11 (1H, t, J_{HH} 2.7 Hz, CHBr), 4.53 (2H, s, Ar-CH₂), 3.82 (2H, m, N-CH₂), 1.31 (3H, s, C(CH₃)₂), 1.27 (3H, s, C(CH₃)₂); δ_{C} (75.5, CDCl_3) 177.5 (C=O), 146.1 (Ar, quaternary), 135.9 (C=C), 128.8, 127.8, 127.6 (Ar), 106.7 (CHBr), 49.6 (Ar-CH₂), 46.2 (N-CH₂), 44.0 (C(CH₃)₂), 25.6, 25.2 (C(CH₃)₂); m/z (ESI) 316

([M]⁺Na), (⁷⁹Br), 318 ([M]⁺Na), (⁸¹Br); [Found: ([M]⁺Na) 316.0307, C₂₀H₂₂⁷⁹BrNNaO₃S requires 316.0313].

6.2.7 General Procedure for Substrates Synthesised in Chapter 4

Substrates **202**, **203**, **210**, **215** (6.2.1) and **249-252** (6.2.5) were prepared previously and procedures and data can be found in the relevant sections above. In addition, compounds **268** and **269** were prepared for 5-*exo trig* radical cyclisation. Substrates **270-275**, **305** and **306** were prepared for 4-*exo* and 5-*endo trig* radical cyclisation via the same general procedure (6.2.8).

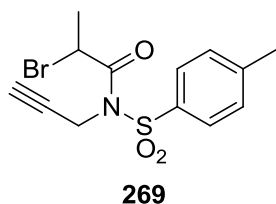
6.2.7.1 2-Bromo-2-methyl-N-[(4-methylphenyl)sulfonyl]-N-(2-methyl-2-propenyl)propanamide **268**²¹



2-Methylallylamine (0.15 g, 2.17 mmol) was dissolved in dichloromethane (10 cm³) and cooled to 0°C. Triethylamine (0.3 cm³, 2.17 mmol) was added followed by *p*-toluenesulfonyl chloride (0.41 g, 2.17 mmol) in dichloromethane (10 cm³), which was added *via* a dropping funnel over 5 minutes. The reaction was allowed to reach room temperature overnight. The reaction was quenched with 1 M HCl (10 cm³) and the aqueous layer was extracted using dichloromethane (3 x 20 cm³). The combined organic extracts were washed with brine (20 cm³), dried using MgSO₄, filtered and concentrated in vacuo to yield a crude product, a portion of which (0.3 g, 1.33 mmol) was dissolved in dry THF (10 cm³) and taken to -78°C at which point *n*-BuLi (1.6 M in hexanes, 0.94 cm³, 1.5

mmol) was added dropwise via syringe. The reaction was allowed to proceed for 30 mins. 2-Bromoisobutyryl bromide (0.19ml, 1.5 mmol) was added and the reaction was allowed to reach room temperature overnight. The reaction was quenched with NH_4Cl (5 cm^3) and partitioned between NaHCO_3 (20 cm^3) and dichloromethane (20 cm^3). The aqueous layer was extracted using dichloromethane (2 x 20 cm^3). The combined organic extracts were washed with brine (20 cm^3), dried with MgSO_4 , filtered and concentrated in *vacuo* to yield a crude yellow which was purified by flash chromatography to yield **268** as a colourless oil (180 mg, 0.48 mmol, 36%). R_f (3:1 pet ether:EtOAc) 0.85; mpt 110-112 °C, lit²¹ 112-113 °C; ν_{max} (cm^{-1}) 3088, 3001, 2974, 2919, 1673, 1597, 1494, 1453, 1352, 1317, 1237, 1165, 1096, 717; δ_{H} (300 MHz, CDCl_3) 7.86 (2H, d, J_{HH} 8.1 Hz, Ar), 7.30 (2H, d, J_{HH} 8.1 Hz, Ar), 5.03 (1H, d, J_{HH} 1.6 Hz, $\text{C}(\text{CH}_3)\text{C}=\underline{\text{CH}}_2$), 5.02 (1H, d, J_{HH} 1.6 Hz, $\text{C}(\text{CH}_3)\text{C}=\underline{\text{CH}}_2$), 4.81 (2H, br s, $\text{N}-\underline{\text{CH}}_2$), 2.43 (3H, s, Ar- $\underline{\text{CH}}_3$), 1.83 (6H, s, ($\underline{\text{CH}}_3$)₂), 1.81 (3H, s, $\underline{\text{CH}}_3$); δ_{C} (75.5 MHz, CDCl_3) 169.8 ($\underline{\text{C}}=\text{O}$), 144.0, 135.3 (Ar, quaternary), 140.2 ($\underline{\text{C}}(\text{CH}_3)\text{CH}_2$), 128.5, 128.2 (Ar), 111.5 ($\text{C}(\text{CH}_3)\underline{\text{C}}\text{H}_2$), 57.0 ($\underline{\text{C}}(\text{CH}_3)\text{Br}$), 52.7 ($\text{N}-\underline{\text{C}}\text{H}_2$), 31.5 ($\text{C}(\underline{\text{C}}\text{H}_3)_2\text{Br}$), 21.1 (Ar- $\underline{\text{C}}\text{H}_3$), 19.7 ($\text{C}(\underline{\text{C}}\text{H}_3)\text{CH}_2$); m/z 396 ($[\text{M}]^+\text{Na}$) (^{79}Br), 398 ($[\text{M}]^+\text{Na}$) (^{81}Br); [Found: ($[\text{M}]^+\text{Na}$) 396.0239, $\text{C}_{15}\text{H}_{20}^{79}\text{BrNNaO}_3\text{S}$ requires 396.0345].

6.2.7.2 2-Bromo-*N*-[(4-methylphenyl)sulfonyl]-*N*-2-propynyl propanamide **269**¹⁵



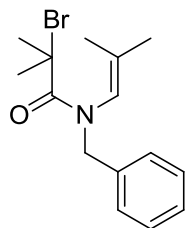
Using the same procedure as 6.2.1.3, 4-methyl-*N*-prop-2-ynyl-benzenesulfonamide (1.02 g, 4.9 mmol) in dry THF (50 cm^3), *n*-BuLi (1.6 M, 4.7 cm^3 , 7.5 mmol) and 2-

bromopropionyl bromide (0.79 cm³, 7.5 mmol) furnished the crude product as a yellow oil which was purified by flash chromatography eluting with 5:1 pet ether/EtOAc to yield **269** as a pale yellow oil (0.89 g, 2.6 mmol, 53%). *R_f* (3:1 Pet ether: EtOAc) 0.50; ν_{\max} (cm⁻¹) 3276, 2989, 2972, 2937, 1698, 1599, 1498, 1369, 1283, 1167, 1088, 812, 718; δ_{H} (300 MHz, CDCl₃) 7.91 (2H, d, J_{HH} 8.1 Hz, Ar-H) 7.34 (2H, d, J_{HH} 8.1 Hz, Ar-H), 4.97 (1H, q, J_{HH} 6.6 Hz, CH(Br)CH₃), 4.84 (1H, dd, J_{HH} 18.6, 2.3 Hz N-CH₂), 4.60 (1H, dd, J_{HH} 18.6, 2.3 Hz, N-CH₂), 2.44 (3H, s, Ar-CH₃), 2.34 (1H, t, J_{HH} 2.3 Hz, CH), 1.74 (3H, d, J_{HH} 6.6 Hz, CH₃); δ_{C} (75.5 MHz, CDCl₃) 168.9 (C=O), 145.5, 135.3 (Ar quaternary), 129.8, 128.4 (Ar), 77.7, 73.5 (CCH), 39.3 (CH(Br)CH₃), 35.7 (N-CH₂), 21.1, 20.2 (CH₃); *m/z* (ESI) 366 ([M]⁺Na) (⁷⁹Br), 368 ([M]⁺Na) (⁸¹Br); [Found: ([M]⁺Na) 365.9770, C₁₃H₁₄⁷⁹BrNNaO3S requires 365.9775].

6.2.8 General Procedure for the Synthesis of Enamides in Chapter 4

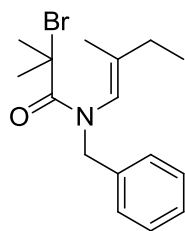
Aldehyde or cyclic ketone (1 equiv) and benzylamine (1 equiv) were added to dry toluene at room temperature. The reaction mixture was heated at reflux overnight, using a dean-stark apparatus. The crude reaction mixture was allowed to cool to room temperature, then cooled further to 0°C before addition of acyl halide (1 equiv), followed by diethylaniline (1 equiv). The reaction was allowed to reach room temperature and stirred for 4 hrs. The reaction mixture was washed with 2M HCl. The resulting organic layer was dried over MgSO₄, filtered and concentrated in *vacuo* to yield a crude product purified *via* flash chromatography eluting with 9:1 pet ether-EtOAc.

6.2.8.1 *N*-Benzyl-2-bromo-*N*-(isobutenyl)-2-methyl-propionamide **270**³⁵

**270**

The general procedure for the synthesis of enamides (6.2.8) was applied using benzylamine (3.00 ml, 27.5 mmol), isobutyraldehyde (2.51 ml, 27.5 mmol) and 2-bromoisobutyryl bromide (3.40 ml, 27.5 mmol) to furnish a crude product which was purified by flash chromatography, eluting with 9:1 pet ether/EtOAc to yield **270** as a colourless oil (4.97 g, 15.8 mmol, 57%). R_f (3:1 pet ether:EtOAc) 0.74; ν_{\max} (cm^{-1}) 3030, 2975, 2933, 1637, 1496, 1463, 1447, 1390, 1366, 1263, 1173, 1107, 829, 697; δ_{H} (400 MHz, CDCl_3) 7.32-7.28 (5H, m, Ar), 6.36 (1H, s, N-CH), 4.72 (2H, s, Ar-CH₂), 1.99 (6H, s, C(CH₃)₂Br), 1.75 (3H, s, CH₃), 1.63 (3H, s, CH₃); δ_{C} (100 MHz, CDCl_3) 170.6 (C=O), 137.3 (Ar quaternary), 134.9 (C(CH₃)₂), 128.4, 127.9, 127.2 (Ar), 125.8 (N-CH), 58.3 (C(CH₃)₂Br), 54.4 (Ar-CH₂), 32.1 (C(CH₃)₂Br), 21.8 (C(CH₃)₂), 18.2 (C(CH₃)₂); m/z (ESI) 332 ($[\text{M}]^+\text{Na}$) (^{79}Br), 334 ($[\text{M}]^+\text{Na}$) (^{81}Br); [Found: ($[\text{M}]^+\text{Na}$) 332.0620, $\text{C}_{15}\text{H}_{20}^{79}\text{BrNNaO}$ requires 332.0626].

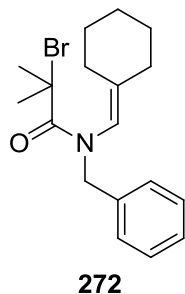
6.2.8.2 *N*-Benzyl-2-bromo-*N*-(2-methylbut-1-enyl)-2-methyl-propionamide **271**³⁵

**271**

The general procedure for the synthesis of enamides (6.2.8) was applied using benzylamine (2.32 ml, 22.1 mmol), 2-methylbutyraldehyde (2.37 ml, 22.1 mmol) and 2-bromoisobutyryl bromide (2.73 ml, 22.1 mmol) to furnish a crude product which was purified by flash chromatography, eluting with 9:1 pet ether/EtOAc to yield **271** as a

pale yellow oil (2.80 g, 8.6 mmol, 39%). R_f (3:1 pet ether:EtOAc) 0.81; ν_{\max} (cm^{-1}) 3031, 2968, 2934, 1637, 1496, 1454, 1388, 1366, 1284, 1263, 1172, 1107, 844, 749, 726, 697; δ_{H} (300 MHz, CDCl_3) 7.33-7.29 (5H, m, Ar), 6.37 (1H, s, N-CH), 4.70 (2H, s, Ar-CH₂), 2.08 (2H, q, J_{HH} 7.5 Hz, CH₂CH₃), 1.98 (6H, s, (CH₃)₂), 1.62 (3H, s, CCH₃), 1.04 (3H, t, J_{HH} 7.5 Hz, CH₂CH₃); δ_{C} (75.5 Hz, CDCl_3) 170.6 (C=O), 139.8 (Ar quaternary), 137.3 (NC=C), 128.4, 128.0, 127.2 (Ar), 125.2 (N-CH), 58.5 (C(CH₃)₂Br), 54.3 (Ar-CH₂), 32.2 (C(CH₃)₂), 29.0 (CCH₃), 16.2 (CCH₂CH₃), 12.2 (CCH₂CH₃); m/z (ESI) 346 ([M]⁺Na) (⁷⁹Br), 348 ([M]⁺Na) (⁸¹Br); [Found: ([M]⁺Na) 346.0779, C₁₆H₂₂⁷⁹BrNNaO requires 346.0782].

6.2.8.3 *N*-Benzyl-2-bromo-*N*-(methylenecyclohexane)-2-methylpropionamide **272**⁵⁶

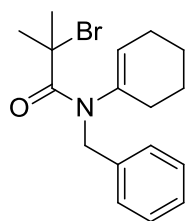


The general procedure for the synthesis of enamides (6.2.8) was applied using benzylamine (1.73 ml, 16.5 mmol), cyclohexane carboxaldehyde (2.00 ml, 16.5 mmol) and 2-bromoisobutyryl bromide (2.04 ml, 16.5 mmol) to furnish a crude product which was purified by flash chromatography, eluting with 9:1 pet ether/EtOAc to yield **272** as a yellow oil (3.90 g, 11.1 mmol, 67%). R_f (3:1 pet ether:EtOAc) 0.83; ν_{\max} (cm^{-1}) 3028, 2929, 2854, 1636, 1495, 1463, 1448, 1389, 1365, 1264, 1177, 1108, 836, 697; δ_{H} (300 MHz, CDCl_3) 7.32-7.27 (5H, m, Ar), 6.33 (1H, s, N-CH), 4.70 (Ar-CH₂), 2.13 (4H, br, CCH₂), 2.00 (6H, s, C(CH₃)₂), 1.57 (6H, br, CH₂); δ_{C} (75.5 MHz, CDCl_3) 170.0 (C=O), 140.5 (Ar quaternary), 136.7 (N-CH), 127.8, 127.3, 126.5 (Ar), 122.2 (N-C(H)C), 57.9 (C(CH₃)₂), 54.4 (Ar-CH₂), 32.2 (C(CH₃)₂), 31.7 (C(CH₃)₂), 28.0 (CH₂), 26.8 (CH₂), 25.5 (CH₂); m/z (ESI) 372 ([M]⁺Na) (⁷⁹Br), 374

([M]⁺Na) (⁸¹Br), 350 [M]⁺; [Found: ([M]⁺Na) 372.0933, C₁₈H₂₄⁷⁹BrNNaO requires 372.0939].

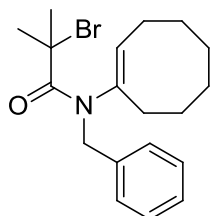
6.2.8.4 *N*-Benzyl-2-bromo-*N*-(cyclohex-1-enyl)-2-methyl-propionamide

273⁵⁵

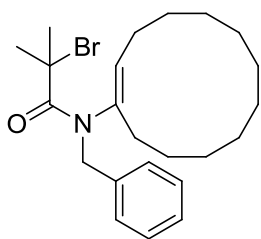


273

The general procedure for the synthesis of enamides (6.2.8) was applied using benzylamine (2.63 ml, 24.1 mmol), cyclohexanone (2.50 ml, 24.1 mmol) and 2-bromoisobutyryl bromide (2.98 ml, 24.1 mmol) to furnish a crude product which was purified by flash chromatography, eluting with 9:1 pet ether/EtOAc to yield **273** as a colourless oil (5.60 g, 16.6 mmol, 69%). R_f (3:1 pet ether:EtOAc) 0.8; ν_{\max} (cm⁻¹) 2931, 2859, 1630, 1495, 1449, 1390, 1364, 1257, 1171, 1107, 920, 726, 697; δ_H (300 MHz CDCl₃) 7.25-7.19 (5H, m, Ar), 5.53 (1H, m, CH), 4.90 (1H, br, Ar-CH₂), 4.19 (1H, br, Ar-CH₂), 2.12 (2H, br, CH₂), 1.96 (8H, br-s, (CH₃)₂ and CH₂), 1.63 (2H, m, CH₂), 1.47 (CH₂); δ_C (75 MHz CDCl₃) 170.5 (C=O), 137.7 (Ar, quaternary), 128.4, 128.2, 127.2 (Ar), 58.5 (C(CH₃)₂Br), 52.4 (Ar-CH₂), 28.0 (CH₂), 24.6 (C(CH₃)₂Br), 22.6 (CH₂), 21.3 (CH₂); m/z (ESI) 358 ([M]⁺Na) (⁷⁹Br), 360 ([M]⁺Na) (⁸¹Br); [Found: ([M]⁺Na) 358.0777; C₁₇H₂₂BrNNaO requires 358.0782]; [Found: C, 60.7; H, 6.7; N, 4.1. C₁₇H₂₂BrNO requires C, 60.7; H, 6.6; N, 4.2].

6.2.8.5 *N*-Benzyl-2-bromo-*N*-(cyclooct-1-enyl)-2-methyl-propionamide**274**²⁵**274**

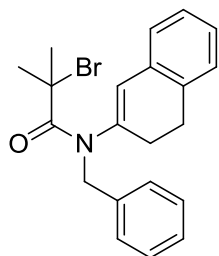
The general procedure for the synthesis of enamides (6.2.8) was applied using benzylamine (1.10 ml, 10.0 mmol), cyclooctanone (1.32 ml, 10.0 mmol) and 2-bromoisobutyryl bromide (1.24 ml, 10.0 mmol) to furnish a crude product which was purified by flash chromatography, eluting with 9:1 pet ether/EtOAc to yield **274** as a colourless oil (3.50 g, 9.5 mmol, 95%). R_f (3:1 pet ether:EtOAc) 0.77; ν_{\max} (cm^{-1}) 2925, 2852, 1630, 1495, 1463, 1453, 1390, 1364, 1273, 1171 1107, 733, 698; δ_{H} (300 MHz, CDCl_3) 7.34-7.28 (5H, m, Ar), 5.61 (1H, t, J_{HH} 8.5 Hz, $\underline{\text{CH}}$), 5.08-4.45 (2H, br, Ar- $\underline{\text{CH}}_2$), 2.07-1.39 (12H, br, $\underline{\text{CH}}_2$), 2.04 (6H, s, ($\underline{\text{CH}}_3$)₂); δ_{C} (75 MHz, CDCl_3) 170.7 ($\underline{\text{C}}=\text{O}$), 137.6 (Ar, quaternary), 129.1 ($\underline{\text{N}}-\underline{\text{C}}$), 128.3, 127.9, 127.1 (Ar), 58.6 ($\underline{\text{C}}(\text{CH}_3)_2$), 42.0 (Ar- $\underline{\text{C}}\text{H}_2$), 33.7, 33.3, 32.4, 29.4, 22.6, 21.1 ($\underline{\text{C}}\text{H}_2$), 26.3 ($\text{C}(\underline{\text{C}}\text{H}_3)_2$); m/z (ESI) 386 ($[\text{M}]^+\text{Na}$) (^{79}Br), 386 ($[\text{M}]^+\text{Na}$) (^{81}Br); [Found: ($[\text{M}]^+\text{Na}$) 386.1090; $\text{C}_{19}\text{H}_{26}^{79}\text{BrNNaO}$ requires 386.1095].

6.2.8.6 *N*-Benzyl-2-bromo-*N*-(cyclododec-1-enyl)-2-methyl-propionamide**275****275**

The general procedure for the synthesis of enamides (6.2.8) was applied using benzylamine (1.10 ml, 10.0 mmol), cyclododecanone (1.82 g, 10.0 mmol) and 2-bromoisobutyryl bromide (1.24 ml, 10.0 mmol) to furnish a crude product

which was purified by flash chromatography, eluting with 9:1 pet ether/EtOAc to yield **275** as a yellow oil (3.30 g, 7.8 mmol, 78%). R_f (3:1 pet ether:EtOAc) 0.84; ν_{\max} (cm^{-1}) 2928, 2861, 1707, 1633, 1495, 1467, 1390, 1366, 1265, 1169, 1107, 734, 696; δ_{H} (300 MHz, CDCl_3) 7.33-7.27 (5H, m, Ar), 5.18 (1H, t, J_{HH} 8.3 Hz, CH), 5.12-4.19 (2H, br, Ar- CH_2), 2.37, 2.00, 1.72, 1.62, 1.5-1.2 (20H, br, CH_2), 2.04 (6H, s, (CH_3)₂); δ_{C} (75 MHz, CDCl_3) 170.4 ($\text{C}=\text{O}$), 139.0 (Ar, quaternary), 137.6 (N- C), 128.5, 128.2, 127.2 (Ar), 54.1 ($\text{C}(\text{CH}_3)_2\text{Br}$), 40.4 (Ar- CH_2), 33.6, 27.5, 26.3, 25.4, 24.7, 24.6, 24.4, 24.2, 22.7, 22.6 (CH_2), 22.3 ((CH_3)₂); m/z (ESI) 442 ($[\text{M}]^+\text{Na}$) (^{79}Br), 444 ($[\text{M}]^+\text{Na}$) (^{81}Br), [Found: ($[\text{M}]^+\text{Na}$) 442.1716; $\text{C}_{23}\text{H}_{34}^{79}\text{BrNNaO}$ requires 442.1721].

6.2.8.7 *N*-Benzyl-2-bromo-*N*-(9,10-dihydronaphthalen-1-yl)-2-methylpropionamide **305**²⁵

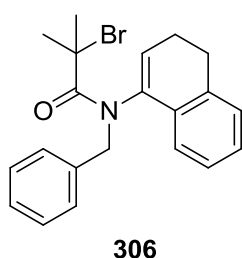


305

The general procedure for the synthesis of enamides (6.2.8) was applied using benzylamine (0.37 ml, 3.4 mmol), β -tetralone (0.45 ml, 3.4 mmol) and 2-bromoisobutyryl bromide (0.42 ml, 3.4 mmol) to furnish a crude product which was purified by flash chromatography, eluting with 9:1 pet ether/EtOAc to yield **305** as a brown oil (1.10 g, 2.9 mmol, 84%). R_f (3:1 pet ether: EtOAc) 0.74; ν_{\max} (cm^{-1}) 3030, 2937, 2835, 1630, 1495, 1486, 1453, 1436, 1390, 1365, 1266, 1166, 1106, 751, 666; δ_{H} (400 MHz, CDCl_3) 7.34-7.08 (9H, m, Ar), 6.27 (1H, s, CH), 4.79 (2H, br s, Ar- CH_2), 2.96 (2H, t, J_{HH} 8.0 Hz, CH_2), 2.55 (2H, t, J_{HH} 8.0 Hz, CH_2), 2.06 (6H, s, (CH_3)₂); δ_{C} (100 MHz, CDCl_3); 170.7 ($\text{C}=\text{O}$), 139.6, 137.2, 134.1 (Ar, quaternary), 132.8 (N- C), 128.6, 128.4, 127.9, 127.6, 127.5, 127.4, 126.9, 126.8, 126.7 (Ar),

126.6 ($\underline{\text{C}}\text{H}$), 58.4 ($\underline{\text{C}}(\text{CH}_3)_2$), 53.1 ($\text{Ar}-\underline{\text{C}}\text{H}_2$), 33.6 ($\text{C}(\underline{\text{C}}\text{H}_3)_2$), 28.3, 27.5 ($\underline{\text{C}}\text{H}_2$); m/z (ESI) 384 ($[\text{M}]^+\text{H}$) (^{79}Br), 386 ($[\text{M}]^+\text{H}$) (^{81}Br); [Found: ($[\text{M}]^+\text{H}$) 383.0963; $\text{C}_{21}\text{H}_{23}^{79}\text{BrNO}$ requires 383.0961].

6.2.8.8 *N*-Benzyl-2-bromo-*N*-(3,4-dihydronaphthalen-1-yl)-2-methylpropion-amide **306²⁵**



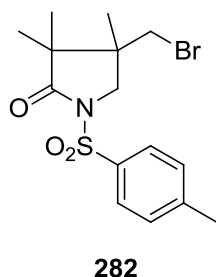
The general procedure for the synthesis of enamides (6.2.8) was applied using benzylamine (3.00ml, 27.5 mmol), α -tetralone (3.66 ml, 27.5 mmol) and 2-bromoisobutyryl bromide (3.40 ml, 27.5 mmol) to furnish a crude product which was purified by flash chromatography, eluting with 9:1 pet ether/EtOAc to yield **306** as a yellow oil (6.10 g, 16.0 mmol, 58%). R_f (3:1 per ether:EtOAc) 0.77; ν_{max} (cm^{-1}) 3062, 2968, 2939, 2893, 2826, 1634, 1497, 1483, 1448, 1425, 1391, 1361, 1351, 1274, 1173, 1102, 978, 916, 782, 773, 733, 696; δ_{H} (400 MHz, CDCl_3) 7.20-7.09 (9H, m, Ar), 5.82 (1H, t, J_{HH} 4.7 Hz, $\underline{\text{C}}\text{H}$), 5.55 (1H, d, J_{HH} 14.2 Hz, $\text{Ar}-\underline{\text{C}}\text{H}_2$), 3.68 (1H, br d J_{HH} 14.2 Hz, $\text{Ar}-\underline{\text{C}}\text{H}_2$), 2.71 (2H, t, J_{HH} 7.7 Hz, $\underline{\text{C}}\text{H}_2$), 2.23 (2H, m, $\text{CH}\underline{\text{C}}\text{H}_2$), 1.97 (3H, s, $\underline{\text{C}}\text{H}_3$), 1.76 (3H, s, $\underline{\text{C}}\text{H}_3$); δ_{C} (100 MHz, CDCl_3) 171.2 ($\underline{\text{C}}=\text{O}$), 137.4, 137.0, 136.8 (Ar quaternary), 132.0 ($\text{N}-\underline{\text{C}}$), 130.3, 129.0, 128.3, 128.2, 128.1, 127.4, 126.8 (Ar), 122.6 ($\underline{\text{C}}\text{H}$), 58.1 ($\underline{\text{C}}(\text{CH}_3)_2$), 52.9 ($\text{Ar}-\underline{\text{C}}\text{H}_2$), 34.6, 31.6 ($\underline{\text{C}}\text{H}_2$), 27.0, 22.7 ($\underline{\text{C}}\text{H}_3$); m/z (ESI) 384 ($[\text{M}]^+\text{H}$) (^{79}Br), 386 ($[\text{M}]^+\text{H}$) (^{81}Br); [Found: ($[\text{M}]^+\text{H}$) 383.0959; $\text{C}_{21}\text{H}_{23}^{79}\text{BrNO}$ requires 383.0963]; [Found: C, 65.7; H, 5.8; N, 3.5 $\text{C}_{21}\text{H}_{22}\text{BrNO}$ requires C, 65.6; H, 5.8; N, 3.6].

6.2.9 General Procedure for Copper Mediated ATRC Using KBH_4 in Chapter 4

The precursor (0.20-0.31 mmol) was dissolved in methanol (0.12 M) at room temperature. A solution (0.01 M) of CuSO_4/TPA (0.1 mol%) was added followed by KBH_4 (10 mol%). The reaction mixture was then stirred at room temperature for 10-30 minutes. The mixture was filtered through a silica plug using DCM (50 ml) and the resulting filtrate was washed with H_2O (30 ml). The organic layer was dried over MgSO_4 , filtered and concentrated in *vacuo* to isolate the crude product which was purified by flash chromatography eluting with 5:1/9:1 petrol-EtOAc.

The cyclisation of substrates **202**, **203**, **206**, **210**, **215** and **249-251** yielded products **218**, **221**, **222**, **233**, **235**, **253-256** and **258**, the data for which can be found in sections above.

6.2.9.1 3,3-Dimethyl-4-methyl-4-bromomethyl-1-(*p*-toluenesulfonyl)-pyrrolidin-2-one **282**⁵⁵



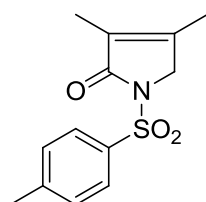
2-Bromo-2-methyl-*N*-[(4-methylphenyl)sulfonyl]-*N*-(2-methyl-2-propenyl)-propanamide (100 mg, 0.27 mmol) was subjected to the general procedure for copper-mediated ATRC using KBH_4 (6.2.9) to yield a crude product. Flash chromatography eluting

with 5:1 pet ether/EtOAc yielded **282** as a white solid (84 mg, 0.23 mmol, 84 %). R_f (3:1 pet ether:EtOAc) 0.48; mpt 174-176 °C, lit⁵⁵ 175-176; ν_{max} (cm^{-1}) 3052, 2982, 2937, 1722, 1596, 1489, 1458, 1383, 1349, 1292, 1261, 1158, 1105, 1091, 817, 767;

δ_{H} (400 MHz CDCl_3) 7.91 (2H, d, J_{HH} 8.3 Hz, Ar-H), 7.34 (2H, d, J_{HH} 8.3 Hz, Ar-H), 3.85 (1H, d, J_{HH} 10.8 Hz N-CH₂), 3.57 (1H, d, J_{HH} 10.8 Hz N-CH₂), 3.27 (1H, d, J_{HH} 10.5 Hz, CH₂Br), 3.22 (1H, d, J_{HH} 10.5 Hz, CH₂Br), 2.44 (3H, s, Ar-CH₃), 1.09 (3H, s, C(CH₃)₂), 1.07 (3H, s, C(CH₃)₂), 0.97 (3H, s, CH₃); δ_{C} (100 MHz CDCl_3) 165.2 (C=O), 145.3 (Ar, quaternary), 135.0 (Ar, quaternary), 129.7, 128.0 (Ar), 54.1 (N-CH₂), 48.5 (C(CH₃)₂), 48.2 (C(CH₃)CH₂Br), 38.5 (CH₂Br), 21.7 (Ar-CH₃), 20.0, 19.1 (C(CH₃)₂), 18.5 (CH₃); m/z (ESI) 396 ($[\text{M}]^+\text{Na}$) (^{79}Br), 398 ($[\text{M}]^+\text{Na}$) (^{81}Br); [Found: ($[\text{M}]^+\text{Na}$) 396.0244, $\text{C}_{15}\text{H}_{20}^{79}\text{BrNNaO}_3\text{S}$ requires 396.0245].

6.2.9.2 3-Methyl-4-methyl-1-(p-toluenesulfonyl)-pyrrolidin-3-en-2-one

286¹⁵

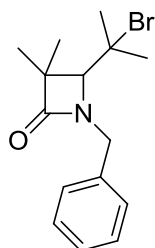
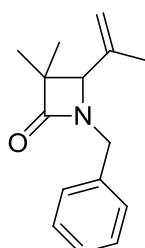


286

2-Bromo-*N*-[(4-methylphenyl)sulfonyl]-*N*-2-propynylpropanamide (100 mg, 0.29 mmol) was subjected to the general procedure for copper-mediated ATRC using KBH_4 (6.2.9) to yield a crude product. Flash chromatography eluting with 5:1 pet ether/EtOAc yielded **286** as a pale yellow oil (35 mg, 0.13 mmol, 45 %). R_f (3:1 pet ether:EtOAc) 0.23; ν_{max} (cm^{-1}) 2923, 2858, 1709, 1595, 1446, 1355, 1317, 1160, 1121, 1084, 749; δ_{H} (400 MHz CDCl_3) 7.94 (2H, d, J_{HH} 8.5 Hz, Ar-H), 7.32 (2H, d, J_{HH} 8.5 Hz, Ar-H), 4.23 (2H, s, N-CH₂), 2.41 (3H, s, Ar-CH₃), 1.98, 1.70 (CH₃); δ_{C} (100 MHz CDCl_3) 169.8 (C=O), 150.8 (C(CH₃)), 144.9, 135.6 (Ar quaternary), 128.5 (C(CH₃)), 129.7, 128.0 (Ar), 53.4 (N-CH₂), 21.7 (Ar-CH₃), 13.5, 8.3 (CH₃); m/z (ESI) 288 ($[\text{M}]^+\text{Na}$); [Found: ($[\text{M}]^+\text{Na}$) 288.0665, $\text{C}_{13}\text{H}_{15}\text{NNaO}_3\text{S}$ requires 288.0670].

6.2.9.3 *N*-Benzyl-4-(2-methyl-2-bromoethyl)-3,3-dimethylazetidine-2-one
287,³⁵

N-Benzyl-4-(isoprop-1-enyl)-3,3-dimethylazetidine-2-one **290a**¹⁷⁰

**287****290a**

2-Bromo-*N*-[(4-methylphenyl)sulfonyl]-*N*-2-propynyl-propanamide (100 mg, 0.32 mmol) was subjected to the general procedure for copper-mediated ATRC using KBH_4 (6.2.9) to yield a crude product. Flash chromatography eluting with 9:1 pet ether/EtOAc

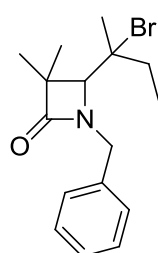
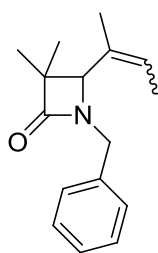
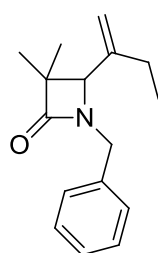
yielded **287** and **290a** as a pale yellow oil (76 mg, 81 %) of a 3 : 1 mixture.

287; R_f (3:1 pet ether:EtOAc) 0.46; ν_{max} (cm^{-1}) 2962, 2925, 1751, 1496, 1455, 1397, 1368, 1349, 1092, 1076, 736, 698; δ_{H} (400 MHz CDCl_3) 7.30-7.15 (5H, m, Ar-H), 4.86 (1H, d J_{HH} 15.1 Hz, Ar- $\underline{\text{CH}_2}$), 4.16 (1H, d J_{HH} 15.1 Hz, Ar- $\underline{\text{CH}_2}$), 3.54 (1H, s, N- $\underline{\text{CH}}$), 1.75 (3H, s, C($\underline{\text{CH}_3}$)Br), 1.74 (3H, s, C($\underline{\text{CH}_3}$)Br), 1.32 (3H, s, C($\underline{\text{CH}_3}$)₂), 1.21 (3H, s, C($\underline{\text{CH}_3}$)₂); δ_{C} (100 MHz CDCl_3) 174.8 ($\underline{\text{C}}=\text{O}$), 140.3 (Ar, quaternary), 128.7, 128.5, 127.7 (Ar), 72.8 (N- $\underline{\text{CH}}$), 65.2 ($\underline{\text{C}}(\text{CH}_3)_2\text{Br}$), 55.4 ($\underline{\text{C}}(\text{CH}_3)_2$), 45.0 (Ar- $\underline{\text{CH}_2}$), 31.5, 31.3 (C($\underline{\text{CH}_3}$)₂Br), 24.1, 17.9 (C($\underline{\text{CH}_3}$)₂); m/z (ESI) 332 ($[\text{M}]^+\text{Na}$) (^{79}Br), 334 ($[\text{M}]^+\text{Na}$) (^{81}Br); [Found: ($[\text{M}]^+\text{Na}$) 332.0628, $\text{C}_{15}\text{H}_{20}^{79}\text{BrNNaO}$ requires 332.0626].

290a; R_f (3:1 pet ether:EtOAc) 0.46; ν_{max} (cm^{-1}) 2962, 2925, 1751, 1496, 1455, 1397, 1368, 1349, 1092, 1076, 736, 698; δ_{H} (400 MHz CDCl_3) 7.30-7.15 (5H, m, Ar- $\underline{\text{H}}$), 4.99 (1H, brs, C $\underline{\text{CH}_2}$), 4.81 (1H, brs, C $\underline{\text{CH}_2}$), 4.79 (1H, d J_{HH} 14.6 Hz, Ar- $\underline{\text{CH}_2}$), 3.81 (1H, d J_{HH} 14.6 Hz, Ar- $\underline{\text{CH}_2}$), 3.34 (1H, s, N- $\underline{\text{CH}}$), 1.55 (3H, s, C $\underline{\text{CH}_3}$), 1.20 (3H, s, C($\underline{\text{CH}_3}$)₂), 1.04 (3H, s, C($\underline{\text{CH}_3}$)₂); δ_{C} (100 MHz CDCl_3) 168.4 ($\underline{\text{C}}=\text{O}$), 136.2 (Ar,

quaternary), 135.9 (CCH₂), 128.8, 128.4, 127.7 (Ar), 111.9 (CCH₂), 66.2 (N-CH), 44.4 (Ar-CH₂), 31.2 (C(CH₃)₂), 29.7 (C(CH₃)₂), 21.0 (CCH₃), 16.6 (C(CH₃)₂); *m/z* (ESI) 252 ([M]⁺Na), 230 ([M]⁺H); [Found: ([M]⁺Na) 252.1361, C₁₅H₁₉NNaO requires 252.1364].

6.2.9.4 ***N*-Benzyl-4-(3-methyl-3-bromopropyl)-3,3-dimethylazetidine-2-one** **288**,³⁵ ***N*-Benzyl-4-(3-methylprop-2-enyl)-3,3-dimethylazetidine-2-one** **291a**, ***N*-Benzyl-4-(but-1-en-2-yl)-3,3-dimethylazetidine-2-one** **291b**

**288****291a****291b**

N-Benzyl-2-bromo-*N*-(2-methylbut-1-enyl)-2-methyl-propionamide (100 mg, 0.31 mmol) was subjected to the general procedure for copper-mediated ATRC using KBH₄ (6.2.9) to furnish a

crude product. Flash chromatography eluting with 9:1 pet ether/EtOAc yielded a 1.7 : 3.7 : 1 mixture of **288**, **291a** and **291b** (78 mg, 89 %) of a pale yellow oil.

288 as a single diastereomer; *R_f* (3:1 pet ether:EtOAc) 0.30; ν_{\max} (cm⁻¹) 2962, 2925, 1751, 1496, 1455, 1397, 1368, 1349, 1092, 1076, 736, 698; δ_{H} (400 MHz CDCl₃) 7.35-7.21 (5H, m, Ar-H), 4.94 (1H, d, *J*_{HH} 14.8 Hz, Ar-CH₂), 4.32 (1H, d, *J*_{HH} 14.8 Hz, Ar-CH₂), 3.76 (1H, s, N-CH), 1.99-1.74 (2H, m, C(Br)CH₂), 1.78 (3H, s, C(CH₃)₂), 1.49 (3H, s, C(Br)CH₃), 1.35 (3H, s, C(CH₃)₂), 1.06 (3H, dd, *J*_{HH} 9.3, 7.8 Hz, CH₂CH₃); δ_{C} (100 MHz CDCl₃) 174.6 (C=O), 145.7 (Ar, quaternary), 128.8, 128.6, 127.7 (Ar), 73.3 (CBr), 72.1 (N-CH), 55.1 (C(CH₃)₂), 44.6 (Ar-CH₂), 35.8

(C(Br)CH2), 27.2 (C(CH3)2), 18.2 (C(CH3)2), 14.8 (C(Br)CH3), 10.0 (CH2CH3); m/z (ESI) 346 ([M]⁺Na) (⁷⁹Br), 348 ([M]⁺Na) (⁸¹Br); [Found: ([M]⁺Na) 346.0779, C₁₆H₂₂⁷⁹BrNNaO requires 346.0782].

291a as a 3:1 mixture of *E* and *Z* isomers; R_f (3:1 pet ether:EtOAc) 0.30; ν_{\max} (cm⁻¹) 2962, 2926, 1746, 1496, 1455, 1398, 1366, 1352, 1115, 1076, 734, 698; δ_H (400 MHz CDCl₃) 7.35-7.21 (10H, m, Ar-H), 5.54 (1H, q, J_{HH} 7.3 Hz, CCHCH₃, *Z*), 5.39 (1H, q, J_{HH} 6.8 Hz, CCHCH₃, *E*), 4.85 (1H, d, J_{HH} 14.8 Hz, Ar-CH₂, *E*), 4.83 (1H, d, J_{HH} 14.8 Hz, Ar-CH₂, *Z*), 3.85 (1H, d, J_{HH} 14.8 Hz, Ar-CH₂, *Z*), 3.80 (1H, d, J_{HH} 14.8 Hz, Ar-CH₂, *E*), 3.42 (2H, s, N-CH, *E* + *Z*), 1.68 (3H, d, J_{HH} 6.8 Hz, CHCH₃, *E*), 1.47 (3H, d, J_{HH} 7.3 Hz, CHCH₃, *Z*), 1.27 (6H, s, C(CH3)₂, *E* + *Z*), 1.26 (6H, s, C(CH3)₂, *E* + *Z*), 1.04 (6H, s, C(CH3)₂, *E* + *Z*); δ_C (100 MHz CDCl₃, *E* + *Z*) 174.4 (C=O), 136.4, 136.1 (Ar, quaternary), 131.8, 130.8 (CCH), 128.8, 128.7, 128.6, 128.4, 127.7, 127.6 (Ar), 124.5, 121.1 (CCH), 67.6, 65.5 (N-CH), 54.9, 54.8 (C(CH3)₂), 45.8, 44.5 (Ar-CH₂), 23.0 (CCH₃), 22.4, 22.2, 16.8, 16.7 (C(CH3)₂), 14.8 (CHCH₃), 13.1 (CHCH₃); m/z (ESI) 266 ([M]⁺Na), 244 ([M]⁺H); [Found: ([M]⁺H) 244.1696, C₁₆H₂₂NO requires 244.1701].

291b; R_f (3:1 pet ether:EtOAc) 0.30; ν_{\max} (cm⁻¹) 2962, 2926, 1746, 1496, 1455, 1398, 1366, 1352, 1115, 1076, 734, 698; δ_H (400 MHz CDCl₃) 7.35-7.21 (5H, m, Ar-H), 5.08 (1H, brs, CCH₂), 4.92 (1H, brs, CCH₂), 4.90 (1H, d, J_{HH} 14.6 Hz, Ar-CH₂), 3.85 (1H, d, J_{HH} 14.6 Hz, Ar-CH₂), 3.92 (1H, s, N-CH), 1.84 (2H, m, CH₂CH₃), 1.35 (3H, s, C(CH3)₂), 1.26 (3H, s, C(CH3)₂), 0.99 (3H, t, J_{HH} 7.5 Hz, CH₂CH3); δ_C (100 MHz CDCl₃) 174.2 (C=O), 135.9 (Ar, quaternary), 135.8 (CCH₂), 128.7, 128.5, 127.7 (Ar), 109.8 (CCH₂), 62.3 (N-CH), 55.9 (C(CH3)₂), 44.1 (Ar-CH₂), 27.5 (CCH₂), 20.9, 13.4,

11.9 ($\underline{\text{C}}\text{H}_3$); m/z (ESI) 266 ($[\text{M}]^+\text{Na}$), 244 ($[\text{M}]^+\text{H}$); [Found: ($[\text{M}]^+\text{H}$) 244.1696, $\text{C}_{16}\text{H}_{22}\text{NO}$ requires 244.1701].

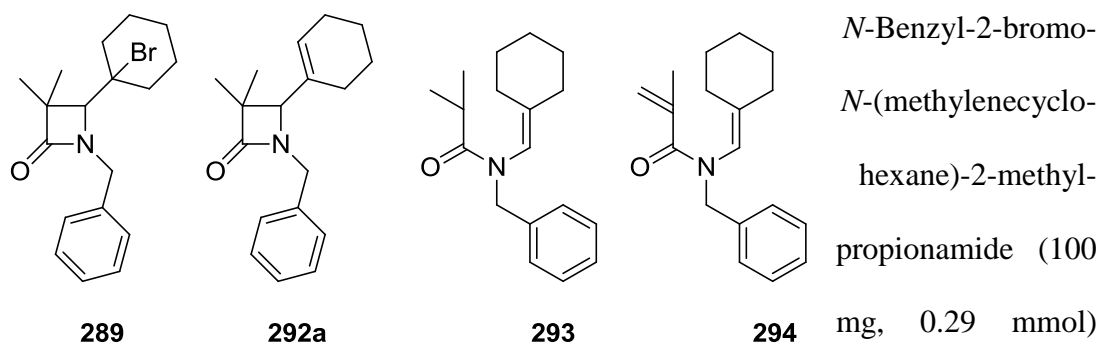
6.2.9.5 *N*-Benzyl-4-bromo-4-cyclohexyl-3,3-dimethylazetidine-2-one

289,³⁵

N-Benzyl-4-cyclohex-1-enyl-3,3-dimethylazetidine-2-one **292a**,⁵⁶

N-Benzyl-*N*-(methylenecyclohexane)-2-methylpropionamide **293**,

N-Benzyl-*N*-(methylene-cyclohexane)-2-methylacrylate **294**



was subjected to the general procedure for copper-mediated ATRC using KBH_4 (6.2.9) to furnish a crude product. Flash chromatography eluting with 9:1 pet ether/EtOAc yielded **289** and **292a** as a 1:1 mixture (74 mg, 80 %) of a pale yellow oil. Compounds **293** (8 mg, 0.03 mmol, 12 %) and **294** (5 mg, 0.02 mmol, 8%) were also isolated as minor byproducts.

289; R_f (3:1 pet ether:EtOAc) 0.33; ν_{max} (cm^{-1}) 2929, 1736, 1496, 1455, 1399, 1366, 1350, 1260, 1106, 1074, 918 806, 729; δ_{H} (400 MHz CDCl_3) 7.29-7.15 (5H, m, Ar-H), 4.86 (1H, d, J_{HH} 15.6 Hz, Ar- $\underline{\text{C}}\text{H}_2$), 4.09 (1H, d, J_{HH} 15.6 Hz, Ar- $\underline{\text{C}}\text{H}_2$), 3.44 (1H, s, N- $\underline{\text{C}}\text{H}$), 2.08-1.48 (10H, m, $\underline{\text{C}}\text{H}_2$) 1.42 (3H, s, $\text{C}(\underline{\text{C}}\text{H}_3)_2$), 1.23 (3H, s, $\text{C}(\underline{\text{C}}\text{H}_3)_2$); δ_{C} (100 MHz CDCl_3) 175.0 ($\underline{\text{C}}=\text{O}$), 136.2 (Ar, quaternary) 127.8, 128.4, 127.7 (Ar),

74.4 (CBr), 72.7 (N-CH), 55.5 (C(CH₃)₂), 45.5 (Ar-CH₂), 37.6, 25.0, 22.6, 22.4, 21.9 (CH₂), 24.5, 18.4 (C(CH₃)₂); *m/z* (ESI) 372 ([M]⁺Na) (⁷⁹Br), 374 ([M]⁺Na) (⁸¹Br); [Found: ([M]⁺Na) 372.0933, C₁₈H₂₄⁷⁹BrNNaO requires 372.0939].

292a; *R_f* (3:1 pet ether:EtOAc) 0.33; ν_{\max} (cm⁻¹) 2929, 1736, 1496, 1455, 1399, 1366, 1350, 1260, 1106, 1074, 918 806, 729; δ_{H} (400 MHz CDCl₃) 7.29-7.15 (5H, m, Ar-H), 5.50 (1H, brs, CH), 4.75 (1H, d, *J*_{HH} 14.8 Hz, Ar-CH₂), 3.79 (1H, d, *J*_{HH} 14.8 Hz, Ar-CH₂), 3.28 (1H, s, N-CH), 2.08-1.48 (8H, m, CH₂) 1.19 (3H, s, C(CH₃)₂), 0.99 (3H, s, C(CH₃)₂); δ_{C} (100 MHz CDCl₃) 174.4 (C=O), 136.2 (Ar, quaternary), 132.8 (CCH), 128.7, 128.4, 127.6 (Ar), 123.4 (CCH), 66.4 (N-CH), 54.9 (C(CH₃)₂), 44.4 (Ar-CH₂), 27.3, 24.8, 22.4, 22.3 (CH₂), 22.5, 16.8 (C(CH₃)₂); *m/z* (ESI) 292 ([M]⁺Na), 270 ([M]⁺H); [Found: ([M]⁺H) 270.1852, C₁₈H₂₄NO requires 270.1858].

293 as a colourless oil; *R_f* (3:1 pet ether:EtOAc) 0.57; ν_{\max} (cm⁻¹) 2931, 2855, 1639, 1495, 1447, 1412, 1240, 1223, 1089, 1078, 908, 714; δ_{H} (400 MHz CDCl₃) 7.30-7.21 (5H, m, Ar-H), 5.74 (1H, brs, N-CH), 4.59 (2H, s, Ar-CH₂), 2.83 (1H, sept, *J*_{HH} 6.8 Hz, CH(CH₃)₂), 2.06 (2H, brt, *J*_{HH} 5.8 Hz, CCH₂), 1.90 (2H, t, *J*_{HH} 5.8 Hz, CCH₂), 1.50 (4H, tt, *J*_{HH} 5.8, 2.7 Hz, CH₂), 1.29-1.23 (2H, m, CH₂), 1.08 (6H, d, *J*_{HH} 6.8 Hz, CH(CH₃)₂); δ_{C} (100 MHz CDCl₃) 177.6 (C=O), 143.2 Ar, quaternary), 137.7 (N-C(H)C), 128.9, 128.3, 127.1 (Ar), 120.1 (N-CH), 51.0 (Ar-CH₂), 33.0 (CH₂), 30.9 (CH(CH₃)₂), 28.0, 27.9, 26.4, 26.3 (CH₂), 19.2 (CH(CH₃)₂); *m/z* (ESI) 294 ([M]⁺Na), 272 ([M]⁺H); [Found: ([M]⁺H) 272.2009, C₁₈H₂₆NO requires 272.2014].

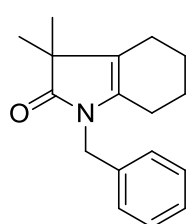
294 as a colourless oil; *R_f* (3:1 pet ether:EtOAc) 0.48; ν_{\max} (cm⁻¹) 2927, 2854, 1619, 1495, 1448, 1417, 1368, 1211, 1196, 1078, 909, 729; δ_{H} (400 MHz CDCl₃) 7.31-

7.23 (5H, m, Ar-H), 5.69 (1H, brs, N-CH), 5.19 (1H, brs, CCH₂), 5.17 (1H, brs, CCH₂), 4.62 (2H, s, Ar-CH₂), 1.99 (2H, brs, CH₂), 1.92 (3H, s, CCH₃), 1.79 (2H, brs, CH₂), 1.45 (4H, brs, CH₂), 1.19 (2H, brs, CH₂); δ_C (100 MHz CDCl₃) 171.5 (C=O), 141.0 (Ar, quaternary), 138.9 (CCH₂), 137.3 (N-C(H)C), 129.0, 128.3, 127.3 (Ar), 120.7 (N-CH), 117.9 (CCH₂), 51.2 (Ar-CH₂), 33.0, 28.2, 27.6, 26.2 (CH₂), 19.8 (CH₃); m/z (ESI) 292 ([M]⁺Na), 270 ([M]⁺H); [Found: ([M]⁺H) 270.1852, C₁₈H₂₄NO requires 270.1858].

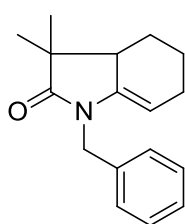
6.2.9.6 *N*-Benzyl-3,3-dimethyl-1,3,4,5,6,7-hexahydroindol-2-one **301a**,⁵⁵

N-Benzyl-3,3-dimethyl-1,3,3',4,5,6-hexahydroindol-2-one **301b**,⁵⁵

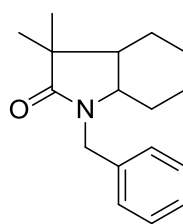
N-Benzyl-3,3-dimethyl-2,3,4,5,6,7-hexahydroindol-2-one **301c**²⁴³



301a



301b



301c

N-Benzyl-2-bromo-*N*-(cyclohex-1-enyl)-2-methyl-propionamide (100 mg, 0.30 mmol) was subjected to the general

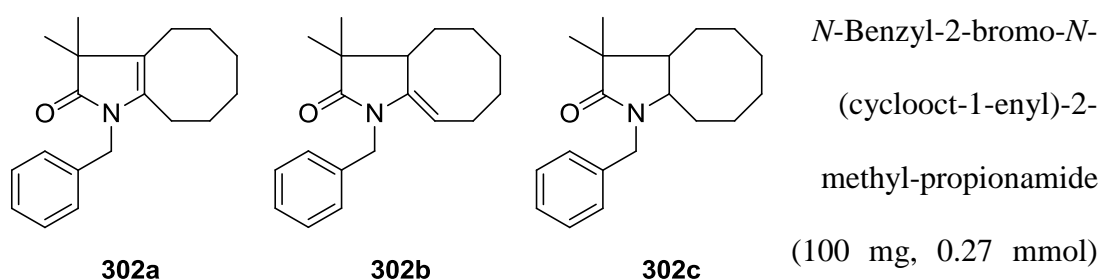
procedure for copper-mediated ATRC using KBH₄ (6.2.9) to furnish a crude product. Flash chromatography eluting with 9:1 pet ether/EtOAc yielded a 2 : 4 : 1 mixture of products **301a**, **301b** and **301c** as a colourless oil (64 mg, 0.25 mmol, 83%). Further purification was achieved *via* flash chromatography eluting with 20:1 pet ether/EtOAc to yield **301b** as a colourless oil (36 mg, 0.14 mmol, 47%), as well as **301a** and **301c** as a 2:1 mixture (28 mg, 0.11 mmol, 36%) of a colourless oil.

301a; R_f (3:1 pet ether:EtOAc) 0.67; ν_{\max} (cm⁻¹) 2924, 2855, 1680, 1495, 1445, 1361, 1273, 1079, 922, 729; δ_H (400 MHz CDCl₃) 7.31-7.16 (5H, m, Ar-H), 4.63

(2H, s, Ar-CH₂), 1.97 (2H, m, CH₂), 1.64-1.47 (6H, m, CH₂), 1.26 (6H, s, C(CH₃)₂); δ_C (100 MHz CDCl₃) 181.1 (C=O), 138.7 (Ar, quaternary), 133.6 (N-C), 128.5, 17.9, 127.3 (Ar), 121.4 (N-CC), 42.7 (Ar-CH₂), 28.5 (C(CH₃)₂), 24.8, 22.6, 22.5, 21.9 (CH₂), 22.2 (C(CH₃)₂); m/z (ESI) 278 ([M]⁺Na), 256 ([M]⁺H); [Found: ([M]⁺Na) 278.1515, C₁₇H₂₁NNaO requires 278.1521].

301b; R_f (3:1 pet ether:EtOAc) 0.56; ν_{\max} (cm⁻¹) 2962, 1669, 1405, 1257, 1078, 1008, 798; δ_H (400 MHz CDCl₃) 7.25-7.12 (5H, m, Ar-H), 4.72 (1H, dd, J_{HH} 6.8, 3.0 Hz, CCH), 4.58 (1H, d, J_{HH} 15.6 Hz, Ar-CH₂), 4.49 (1H, d, J_{HH} 15.6 Hz, Ar-CH₂), 2.35 (1H, m, CH), 1.99, 1.44 (1H, m, CH₂), 1.96, 1.83 (1H, m, CHCH₂), 1.70, 1.32 (1H, m, CH₂), 1.19 (3H, s, C(CH₃)₂) 0.94 (3H, s, C(CH₃)₂); δ_C (100 MHz CDCl₃) 180.6 (C=O), 139.7 (Ar, quaternary), 137.0 (N-C), 128.7, 128.5, 127.2 (Ar), 98.5 (CCH), 45.8 (CH), 43.6 (Ar-CH₂), 43.0 (C(CH₃)₃) 23.5 (CCHCH₂), 23.1 (C(CH₃)₂), 22.2 (CH₂), 21.9 (CH₂), 20.8 (C(CH₃)₂); m/z (ESI) 278 ([M]⁺Na), 256 ([M]⁺H); [Found: ([M]⁺Na) 278.1515, C₁₇H₂₁NNaO requires 278.1521].

301c; R_f (3:1 pet ether:EtOAc) 0.56; ν_{\max} (cm⁻¹) 2924, 2855, 1680, 1495, 1445, 1361, 1273, 1079, 922, 729; δ_H (400 MHz CDCl₃) 7.31-7.16 (5H, m, Ar-H), 5.00 (1H, d, J_{HH} 15.1 Hz, Ar-CH₂), 3.91 (1H, d, J_{HH} 15.1 Hz, Ar-CH₂), 2.81 (1H, ddd, J_{HH} 10.0, 3.5, 2.8 Hz, N-CH), 2.00 (1H, m, CH), 1.78 (4H, m, CH₂), 1.41 (2H, m, CH₂), 1.17 (2H, m, CH₂), 1.13 (3H, s, C(CH₃)₂), 1.10 (3H, s, C(CH₃)₂); δ_C (100 MHz CDCl₃) 180.6 (C=O), 138.3 (Ar, quaternary), 128.6, 128.2, 127.2 (Ar), 58.7 (N-CH), 43.0 (Ar-CH₂), 32.6 (CH), 29.8 (C(CH₃)₂), 24.6 23.9, 23.6, 19.5 (CH₂), 20.8, 20.6 (C(CH₃)₂); m/z (ESI) 280 ([M]⁺Na), 258 ([M]⁺H); [Found: ([M]⁺Na) 280.1672, C₁₇H₂₃NNaO requires 280.1677].

6.2.9.7 *N*-Benzyl-3,3-dimethyl-*N*-(cyclooct-1-enyl)-pyrrolidin-2-one**302a**,²⁵*N*-Benzyl-3,3-dimethyl-*N*-(cyclooct-2-enyl)-pyrrolidin-2-one**302b**,²⁵*N*-Benzyl-3,3-dimethyl-*N*-(cyclooctyl)-pyrrolidin-2-one **302c**

was subjected to the general procedure for copper-mediated ATRC using KBH_4 (6.2.9) to furnish a crude product. Flash chromatography eluting with 9:1 pet ether/EtOAc yielded **302b** as a pale yellow oil (53 mg, 0.19 mmol, 69%), as well as **302a**²⁵ and **302c** as a 1:2 mixture (15 mg, 0.05 mmol, 17%) of a yellow oil.

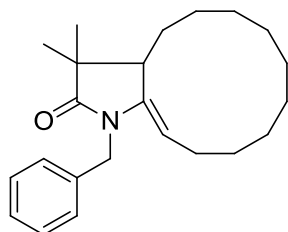
302a; R_f (3:1 pet ether:EtOAc) 0.63; ν_{max} (cm^{-1}) 2925, 2855, 1755, 1596, 1454, 1404, 1353, 1152, 1066, 730, 670; δ_{H} (400 MHz CDCl_3) 7.35-7.12 (5H, m, Ar-H), 4.68 (2H, s, Ar-CH₂), 2.28 (2H, t, J_{HH} 6.5 Hz, N-CCH₂), 2.22 (2H, t, J_{HH} 6.5 Hz, CCH₂), 2.04-1.39 (8H, m, CH₂), 1.20 (6H, s, C(CH₃)₂); δ_{C} (100 MHz CDCl_3) 175.3 (C=O), 142.3 (Ar, quaternary), 142.2 (N-C), 128.6, 127.2, 127.0 (Ar), 120.8 (N-CC), 49.0 (C(CH₃)₂), 43.0 (Ar-CH₂), 32.3, 30.3, 30.0, 28.5, 26.0, 23.0 (CH₂), 22.4 (C(CH₃)₂); m/z (ESI) 306 ($[\text{M}]^+\text{Na}$), 284 ($[\text{M}]^+\text{H}$); [Found: ($[\text{M}]^+\text{Na}$) 306.1828, $\text{C}_{19}\text{H}_{25}\text{NNaO}$ requires 306.1834].

302b; R_f (3:1 pet ether:EtOAc) 0.74; ν_{\max} (cm^{-1}) 2926, 2854, 1702, 1496, 1454, 1407, 1385, 1338, 1153, 1078, 909, 696; δ_{H} (400 MHz CDCl_3) 7.33-7.17 (5H, m, Ar-H), 4.74 (1H, dd, J_{HH} 9.8, 7.2 Hz, N-CCH), 4.71 (1H, d, J_{HH} 15.1 Hz, Ar-CH₂), 4.59 (1H, d, J_{HH} 15.1 Hz, Ar-CH₂), 2.55 (1H, dd, J_{HH} 12.5, 3.0 Hz, CH), 2.21-2.10 (1H, m, N-CCHCH₂), 2.08-2.00 (1H, m, N-CCHCH₂), 1.82-1.69 (2H, m, CH₂), 1.57-1.46 (2H, m, CH₂), 1.37-1.09 (4H, m, CH₂) 1.19 (3H, s, C(CH₃)₂), 1.18 (3H, s, C(CH₃)₂); δ_{C} (100 MHz CDCl_3) 180.4 (C=O), 142.3, Ar, quaternary), 136.8 (N-C), 128.4, 127.1 (Ar), 101.9 (N-CCH), 47.3 (CH), 43.6 (Ar-CH₂), 41.4 (C(CH₃)₂), 32.1, 29.4, 25.4, 23.8, 20.5 (CH₂), 27.6, 22.6 (C(CH₃)₂); m/z (ESI) 306 ($[\text{M}]^+\text{Na}$), 284 ($[\text{M}]^+\text{H}$); [Found: ($[\text{M}]^+\text{Na}$) 306.1829, $\text{C}_{19}\text{H}_{25}\text{NNaO}$ requires 306.1834].

302c; R_f (3:1 pet ether:EtOAc) 0.63; ν_{\max} (cm^{-1}) 2925, 2855, 1755, 1596, 1454, 1404, 1353, 1152, 1066, 730, 670; δ_{H} (400 MHz CDCl_3) 7.28-7.10 (5H, m, Ar-H), 4.95 (1H, d, J_{HH} 14.8 Hz, Ar-CH₂), 3.90 (1H, d, J_{HH} 14.8 Hz, Ar-CH₂), 3.04 (1H, ddd, J_{HH} 9.5, 5.0, 4.0 Hz, N-CH), 1.98 (1H, m, CH₂), 1.80-1.16 (11H, m, CH₂), 1.10 (3H, s, C(CH₃)₂), 0.88 (3H, s, C(CH₃)₂), 0.81 (1H, m, CH₂); δ_{C} (100 MHz CDCl_3) 174.9 (C=O), 137.0 (Ar, quaternary), 128.6, 127.9, 127.3 (Ar), 59.4 (N-CH), 48.8 (CH), 44.2 (C(CH₃)₂), 43.6 (Ar-CH₂), 32.1, 29.8, 27.4, 27.1, 25.5, 20.9 (CH₂), 24.1, 19.7 (C(CH₃)₂); m/z (ESI) 308 ($[\text{M}]^+\text{Na}$), 286 ($[\text{M}]^+\text{H}$); [Found: ($[\text{M}]^+\text{Na}$) 308.1985, $\text{C}_{19}\text{H}_{27}\text{NNaO}$ requires 308.1990].

6.2.9.8 *N*-Benzyl-3,3-dimethyl-*N*-(cyclododec-2-enyl)-pyrrolidin-2-one

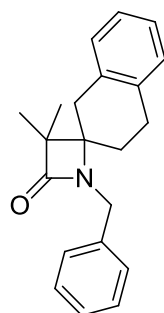
303b



303b

N-Benzyl-2-bromo-*N*-(cyclododec-1-enyl)-2-methyl-propionamide (100 mg, 0.24 mmol) was subjected to the general procedure for copper-mediated ATRC using KBH_4 (6.2.9) to furnish a crude product. Flash chromatography eluting with

9:1 pet ether/EtOAc yielded **303b** as a pale yellow oil (44 mg, 0.13 mmol, 55%). R_f (3:1 pet ether:EtOAc) 0.43; ν_{max} (cm^{-1}) 2928, 2859, 1687, 1496, 1467, 1444, 1383, 1361, 1148, 1079, 908, 710; δ_{H} (400 MHz CDCl_3) 7.30-7.19 (5H, m, Ar-H), 4.79 (1H, dd, J_{HH} 12.0, 3.8 Hz, N-CCH), 4.65 (1H, d, J_{HH} 15.3 Hz, Ar-CH₂), 4.60 (1H, d, J_{HH} 15.3 Hz, Ar-CH₂), 2.64 (1H, dd, J_{HH} 8.8, 4.3 Hz, CH), 2.15 (1H, m, N-CCHCH₂), 1.80 (1H, m, N-CCHCH₂), 1.65-1.51, 1.36-1.12 (15H, m, CH₂), 1.19 (3H, s, C(CH₃)₂), 1.17 (3H, s, C(CH₃)₂), 0.87 (1H, m, CH₂); δ_{C} (100 MHz CDCl_3) 180.1 (C=O), 140.7 (N-C), 137.0 (Ar, quaternary), 128.4, 127.2, 127.1 (Ar), 106.6 (N-CCH), 45.5 (CH), 44.2 (C(CH₃)₂), 43.7 (Ar-CH₂), 30.2, 27.1, 26.5, 25.9, 25.8, 25.1, 23.9, 23.2, 22.3 (CH₂), 27.0, 18.5 (C(CH₃)₂); m/z (ESI) 362 ($[\text{M}]^+\text{Na}$) 340 ($[\text{M}]^+\text{H}$); [Found: ($[\text{M}]^+\text{Na}$) 362.2459, $\text{C}_{10}\text{H}_{17}\text{NNaO}$ requires 362.2460].

6.2.9.9 *N*-Benzyl-4-(1,8,9-hexahydronaphthalenyl)-3,3-dimethylazetidione-2-one 308

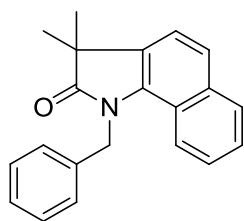
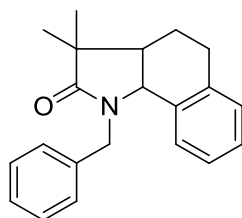
308

N-Benzyl-2-bromo-*N*-(9,10-dihydronaphthalen-1-yl)-2-methyl-propionamide (100 mg, 0.26 mmol) was subjected to the general procedure for copper-mediated ATRC using KBH_4 (6.2.9) to furnish a

crude product. Flash chromatography eluting with 9:1 pet ether/EtOAc afforded **308** as a pale yellow oil (18 mg, 0.06 mmol, 23%). R_f (3:1 pet ether:EtOAc) 0.19; ν_{\max} (cm^{-1}) 2962, 2927, 1731, 1495, 1454, 1401, 1257, 1078, 1009, 790; δ_{H} (400 MHz CDCl_3) 7.21-6.85 (9H, m, Ar-H), 4.27 (1H, d, J_{HH} 15.3 Hz, Ar-CH₂), 4.09 (1H, d, J_{HH} 15.3 Hz, Ar-CH₂), 2.80 (2H, s, CH₂), 2.80 (1H, dt J_{HH} 17.8, 6.5 Hz, N-CCH₂), 2.69 (1H, dt J_{HH} 17.8, 6.5 Hz, N-CCH₂), 1.85 (2H, t, J_{HH} 6.5 Hz, CH₂), 1.25 (3H, s, C(CH₃)₂), 1.09 (3H, s, C(CH₃)₂); δ_{C} (100 MHz CDCl_3) 174.3 (C=O), 137.8, 134.8, 134.2 (Ar, quaternary), 129.1, 128.5, 128.5, 127.9, 127.4, 126.3, 126.1 (Ar), 64.5 (C(CH₃)₂), 55.6 (N-C), 43.0 (Ar-CH₂), 35.9, 29.1, 27.1 (CH₂), 18.7, 18.6 (C(CH₃)₂); m/z 328 ([M]⁺Na); [Found: ([M]⁺Na) 328.1672, C₂₁H₂₃NNaO requires 328.1677].

6.2.9.10 *N*-Benzyl-4-(naphthalenyl)-pyrrolidin-2-one **312**,

N-Benzyl-4-(2,4,5,6-tetrahydronaphthalenyl)-pyrrolidin-2-one **313**

**312****313**

N-Benzyl-2-bromo-*N*-(3,4-dihydronaphthalen-1-yl)-2-methyl-propionamide (100 mg, 0.26 mmol) was subjected to the general procedure for copper-

mediated ATRC using KBH_4 (6.2.9) to furnish a crude product. Flash chromatography eluting with 9:1 pet ether/EtOAc yielded the pure products **312** (24 mg, 0.08 mmol, 31%), and **313** (31 mg, 0.10 mmol, 38%).

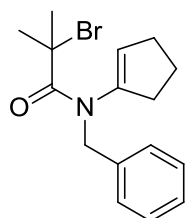
312 as a colourless oil; R_f (3:1 pet ether:EtOAc) 0.59; ν_{\max} (cm^{-1}) 3031, 2964, 2928, 1703, 1523, 1495, 1454, 1440, 1368, 1339, 1159, 1076, 731; δ_{H} (400 MHz CDCl_3) 8.00 (1H, d, J_{HH} 9.0 Hz, Ar-H), 7.81 (1H, d, J_{HH} 9.0 Hz, Ar-H), 7.62 (1H, d, J_{HH} 8.5

Hz, Ar-H), 7.42 (1H, d, J_{HH} 8.5 Hz, Ar-H), 7.36-7.21 (7H, m, Ar-H), 5.51 (2H, s, Ar-CH₂), 1.53 (6H, s, C(CH₃)₂); δ_{C} (100 MHz CDCl₃) 170.7 (C=O), 129.0, 127.3, 125.9, 125.8, 125.1, 122.0, 120.1 (Ar), 45.8 (Ar-CH₂), 24.7 (C(CH₃)₂); m/z (ESI) 324 ([M]⁺Na); [Found: ([M]⁺Na) 324.1359, C₂₁H₁₉NNaO requires 324.1364].

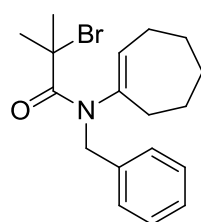
313 as a colourless oil; R_f (3:1 pet ether:EtOAc) 0.48; ν_{max} (cm⁻¹) 3029, 2927, 1679, 1495, 1454, 1408, 1361, 1269, 908, 726, 697; δ_{H} (400 MHz CDCl₃) 7.27-6.92 (9H, m, Ar-H), 4.93 (1H, d, J_{HH} 15.1 Hz, Ar-CH₂), 4.58 (1H, d, J_{HH} 5.3 Hz, N-CH), 3.56 (1H, d, J_{HH} 15.1 Hz, Ar-CH₂), 2.66 (1H, dt, J_{HH} 16.1, 5.5 Hz, CH₂), 2.55 (1H, dt, J_{HH} 16.1, 5.5 Hz, CH₂), 2.20 (1H, m, CH), 1.66 (2H, m, Hz, CHCH₂), 1.27 (3H, s, C(CH₃)₂), 1.17 (3H, s, C(CH₃)₂); δ_{C} (100 MHz CDCl₃) 169.5 (C=O), 139.7, 137.3, 131.8 (Ar, quaternary), 131.1, 128.7, 128.6, 128.2, 127.5, 127.1, 125.7 (Ar), 61.8 (C(CH₃)₂), 55.8 (N-CH), 43.5 (Ar-CH₂), 43.4 (CH), 28.1, 22.9 (CH₂), 25.1, 20.1 (C(CH₃)₂); m/z (ESI) 328 ([M]⁺Na); [Found: ([M]⁺Na) 328.1672, C₂₁H₂₃NNaO requires 328.1677].

6.2.10 General Procedures for the Synthesis of Enamides in Chapter 5

Substrates **273-275**, **305** and **306** were prepared for use in chapter 4 and the relevant procedures and data can be found in section 6.2.8. The majority of the other enamides were prepared in identical fashion. For tetrasubstituted enamides an alternative approach was used detailed in section 6.2.11.

6.2.10.1 *N*-Benzyl-2-bromo-*N*-(cyclopent-1-enyl)-2-methyl-propionamide**331**²⁵**331**

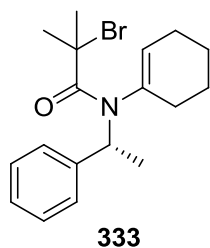
The general procedure for the synthesis of enamides (6.2.8) was applied using benzylamine (1.10 ml, 10.0 mmol), cyclopentanone (1.04 ml, 10.0 mmol) and 2-bromoisobutyryl bromide (1.24 ml, 10.0 mmol) to furnish a crude product which was purified by flash chromatography, eluting with 9:1 pet ether/EtOAc to yield **331** as a yellow oil (1.90 g, 6.0 mmol, 60%). R_f (3:1 pet ether:EtOAc) 0.83; ν_{\max} (cm^{-1}) 2932, 2850, 1633, 1496, 1464, 1453, 1392, 1365, 1173, 1108, 729, 697; δ_{H} (300 MHz, CDCl_3) 7-25-7.19 (5H, m, Ar-H), 5.53 (1H, t, J_{HH} 6.0 Hz, CH), 4.62 (2H, s, Ar-CH₂), 2.39 (2H, m, CCH₂), 2.22 (2H, m, CHCH₂), 1.94 (6H, s, (CH₃)₂), 1.85 (2H, m, CH₂CH₂CH₂); δ_{C} (100 MHz CDCl_3) 170.5 (C=O), 142.3 (Ar, quaternary), 137.6 (N-C), 128.3, 127.9, 127.2 (Ar), 58.0 (C(CH₃)₂Br), 52.1 (Ar-CH₂) 33.3 (CH₂), 32.6 (CH₂), 30.2 (CH₂), 22.1 (C(CH₃)₂Br); m/z (ESI) 344 ([M]⁺Na) (⁷⁹Br), 346 ([M]⁺Na) (⁸¹Br); [Found: ([M]⁺Na) 344.0620; C₁₆H₂₀⁷⁹BrNNaO requires 344.0626].

6.2.10.2 *N*-Benzyl-2-bromo-*N*-(cyclohept-1-enyl)-2-methyl-propionamide**332****332**

The general procedure for the synthesis of enamides (6.2.8) was applied using benzylamine (1.10 ml, 10.0 mmol), cyclohexanone (1.04 ml, 10.0 mmol) and bromoacetyl bromide (1.24 ml, 10.0 mmol) to furnish a crude product which was purified by flash

chromatography, eluting with 9:1 pet ether/EtOAc to yield **332** as a pale yellow oil (2.51 g, 7.1 mmol, 71%). R_f (3:1 pet ether:EtOAc) 0.77; ν_{\max} (cm^{-1}) 2922, 2851, 1629, 1495, 1446, 1392, 1365, 1173, 1108, 739, 693; δ_{H} (300 MHz, CDCl_3) 7.26-7.20 (5H, m, Ar-H), 5.54 (1H, t, J_{HH} 6.6 Hz, CH), 5.07 (1H, br, Ar-CH₂), 3.99 (1H, br, Ar-CH₂), 2.54-1.19 (10H, br, CH₂), 1.95 (6H, s, (CH₃)₂); δ_{C} (75 MHz CDCl_3) 170.1 (C=O), 137.4 (Ar quaternary), 129.1 (N-C), 128.9, 128.2, 127.3 (Ar), 125.3 (CH), 47.8 (C(CH₃)₂), 44.4 (Ar-CH₂), 34.8, 33.2, 31.7, 26.6, 26.0 (CH₂), 26.9 (C(CH₃)₂); m/z (ESI) 372 ($[\text{M}]^+\text{Na}$) (^{79}Br), 374 ($[\text{M}]^+\text{Na}$) (^{81}Br); [Found: ($[\text{M}]^+\text{Na}$) 372.0933; $\text{C}_{18}\text{H}_{24}^{79}\text{BrNNaO}$ requires 372.0939]; [Found: C, 61.6; H, 6.9; N, 3.9; $\text{C}_{18}\text{H}_{24}\text{BrNNaO}$ requires C, 61.7; H, 6.9; N, 4.0].

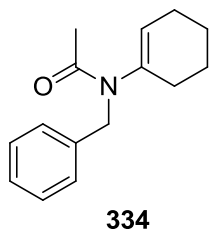
6.2.10.3 (*R*)-*N*-(1-phenylethyl)-2-bromo-*N*-(cyclohex-1-enyl)-2-methylpropionamide **333**²⁵



The general procedure for the synthesis of enamides (6.2.8) was applied using (*R*)- α -methylbenzylamine (1.29 ml, 10.0 mmol), cyclohexanone (1.04 ml, 10.0 mmol) and bromoacetyl bromide (1.24 ml, 10.0 mmol) to furnish a crude product which was purified by flash chromatography, eluting with 9:1 pet ether/EtOAc to yield **333** as a pale yellow oil (1.49 g, 4.4 mmol, 44%). R_f (3:1 pet ether:EtOAc) 0.81; ν_{\max} (cm^{-1}) 3061, 2966, 2963, 2857, 1615, 1486, 1454, 1379, 1367, 1318, 1168, 773, 700; δ_{H} (400 MHz, CDCl_3) 7.35-7.27 (5H, m, Ar-H), 5.86 (1H, br, CH), 5.44 (1H, br, CHCH₃), 2.53-1.93 (9H, br, CH₃), 1.92-1.04 (8H, br, CH₂); δ_{C} (100 MHz, CDCl_3) 170.6 (C=O), 140.9 (Ar quaternary), 135.7 (N-C), 131.7 (CH), 128.1, 127.6, 127.1 (Ar), 59.5 (C(CH₃)₂), 54.5 (N-CH), 34.8 (N-C(H)CH₃), 32.4, 30.6, 24.9, 22.7 (CH₂),

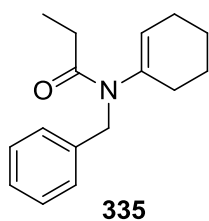
21.1, 16.6 (C(CH₃)₂); *m/z* (ESI) 372 ([M]⁺Na) (⁷⁹Br), 374 ([M]⁺Na) (⁸¹Br); [Found: ([M]⁺Na) 372.0933; C₁₈H₂₄⁷⁹BrNNaO expect 372.0939].

6.2.10.4 *N*-cyclohex-1-enyl-*N*-benzylacetamide **334**²¹³



The general procedure for the synthesis of enamides (6.2.8) was applied using benzylamine (1.10 ml, 10.0 mmol), cyclohexanone (1.04 ml, 10.0 mmol) and acetyl chloride (0.62 ml, 10.0 mmol) to furnish a crude product which was purified by flash chromatography, eluting with 9:1 pet ether/EtOAc to yield **334** as a colourless oil (757 mg, 3.3 mmol, 33%). *R_f* (3:1 pet ether:EtOAc) 0.6; ν_{\max} (cm⁻¹) 2928, 1644; δ_{H} (CDCl₃, 300MHz) 7.27-7.21 (5H, m, Ar-H), 5.37 (1H, m, N-CCH), 4.60 (2H, s, Ar-CH₂), 2.06 (3H, s, CH₃), 1.95 (4H, m, CH₂), 1.62 (2H, m, CH₂), 1.49 (2H, m, N-CH₂); δ_{C} (CDCl₃, 75.5MHz) 170.1 (C=O), 138.9 (Ar, quaternary), 138.1 (N-C), 128.7, 128.2, 128.1 (Ar), 127.1 (C-H), 49.5 (Ar-CH₂), 28.1, 24.7, 23.9, 21.7 (CH₂), 21.7 (CH₃); *m/z* (ESI) 252 ([M]⁺Na); [Found ([M]⁺Na) 252.1359, C₁₅H₁₉NNaO requires 252.1364].

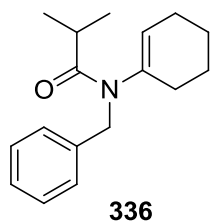
6.2.10.5 *N*-cyclohex-1-enyl-*N*-benzylpropionamide **335**



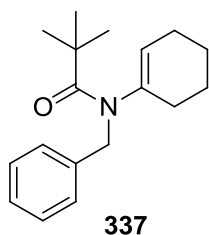
The general procedure for the synthesis of enamides (6.2.8) was applied using benzylamine (1.10 ml, 10.0 mmol), cyclohexanone (1.04 ml, 10.0 mmol) and propionyl chloride (0.87 ml, 10.0 mmol) to furnish a crude product which was purified by flash chromatography, eluting with 9:1 pet ether/EtOAc to **335** as a pale yellow oil (487

mg, 2.0 mmol, 20%). R_f (3:1 pet ether:EtOAc) 0.6; ν_{\max} (cm^{-1}) 2935, 1634; δ_{H} (CDCl_3 , 300MHz) 7.31-7.28 (5H, m, Ar-H), 5.38, (1H, s, N-CCH), 4.60 (2H, s, Ar-CH₂), 2.33 (2H, q, J_{HH} 7.5 Hz, CH₂CH₃), 2.00 (4H, m, CH₂), 1.64 (2H, m, CH₂), 1.53 (2H, m, CH₂), 1.12 (3H, t, J_{HH} 7.5 Hz, CH₂CH₃); δ_{C} (CDCl_3 , 75.5MHz) 164.3 (C=O), 138.5 (Ar, quaternary), 138.3 (N-C), 128.8, 128.2, 128.1 (Ar), 127.1 (C-H), 49.6 (Ar-CH₂), 28.2, 26.8, 24.8, 22.8 (CH₂), 21.3 (CH₂CH₃), 10.1 (CH₂CH₃); m/z (ESI) 266 ($[\text{M}]^+\text{Na}$); [Found ($[\text{M}]^+\text{Na}$) 266.1515, C₁₆H₂₁NNaO requires 266.1521].

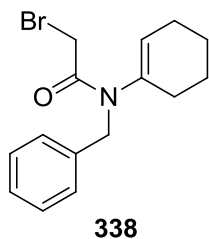
6.2.10.6 *N*-cyclohex-1-enyl-*N*-benzyl-2-methylpropionamide **336**



The general procedure for the synthesis of enamides (6.2.8) was applied using benzylamine (1.10 ml, 10.0 mmol), cyclohexanone (1.04 ml, 10.0 mmol) and 2-methylpropionyl chloride (1.05 ml, 10.0 mmol) to furnish a crude product which was purified by flash chromatography, eluting with 9:1 pet ether/EtOAc to yield **336** as a pale yellow oil (206 mg, 0.8 mmol, 8%). R_f (3:1 pet ether:EtOAc) 0.8; ν_{\max} (cm^{-1}) 2929, 1634; δ_{H} (CDCl_3 , 400MHz) 7.25-7.20 (5H, m, Ar-H), 5.40 (1H, s, N-CCH), 4.59 (2H, s, Ar-CH₂), 2.81 (1H, sept, J_{HH} 6.5 Hz, CH(CH₃)₂), 1.99 (4H, m, CH₂), 1.68 (2H, m, CH₂), 1.52 (2H, m, CH₂), 1.12 (6H, d, J_{HH} 6.5 Hz, CH(CH₃)₂); δ_{C} (CDCl_3 , 100 MHz) 177.0 (C=O), 138.6 (Ar, quaternary), 138.5 (N-C), 128.7, 128.2, 127.5 (Ar), 127.0 (CH), 49.7 (Ar-CH₂), 31.4 (CH(CH₃)₂), 28.8 (CH(CH₃)₂), 24.7, 22.9, 21.5, 20.2 (CH₂); m/z (ESI) 280 ($[\text{M}]^+\text{Na}$); [Found ($[\text{M}]^+\text{Na}$) 280.1672, C₁₇H₂₃NNaO requires 280.1677].

6.2.10.7 *N*-cyclohex-1-enyl-*N*-benzyl-2-dimethylpropionamide **337**

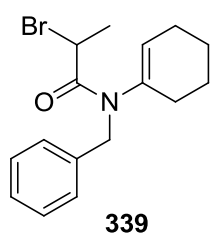
The general procedure for the synthesis of enamides (6.2.8) was applied using benzylamine (1.10 ml, 10.0 mmol), cyclohexanone (1.04 ml, 10.0 mmol) and pivaloyl chloride (1.23 ml, 10.0 mmol) to furnish a crude product which was purified by flash chromatography, eluting with 9:1 pet ether/EtOAc to yield **337** as a brown oil (163 mg, 0.6 mmol, 6%). R_f (3:1 pet ether:EtOAc) 0.9; ν_{\max} (cm^{-1}) 2928, 1625; δ_{H} (CDCl_3 , 400MHz) 7.25-7.19 (5H, m, Ar-H), 5.28 (1H, m, N-CCH), 4.42 (2H, brs, Ar-CH₂), 2.07 (4H, m, CH₂), 1.67 (2H, m, CH₂), 1.54 (2H, m, CH₂), 1.25 (9H, s, C(CH₃)₃); δ_{C} (CDCl_3 , 75.5MHz) 178.0 (C=O), 138.7 (Ar, quaternary), 132.6 (N-C) 128.5, 128.2, 128.1 (Ar), 126.9 (CH), 51.7 (Ar-CH₂), 40.9 (C(CH₃)₃), 29.3, 28.5, 24.7, 22.7 (CH₂), 21.4 (C(CH₃)₃); m/z (ESI) 294 ([M]⁺Na); [Found ([M]⁺Na) 294.1828, C₁₈H₂₅NNaO requires ([M]⁺Na) 294.1834].

6.2.10.8 **2-Bromo-*N*-cyclohex-1-enyl-*N*-benzylacetamide **338****²¹³

The general procedure for the synthesis of enamides (6.2.8) was applied using benzylamine (1.10 ml, 10.0 mmol), cyclohexanone (1.04 ml, 10.0 mmol) and bromoacetyl bromide (0.87 ml, 10.0 mmol) to furnish a crude product which was purified by flash chromatography, eluting with 9:1 pet ether/EtOAc to yield **338** as a pale yellow oil (925 mg, 3.0 mmol, 30%). R_f (3:1 pet ether:EtOAc) 0.6; ν_{\max} (cm^{-1}) 2934, 1646; δ_{H} (CDCl_3 , 400MHz) 7.31-7.25 (5H, m, Ar-H), 5.50 (1H, s, N-CCH), 4.62 (2H, s, Ar-CH₂), 3.95 (2H, s, CH₂Br), 2.07 (4H, m, CH₂), 1.69 (2H, m, CH₂), 1.4 (2H, m, CH₂);

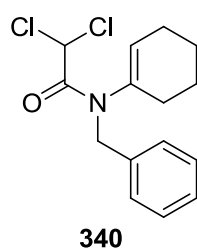
δ_{C} (CDCl₃, 100 MHz) 166.1 (C=O), 137.8 (Ar, quaternary), 137.4 (N-C), 129.2, 128.7, 128.4 (Ar), 127.4 (CH), 49.9 (Ar-CH₂), 41.9 (CH₂Br), 27.4, 25.0, 24.7, 21.4 (CH₂); m/z (ESI) 330 ([M]⁺Na) (⁷⁹Br), 332 ([M]⁺Na) (⁸¹Br); [Found ([M]⁺Na) 330.0464, C₁₅H₁₈⁷⁹BrNNaO requires 330.0469].

6.2.10.9 N-Cyclohex-1-enyl-N-benzyl-2-bromopropionamide **339**⁵⁶



The general procedure for the synthesis of enamides (6.2.8) was applied using benzylamine (1.10 ml, 10.0 mmol), cyclohexanone (1.04 ml, 10.0 mmol) and 2-bromopropionyl bromide (1.05 ml, 10.0 mmol) to furnish a crude product which was purified by flash chromatography, eluting with 9:1 pet ether/EtOAc to yield **339** as a pale brown solid (1.31 g, 3.9 mmol, 39%). R_f (3:1 pet ether:EtOAc) 0.8; mpt 86-88 °C, lit⁵⁶ 87-88°C; ν_{max} (cm⁻¹) 2922, 1651; δ_{H} (CDCl₃, 400MHz) 7.25-7.17 (5H, m, Ar-H), 5.50 (1H, m, N-CCH), 4.64 (2H, brs, N-CH₂), 2.16 (2H, m, CH₂), 2.00 (2H, m, CH₂), 1.79 (3H, d, J_{HH} 6.8 Hz, CH(Br)CH₃), 1.64 (2H, m, CH₂), 1.60 (1H, q, J_{HH} 6.8 Hz, (CH(Br)CH₃), 1.53 (2H, m, CH₂); (CDCl₃, 100 MHz) 169.3 (C=O), 137.4 (Ar, quaternary), 136.5 (N-C), 129.0, 128.7, 128.4 (Ar), 127.4 (CH), 50.0 (Ar-CH₂), 39.5 (C(CH₃)Br), 28.0, 24.7, 22.7, 21.4 (CH₂), 20.9 (CH₃); m/z (ESI) 344 ([M]⁺Na) (⁷⁹Br), 346 ([M]⁺Na) (⁸¹Br); [Found ([M]⁺Na) 344.0620, C₁₆H₂₀⁷⁹BrNNaO requires 344.0626].

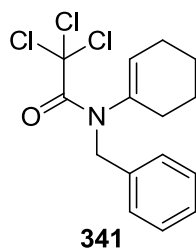
6.2.10.10 N-Cyclohex-1-enyl-N-benzyl-dichloroacetamide **340**



The general procedure for the synthesis of enamides (6.2.8) was applied using benzylamine (2.73 ml, 25.0 mmol), cyclohexanone

(2.60 ml, 25.0 mmol) and dichloroacetyl chloride (2.41 ml, 25.0 mmol) to furnish a crude product which was purified by flash chromatography, eluting with 9:1 pet ether/EtOAc to yield **340** as a pale yellow oil (2.32 g, 7.8 mmol, 31%). R_f (3:1 pet ether:EtOAc) 0.67; ν_{\max} (cm^{-1}) 3030, 2927, 1673, 1495, 1440, 1403, 1210, 1177, 1078, 922, 803, 744, 670; δ_{H} (300 MHz CDCl_3) 7.34-7.24 (5H, m, Ar-H), 6.39 (1H, s, CHCl_2), 5.53 (1H, br m, CH), 4.65 (2H, br s, Ar- CH_2), 2.06 (4H, m, CH_2), 1.74-1.52 (4H, m, CH_2); δ_{C} (75 MHz CDCl_3) 164.2 ($\text{C}=\text{O}$), 136.3 (N-C), 135.8 (Ar, quaternary), 129.8, 128.2, 127.9 (Ar), 127.1 (N-CCH), 63.5 (CHCl_2), 49.8 (Ar- CH_2), 27.3, 24.1, 21.9, 20.6 (CH_2); m/z (ESI) 320 ($[\text{M}]^+\text{Na}$) (^{35}Cl), (ESI) 322 ($[\text{M}]^+\text{Na}$) (^{37}Cl); [Found: ($[\text{M}]^+\text{Na}$) 320.0579, $\text{C}_{15}\text{H}_{17}^{35}\text{Cl}_2\text{NNaO}$ requires 320.0585].

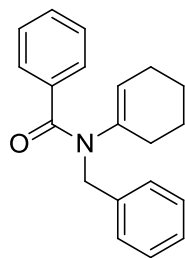
6.2.10.11 *N*-Cyclohex-1-enyl-*N*-benzyltrichloroacetamide **341**³⁶



The general procedure for the synthesis of enamides (6.2.8) was applied using benzylamine (2.73 ml, 25.0 mmol), cyclohexanone (2.60 ml, 25.0 mmol) and trichloroacetyl chloride (2.79 ml, 25.0 mmol) to furnish a crude product which was purified by flash chromatography, eluting with 9:1 pet ether/EtOAc to yield **341** as a pale brown oil (1.69 g, 5.1 mmol, 20%). R_f (3:1 pet ether:EtOAc) 0.78; ν_{\max} (cm^{-1}) 3032, 2928, 2859, 1665, 1496, 1438, 1389, 1246, 1175, 848, 808, 697; δ_{H} (300 MHz CDCl_3) 7.34-7.28 (5H, m, Ar-H), 5.59 (1H, m, CH), 5.05 (1H, br s, Ar- CH_2), 4.26 (1H, br s, Ar- CH_2), 2.22 (2H, br, CH_2), 2.01 (2H, br, CH_2), 1.68-1.51 (4H, br, CH_2); δ_{C} (75 MHz CDCl_3) 178.1 ($\text{C}=\text{O}$), 141.4 (N-C), 131.8 (Ar, quaternary), 128.2, 127.8, 127.1 (Ar), 127.6 (N-CCH), 74.0 (CCl_3), 52.7 (Ar- CH_2), 27.0, 24.0, 21.8, 20.5 (CH_2); m/z

(ESI) 354 ($[M]^+Na$) (^{35}Cl), 356 ($[M]^+Na$) (^{37}Cl); [Found: ($[M]^+Na$) 354.0193, $C_{15}H_{16}^{35}Cl_3NNaO$ requires 354.0195].

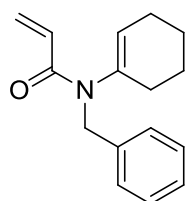
6.2.10.12 *N*-Cyclohex-1-enyl-*N*-benzamide **342**²⁴⁴



342

The general procedure for the synthesis of enamides (6.2.8) was applied using benzylamine (2.73 ml, 25.0 mmol), cyclohexanone (2.60 ml, 25.0 mmol) and benzoyl chloride (2.90 ml, 25.0 mmol) to furnish a crude product which was purified by flash chromatography, eluting with 9:1 pet ether/EtOAc to yield **342** as a brown oil (2.61 g, 9.0 mmol, 36%). R_f (3:1 pet ether:EtOAc) 0.54; ν_{max} (cm^{-1}) 3061, 3029, 2929, 2858, 2837, 1632, 1576, 1495, 1446, 1436, 1388; δ_H (300 MHz, $CDCl_3$) 7.44-7.40 (2H, m, Ar-H), 7.29-7.15 (8H, m, Ar-H), 5.18 (1H, br t, J_{HH} 3.5 Hz, N-C=CH), 4.73 (2H, s, Ar-CH₂), 1.84-1.66 (4H, m, CH₂), 1.40-1.19 (4H, m, CH₂); δ_C (75.5 MHz $CDCl_3$) 169.9 (C=O), 138.2, 136.5 (Ar, quaternary), 137.4 (N-C=CH), 128.9, 127.9, 127.7, 127.5, 127.1, 126.9 (Ar), 126.6 (NC=CH), 50.0 (CH₂Ph), 28.2, 24.1, 21.9, 20.7 (CH₂); m/z (ESI) 314 ($[M]^+Na$); [Found: $[M]^+$ 292.1696, $C_{20}H_{22}NO$ requires 292.1701]; [Found: C, 81.9; H, 7.3; N, 4.5. $C_{20}H_{21}NO$ requires C, 82.4; H, 7.3; N, 4.8].

6.2.10.13 *N*-Cyclohex-1-enyl-*N*-benzylprop-2-enamide **343**²⁴⁵

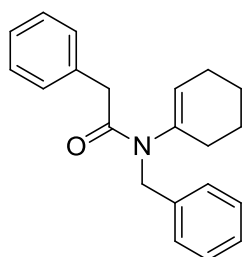


343

The general procedure for the synthesis of enamides (6.2.8) was applied using benzylamine (2.73 ml, 25.0 mmol), cyclohexanone

(2.60 ml, 25.0 mmol) and acryloyl chloride (2.03 ml, 25.0 mmol) to furnish a crude product which was purified by flash chromatography, eluting with 9:1 pet ether/EtOAc to yield **343** as an off-white solid (2.78 g, 11.5 mmol, 46%). R_f (3:1 pet ether:EtOAc) 0.41; mpt 66-67 °C, lit²⁴⁵ 67-68 °C; ν_{\max} (cm⁻¹) 2926, 1648, 1408, 1350, 1236, 1138, 1079, 980, 698; δ_H (300 MHz, CDCl₃) 7.29-7.18 (5H, m, Ar-H), 6.54-6.45 (1H, dd, J_{HH} 17.0, 9.7 Hz, CH₂=CH), 6.42-6.35 (1H, dd, J_{HH} 17.0, 2.8 Hz, CH₂=CH), 5.63-5.59 (1H, dd, J_{HH} 9.7, 2.8 Hz, CH₂=CH), 5.39 (1H, brs, NCCH), 4.67 (2H, s, Ar-CH₂), 2.06-1.92 (4H, m, CH₂), 1.68-1.48 (4H, m, CH₂); δ_C (75.5 MHz CDCl₃) 165.2 (C=O), 137.9 (NCCH), 136.6 (Ar, quaternary) 128.7, 128.6, 128.6, 128.3, 128.3, 127.2 (Ar, CH₂=CH, CH₂=CH, NCCH), 49.8 (Ar-CH₂), 28.7, 24.7, 22.7, 21.5 (CH₂); m/z (ESI) 264 ([M]⁺Na); [Found: ([M]⁺Na) 264.1359, C₁₆H₁₉NNaO requires 264.1364].

6.2.10.14 *N*-Cyclohex-1-enyl-*N*-benzyl-2-phenylacetamide **344**



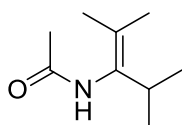
344

The general procedure for the synthesis of enamides (6.2.8) was applied using benzylamine (2.73 ml, 25.0 mmol), cyclohexanone (2.60 ml, 25.0 mmol) and phenylacetyl chloride (3.31 ml, 25.0 mmol) to furnish a crude product which was purified by flash chromatography, eluting with 9:1 pet ether/EtOAc to yield **344** as a pale yellow oil (1.72 g, 5.6 mmol, 23%). R_f (3:1 pet ether:EtOAc) 0.52; ν_{\max} (cm⁻¹) 3028, 2937, 1632, 1581, 1451, 1427, 1399, 1248, 1166, 1026, 702; δ_H (300 MHz, CDCl₃) 7.33-7.19 (10H, m, Ar-H), 5.29 (1H, brs, NCCH), 4.61 (2H, s, Ar-CH₂), 3.70 (2H, s, Ar-CH₂), 2.03-1.86 (4H, m, CH₂), 1.67-1.49 (4H, m, CH₂); δ_C (75.5 MHz CDCl₃) 169.9 (C=O), 137.5, 137.4 (Ar,

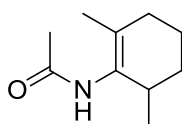
quaternary), 135.5 (N \overline{C} CH), 128.4, 128.3, 128.1, 127.8, 127.7, 126.5 (Ar), 125.9 (N \overline{C} CH), 49.0 (Ar- \overline{C} H₂), 40.3, (Ar- \overline{C} H₂), 27.6, 24.1, 22.1, 20.9 (\overline{C} H₂); *m/z* (ESI) 328 ([M]⁺Na); [Found: ([M]⁺Na) 328.1672, C₂₁H₂₃NNaO requires 328.1677]; [Found: C, 82.4; H, 7.5; N, 4.5. C₂₁H₂₃NO requires C, 82.6; H, 7.6; N, 4.6].

6.2.11 General Procedures for the Synthesis of Tetrasubstituted enamides in Chapter 5

Cyclic ketone (1 equiv) was dissolved in methanol. Hydroxylamine hydrochloride (1.1 equiv) was added followed by sodium acetate (1.1 equiv) and the reaction mixture was heated at reflux for 5 h. The reaction was allowed to cool and quenched by addition of H₂O (50 ml) over 1 h. After stirring at room temperature for a further hour, Et₂O (50 ml) was added and the organic layer was dried, filtered and concentrated in *vacuo* to yield a crude product. The crude product (1 equiv) was dissolved in dry toluene at room temperature. An anhydride (3 equiv) was added followed by acetic acid (3 equiv). Finally Fe powder (2 equiv) was added and the mixture was heated at 70 °C for 4 h. The mixture was allowed to cool to room temperature then filtered through celite and diluted with DCM (50 ml). The filtrate was then washed with 2 M NaOH (2 x 25 ml). The resulting organic layer was dried, filtered and concentrated in *vacuo* to yield a crude product that was purified by flash chromatography eluting with 5:1 hexane-EtOAc.

6.2.11.1 *N*-(2,4-dimethylpent-2-en-3-yl)-acetamide **355****355**

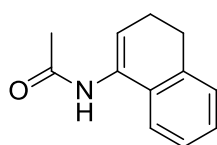
The general procedure for the synthesis of tetrasubstituted enamides (6.2.11) was applied using diisopropylketone (1.74 ml, 12.3 mmol), acetic acid (2.11 ml, 36.9 mmol), acetic anhydride (3.49 ml, 36.9 mmol) and Fe powder (1.37 g, 24.6 mmol). Flash chromatography eluting with 5:1 hexane/EtOAc yielded **355** as a pale yellow oil (435 mg, 2.8 mmol, 23%) of a 2:1 mixture of rotamers. R_f (3:1 pet ether:EtOAc) 0.09; ν_{\max} (cm^{-1}) 3243, 2965, 2930, 1643, 1522, 1465, 1370, 1280, 715; δ_{H} (300 MHz CDCl_3) 6.19 (1H, brs, NH , min), 6.09 (1H, brs, NH , maj), 3.02-2.88 (1H, sept, J_{HH} 7.0 Hz, $\text{CH}(\text{CH}_3)_2$, min), 2.99-2.86 (1H, sept, J_{HH} 7.0 Hz, $\text{CH}(\text{CH}_3)_2$, maj), 2.07 (3H, s, COCH_3 , maj), 1.87 (3H, s, COCH_3 , min), 1.76 (3H, s, $\text{C}(\text{CH}_3)_2$, maj), 1.74 (3H, s, $\text{C}(\text{CH}_3)_2$, min), 1.66 (3H, s, $\text{C}(\text{CH}_3)_2$, min), 1.58 (3H, s, $\text{C}(\text{CH}_3)_2$, maj), 0.95 (6H, d, J_{HH} 7.0 Hz, $\text{CH}(\text{CH}_3)_2$, min), 0.94 (6H, d, J_{HH} 7.0 Hz, $\text{CH}(\text{CH}_3)_2$, maj); δ_{C} (75 MHz CDCl_3); 173.8 (min), 168.8 (maj) ($\text{C}=\text{O}$), 133.6 (min), 131.3 (maj) ($\text{N}-\text{C}$), 128.4 (min), 127.4 (maj) ($\text{C}(\text{CH}_3)_2$), 29.5 (min), 29.2 (maj) (COCH_3), 23.2 (min), 20.0 (maj) ($\text{C}(\text{CH}_3)_2$), 20.5 (maj), 20.4 (min) (CH), 20.0 (min), 19.7 (maj), 19.5 (min), 19.2 (maj) ($\text{CH}(\text{CH}_3)_2$); m/z (ESI) 178 ($[\text{M}]^+\text{Na}$); [Found: ($[\text{M}]^+\text{Na}$) 178.1202, $\text{C}_9\text{H}_{17}\text{NNaO}$ requires 178.1208].

6.2.11.2 *N*-(2,6-dimethylcyclohexen-1-yl)-acetamide **357****357**

The general procedure for the synthesis of tetrasubstituted enamides (6.2.11) was applied using 2,6-dimethylcyclohexanone (1.60 ml, 12.7 mmol), acetic acid (2.18 ml, 38.1 mmol), acetic anhydride (38.1 mmol) and Fe powder (1.42 g, 25.4 mmol). Flash chromatography eluting

with 5:1 hexane/EtOAc yielded **357** as a yellow oil (552 mg, 3.3 mmol, 26%) of a 5 : 1 mixture of rotomers. R_f (3:1 pet ether:EtOAc) 0.13; ν_{\max} (cm^{-1}) 3260, 2928, 2864, 1641, 1514, 1453, 1369, 1280, 709; δ_{H} (300 MHz CDCl_3) 6.43 (1H, br, NH , min), 6.43 (1H, br, NH , maj), 2.42 (1H, br, $\text{C}(\text{H})\text{CH}_3$, maj), 2.40 (1H, br, $\text{C}(\text{H})\text{CH}_3$, min), 2.06 (2H, m, CH_2 , min), 2.05 (3H, s, $\text{C}(\text{O})\text{CH}_3$, maj), 1.99 (2H, m, CH_2 , maj), 1.84 (3H, s, $\text{C}(\text{O})\text{CH}_3$, min), 1.79-1.69 (4H, m, CH_2 , min), 1.58 (3H, s, CH_3) 1.61-1.48 (4H, m, CH_2 , maj), 1.01 (3H, s, CH_3 , maj), 0.99 (3H, s, CH_3 , min), 0.98 (3H, d, J_{HH} 7.0 Hz, $\text{C}(\text{H})\text{CH}_3$, min), 0.93 (3H, d, J_{HH} 7.0 Hz, $\text{C}(\text{H})\text{CH}_3$, maj); δ_{C} (75 MHz CDCl_3) 169.0 (min), 168.5 (maj) ($\text{C}=\text{O}$), 138.1 (maj) 138.0 (min) ($\text{N}-\text{C}$), 132.0 (maj) 131.8 (min) ($\text{N}-\text{CC}$), 34.1 (min) 32.0 (maj) (CH), 33.3 (min) 31.2 (maj) (CH_2), 31.1 (min) 30.9 (maj) (CH_2), 27.2 (maj) 26.6 (min) (CH_3), 24.3 (min) 23.3 (maj) (CH_3), 19.4 (maj), 18.8 (min) (CH_2); m/z (ESI) 190 ($[\text{M}]^+\text{Na}$); [Found: ($[\text{M}]^+\text{Na}$) 190.1204, $\text{C}_{10}\text{H}_{17}\text{NNaO}$ requires 190.1208].

6.2.11.3 *N*-(3,4-dihydronaphthalen-1-yl)-acetamide **358**²⁴⁶

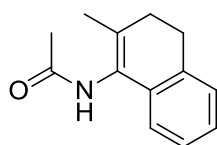


358

The general procedure for the synthesis of tetrasubstituted enamides (6.2.11) was applied using α -tetralone (0.82 ml, 6.2 mmol), acetic acid (1.06 mmol, 18.6 mmol), acetic anhydride (1.76 mmol, 18.6 mmol) and Fe powder (693 mg, 12.4 mmol). Flash chromatography eluting with 5:1 hexane/EtOAc yielded **358** as an off-white solid (580 mg, 3.1 mmol, 50%) of a 3:1 mixture of amide rotomers. R_f (3:1 pet ether:EtOAc) 0.11; mpt 130-132, lit²⁴⁶ 133-134 °C; ν_{\max} (cm^{-1}) 3243, 3028, 2930, 2833, 1655, 1522, 1486, 1368, 1284, 768, 731; δ_{H} (300 MHz CDCl_3) 7.36-7.21 (8H, m, Ar- H , maj + min), 7.06 (1H, brs, NH maj), 6.91 (1H, brs, NH min), 6.50 (1H, t,

J_{HH} 4.9 Hz, N-CCH maj), 6.06 (1H, t, J_{HH} 4.9 Hz, N-CCH min), 2.93 (2H, t, J_{HH} 7.7 Hz, CH₂ min), 2.85 (2H, t, J_{HH} 7.7 Hz, CH₂ maj), 2.55-2.38 (4H, m, CHCH₂, maj + min), 2.25 (3H, s, C(O)CH₃ maj), 2.05 (3H, s, C(O)CH₃ min); δ_{C} (75 MHz CDCl₃) 169.3, 164.2 (C=O), 149.1, 147.9, 136.9, 136.8, 131.6, 131.5, (quaternary), 128.2, 127.9, 127.6, 126.9, 126.4, 120.6 (Ar), 126.0, 119.7 (CH), 27.6, 27.3 (CH₂), 22.6, 22.2 (CHCH₂), 24.2, 20.4 (CH₃); m/z (ESI) 210 ([M]⁺Na), 188 ([M]⁺H); [Found ([M]⁺H) 188.1070, C₁₂H₁₄NO requires 188.1075].

6.2.11.4 *N*-(2-methyl-3,4-dihydronaphthalen-1-yl)-acetamide **359**²²⁹

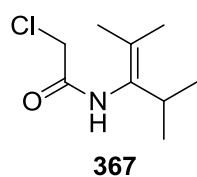


359

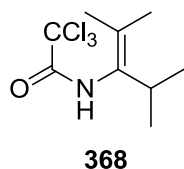
The general procedure for the synthesis of tetrasubstituted enamides (6.2.11) was applied using 2-methyl-1-tetralone (0.90 ml, 5.6 mmol), acetic acid (0.96 ml, 16.8 mmol), acetic anhydride (1.57 ml, 16.8 mmol) and Fe powder (626 mg, 11.2 mmol). Flash chromatography eluting with 5:1 hexane/EtOAc yielded **359** as a white solid (403 mg, 2.0 mmol, 36%) of a 1 : 1 mixture of amide rotomers (1 + 2). R_f (3:1 pet ether:EtOAc) 0.07; mpt 151-153 °C, lit²²⁹ 152-154 °C; ν_{max} (cm⁻¹) 3225, 2936, 2892, 2831, 1646, 1531, 1487, 1368, 1283, 1229, 990, 761; δ_{H} (300 MHz CDCl₃) 7.43-7.21 (8H, m, Ar-H, 1 + 2), 6.94 (2H, brs, NH, 1 + 2), 3.02-2.96 (2H, t, J_{HH} 8.4 Hz, CH₂CH, 2), 2.99-2.93 (2H, t, J_{HH} 8.8 Hz, CH₂CH, 1), 2.58-2.53 (2H, t, J_{HH} 8.4 Hz, CHCH₂, 2), 2.56-2.51 (2H, t, J_{HH} 8.8 Hz, CHCH₂, 1), 2.33 (3H, s, COCH₃, 1), 2.10 (3H, s, CCH₃, 2), 2.01 (3H, s, CCH₃, 1), 1.99 (3H, s, COCH₃, 2); δ_{C} (75 MHz CDCl₃) 174.1 (2), 169.1 (1) (C=O), 135.2 (2) 135.1 (1) (N-C), 135.7 (1), 134.4 (1), 133.5 (2), 133.0 (2) (Ar quaternary), 127.9 (1), 126.2 (2) (CCH₃), 127.5, 127.3, 127.2, 126.8, 126.4, 126.2, 121.8, 121.5 (Ar 1 + 2), 29.6 (2), 29.5 (1), 27.5 (1), 27.4 (2) (CH₂), 23.2 (2), 19.9 (1) (COCH₃),

19.5 (1), 19.1 (2) (CCH₃); *m/z* (ESI) 224 ([M]⁺Na), 202 ([M]⁺H); [Found: ([M]⁺H) 202.1226, C₁₃H₁₆NO requires 202.1232]; [Found: C, 77.5; H, 7.5; N, 6.9. C₁₃H₁₅NO requires C, 77.6; H, 7.5; N, 6.9].

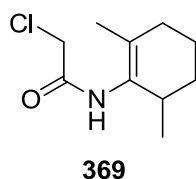
6.2.11.5 *N*-(2,4-dimethylpent-2-en-3-yl)-2-chloroacetamide **367**



The general procedure for the synthesis of tetrasubstituted enamides (6.2.11) was applied using diisopropyl ketone (1.09 ml, 7.7 mmol), acetic acid (1.32 ml, 23.0 mmol), chloroacetic anhydride (3.81 ml, 23.0 mmol) and Fe powder (860 mg, 15.4 mmol). Flash chromatography eluting with 5 : 1 hexane/EtOAc yielded **367** as a yellow oil (550 mg, 2.9 mmol, 38%) of a 20 : 1 mixture of amide rotamers. *R_f* (3:1 pet ether:EtOAc) 0.41; ν_{\max} (cm⁻¹) 3243, 2973, 2933, 2869, 1656, 1535, 1461, 1421, 1329, 1231, 804, 717, 678; δ_{H} (300 MHz CDCl₃) 7.18 (2H, brs, NH, maj + min), 4.10 (2H, s, CH₂Cl, maj), 4.07 (2H, s, CH₂Cl, min), 2.90 (2H, sept, *J*_{HH} 6.9 Hz, CH, maj + min), 1.75 (3H, s, C(CH₃)₂, maj), 1.67 (3H, s, C(CH₃)₂, min), 1.61 (3H, s, C(CH₃)₂, min), 1.56 (3H, s, C(CH₃)₂, maj), 1.18 (6H, d, *J*_{HH} 6.9 Hz, CH(CH₃)₂, min), 0.91 (6H, d, *J*_{HH} 6.9 Hz, CH(CH₃)₂, maj); δ_{C} (75 MHz CDCl₃) 164.4 (min) 163.6 (maj) (C=O), 129.6 (maj) 129.5 (min) (N-C), 127.4 (min) 127.3 (maj) (C=C), 42.4 (maj) 42.1 (min) (CH₂Cl), 28.7 (maj) 28.4 (min) (CH), 19.8, 18.6 (C(CH₃)₂ maj + min), 19.3 (CH(CH₃)₂ maj + min); *m/z* (ESI) 190 ([M]⁺H) (³⁵Cl), 192 ([M]⁺H) (³⁷Cl); [Found: ([M]⁺H) 190.0993, C₉H₁₇³⁵ClNO requires 190.0999]; [Found: C, 56.9; H, 8.4; N, 7.3. C₁₀H₁₇NO requires C, 57.0; H, 8.5; N, 7.4].

6.2.11.6 *N*-(2,4-dimethylpent-2-en-3-yl)-trichloroacetamide **368**

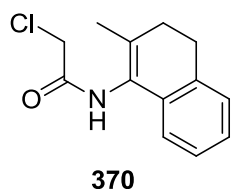
The general procedure for the synthesis of tetrasubstituted enamides (6.2.11) was applied using diisopropyl ketone (1.18 ml, 8.3 mmol), acetic acid (1.43 ml, 24.9 mmol), trichloroacetic anhydride (4.55 ml, 24.9 mmol) and Fe powder (927 mg, 16.6 mmol). Flash chromatography eluting with 5:1 hexane/EtOAc yielded **368** as a yellow oil (517 mg, 2.0 mmol, 24%) of a 1 : 1 mixture of amide rotamers (1 + 2). R_f (3:1 pet ether:EtOAc) 0.77; ν_{\max} (cm^{-1}) 3275, 2965, 2917, 2856, 1699, 1496, 1459, 1263, 1249, 843, 818, 681; δ_{H} (300 MHz CDCl_3) 7.29 (1H, brs, NH , 1), 7.12 (1H, brs, NH , 2), 3.07-2.94 (1H, sept, J_{HH} 6.9 Hz, $\text{CH}(\text{CH}_3)_2$, 1), 3.05, 2.92 (1H, sept, J_{HH} 6.9 Hz, $\text{CH}(\text{CH}_3)_2$, 2), 1.78 (H, brs, $\text{C}(\text{CH}_3)_2$, 1), 1.77 (H, brs, $\text{C}(\text{CH}_3)_2$, 2), 1.64 (3H, brs, $\text{C}(\text{CH}_3)_2$, 1), 1.62 (3H, brs, $\text{C}(\text{CH}_3)_2$, 2), 1.02 (6H, d, J_{HH} 6.9 Hz, $\text{CH}(\text{CH}_3)_2$, 1), 1.00 (6H, d, J_{HH} 6.9 Hz, $\text{CH}(\text{CH}_3)_2$, 2); δ_{C} (75 MHz CDCl_3) 164.1, 162.7 ($\text{C}=\text{O}$ 1 + 2), 129.8, 129.5, ($\text{N}-\text{C}$ 1 + 2) 129.2, 128.8 ($\text{C}(\text{CH}_3)_2$ 1 + 2), 29.6, 29.5 ($\text{CH}(\text{CH}_3)_2$ 1 + 2), 20.1, 20.0, 19.9, 19.9, 19.3, 19.3 (CH_3 1 + 2); m/z (ESI) 280 ($[\text{M}]^+\text{Na}$) (^{35}Cl), 282 ($[\text{M}]^+\text{Na}$) (^{37}Cl); [Found: ($[\text{M}]^+\text{Na}$) 280.0033, $\text{C}_9\text{H}_{14}\text{Cl}_3\text{NNaO}$ requires 280.0039].

6.2.11.7 *N*-(2,6-dimethylcyclohexen-1-yl)-2-chloroacetamide **369**

The general procedure for the synthesis of tetrasubstituted enamides was applied using 2,6-dimethylcyclohexanone (1.09 ml, 8.6 mmol), acetic acid (1.48 ml, 25.8 mmol) chloroacetic anhydride (4.27 ml, 25.8 mmol) and Fe powder (961 mg, 17.2 mmol). Flash chromatography

eluting with 5:1 hexane/EtOAc yielded **369** (666 mg, 3.3 mmol, 38%) as a pale yellow oil. R_f (3:1 pet ether:EtOAc) 0.48; ν_{\max} (cm^{-1}) 3246, 2928, 2867, 1672, 1527, 1452, 1426, 1329, 1230, 1174, 971, 788; δ_{H} (300 MHz CDCl_3) 7.30 (1H, brs, NH), 4.11 (2H, s, CH_2Cl), 2.47 (1H, m, $\text{CH}(\text{CH}_3)$), 2.06 (2H, br t, J_{HH} 6.0 Hz, $\text{C}(\text{CH}_3)\text{CH}_2$), 1.59 (3H, s, $\text{C}(\text{CH}_3)_3$), 1.87-1.77 (1H, m, $\text{CH}(\text{CH}_3)\text{CH}_2$) 1.73-1.51 (2H, m, $\text{CH}_2\text{CH}_2\text{CH}_2$), 1.47-1.37 (1H, m, $\text{CH}(\text{CH}_3)\text{CH}_2$), 1.00 (3H, d, J_{HH} 6.7 Hz, $\text{CH}(\text{CH}_3)$); δ_{C} (75 MHz CDCl_3) 164.1 ($\text{C}=\text{O}$), 139.9 ($\text{N}-\text{C}$), 128.9 ($\text{C}=\text{C}$), 42.2 (CH_2Cl), 30.7, 30.4, 18.9 (CH_2) 31.3 (CH), 18.3, 18.1 (CH_3); m/z (ESI) 202 ($[\text{M}]^+\text{Na}$) (^{35}Cl), 204 ($[\text{M}]^+\text{H}$) (^{37}Cl); [Found: ($[\text{M}]^+\text{H}$) 202.0993, $\text{C}_{10}\text{H}_{17}^{35}\text{ClNO}$ requires 202.0999]; [Found: C, 59.2; H, 7.9; N, 6.8. $\text{C}_{10}\text{H}_{17}\text{NO}$ requires C, 59.6; H, 8.0; N, 6.9].

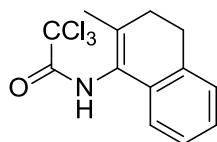
6.2.11.8 *N*-(2-methyl-3,4-dihydronaphthalen-1-yl)-2-chloroacetamide **370**



The general procedure for the synthesis of tetrasubstituted enamides was applied using 2-methyl-1-tetralone (0.70 ml, 4.6 mmol), acetic acid (0.79 ml, 13.8 mmol), chloroacetic anhydride (2.29 ml, 13.8 mmol) and Fe powder (514 mg, 9.2 mmol). Flash chromatography eluting with 5:1 hexane/EtOAc yielded **370** (236 mg, 1.0 mmol, 22%) as an off white solid. R_f (3:1 pet ether:EtOAc) 0.36; mpt 140-142 °C; ν_{\max} (cm^{-1}) 3180, 3026, 2937, 1664, 1535, 1419, 1238, 1161, 807, 742, 728; δ_{H} (300 MHz CDCl_3) 7.53 (1H, brs, NH), 7.14-6.98 (4H, m, Ar-H), 4.18 (2H, s, CH_2Cl), 2.77 (2H, t, J_{HH} 8.2 Hz, $\text{CH}_2\text{-Ar}$), 2.36 (2H, t, J_{HH} 8.2 Hz, CH_2C), 1.81 (3H, s, CH_3); δ_{C} (75 MHz CDCl_3) 170.2 ($\text{C}=\text{O}$), 134.5, 124.4 (Ar quaternary), 126.9, 126.3, 125.9, 120.5 (Ar), 42.2 (CH_2Cl), 29.0 (CH_2C), 26.8 ($\text{CH}_2\text{-Ar}$), 18.8 (CH_3); m/z (ESI) 258 ($[\text{M}]^+\text{Na}$), 236

([M]⁺H); [Found: ([M]⁺H) 236.0838, C₁₃H₁₅³⁵ClNO requires 236.0842]; [Found: C, 66.2; H, 5.9; N, 5.8. C₁₃H₁₄ClNO requires C, 66.2; H, 6.0; N 5.8].

6.2.11.9 N-(2-methyl-3,4-dihydronaphthalen-1-yl)-trichloroacetamide **371**



371

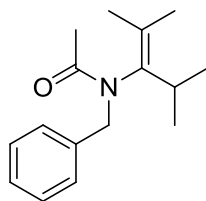
The general procedure for the synthesis of tetrasubstituted enamides was applied using 2-methyl-1-tetralone (0.58 ml, 3.8 mmol), acetic acid (0.65 ml, 11.4 mmol), trichloroacetic anhydride (2.08 ml, 11.4 mmol) and Fe powder (424 mg, 7.6 mmol). Flash chromatography eluting with 5:1 hexane/EtOAc yielded **371** (287 mg, 0.95 mmol, 25%) as a yellow oil. R_f (3:1 pet ether:EtOAc) 0.50; ν_{\max} (cm⁻¹) 3302, 3027, 2939, 2894, 2831, 1698, 1486, 1454, 1224, 809, 798, 756, 679; δ_H (300 MHz CDCl₃) 7.66 (1H, brs, NH), 7.22-7.09 (4H, m, Ar-H), 2.85 (2H, t, J_{HH} 7.9 Hz, CH₂-Ar), 2.44 (2H, t, J_{HH} 7.9 Hz, CH₂), 1.92 (3H, s, CH₃); δ_C (75 MHz CDCl₃) 160.3 (C=O), 135.9, 135.1 (NCCCH₃), 132.0, 124.6 (Ar quaternary), 127.6, 127.2, 126.7, 120.9 (Ar), 29.7, 27.4 (CH₂), 19.2 (CH₃); m/z (ESI) 304 ([M]⁺H) (³⁵Cl), 306 ([M]⁺H) (³⁷Cl); [Found: ([M]⁺H) 304.0057, C₁₃H₁₃³⁵Cl₃NO requires 304.0063].

6.2.12 General Procedures for the Alkylation of Enamides

Enamide (1 equiv) in dry THF was added to NaH (5 equiv) in dry THF and cooled to 0°C. Alkyl halide (1.05-8.00 equiv) was then added in the single portion and the reaction was heated at reflux for 24 hrs. The reaction was allowed to cool to room temperature then poured into H₂O. The aqueous layer was then extracted using three portions of DCM. The resulting organic layer was dried over MgSO₄, filtered and

concentrated in *vacuo* to yield a crude product which could be purified *via* flash chromatography eluting with pet ether and EtOAc.

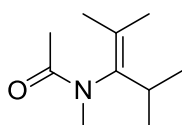
6.2.12.1 *N*-Benzyl-*N*-(2,4-dimethylpent-2-en-3-yl)-acetamide **360**²²⁰



360

The general procedure for enamide alkylation (6.2.12) was applied using *N*-(2,4-dimethylpent-2-en-3-yl)-acetamide (149 mg, 0.96 mmol), sodium hydride (192 mg, 4.8 mmol) and benzyl bromide (0.12 ml, 1.01 mmol). Flash chromatography eluting with 9:1 pet ether/EtOAc yielded **360** as a colourless oil (52 mg, 0.21 mmol, 22%). R_f (3:1 pet ether:EtOAc) 0.36; ν_{\max} (cm^{-1}) 2965, 1642, 1438, 1395, 1278, 1238, 682; δ_{H} (300 MHz CDCl_3) 7.38-7.22 (5H, m, Ar-H), 5.25 (1H, d, J_{HH} 14.0 Hz, Ar-CH₂), 3.96 (1H, d, J_{HH} 14.0 Hz, Ar-CH₂), 2.96 (1H, sept, J_{HH} 7.5 Hz, CH), 1.94 (3H, s, CH₃), 1.69 (3H, s, C(CH₃)₂), 1.25 (3H, d, J_{HH} 7.5 Hz, CH(CH₃)₂), 1.02 (3H, d, J_{HH} 7.5 Hz, CH(CH₃)₂), 1.01 (3H, s, C(CH₃)₂); δ_{C} (75 MHz CDCl_3) 170.5 (C=O), 136.8 (Ar, quaternary), 136.8, (N-C), 130.9 (C(CH₃)₂), 129.2, 127.5, 126.6 (Ar), 49.9 (Ar-CH₂), 29.4 (CH), 23.2 (CH(CH₃)₂), 21.0 (C(CH₃)₂), 19.7(CH(CH₃)₂), 18.8 (CH₃), 18.7 (C(CH₃)₂); m/z (ESI) 268 ($[\text{M}]^+\text{Na}$), 268 ($[\text{M}]^+\text{Na}$); [Found: ($[\text{M}]^+\text{Na}$) 268.1672, $\text{C}_{16}\text{H}_{23}\text{NNaO}$ requires 268.1677].

6.1.12.2 *N*-Methyl-*N*-(2,4-dimethylpent-2-en-3-yl)-acetamide **361**

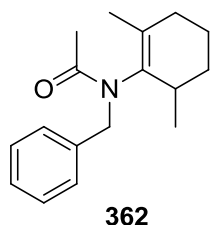


361

The general procedure for enamide alkylation (6.2.12) was applied using *N*-(2,4-dimethylpent-2-en-3-yl)-acetamide (497 mg, 3.2

mmol), sodium hydride (640 mg, 16.0 mmol) and methyl iodide (1.60 ml, 25.6 mmol). Flash chromatography eluting with 9:1 pet ether/EtOAc yielded **361** as a colourless oil (186 mg, 1.1 mmol, 33%). R_f (3:1 pet ether:EtOAc) 0.16; ν_{\max} (cm^{-1}) 2965, 2931, 2873, 1637, 1421, 1371, 1345, 1138, 1027; δ_{H} (300 MHz CDCl_3) 3.05-2.91 (1H, sept, J_{HH} 6.9 Hz, CH), 2.99 (3H, s, N- CH_3), 1.94 (3H, COCH_3), 1.76 (3H, s, $\text{C}(\text{CH}_3)_2$), 1.58 (3H, s, $\text{C}(\text{CH}_3)_2$), 1.11 (3H, d, J_{HH} 6.9 Hz, $\text{CH}(\text{CH}_3)_2$), 0.99 (3H, d, J_{HH} 6.9 Hz, $\text{CH}(\text{CH}_3)_2$); δ_{C} (75 MHz CDCl_3) 170.8 ($\text{C}=\text{O}$), 139.8 (N- C), 128.7 ($\text{C}(\text{CH}_3)_2$), 35.6 (N- CH_3), 29.5 (CH), 22.2 ($\text{CH}(\text{CH}_3)_2$), 20.6 (COCH_3), 19.2 ($\text{C}(\text{CH}_3)_2$), 19.0 ($\text{CH}(\text{CH}_3)_2$), 18.6 ($\text{C}(\text{CH}_3)_2$); m/z (ESI) 192 ($[\text{M}]^+\text{Na}$), 170 ($[\text{M}]^+\text{H}$); [Found: ($[\text{M}]^+\text{H}$) 170.1541, $\text{C}_{10}\text{H}_{20}\text{NO}$ requires 170.1545]; [Found: C, 69.6; H, 11.2; N, 7.9. $\text{C}_{10}\text{H}_{20}\text{NO}$ requires C, 71.0; H, 11.3; N, 8.3].

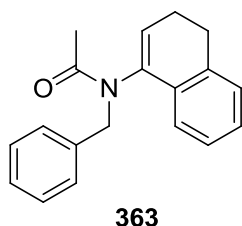
6.2.12.3 *N*-Benzyl-*N*-(2,6-dimethylcyclohexen-1-yl)-acetamide **362**



The general procedure for enamide alkylation (6.2.12) was applied using *N*-(2,6-dimethylcyclohexen-1-yl)-acetamide (184 mg, 1.1 mmol), sodium hydride (220 mg, 5.5 mmol) and benzyl bromide (0.14 ml, 1.2 mmol). Flash chromatography eluting with 9:1 pet ether/EtOAc yielded **362** as a pale yellow oil (111 mg, 0.43 mmol, 39%) of a 2 : 1 mixture of diastereomers. R_f (3:1 pet ether:EtOAc) 0.25; ν_{\max} (cm^{-1}) 2930, 1641, 1454, 1385, 1358, 1268, 1178, 702; δ_{H} (300 MHz CDCl_3) 7.33-7.22 (10H, m Ar- H , maj + min), 5.40 (1H, d, J_{HH} 14.6 Hz, Ar- CH_2 , min), 5.13 (1H, d, J_{HH} 13.8 Hz, Ar- CH_2 , maj), 4.05 (1H, d, J_{HH} 13.8 Hz, Ar- CH_2 , maj), 3.96 (1H, d, J_{HH} 14.6 Hz, Ar- CH_2 , min), 2.43 (1H, m, $\text{CH}(\text{CH}_3)$, maj), 2.41 (1H, m, $\text{CH}(\text{CH}_3)$, min), 2.04 (3H, s, CH_3 , min), 2.02-1.41 (12H, m, CH_2 , maj + min), 1.97 (3H, s, CH_3 , maj), 1.19 (3H,

brs, C(CH₃), min), 1.08 (3H, brs, C(CH₃), maj), 1.03 (3H, br d, CH(CH₃), min), 0.95 (3H, d, J_{HH} 7.1 Hz, CH(CH₃), maj); δ_{C} (75 MHz CDCl₃) 171.6 (C=O) (min), 170.9 (C=O) (maj), 138.0 (N-C) (maj), 137.9 (N-C) (min), 135.1 (Ar, quaternary) (maj), 135.0 (Ar, quaternary) (min), 133.3 (C(CH₃)) (maj), 133.2 (C(CH₃)) (min), 130.1, 128.9, 128.8, 128.1, 127.3, 127.0 (Ar) (maj + min), 50.8 (Ar-CH₂) (min), 48.1 (Ar-CH₂) (maj), 31.6, 31.4, 25.6 (CH₂) (maj + min), 29.9 (CH₃) (maj + min), 27.6 (CH) (maj + min), 18.8 (C(CH₃)) (maj + min), 18.4 (CH(CH₃)) (maj + min); m/z (ESI) 280 ([M]⁺Na), 258 ([M]⁺H); [Found: ([M]⁺H) 258.1852, C₁₇H₂₄NO requires 258.1858].

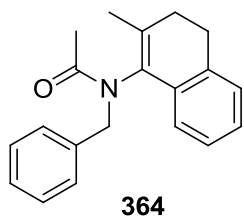
6.2.12.4 *N*-Benzyl-*N*-(3,4-dihydronaphthalen-1-yl)-acetamide **363**



The general procedure for enamide alkylation (6.2.12) was applied using *N*-(3,4-dihydronaphthalen-1-yl)-acetamide (100 mg, 0.53 mmol), sodium hydride (108 mg, 2.7 mmol) and benzyl bromide (0.067 ml, 0.56 mmol). Flash chromatography eluting with 9:1 pet ether/EtOAc yielded **363** as an off white solid (33 mg, 0.12 mmol, 22%). R_f (3:1 pet ether:EtOAc) 0.36; mpt 152-154 °C; ν_{max} (cm⁻¹) 2934, 1646, 1427, 1393, 1273, 1224, 982, 912, 728; δ_{H} (300 MHz CDCl₃) 7.28-7.04 (9H, m, Ar-H), 5.58 (1H, t, J_{HH} 4.3 Hz, CH), 5.54 (1H, d, J_{HH} 14.6 Hz, Ar-CH₂), 3.84 (1H, d, J_{HH} 14.6 Hz, Ar-CH₂), 2.77 (2H, t, J_{HH} 8.2 Hz, CH₂), 2.29 (2H, m, CHCH₂), 2.02 (3H, s, CH₃); δ_{C} (75 MHz CDCl₃) 170.6 (C=O), 137.6 (N-C), 137.3, 136.3, 130.7 (Ar quaternary), 128.5, 128.1, 127.6, 127.6, 127.4, 126.7, 126.3 (Ar), 121.3 (CH), 49.4 (Ar-CH₂), 26.6 (CH₂), 22.1 (CHCH₂CH₂), 21.1 (CH₃); m/z (ESI) 300 ([M]⁺Na), 278 ([M]⁺H); [Found ([M]⁺H) 278.1546, C₁₉H₂₀NO requires 278.1545].

6.2.12.5 *N*-Benzyl-*N*-(2-methyl-3,4-dihydronaphthalen-1-yl)-acetamide

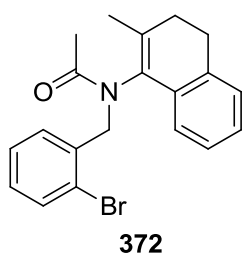
364



The general procedure for enamide alkylation (6.2.12) was applied using *N*-(2-methyl-3,4-dihydronaphthalen-1-yl)-acetamide (141 mg, 0.70 mmol), sodium hydride (140 mg, 3.5 mmol) and benzyl bromide (0.088 ml, 0.74 mmol). Flash chromatography eluting with 9:1 pet ether/EtOAc yielded **364** as a white solid (99 mg, 0.34 mmol, 49%). R_f (3:1 pet ether:EtOAc) 0.36; mpt 158-159 °C; ν_{\max} (cm^{-1}) 2927, 2882, 2924, 1643, 1488, 1396, 1297, 1249, 774, 757, 706; δ_{H} (300 MHz CDCl_3) 7.30-7.17 (8H, m, Ar-H), 6.98 (1H, m, Ar-H), 5.49 (1H, d, J_{HH} 13.5 Hz, Ar-CH₂), 3.74 (1H, d, J_{HH} 13.5 Hz, Ar-CH₂), 2.87-2.69 (2H, m, CH₂), 2.35 (1H, ddd, J_{HH} 16.5, 6.4, 4.1 Hz C(CH₃)CH₂), 2.14 (1H, ddd, J_{HH} 16.6, 6.4, 4.1 Hz, C(CH₃)CH₂), 1.90 (3H, s, C(O)CH₃), 1.24 (3H, brs, CCH₃); δ_{C} (75 MHz CDCl_3) 170.6 (C=O), 136.5, 136.2, 135.6 (Ar, quaternary), 135.5 (N-C), 131.2 (N-CCCH₃), 129.6, 127.5, 127.1, 126.8, 126.6, 126.3, 121.2 (Ar), 48.8 (Ar-CH₂), 28.9 C(CH₃)CH₂, 26.8 (CH₂), 20.6 (C(O)CH₃), 18.3 (CH₃); m/z (ESI) 314 ($[\text{M}]^+\text{Na}$), 292 ($[\text{M}]^+\text{H}$); [Found: ($[\text{M}]^+\text{H}$) 292.1696, $\text{C}_{20}\text{H}_{22}\text{NO}$ requires 292.1701].

6.2.12.6 *N*-2-Bromobenzyl-*N*-(2-methylnaphthalen-1-yl)-2-iodoacetamide

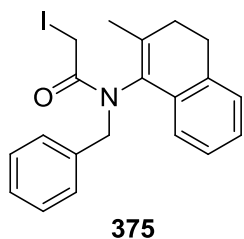
372



The general procedure for enamide alkylation (6.2.12) was applied using *N*-(2-methyl-3,4-dihydronaphthalen-1-yl)-

acetamide (60 mg, 0.30 mmol), sodium hydride (60 mg, 1.5 mmol) and 2-bromobenzyl bromide (0.038 ml, 0.32 mmol). Flash chromatography eluting with 9:1 pet ether/EtOAc yielded **372** as a white solid (59 mg, 0.16 mmol, 54%). R_f (3:1 pet ether:EtOAc) 0.46; mpt 179-180 °C; ν_{\max} (cm^{-1}) 2927, 2881, 2824, 1654, 1566, 1488, 1425, 1390, 1298, 1241, 1026, 760; δ_{H} (300 MHz CDCl_3) 7.51 (1H, dd, J_{HH} 7.7, 1.7 Hz, Ar-H), 7.36 (1H, dd, J_{HH} 7.7, 1.7 Hz, Ar-H), 7.19-6.86 (6H, m, Ar-H), 5.45 (2H, d, J_{HH} 13.8 Hz, Ar-CH₂), 4.20 (2H, d, J_{HH} 13.8 Hz, Ar-CH₂), 2.80 (1H, dt, J_{HH} 15.1, 6.5 Hz CH₂), 2.62 (1H, ddd, J_{HH} 15.1, 6.5, 4.1 Hz, CH₂), 2.28 (1H, dt, J_{HH} 15.1, 6.5 Hz, C(CH₃)CH₂), 2.07 (1H, ddd, 15.1, 6.5, 4.1 Hz, C(CH₃)CH₂), 1.85 (3H, s, CH₃), 1.27 (3H, s, C(CH₃)); δ_{C} (75 MHz CDCl_3) 171.0 (C=O), 136.4 (Ar-Br), 135.8 (N-C), 135.6, 131.4, 131.3 (Ar, quaternary), 132.4, 131.9, 128.5, 127.0, 126.5, 126.8, 126.2, 120.9 (Ar), 124.4 (C(CH₃)), 47.4 (Ar-CH₂), 28.9 (C(CH₃)CH₂), 26.6 (CH₂), 20.5 (CH₃), 18.1 (C(CH₃)); m/z (ESI) 392 ([M]⁺Na) (⁷⁹Br), 394 ([M]⁺Na) (⁸¹Br); [Found: ([M]⁺Na) 392.0627, C₂₀H₂₀⁷⁹BrNNaO requires 392.0626]; [Found: C, 64.8; H, 5.4; N, 3.6. C₂₀H₂₀BrNO requires C, 64.9; H, 5.4; N, 3.8].

6.2.12.7 *N*-Benzyl-*N*-(2-methyl-3,4-dihydronaphthalen-1-yl)-2-iodoacetamide **375**

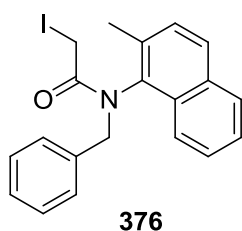


The general procedure for enamide alkylation (6.2.12) was applied using *N*-(2-methyl-3,4-dihydronaphthalen-1-yl)-2-chloroacetamide (146 mg, 0.62 mmol), sodium hydride (214 mg, 3.1 mmol) and benzyl bromide (0.077 ml, 0.65 mmol) afforded a 5:1 mixture of *N*-Benzyl-*N*-(2-methyl-3,4-dihydronaphthalen-1-yl)-2-chloroacetamide **373** and *N*-(2-methyl-3,4-dihydronaphthalen-1-yl)-2-

bromoacetamide **374**. The mixture was dissolved in acetone and sodium iodide was added before being stirred at room temperature for 36 hours. The mixture was then diluted with H₂O (20 ml), and extracted using EtOAc (2 x 50 ml). The organic extracts were washed consecutively with Na₂S₂O₃ (100 ml) and brine (100 ml), then dried filtered and concentrated in *vacuo* to yield a crude product which was purified by flash chromatography to yield **375** as an off-white solid (191 mg, 0.46 mmol, 74% *R_f* (3:1 pet ether:EtOAc) 0.60; mpt 163-165 °C; ν_{\max} (cm⁻¹) 3062, 3030, 2929, 2830, 1652, 1493, 1454, 1415, 1388, 1293, 1246, 1164, 1976, 757; δ_{H} (300 MHz, CDCl₃) 7.31-7.18 (8H, m, Ar-H), 6.96 (1H, m, Ar-H), 5.36 (1H, d, *J*_{HH} 14.1 Hz, Ar-CH₂), 3.98 (1H, d, *J*_{HH} 14.1 Hz, Ar-CH₂), 3.73 (1H, d, *J*_{HH} 12.1 Hz, CH₂I), 3.70 (1H, d, *J*_{HH} 12.1 Hz, CH₂I), 2.83-2.77 (2H, m, CH₂), 2.40 (1H, m, C(CH₃)CH₂), 2.20 (1H, dt, *J*_{HH} 16.6, 6.0 Hz, C(CH₃)CH₂), 1.34 (3H, s, CH₃); δ_{C} (75.5 MHz, CDCl₃) 168.3 (C=O), 137.7 (N-C), 136.4, 136.1, 131.6 (Ar, quaternary), 131.4 (C(CH₃)), 130.3, 128.2, 128.1, 127.9, 127.8, 127.7, 127.4, 126.9, 122.3 (Ar), 50.7 (Ar-CH₂), 29.6 (CH₂), 27.4 (CH₂), 19.8 (CH₃), -1.7 (CH₂I); *m/z* 440 ([M]⁺Na), 418 ([M]⁺H); [Found: ([M]⁺Na) 440.0482, C₂₀H₂₀INNaO requires 440.0487].

6.2.13 Products of Attempted Cyclisations Performed in Chapter 5

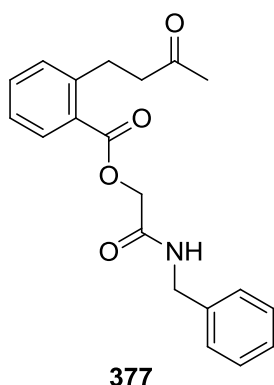
6.2.13.1 *N*-Benzyl-*N*-(2-methylnaphthalen-1-yl)-2-iodoacetamide **376**



N-Benzyl-*N*-(2-methyl-3,4-dihydronaphthalen-1-yl)-2-iodoacetamide (62 mg, 0.15 mmol) was dissolved in dry toluene (7.5 ml) and a mixture of Bu₃SnH (52 μ l, 0.18 mmol) and AIBN (2.5 mg, 0.015 mmol) in toluene (7.5 ml) was degassed simultaneously.

N-Benzyl-*N*-(2-methyl-3,4-dihydronaphthalen-1-yl)-2-iodoacetamide in dry toluene was heated to reflux and the reagent mixture was added *via* syringe pump over 2 hours. A second portion of the Bu₃SnH and AIBN was then added over 1 hour and the resulting mixture was stirred at reflux overnight. The solvent was removed in *vacuo* and the residue was partitioned between 8% KF (50 ml) and Et₂O (20 ml) and stirred for 3 hours. The resulting organic layer was filtered through celite and concentrated to yield a crude product which was purified by gradient chromatography eluting with 100-50% pet ether/EtOAc to yield **376** as a white solid (12 mg, 0.03 mmol, 21%). *R_f* (3:1 pet ether:EtOAc) 0.68; mpt 174-175 °C; ν_{\max} (cm⁻¹) 3064, 2838, 1662, 1495, 1452, 1415, 1388, 1290, 1245, 1164, 1084, 760; δ_{H} (300 MHz, CDCl₃) 7.75-7.62 (2H, m, Ar-H), 7.38-7.19 (9H, m, Ar-H), 5.07 (1H, d, *J*_{HH} 13.4 Hz, Ar-CH₂), 4.49 (1H, d, *J*_{HH} 13.4 Hz, Ar-CH₂), 3.32 (1H, d, *J*_{HH} 10.7 Hz, CH₂I), 3.28 (1H, d, *J*_{HH} 10.7 Hz, CH₂I), 1.85 (CH₃); δ_{C} (75.5 MHz, CDCl₃) 170.3 (C=O), 137.9 (N-C), 136.3, 135.1, 133.2 (Ar, quaternary), 132.1, 130.8, 130.4, 130.1, 130.1, 130.0, 129.7, 129.5, 129.2, 127.7, 124.4 (Ar), 123.2 (C(CH₃)), 55.1 (Ar-CH₂), 25.2 (CH₃), -0.1 (CH₂I); *m/z* 438 ([M]⁺Na), 416 ([M]⁺H); [Found: ([M]⁺Na) 438.0329, C₂₀H₂₀INNaO requires 438.0331].

6.2.13.2 2-(3-Oxobutyl)benzoic acid benzyl carbamoyl methyl ester **377**



N-Benzyl-*N*-(2-methyl-3,4-dihydronaphthalen-1-yl)-2-iodoacetamide (62 mg, 0.15 mmol) was dissolved in dry toluene (7.5 ml) and a mixture of Bu₃SnH (52 μ l, 0.18 mmol) and AIBN (2.5 mg, 0.015 mmol) in toluene (7.5 ml) were degassed simultaneously. *N*-Benzyl-*N*-(2-methyl-3,4-

dihydronaphthalen-1-yl)-2-iodoacetamide in dry toluene was heated to reflux and the reagent mixture was added *via* syringe pump over 2 hours. A second portion of the Bu_3SnH and AIBN was then added over 1 hour and the resulting mixture was stirred at reflux overnight. The solvent was removed in *vacuo* and the residue was partitioned between 8% KF (50 ml) and Et_2O (20 ml) and stirred for 3 hours. The resulting organic layer was filtered through celite and concentrated to yield a crude product which was purified to gradient chromatography eluting with 100-50% pet ether/EtOAc to yield **377** as a colourless oil (14 mg, 0.04 mmol, 26%). R_f (3:1 pet ether:EtOAc) 0.23; ν_{max} (cm^{-1}) 3278, 3067, 2988, 2902, 1730, 1707, 1664, 1555, 1499, 1485, 1454, 1421, 1270, 1248, 1167, 1136, 1102, 744, 691; δ_{H} (300 MHz, CDCl_3) 7.84 (1H, d, J_{HH} 8.3 Hz, Ar-H), 7.45 (1H, dd, J_{HH} 8.3, 1.5 Hz, Ar-H) 7.36-7.24 (8H, m, Ar-H), 6.83 (1H, br, NH), 4.87 (2H, s, C(O)CH₂O), 4.54 (2H, d, J_{HH} 6.0 Hz, Ar-CH₂NH), 3.18 (2H, t, J_{HH} 7.3 Hz, Ar-CH₂), 2.75 (2H, t, J_{HH} 7.3 Hz, CH₂C(O)), 2.04 (3H, s, CH₃); δ_{C} (75.5 MHz, CDCl_3) 208.2, 167.3, 166.1 (C=O), 143.4, 137.9, 128.8 (Ar, quaternary), 132.7, 131.2, 130.5, 128.7, 127.9, 127.7, 127.6, 126.5, 126.4 (Ar), 63.5 (C(O)CH₂O), 44.9 (Ar-CH₂CH₂), 43.2 (Ar-CH₂), 29.9 (CH₃), 28.0 (Ar-CH₂-CH₂); m/z 362 ($[\text{M}]^+\text{Na}$); [Found: ($[\text{M}]^+\text{Na}$) 362.1363, $\text{C}_{20}\text{H}_{21}\text{NNaO}$ requires 362.1368].

Appendix A

N-CYCLOALKENYL BOND ROTATION STUDIES

For each compound a sample was dissolved in the appropriate solvent, which had been spiked with tetramethylsilane, and placed in a precision 5 mm NMR tube. The samples were submitted to the NMR service for variable temperature NMR at temperature intervals which were solvent dependant. Experiments were performed by Dr Adam Clarke or Dr Ivan Prokes then processed using NUTS data processing software (www.acornnmr.com). As the benzylic signals were well defined at lower temperature they were ideal for line-shape analysis.

At all temperatures, for each compound, the standard peak width was determined by measuring the half-height width of the tetramethylsilane internal standard. In order to calculate the $\Delta\nu$ at higher temperatures (during coalescence), for at least two of low temperature spectra (decoalesced) ν_a and ν_b were measured and plotted as $\log \Delta\nu$ (y-axis) verses $1/T$ (x-axis).

Line-shape analysis was performed using WINDNMR software. Appropriate values for $\Delta\nu$ and line width were inputted and line-shape analysis was accomplished by altering the rate (k) variable until the best fit was achieved. An Eyring plot was then derived from the rate data by plotting $1/T$ (x-axis) verses $\ln(k/T)$ (y-axis) according to the equation:

$$\ln\left(\frac{k}{T}\right) = \left(\frac{-\Delta H^\ddagger}{R}\right)\left(\frac{1}{T}\right) + \frac{\Delta S^\ddagger}{R} + \ln\left(\frac{k_B}{h}\right)$$

From the Eyring plots, it was possible to calculate the thermodynamic parameters for rotation from the following equations:

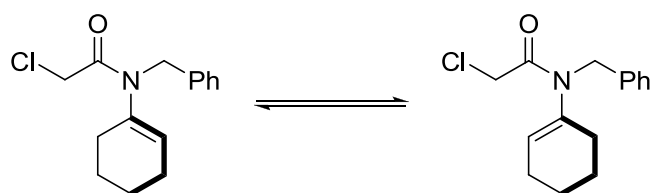
$$k_{298} = 298K \cdot e^{\left(\frac{slope}{298K} + int.\right)}$$

$$\Delta H^{\ddagger} = -R \cdot slope$$

$$\Delta S^{\ddagger} = R \cdot \left(int. - \ln\left(\frac{k_B}{h}\right) \right)$$

$$\Delta G_{298}^{\ddagger} = -R \cdot 298K \cdot \ln\left(\frac{k_{298} \cdot h}{k_B \cdot 298K}\right)$$

To obtain thermodynamic parameters in calories the conversion factor 1 cal = 4.184 J was used in all calculations.

Table A1. Rotational Data for 328 in CDCl₃

temp. (K)	k (s ⁻¹)	calc. $\nu_a - \nu_b$ (Hz)	obs. $\nu_a - \nu_b$ (Hz)
216	21.5	263.0	263.0
220	30.1	259.5	259.5
227	52.2	253.8	253.8
232	82.2	250.0	250.0
238	159	245.8	245.8
244	242	241.8	241.8
249	386	238.7	238.7
257	673	234.0	234.0
263	1.06×10^3	230.8	230.8
270	1.51×10^3	227.2	227.2

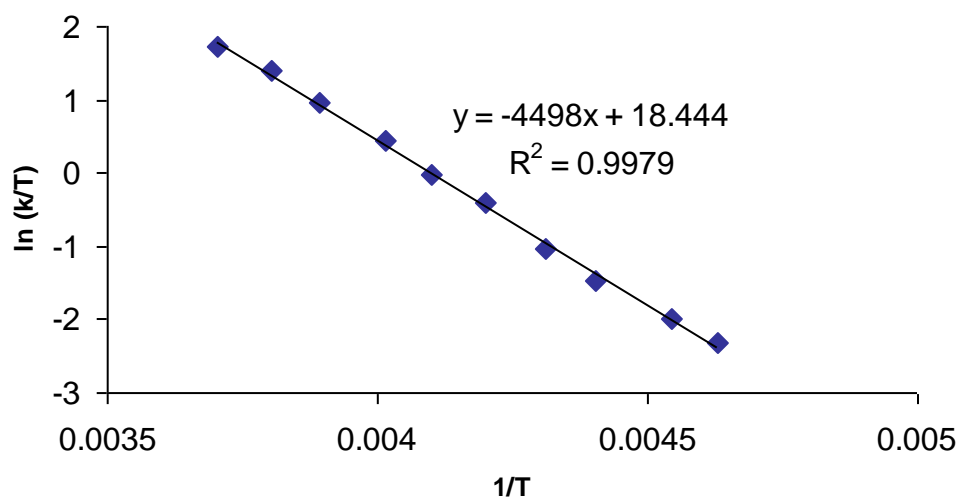
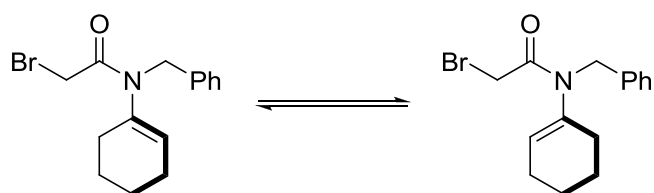
Figure A1. Eyring Plot for 328 in CDCl₃

Table A2. Rotational Data for 338 in CDCl₃

temp. (K)	k (s ⁻¹)	calc. $\nu_a - \nu_b$ (Hz)	obs. $\nu_a - \nu_b$ (Hz)
213	32.8	408.3	408.3
223	81.0	394.9	394.9
233	230	383.0	383.0
243	421	372.5	372.5
245	661	370.5	370.5
247	755	368.5	368.5
249	895	366.7	366.7
251	989	364.8	364.8
253	1.01×10^3	363.0	363.0
263	1.99×10^3	354.4	354.4
273	3.90×10^3	346.7	346.7
283	7.46×10^3	339.7	339.7
298	1.69×10^4	330.2	330.2
313	3.19×10^4	321.9	321.9
323	4.53×10^4	316.9	316.9

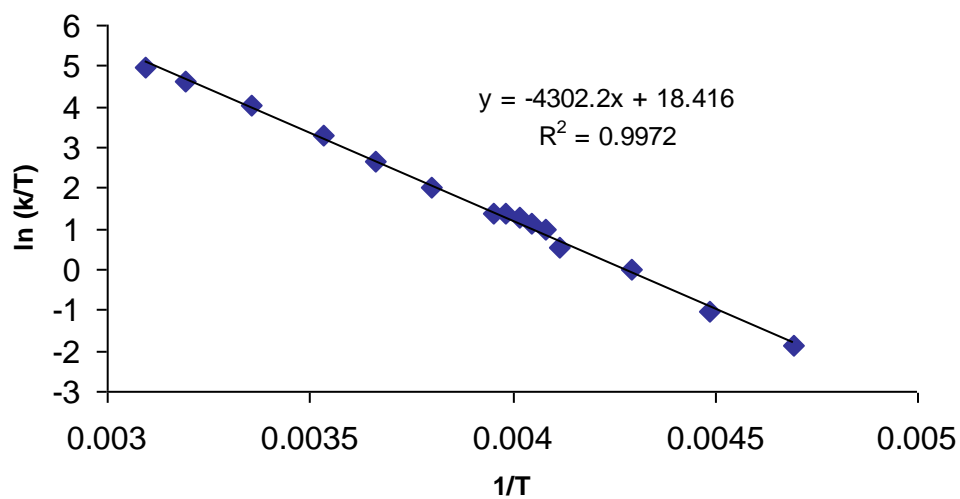
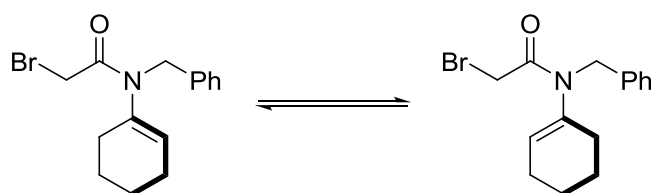
Figure A2. Eyring Plot for X in CDCl₃

Table A3. Rotational Data for 338 in methanol-*d*₄

temp. (K)	<i>k</i> (s ⁻¹)	calc. $\nu_a - \nu_b$ (Hz)	obs. $\nu_a - \nu_b$ (Hz)
213	56.2	390.3	390.0
223	140	379.2	379.2
233	298	369.3	369.3
235	336	367.5	367.5
237	484	365.7	365.7
239	513	363.9	363.9
241	605	362.2	362.2
243	686	360.5	360.5
245	806	358.8	358.8
247	915	357.2	357.2
249	1.08×10^3	355.6	355.6
251	1.23×10^3	354.1	354.1
253	1.38×10^3	352.5	352.5
263	2.68×10^3	345.4	345.4
273	4.70×10^3	338.8	338.8
283	9.00×10^3	332.9	332.9
298	2.06×10^4	324.9	324.9

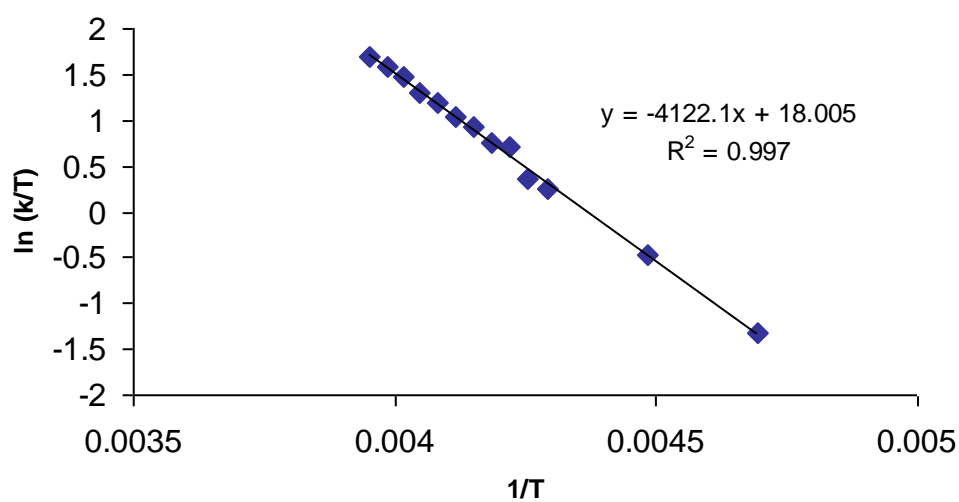
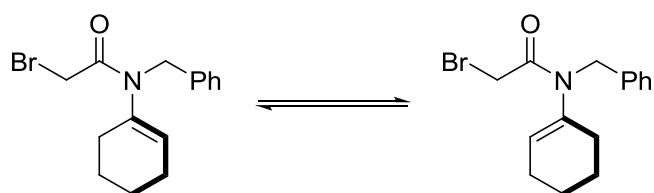
Figure A3. Eyring Plot for 338 in methanol-*d*₄

Table A4. Rotational Data for 338 in toluene- d_8 

temp. (K)	k (s^{-1})	calc. $\nu_a - \nu_b$ (Hz)	obs. $\nu_a - \nu_b$ (Hz)
193	18.6	744.7	744.6
203	46.5	712.1	712.1
213	124	683.8	683.8
223	360	659.0	659.0
233	752	637.1	637.1
243	1.65×10^3	617.7	617.7
253	3.26×10^3	600.3	600.3
263	6.83×10^3	584.7	584.7
273	1.31×10^4	570.6	570.6
283	2.36×10^4	557.8	557.8
293	4.20×10^4	546.1	546.1
298	4.55×10^4	540.7	540.7
303	5.70×10^4	535.5	535.5
313	8.31×10^4	525.7	525.7
323	1.21×10^5	516.6	516.6

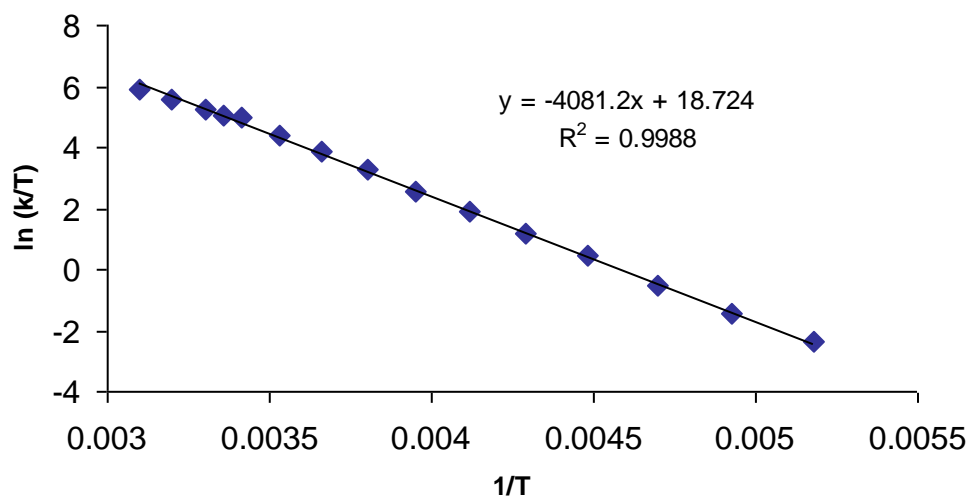
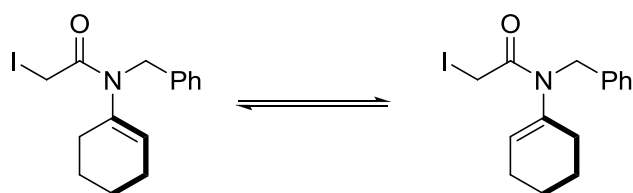
Figure A4. Eyring Plot for 338 in toluene- d_8 

Table A5. Rotational Data for 330 in CDCl₃

Temp. (K)	k (s ⁻¹)	calc. $\nu_a - \nu_b$ (Hz)	obs. $\nu_a - \nu_b$ (Hz)
215	20.5	246.5	246.5
220	32.2	242.6	242.6
228	68.2	236.8	236.8
234	131	232.9	232.9
237	166	231.0	231.0
240	211	229.2	229.2
249	418	224.0	224.0
252	508	222.4	222.4
254	632	221.4	221.4
258	826	219.3	219.3
265	1.35×10^3	216.0	216.0
275	2.92×10^3	211.6	211.6
297	1.14×10^4	203.2	203.2

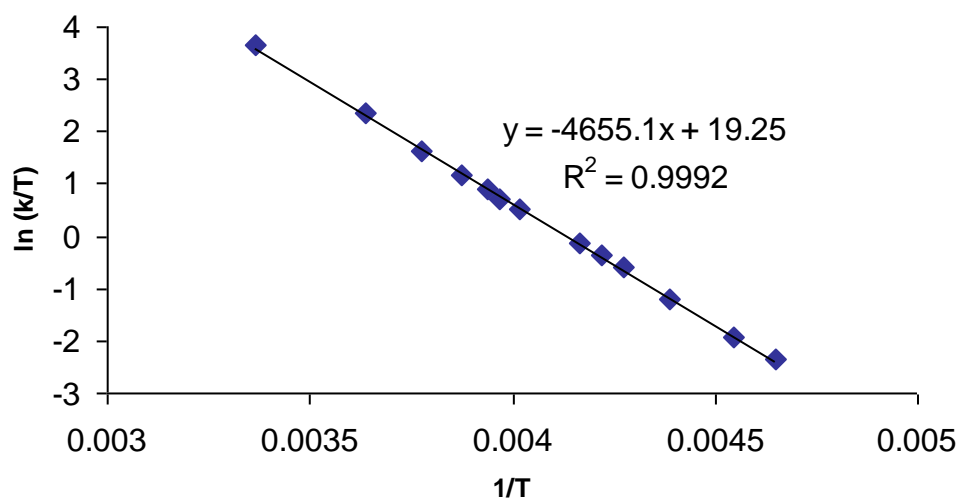
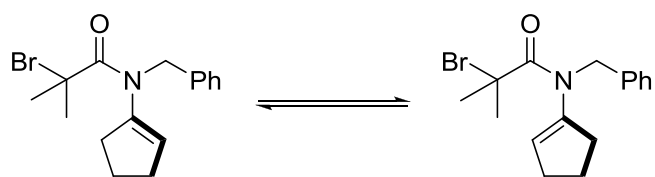
Figure A5. Eyring Plot for 330 in CDCl₃

Table A6. Rotational Data for 331 in toluene- d_8 

temp. (K)	k (s^{-1})	Calc. $\nu_a - \nu_b$ (Hz)	obs. $\nu_a - \nu_b$ (Hz)
186	57.7	546.3	546.5
191	102	533.3	533.5
202	303	507.9	507.9
222	2.40×10^3	470.6	470.6
233	6.90×10^3	453.8	453.8
245	1.42×10^4	437.7	437.7
256	2.90×10^4	424.8	424.8
266	5.75×10^4	414.3	414.3
279	1.05×10^5	402.0	402.0
290	1.97×10^5	392.8	392.8

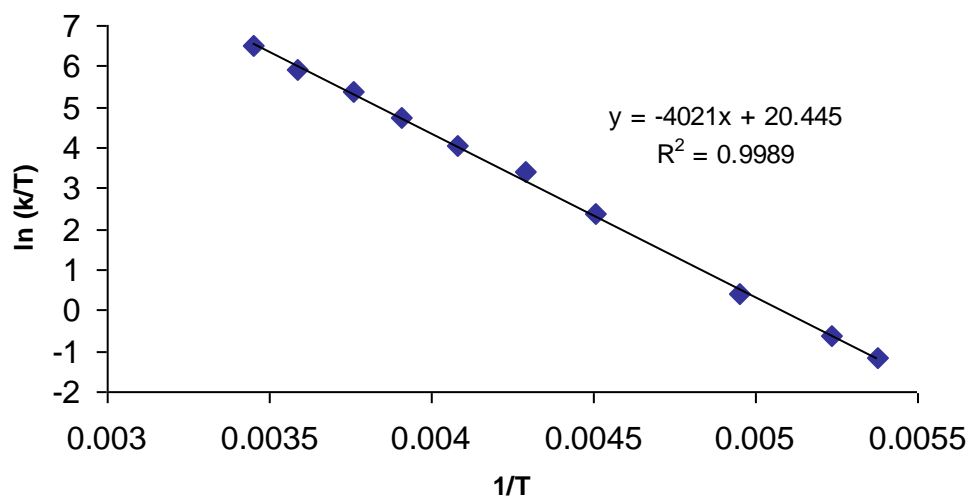
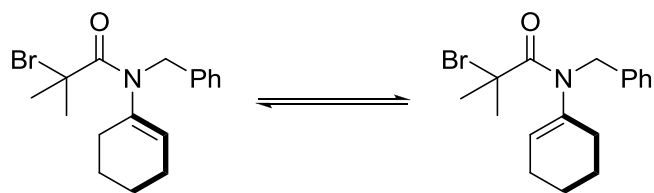
Figure A6. Eyring Plot for 331 toluene- d_8 

Table A7. Rotational Data for 273 in toluene-*d*₈

temp. (K)	k (s ⁻¹)	calc. $\nu_a - \nu_b$ (Hz)	obs. $\nu_a - \nu_b$ (Hz)
233	5.4	431.8	432.8
245	15.0	409.7	411.1
256	31.9	392.1	391.8
266	80.0	378.0	366.9
279	207	361.9	346.7
311	2.43×10^3	330.0	331.2
327	5.99×10^3	317.3	318.2
339	1.67×10^4	308.9	308.2

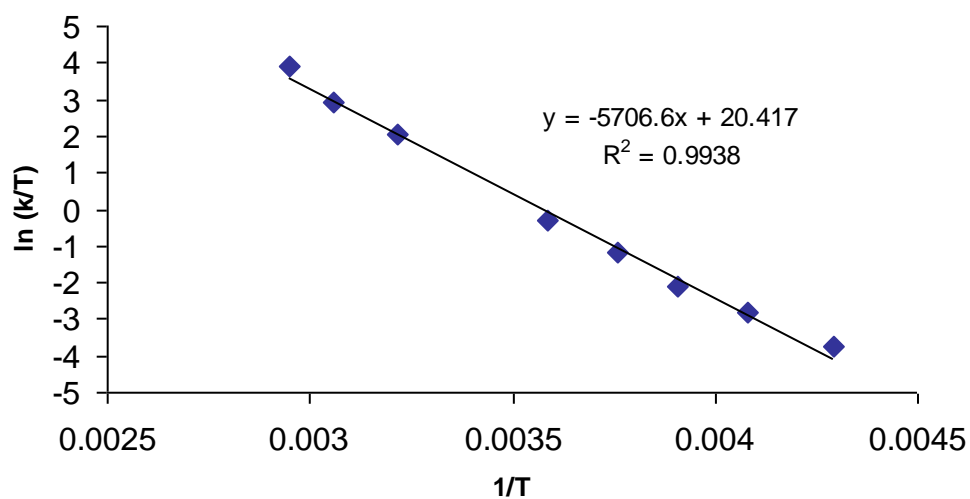
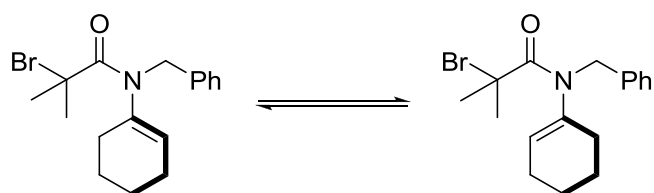
Figure A7. Eyring Plot for 273 toluene-*d*₈

Table A8. Rotational Data for 273 in CDCl₃

temp. (K)	k (s ⁻¹)	calc. $\nu_a - \nu_b$ (Hz)	obs. $\nu_a - \nu_b$ (Hz)
273	26.7	418.5	417.9
283	51.6	415.0	415.0
298	210	410.3	410.1
303	335	408.8	408.5
305	438	408.2	408.0
307	611	407.6	407.6
309	690	407.1	406.8
311	790	406.5	405.9
313	863	406.0	405.7
315	1.12×10^3	405.4	405.4
317	1.34×10^3	404.9	404.4
319	1.60×10^3	404.4	404.0
321	1.83×10^3	403.9	403.9
323	2.12×10^3	403.4	403.2

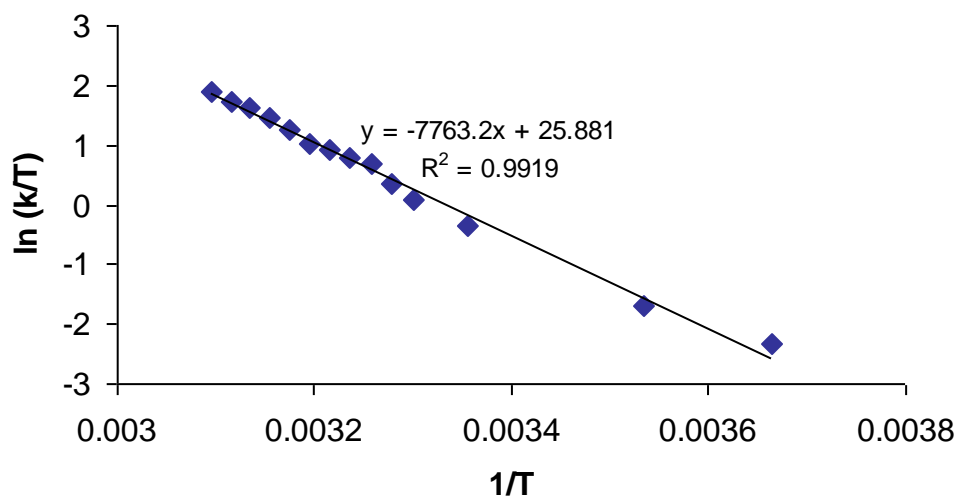
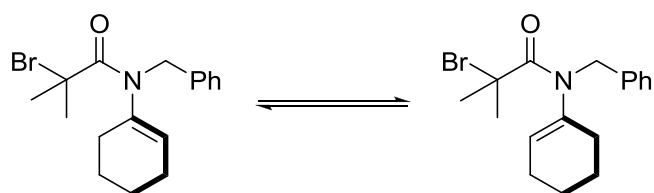
Figure A8. Eyring Plot for 273 CDCl₃

Table A9. Rotational Data for 273 in methanol- d_4 

temp. (K)	k (s^{-1})	calc. $\nu_a - \nu_b$ (Hz)	obs. $\nu_a - \nu_b$ (Hz)
253	8.7	445.0	444.6
263	14.9	440.1	440.5
273	37.0	435.5	435.5
283	84.0	431.3	431.1
298	257	425.6	425.6
303	437	423.9	423.7
305	539	423.2	423.1
307	606	422.5	422.5
309	699	421.9	421.8
311	777	421.2	421.1
313	908	420.6	420.2
315	1.16×10^3	419.9	419.8
317	1.37×10^3	419.3	419.0
319	1.51×10^3	418.7	418.5
321	1.83×10^3	418.1	418.0
323	2.14×10^3	417.5	417.3
333	3.98×10^3	414.6	414.0

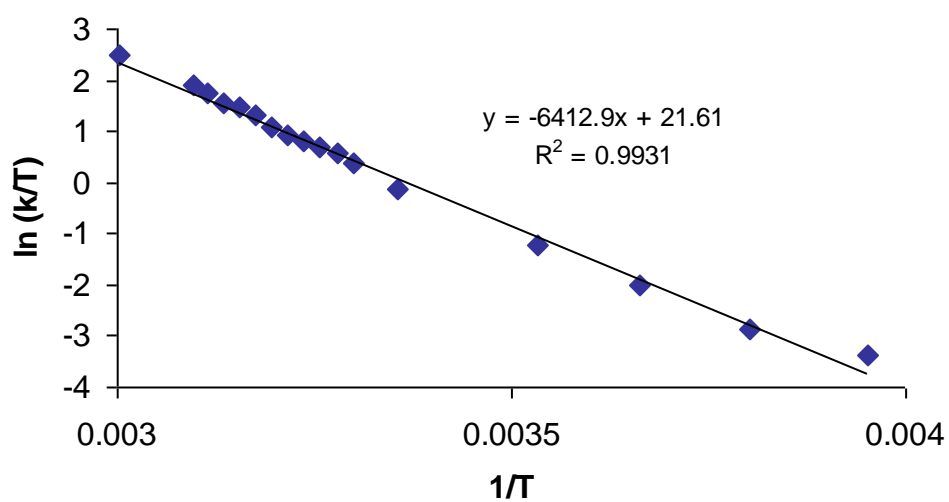
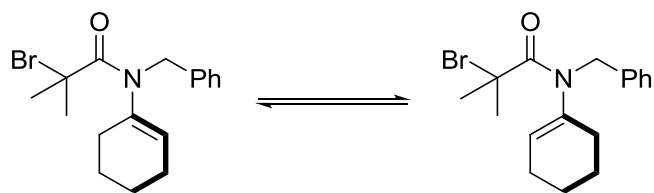
Figure A9. Eyring Plot for 273 methanol- d_4 

Table A10. Rotational Data for 273 in CD₃CN

temp. (K)	k (s ⁻¹)	calc. $\nu_a - \nu_b$ (Hz)	obs. $\nu_a - \nu_b$ (Hz)
263	9.2	347.8	347.3
273	30.2	338.4	337.9
283	68.2	329.9	330.0
298	381	318.5	318.2
300	473	317.1	317.3
302	539	315.8	315.5
304	601	314.4	314.4
306	856	313.1	312.6
308	991	311.8	311.1
310	1.12×10^3	310.5	310.0
312	1.38×10^3	309.2	309.1
318	2.10×10^3	305.6	305.3
323	3.36×10^3	302.7	302.7
333	6.33×10^3	297.2	297.2

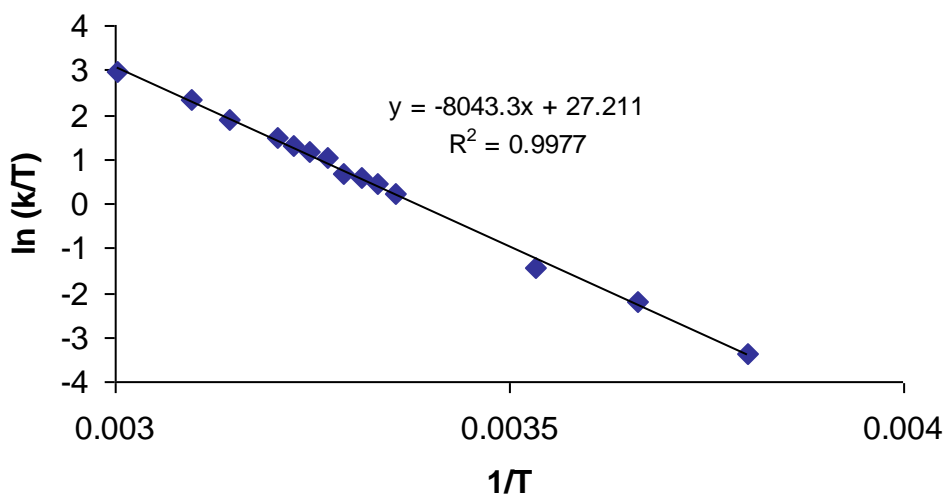
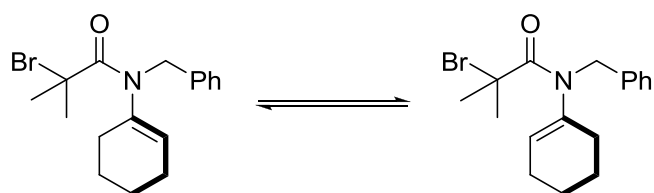
Figure 10. Eyring Plot for 273 CD₃CN

Table A11. Rotational Data for 273 in THF-*d*₈

temp. (K)	k (s ⁻¹)	Calc. $\nu_a - \nu_b$ (Hz)	obs. $\nu_a - \nu_b$ (Hz)
243	4.2	498.2	498.2
253	12.0	491.8	491.2
263	34.1	486.0	486.1
273	86.8	480.7	480.5
283	207	475.8	475.5
298	810	469.2	469.0
300	1.21×10^3	468.3	468.2
302	1.48×10^3	467.5	465.1
304	1.67×10^3	466.7	466.0
306	2.01×10^3	465.9	465.7
308	2.40×10^3	465.2	465.1
313	3.49×10^3	463.3	463.3
323	7.16×10^3	459.6	459.6
333	1.47×10^4	456.3	456.3

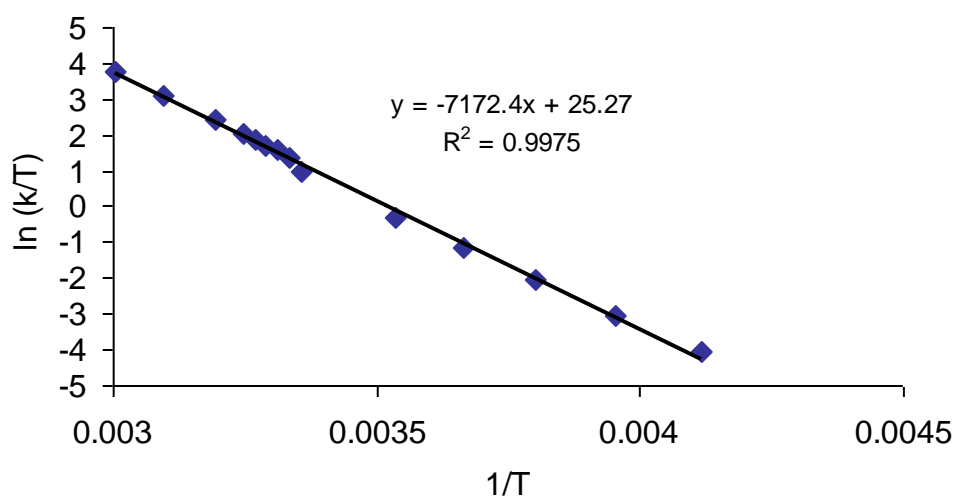
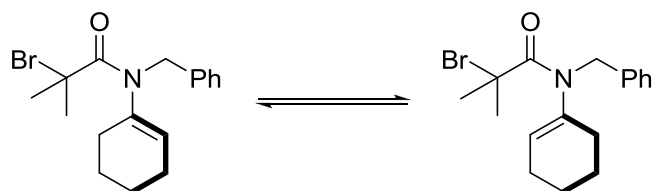
Figure A11. Eyring Plot for 273 THF-*d*₈

Table A12. Rotational Data for 273 in CD₃NO₂

temp. (K)	k (s ⁻¹)	Calc. $\nu_a - \nu_b$ (Hz)	obs. $\nu_a - \nu_b$ (Hz)
248	3.2	337.1	336.9
253	5.7	332.3	332.6
263	15.2	323.5	323.4
273	37.2	315.5	315.6
278	52.1	311.8	311.4
280	54.7	310.4	310.7
282	62.9	309.0	309.0
283	73.7	308.3	308.1
284	76.5	307.6	307.7
286	84.1	306.2	306.0
288	93.4	304.9	304.9
290	107	303.6	303.8
292	139	302.3	302.1
294	179	301.1	301.1
298	233	298.6	298.9
303	391	295.7	297.6
313	591	290.2	290.2
323	1.76×10^3	285.1	285.1
333	3.38×10^3	280.4	280.3

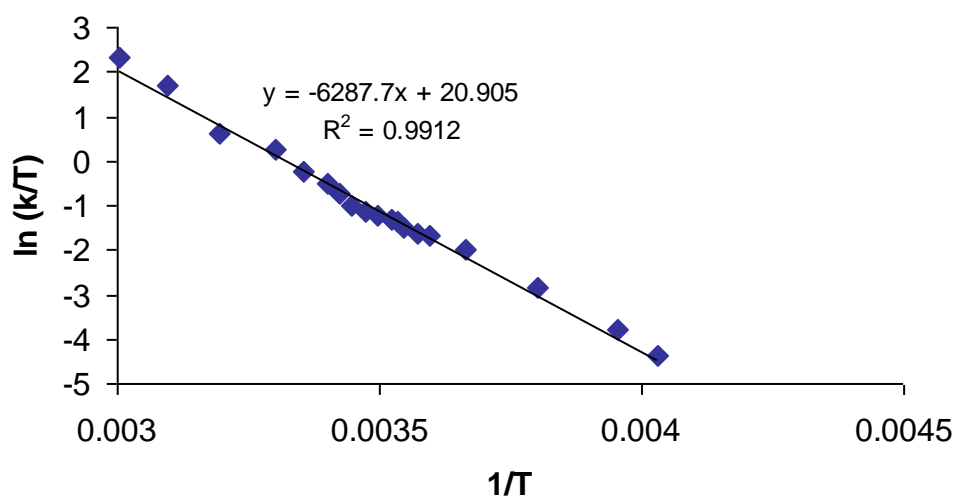
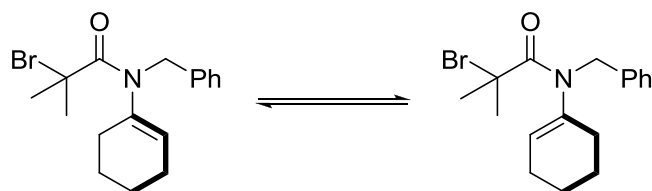
Figure A12. Eyring Plot for 273 CD₃NO₂

Table A13. Rotational Data for 273 in DMF-*d*₇

temp. (K)	k (s ⁻¹)	Calc. $\nu_a - \nu_b$ (Hz)	obs. $\nu_a - \nu_b$ (Hz)
243	5.8	366.2	360.0
253	11.4	358.1	358.4
263	26.8	350.8	350.8
273	52.1	344.2	344.0
283	114	338.1	338.4
298	339	330.0	330.1
303	767	327.5	327.3
305	825	326.5	326.5
307	940	325.5	325.4
309	1.10×10^3	324.6	324.5
311	1.24×10^3	323.7	323.5
313	1.44×10^3	322.8	322.9
315	1.80×10^3	321.9	321.8
317	2.17×10^3	321.0	321.0
319	2.49×10^3	320.1	320.0
321	2.88×10^3	319.3	319.1
323	3.21×10^3	318.4	318.2
333	6.30×10^3	314.4	314.2
343	1.21×10^4	310.6	310.6
353	1.26×10^4	307.1	307.1

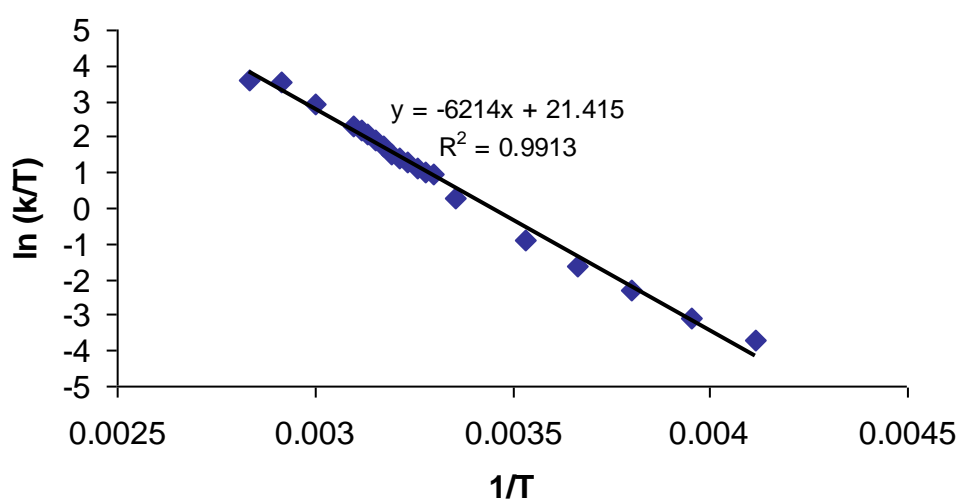
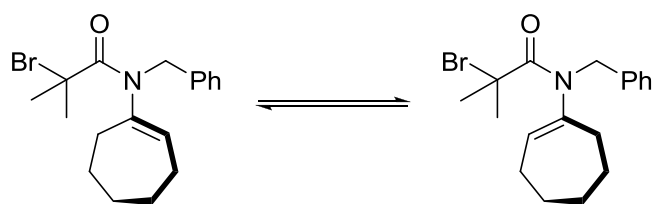
Figure A13. Eyring Plot for 273 DMF-*d*₇

Table A14. Rotational Data for 332 in Toluene-*d*₈

temp. (K)	k (s ⁻¹)	calc. $\nu_a - \nu_b$ (Hz)	obs. $\nu_a - \nu_b$ (Hz)
250	16.7	548.5	549.2
261	40.5	522.8	522.3
271	91.5	489.3	491.6
281	172	460.1	459.6
292	374	432.1	412.6
311	1.62×10^3	391.8	392.4
321	3.12×10^3	373.8	374.4
331	5.76×10^3	357.7	356.4
341	1.19×10^4	343.1	344.4
350	2.11×10^4	331.2	331.6

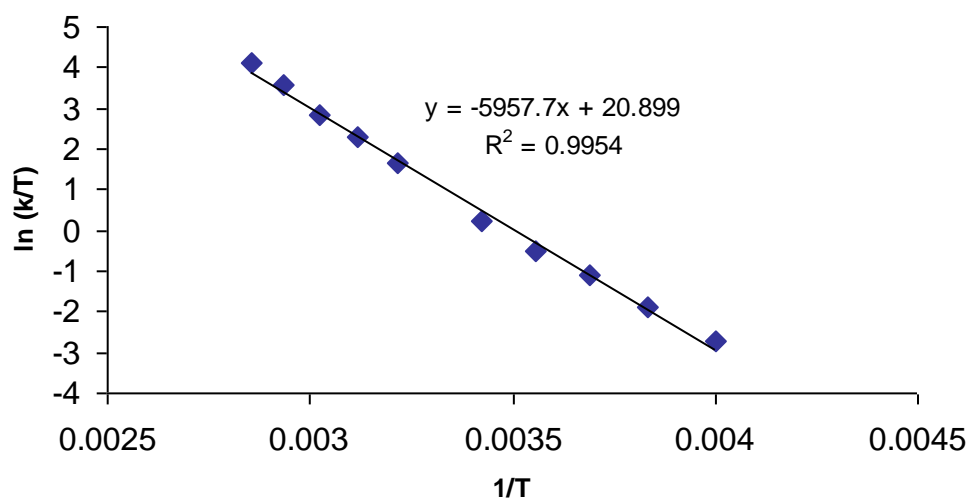
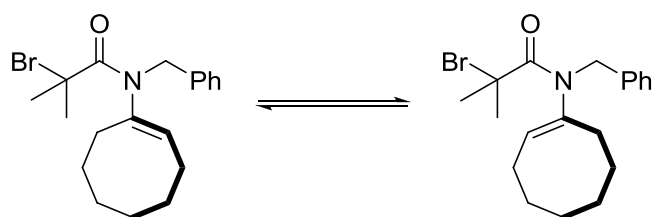
Figure A14. Eyring Plot for 332 in Toluene-*d*₈

Table A15. Rotational Data for 274 in Toluene- d_8 

temp. (K)	k (s^{-1})	calc. $\nu_a - \nu_b$ (Hz)	obs. $\nu_a - \nu_b$ (Hz)
230	11.0	506.6	508.5
240	22.5	483.5	484.1
250	60.0	463.2	461.6
261	161	443.6	440.6
271	365	427.7	426.1
292	1.73×10^3	399.5	399.6
301	3.43×10^3	389.1	388.6
311	7.33×10^3	378.6	379.6
321	1.41×10^4	369.0	369.6
331	2.63×10^4	360.1	359.9
341	4.62×10^4	352.0	350.9

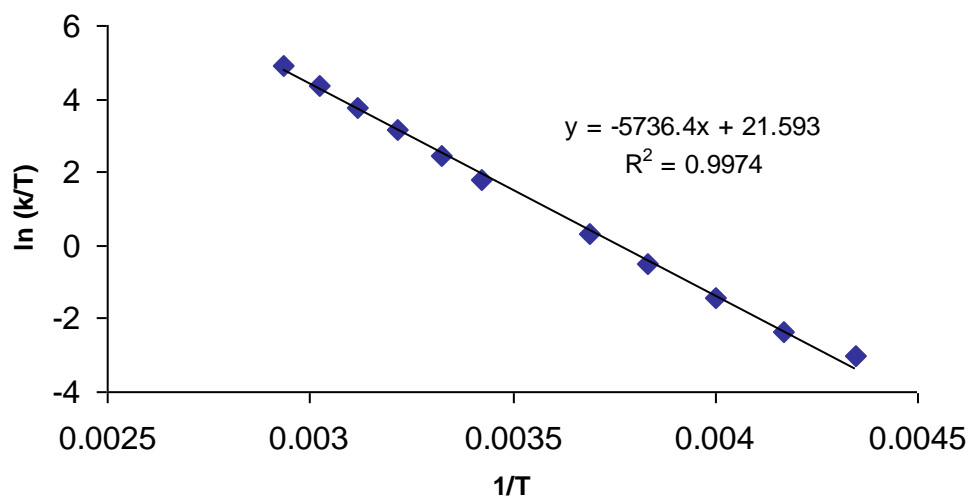
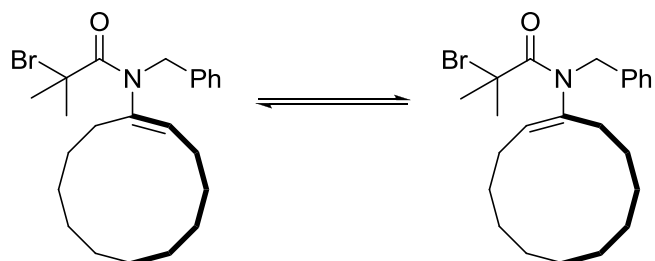
Figure A15. Eyring Plot for 274 in Toluene- d_8 

Table A16. Rotational Data for 275 in Toluene- d_8 

temp. (K)	k (s^{-1})	calc. $\nu_a - \nu_b$ (Hz)	obs. $\nu_a - \nu_b$ (Hz)
230	15.1	603.9	604.8
240	35.4	584.2	583.8
250	101	566.7	565.9
261	280	549.4	549.9
292	2.80×10^3	510.0	510.0
301	5.17×10^3	500.5	500.0
311	1.06×10^4	490.8	490.0
321	2.36×10^4	481.9	481.7
331	3.94×10^4	473.6	473.4
341	7.01×10^4	466.0	467.1

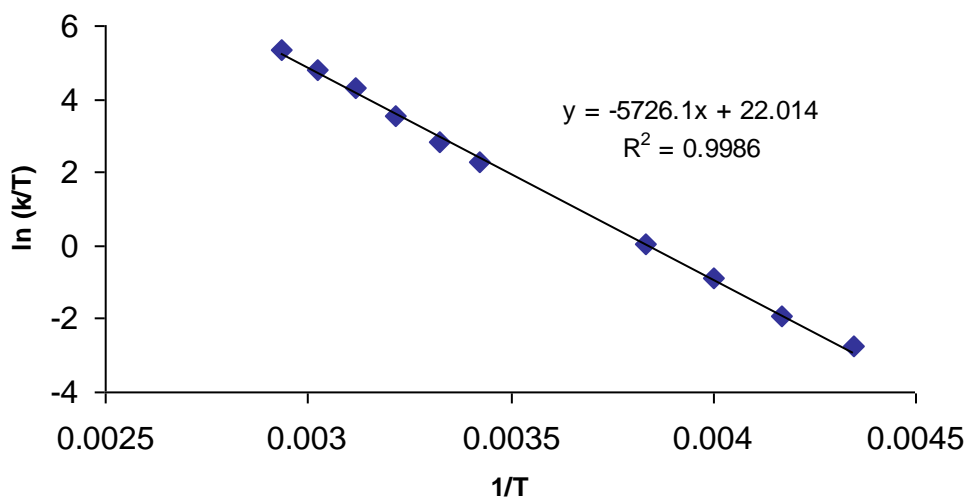
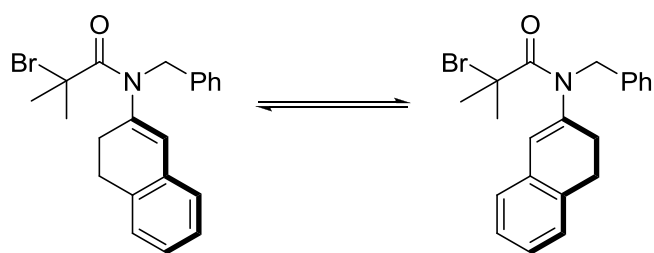
Figure A16. Eyring Plot for 275 in Toluene- d_8 

Table A17. Rotational Data for 305 in Toluene-*d*₈

temp. (K)	k (s ⁻¹)	calc. $\nu_a - \nu_b$ (Hz)	obs. $\nu_a - \nu_b$ (Hz)
220	8.0	110.9	111.2
230	17.8	105.8	105.8
240	42.8	101.3	101.4
250	106	97.4	97.4
271	432	90.4	90.4
281	836	87.6	87.6
292	1.80×10^3	84.9	84.9
301	3.03×10^3	82.8	82.7
311	5.58×10^3	80.7	80.6

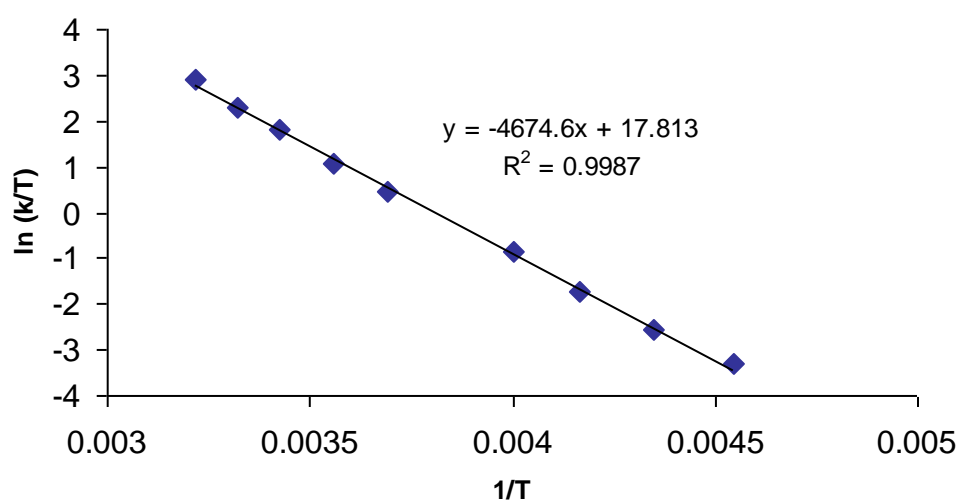
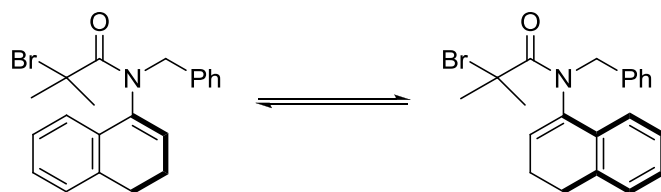
Figure A17. Eyring Plot for 305 in *d*₈-Toluene

Table A18. Rotational Data for 306 in Toluene-*d*₈

temp. (K)	k (s^{-1})	calc. $\nu_a - \nu_b$ (Hz)	obs. $\nu_a - \nu_b$ (Hz)
341	6.0	600.5	599.3
349	8.9	592.4	587.0
359	14.6	582.9	576.6
369	23.6	574.1	564.7
379	38.9	565.9	553.5

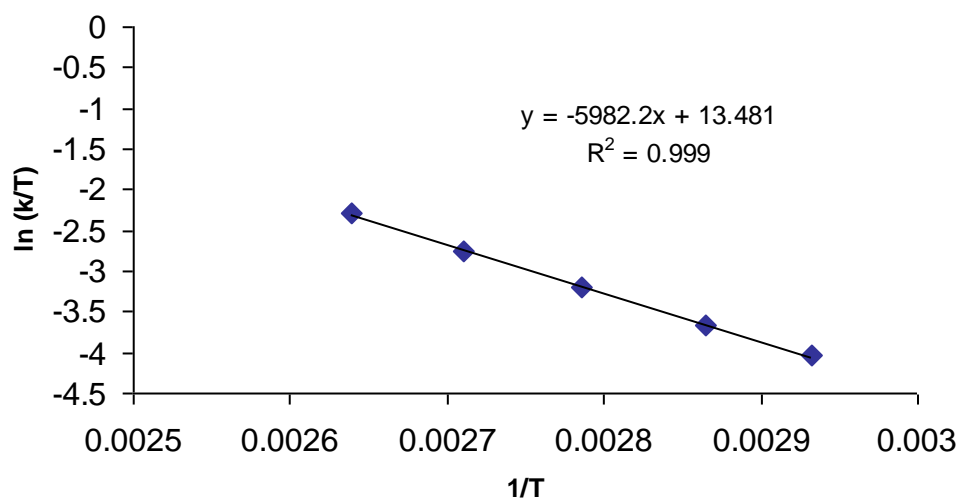
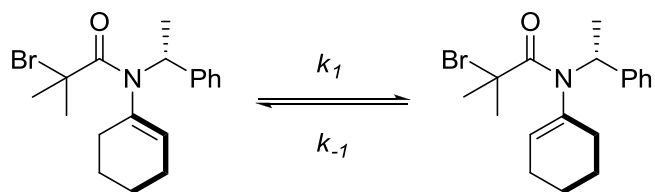
Figure A18. Eyring Plot for 306 in Toluene-*d*₈

Table A19. Rotational Data for 333 in Toluene- d_8 

temp. (K)	$k_1 + k_{-1}$ (s^{-1})	calc. $\nu_a - \nu_b$ (Hz)	obs. $\nu_a - \nu_b$ (Hz)
271	67.0	182.9	180.7
281	136	175.5	175.5
292	316	168.1	168.3
301	656	162.7	162.7
311	1.39×10^3	157.3	157.1
321	2.66×10^3	152.3	152.4
331	4.88×10^3	147.9	148.0
341	1.02×10^4	143.7	143.7
350	1.70×10^4	140.3	140.2

Upon cooling, two diastereomers were seen in a 2:1 ratio.

Therefore, $k_1 = (1/3)(k_1 + k_{-1})$, and $k_{-1} = (2/3)(k_1 + k_{-1})$ for each temperature.

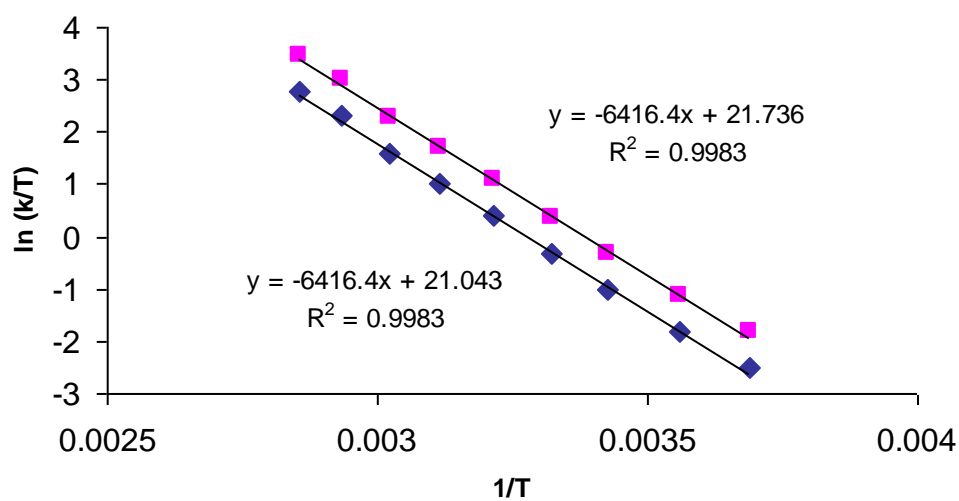
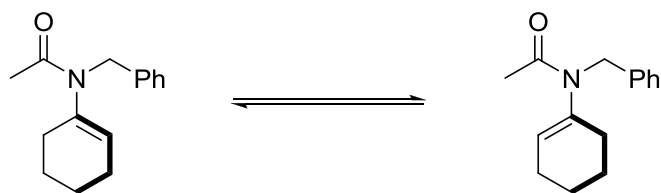
Figure A19. Eyring Plot for 333 in Toluene- d_8 

Table A20. Rotational Data for 334 in d_8 -Toluene

temp. (K)	k (s^{-1})	calc. $\nu_a - \nu_b$ (Hz)	obs. $\nu_a - \nu_b$ (Hz)
193	50.0	743.4	743.4
203	98.0	690.9	690.9
213	251	646.5	646.5
223	967	608.6	608.6
233	2.12×10^3	575.9	575.9
243	6.53×10^3	547.4	547.4
253	1.41×10^4	522.5	522.5
263	3.89×10^4	500.4	500.4
273	6.08×10^4	480.8	480.8
283	8.27×10^4	463.3	463.3

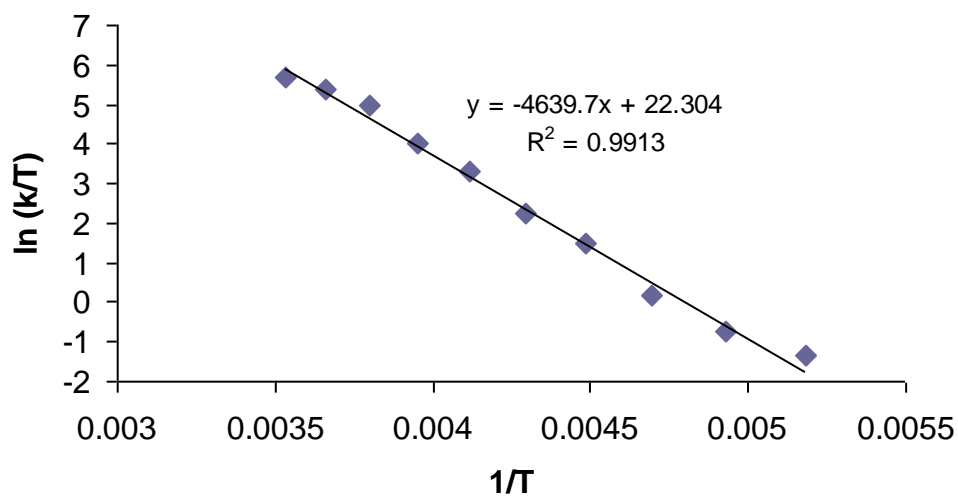
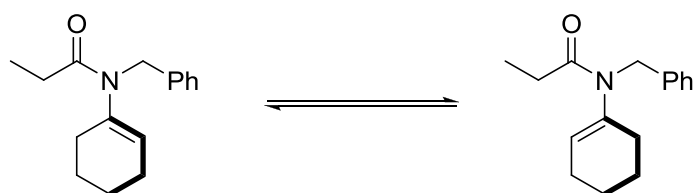
Figure A20. Eyring Plot for 334 in d_8 -Toluene

Table A21. Rotational Data for 335 in toluene-*d*₈

temp. (K)	k (s ⁻¹)	calc. $\nu_a - \nu_b$ (Hz)	obs. $\nu_a - \nu_b$ (Hz)
183	62.4	702.8	702.7
193	118	670.3	670.2
203	306	642.3	642.3
213	612	617.9	617.6
223	1.18×10^3	596.5	596.1
233	2.56×10^3	577.6	577.5
243	5.08×10^3	560.8	560.8
253	1.07×10^4	545.8	545.8
263	2.06×10^4	532.2	532.2
273	3.60×10^4	520.0	520.0
283	5.48×10^4	508.8	508.8
298	6.70×10^4	493.9	493.9
303	7.80×10^4	489.3	489.3
313	1.00×10^5	480.8	480.8
323	1.71×10^5	472.9	472.9

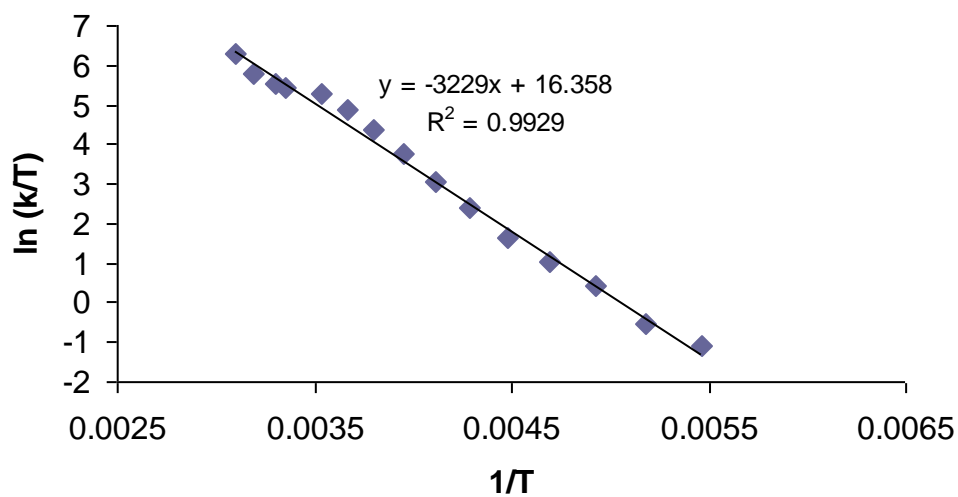
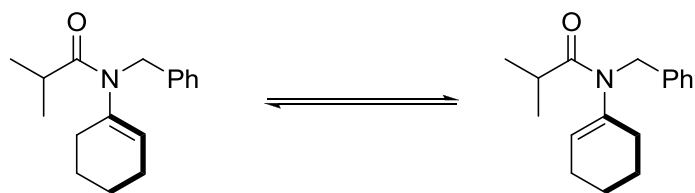
Figure A21. Eyring Plot for 335 in toluene-*d*₈

Table A22. Rotational Data for 336 in Toluene- d_8 

temp. (K)	k (s^{-1})	calc. $\nu_a - \nu_b$ (Hz)	obs. $\nu_a - \nu_b$ (Hz)
203	9.7	594.1	593.3
213	27.8	569.4	567.8
223	81.9	547.9	546.0
233	188	529.0	527.2
243	454	512.1	511.3
253	874	497.1	496.1
263	1.57×10^3	483.6	483.2
273	3.50×10^3	471.5	471.3
283	7.41×10^3	460.4	460.3
298	1.73×10^4	445.7	445.6
303	2.06×10^4	441.2	441.2
313	3.48×10^4	432.8	432.8
323	6.10×10^4	425.0	425.0
333	1.28×10^5	417.8	417.8
343	2.04×10^5	411.2	411.2
353	3.90×10^5	405.0	405.0

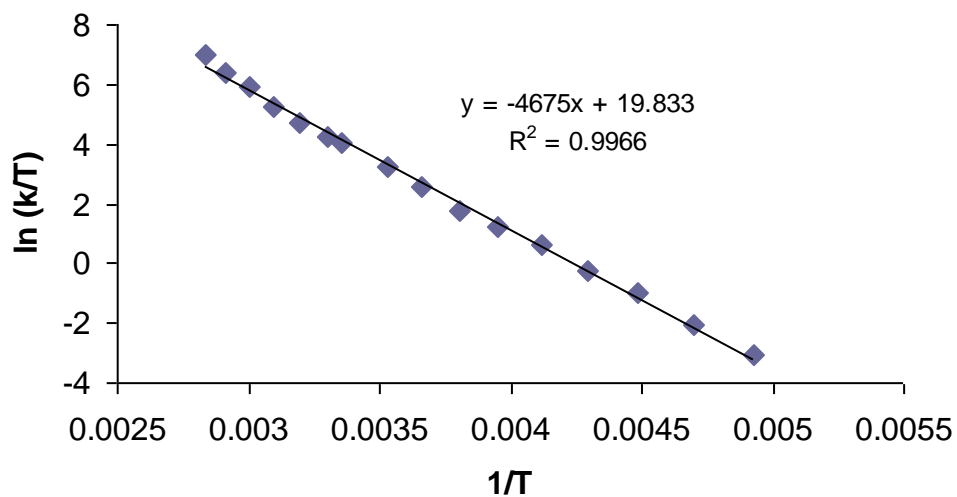
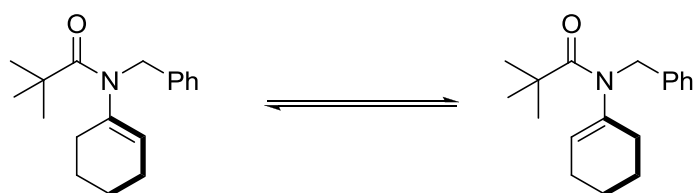
Figure A22. Eyring Plot for 336 in Toluene- d_8 

Table A23. Rotational Data for 337 in Toluene-*d*₈

temp. (K)	k (s ⁻¹)	calc. $\nu_a - \nu_b$ (Hz)	obs. $\nu_a - \nu_b$ (Hz)
223	7.1	785.3	785.3
233	15.4	760.4	760.4
243	35.7	738.3	738.3
253	102	718.6	718.6
263	260	700.8	700.8
273	602	684.7	684.7
283	1.77×10^3	670.0	670.0
298	6.41×10^3	650.4	650.4
303	7.93×10^3	644.4	644.4
313	1.80×10^4	633.2	633.2
323	3.74×10^4	622.8	622.8
333	7.19×10^4	613.2	613.2
343	1.34×10^5	604.3	604.3
353	2.95×10^5	596.1	596.1

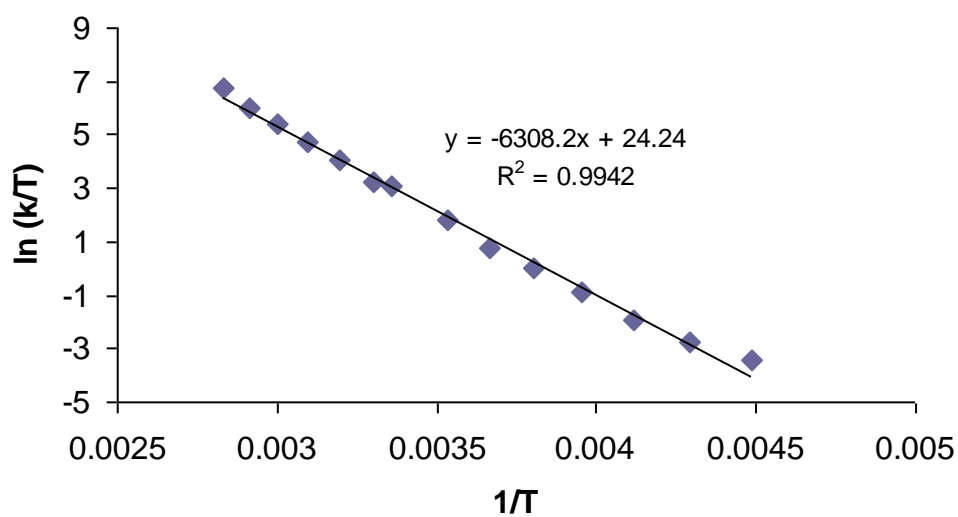
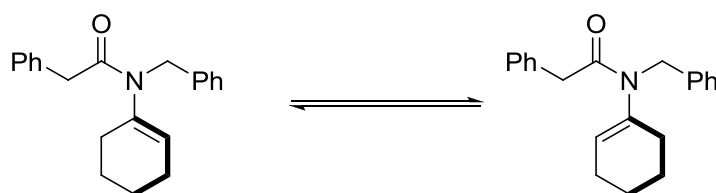
Figure A23. Eyring Plot for 337 in Toluene-*d*₈

Table A24. Rotational Data for 344 in Toluene-*d*₈

temp. (K)	<i>k</i> (s ⁻¹)	calc. $\nu_a - \nu_b$ (Hz)	obs. $\nu_a - \nu_b$ (Hz)
183	7.7	706.3	705.0
193	12.5	672.7	673.8
203	29.1	643.8	645.8
213	63.4	618.1	617.1
223	139	596.7	596.0
233	325	577.3	576.6
243	734	560.0	559.9
253	1.49 × 10 ³	544.6	544.1
263	3.16 × 10 ³	530.7	530.5
273	6.02 × 10 ³	518.1	518.0
283	1.10 × 10 ⁴	506.7	506.7
298	2.57 × 10 ⁴	491.4	491.1
303	3.09 × 10 ⁴	486.8	486.6
313	4.50 × 10 ⁴	478.0	478.0
323	7.00 × 10 ⁴	470.0	470.0
333	1.45 × 10 ⁵	462.5	462.4
343	1.87 × 10 ⁵	455.6	455.5

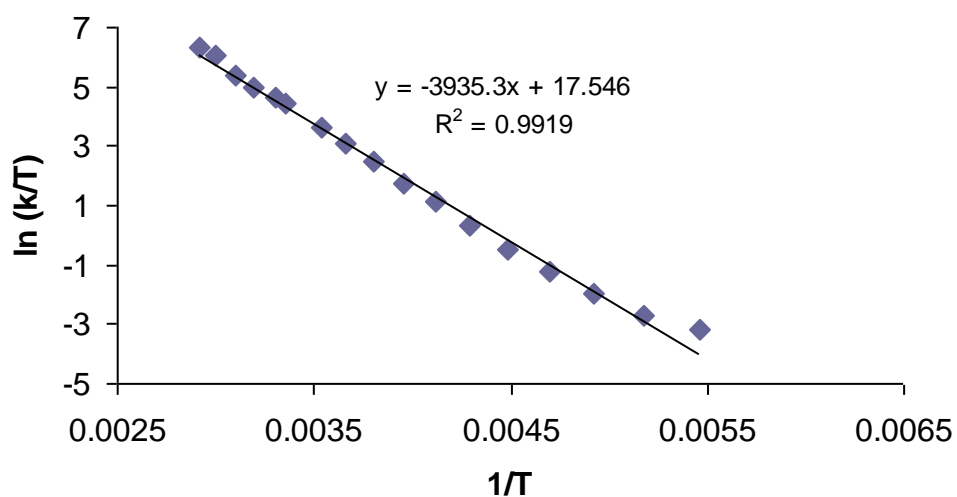
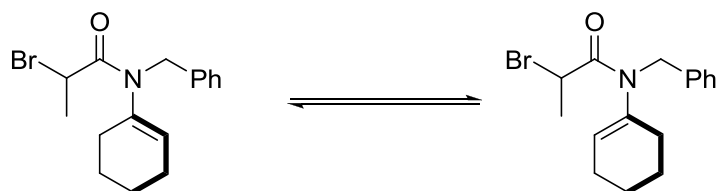
Figure A24. Eyring Plot for 344 in Toluene-*d*₈

Table A25. Rotational Data for 339 in Toluene-*d*₈

temp. (K)	$k_1 + k_{-1}$ (s^{-1})	calc. $\nu_a - \nu_b$ (Hz)	obs. $\nu_a - \nu_b$ (Hz)
213	69.1	620.6	620.7
223	134	597.3	594.6
233	312	576.8	575.1
243	668	558.7	557.2
253	1.34×10^3	542.4	540.9
263	2.70×10^3	527.8	527.2
273	4.74×10^3	514.7	513.8
283	8.16×10^3	502.7	501.9
298	2.00×10^4	486.8	485.2
303	2.96×10^4	481.9	481.3
313	4.37×10^4	472.8	472.1
323	6.20×10^4	464.4	464.0
333	8.60×10^4	456.6	456.1
343	1.07×10^5	449.4	448.9
353	1.57×10^5	442.8	442.5
363	1.93×10^5	436.5	436.0

Upon cooling, two diastereomers were seen in a 1:1 ratio.

Therefore, $k_1 = (1/2)(k_1 + k_{-1})$, and $k_{-1} = (1/2)(k_1 + k_{-1})$ for each temperature.

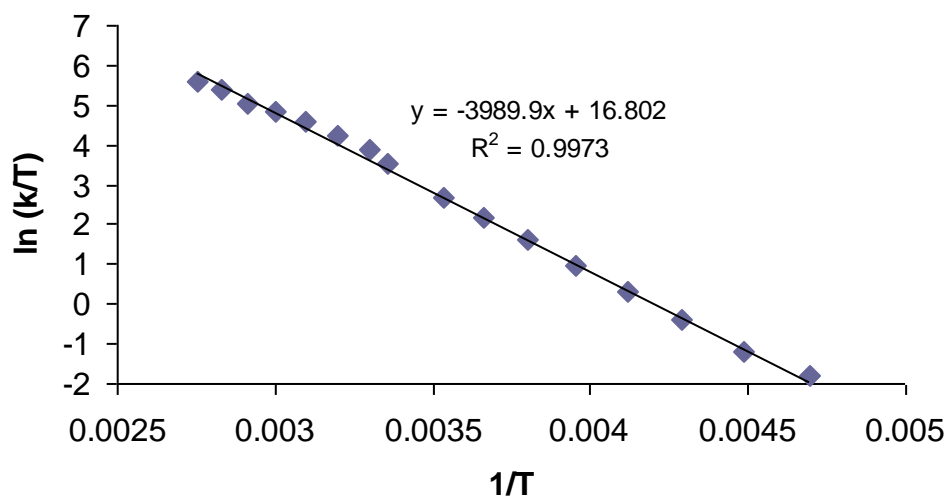
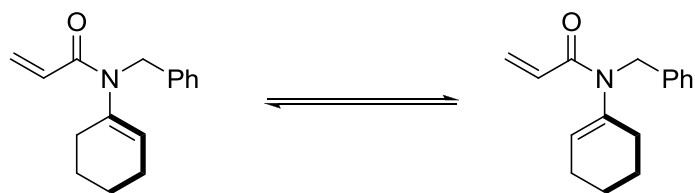
Figure A25. Eyring Plot for 339 in Toluene-*d*₈

Table A26. Rotational Data for 343 in Toluene-*d*₈

temp. (K)	<i>k</i> (s ⁻¹)	calc. $\nu_a - \nu_b$ (Hz)	obs. $\nu_a - \nu_b$ (Hz)
183	22.8	590.7	590.2
193	52.9	559.2	560.3
203	117	532.1	531.6
213	220	508.8	508.1
223	630	488.4	487.7
233	1.69×10^3	470.5	470.0
243	3.71×10^3	454.7	454.1
253	7.69×10^3	440.5	439.9
263	1.50×10^4	427.9	427.4
273	2.59×10^4	416.5	416.2
283	3.69×10^4	406.1	405.5
298	6.24×10^4	392.4	392.1
303	9.10×10^4	388.2	388.0
313	1.48×10^5	380.3	380.0

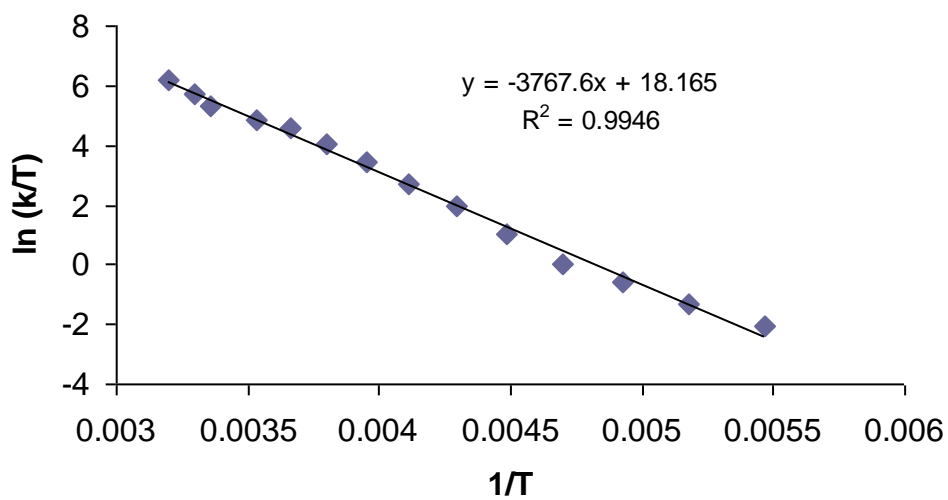
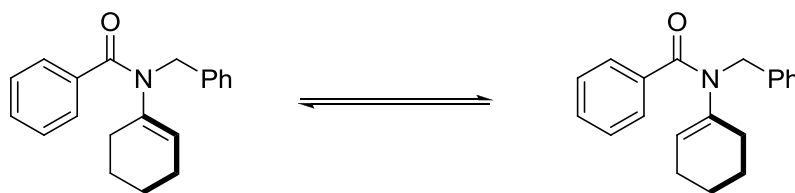
Figure A26. Eyring Plot for 343 in Toluene-*d*₈

Table A27. Rotational Data for 342 in Toluene-*d*₈

temp. (K)	k (s ⁻¹)	calc. $\nu_a - \nu_b$ (Hz)	obs. $\nu_a - \nu_b$ (Hz)
183	478	318.3	318.3
193	1.32×10^3	309.8	309.8
203	2.74×10^3	301.4	301.4
213	5.46×10^3	295.6	295.6
223	1.15×10^4	289.9	289.9
233	2.35×10^4	285.2	285.2

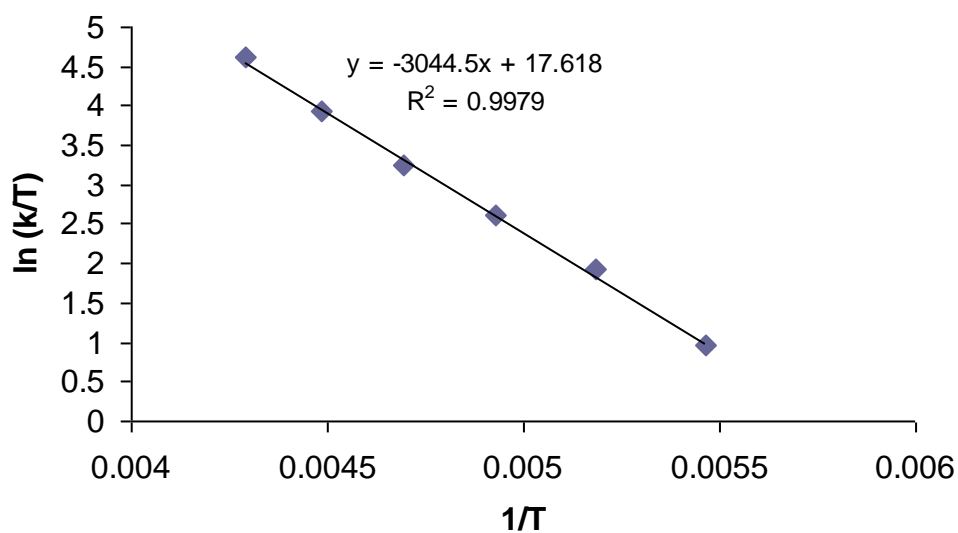
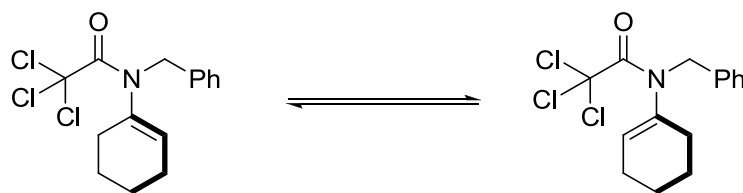
Figure A27. Eyring Plot for 342 in Toluene-*d*₈

Table A28. Rotational Data for 341 in Toluene- d_8 

temp. (K)	k (s^{-1})	calc. $\nu_a - \nu_b$ (Hz)	obs. $\nu_a - \nu_b$ (Hz)
253	4.0	681.3	681.3
263	8.8	668.7	668.7
273	28.9	657.3	657.3
283	51.6	646.9	646.9
298	161	632.8	632.8
303	260	628.5	628.5
313	494	620.4	620.4
323	1.91×10^3	612.8	612.8
333	4.75×10^3	605.8	605.8
343	9.14×10^3	599.3	599.3
353	1.88×10^4	593.2	593.2
363	3.03×10^4	587.5	587.5
373	5.38×10^4	582.2	582.2

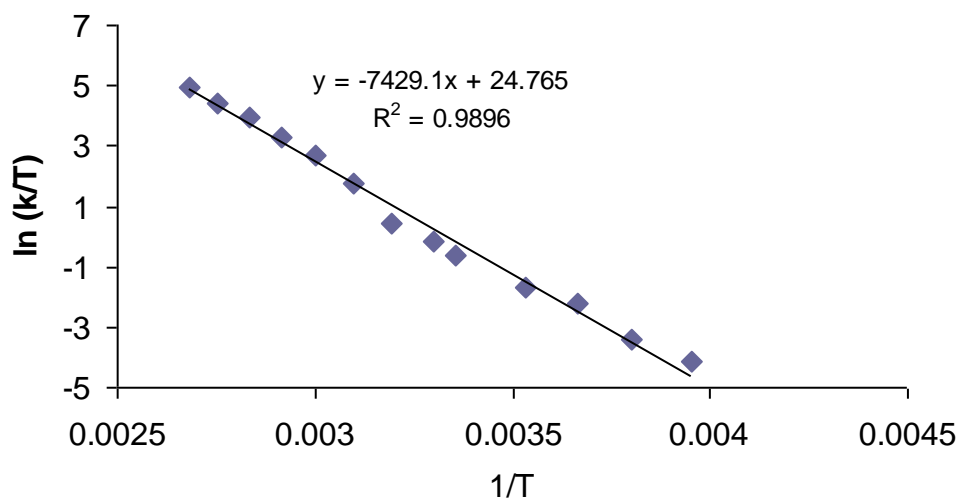
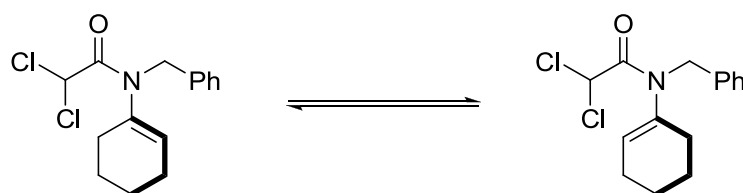
Figure A28. Eyring Plot for 341 in Toluene- d_8 

Table A29. Rotational Data for 340 in Toluene-*d*₈

temp. (K)	k (s ⁻¹)	calc. $\nu_a - \nu_b$ (Hz)	obs. $\nu_a - \nu_b$ (Hz)
213	8.9	620.4	620.4
223	21.6	602.0	602.0
233	45.9	585.6	585.6
243	100	571.0	571.0
253	206	557.9	557.9
263	417	546.0	546.0
273	748	535.2	535.2
283	2.31×10^3	525.2	525.2
298	7.38×10^3	512.2	512.2
303	9.99×10^3	508.1	508.1
313	1.77×10^4	500.5	500.5
323	2.83×10^4	493.5	493.5
333	4.61×10^4	487.0	487.0
343	7.45×10^4	480.9	480.9
353	1.28×10^5	475.2	475.2
363	1.99×10^5	470.0	470.0

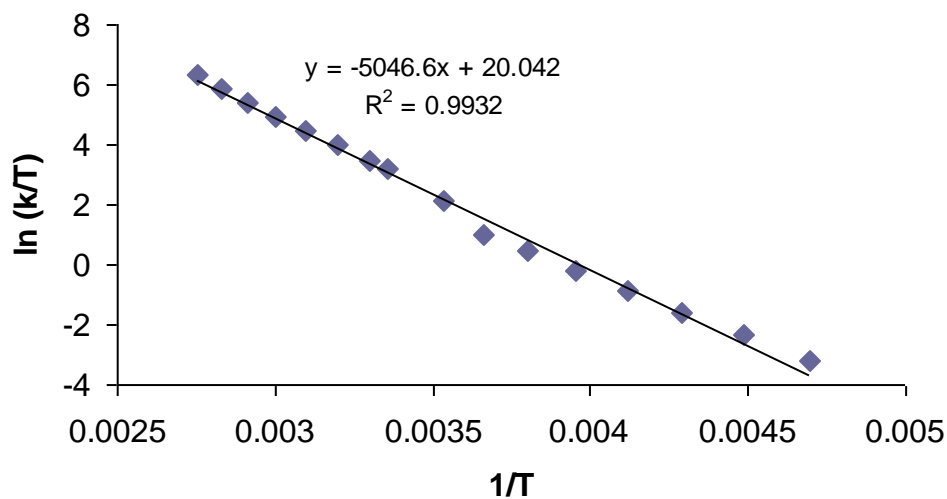
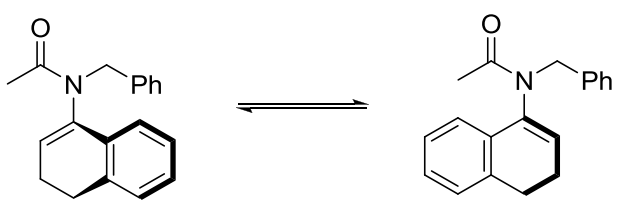
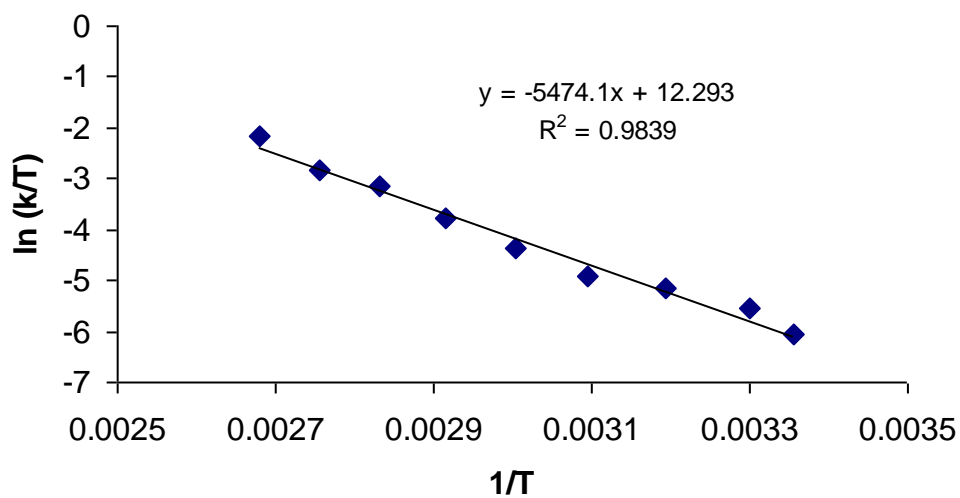
Figure A29. Eyring Plot for 340 in Toluene-*d*₈

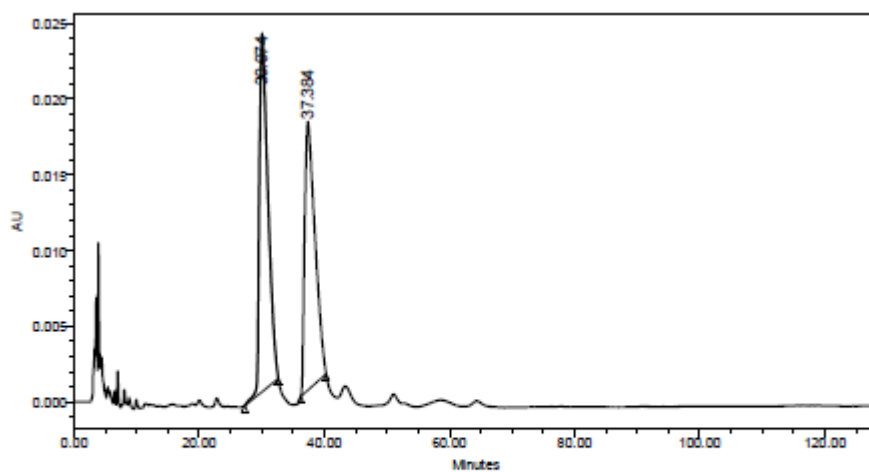
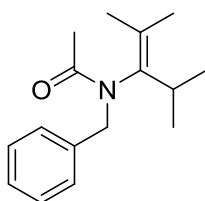
Table A30. Rotational Data for 363 in Toluene-*d*₈


temp. (K)	<i>k</i> (s ⁻¹)	calc. $\nu_a - \nu_b$ (Hz)	obs. $\nu_a - \nu_b$ (Hz)
298	0.7	985.9	979.6
303	1.2	970.7	968.6
313	1.8	942.5	943.6
323	2.4	916.8	921.0
333	4.3	893.3	898.4
343	7.9	871.7	875.9
353	15.0	851.9	852.7
363	21.8	833.5	831.9
373	42.8	816.5	810.5

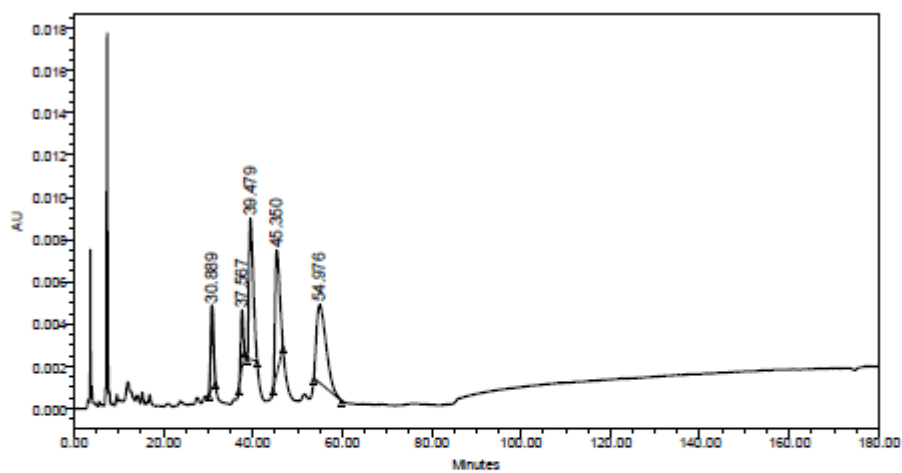
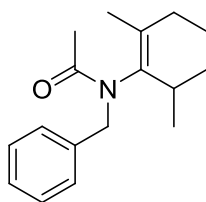
Figure A30. Eyring Plot for 363 in Toluene-*d*₈

Appendix B

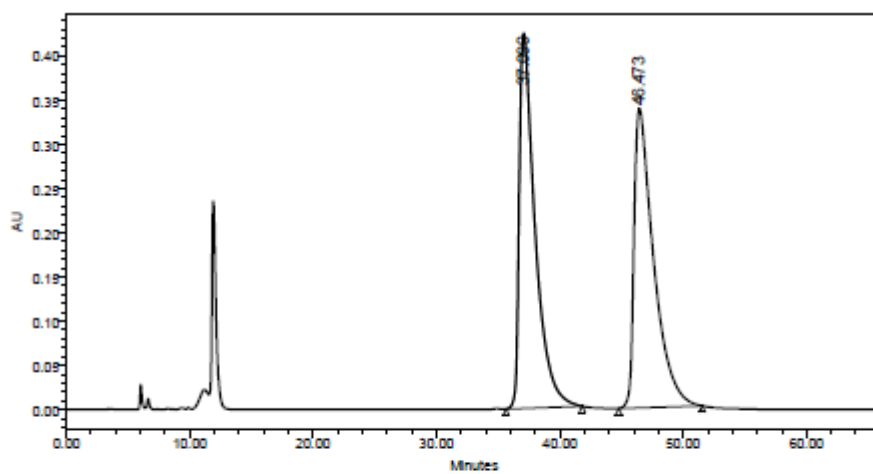
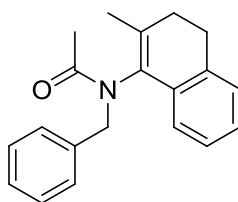
CHIRAL HPLC REPORTS

360 *N*-Benzyl-*N*-(2,4-dimethylpent-2-en-3-yl)-acetamide

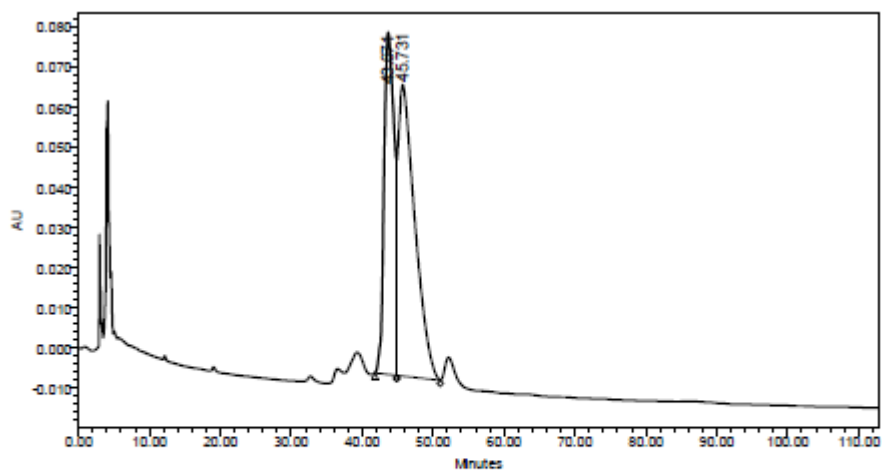
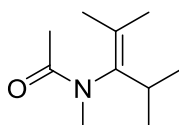
	RT	Area	% Area	Height
1	30.074	2241682	52.59	23676
2	37.384	2020514	47.41	17741

362 *N*-Benzyl-*N*-(2,6-dimethylcyclohexen-1-yl)-acetamide

	RT	Area	% Area	Height
1	30.889	166281	9.95	3953
2	37.567	108667	6.50	2755
3	39.479	439918	26.33	6651
4	45.350	409018	24.48	5837
5	54.976	546651	32.72	3688

364 *N*-Benzyl-*N*-(2-methyl-3,4-dihydronaphthalen-1-yl)-acetamide

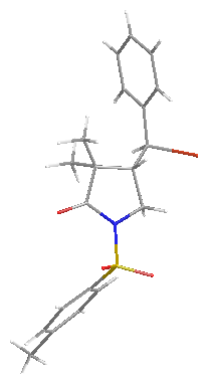
	RT	Area	% Area	Height
1	37.090	37706252	50.23	423991
2	46.473	37354863	49.77	338254

361 *N*-Methyl-*N*-(2,4-dimethylpent-2-en-3-yl)-acetamide

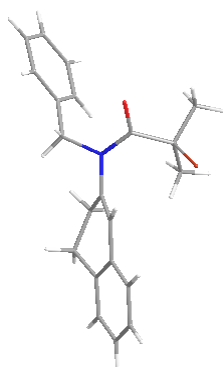
	RT	Area	% Area	Height
1	43.671	8431273	41.24	85233
2	45.731	12012638	58.76	72576

Appendix C

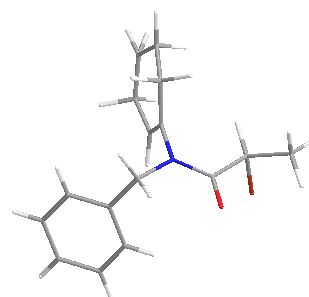
X-RAY CRYSTALLOGRAPHY DATA



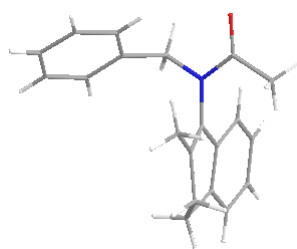
254



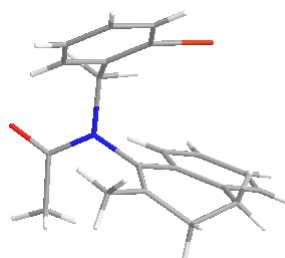
305



339



364



372

	254	305	339	364	372
Empirical	C ₂₀ H ₂₂ BrNO ₃ S	C ₂₁ H ₂₂ BrNO	C ₁₆ H ₂₀ BrNO	C ₂₀ H ₂₁ NO	C ₂₀ H ₂₀ BrNO
FW	436.36	384.31	322.24	291.38	370.28
Crystal Size	0.26 x 0.14 x 0.12	0.30 x 0.30 x 0.20	0.40 x 0.40 x 0.25	0.30 x 0.10 x 0.10	0.35 x 0.20 x 0.15
System	Monoclinic	Monoclinic	Orthorhombic	Orthorhombic	Monoclinic
Space group	P2 (1)/c	P2 (1)/c	Pbca	P2 (1)	P2 (1)/n
<i>a</i> (Å)	20.9783(10)	18.1071(3)	14.1009(3)	7.3684(3)	14.9163(3)
<i>b</i> (Å)	7.8705(4)	6.0419(10)	12.1784(2)	9.7503(4)	7.5696(13)
<i>c</i> (Å)	11.6620(5)	16.1361(2)	17.5284(4)	22.0856(9)	15.2555(2)
<i>α</i> (deg)	90	90	90	90	90
<i>β</i> (deg)	91.72	92.7860(10)	90	90	99.5960(16)
<i>γ</i> (deg)	90	90	90	90	90
<i>V</i> (Å³)	1924.64(16)	1763.22(5)	3010.10(11)	1586.74(11)	1698.39(5)
<i>D</i>_{cal} (Mgm⁻³)	1.506	1.448	1.422	1.220	1.448
<i>μ</i> (mm⁻¹)	2.264	2.338	2.724	0.074	2.425
<i>F</i>₀₀₀	896	792	1328	624	760
Total	24210	15270	14040	8310	13615
Reflections					
Independent	4389	4353	3691	3063	6820
<i>R</i>_{int}	0.0718	0.0248	0.0287	0.0415	0.0218
Data/Restraints/Parameters	4389/0/238	4353/0/219	3691/28/190	3063/0/201	6820/47/231
<i>R</i>₁, [<i>I</i> > 2σ(<i>I</i>)]	0.0606	0.0244	0.0368	0.0542	0.0366
w<i>R</i>₂	0.1547	0.0559	0.0948	0.1182	0.0839
GoF on <i>F</i>²	1.023	0.955	1.038	0.941	0.900

-
1. Bowman, W. R.; Bridge, C. F.; Brookes, P.; *J. Chem. Soc., Perkin Trans. 1*, **2000**, 1-14.
 2. Bowman, W. R.; Cloonan, M. O.; Krintel, S. L.; *J. Chem. Soc., Perkin Trans. 1*, **2001**, 2885-2902.
 3. Majumdar, K. C.; Basu, P. K.; Mukhopadhyay, P. P.; *Tetrahedron*, **2004**, 60, 6239-6278.
 4. Curran, D. P.; Tamine, J.; *J. Org. Chem.*, **1991**, 56, 2746-2750.
 5. Curran, D. P.; Kim, D.; *Tetrahedron*, **1991**, 47, 6171-6188.
 6. Kharasch, M. S.; Jensen, Elwood V.; Urry, W. H.; *J. Am. Chem. Soc.*, **1946**, 68 154-5.
 7. Kharasch, M. S.; Jensen, Elwood V.; Urry, W. H.; *Science*, **1945**, 102, 128.
 8. Kharasch, M. S.; Jensen, Elwood V.; Urry, W. H.; *J. Am. Chem. Soc.*, **1945**, 67, 1626.
 9. Murai, S.; Sonoda, N.; Tsutsumi, S.; *J. Org. Chem.*, **1964**, 29, 2104.
 10. Nagashima, H.; Wakamatsu, H.; Itoh, K.; Tomo, Y.; Tsuji, J.; *Tetrahedron Lett.*, **1983**, 24, 2395.
 11. Kropp, P.; *Acc. Chem. Res.*, **1984**, 17, 131-137.
 12. Lin, L. J.; Bent, B. E.; *J. Phys. Chem.*, **1992**, 96, 8529-8538.
 13. Zhang, X. M.; *J. Chem. Soc. Perkin Trans 2*, **1993**, 2275-2279.
 14. Iwamatsu, K.; Matsubara, K.; Nagashima, H.; *J. Org. Chem.*, **1999**, 64, 9625.
 15. Clark, A. J.; Battle, G. M.; Bridge, A. *Tetrahedron Letts.*, **2001**, 42, 1999.
 16. Nagashima, H.; Seji, K.; Ozaki, N.; Wakamatsu, H.; Itoh, K.; Tomo, Y.; Tsuji, J.; *J. Org. Chem.*, **1990**, 55, 986.
 17. Nagashima, H.; Ozaki, N.; Ishii, M.; Seki, K.; Washiyama, M.; Itoh, K.; *J. Org. Chem.*, **1993**, 58, 464.
 18. Clark, A. J. *Chem. Soc. Rev.*, **2002**, 31, 1-11.
 19. Nagashima, H.; Wakamatsu, H.; Itoh, K.; *J. Chem. Soc. Chem. Commun.*, **1984**, 652.
 20. Nagashima, H.; Ara, K.; Wakamatsu, H.; Itoh, K.; *J. Chem. Soc. Chem. Commun.*, **1985**, 518.
 21. Clark, A. J.; De Campo, F.; Deeth, R. J.; Filik, R. P.; Gatard, S.; Hunt, N. A.; Lastecoueres, D.; Thomas, G. H.; Verhlac, J. B.; Wongtap, H. *J. Chem. Soc., Perkin Trans. 1*, **2000**, 1, 671.
 22. Haddleton, D. M.; Clark, A. J.; Duncalf, D. J.; Heming, A. M.; Kukulj, D.; Shooter, A. J.; *J. Chem. Soc., Dalton Trans.*, **1998**, 381.
 23. Clark, A. J.; Duncalf, D. J.; Filik, R. P.; Haddleton, D. M.; Thomas, G. H.; Wongtap, H.; *Tetrahedron Lett.*, **1999**, 40, 3807.
 24. Clark, A. J.; Battle, G. M.; Heming, A. M.; Haddleton, D. M.; Bridge, A.; *Tetrahedron Lett.*, **2001**, 42, 2003.
 25. Clark, A. J.; Dell, C. P.; Ellard, J. M.; Hunt, N. A.; McDonagh, J. P.; *Tetrahedron Lett.*, **1999**, 40, 8619.

26. Benedetti, M.; Forti, L.; Ghelfi, F.; Pagnoni, U. M.; Ronzoni, R.; *Tetrahedron*, **1997**, 41, 14031.
27. Ghelfi, F.; Bellesia, F.; Forti, L.; Ghirardini, G.; Grandi, R.; Libertini, E.; Montemaggi, M. C.; Pagnoni, U. M.; Pinetti, A.; De Buyck, L.; Parsons, A. F.; *Tetrahedron*, **1999**, 55, 5839.
28. Ghelfi, F.; Parsons, A. F.; *J. Org. Chem.*, **2000**, 65, 6249.
29. Ghelfi, F.; Ghirardini, G.; Libertini, E.; Forti, L.; Pagnoni, U. M.; *Tetrahedron Lett.* **1999**, 40, 8595.
30. Stevens, C. V.; Van Meenen, E.; Masschelein, K. G. R.; Eeckhout, Y.; Hooghe, W.; D'honte, B.; Nemykin, V. N.; Zhdankin, V. V.; *Tetrahedron Lett.*, **2007**, 48, 7108-7111.
31. Ghelfi, F.; Rancaglia, F.; Pattarozzi, M.; Giangiordano, V.; Petrillo, G.; Sancassan, F.; Parsons, A. F.; *Tetrahedron*, **2009**, 65, 10323-10333.
32. Clark, A. J.; Filik, R. P.; Thomas, G. H.; *Tetrahedron Lett.*, **1999**, 40, 4885.
33. Clark, A. J.; Wilson, P. *Tetrahedron Lett.*, **2008**, 49, 4848.
34. Clark, A. J.; Dell, C. P.; McDonagh, J. P. C. R.; *Acad. Sci. Ser IIC: Chim.*, **2001**, 4, 575.
35. Clark, A. J.; Battle, G. M.; Bridge, A.; *Tetrahedron Lett.*, **2001**, 42, 4409.
36. Davies, T. D.; Kapur, N.; Parsons, A. F.; *Tetrahedron Lett.*, **1999**, 40, 8615.
37. Davies, T. D.; Kapur, N.; Parsons, A. F.; *Tetrahedron*, **2000**, 56, 3941.
38. Clark, A. J.; Geden, J. V.; Thom, S.; Wilson, P.; *J. Org. Chem.*, **2007**, 72, 5923-5926.
39. De Campo, F.; Lastecoueres, D.; Verlhac, J. B.; *Chem. Commun.*, **1998**, 2117.
40. De Campo, F.; Lastecoueres, D.; Verlhac, J. B.; *J. Chem. Soc., Perkin Trans. 1*, **2000**, 575.
41. Ram, R. N.; Tittal, R. K.; Upreti, S.; *Tetrahedron Lett.*, **2007**, 48, 7994-7997.
42. Arduengo, A. J.; III. *Acc. Chem. Res.*, **1999**, 32, 913-921.
43. Jurkauskas, V.; Sadighi, J. P.; Buchwald, S. L.; *Org. Lett.*, **2003**, 5, 2417-2420.
44. Kaur, H.; Zinn, F. K.; Stevens, E. D.; Nolan, S. P.; *Organometallics*, **2004**, 23, 1157-1160.
45. Fructos, M. R.; De Fremont, P.; Nolan, S.P.; Mar, D.-R. M.; Perez, P. J.; *Organometallics*, **2006**, 25, 2237-2241.
46. Diez-Gonzalez, S.; Correa, A.; Cavallo, L.; Nolan, S. P.; *Chem. Eur. J.*, **2006**, 12, 7558-7564.
47. Bull, J. A.; Hutchings, M. G.; Lujan, C.; Quayle, P.; *Tetrahedron Lett.*, **2008**, 49, 1352-1356.
48. Motherwell, W. B.; Pennell, A. M. K.; *Chem. Commun.*, **1991**, 877.
49. da Mata, M. L. E. N.; Motherwell, W. B.; Ujjainwalla, F.; *Tetrahedron Letts.*, **1997**, 38, 137.
50. da Mata, M. L. E. N.; Motherwell, W. B.; Ujjainwalla, F.; *Tetrahedron Letts.*, **1997**, 38, 141.
51. Bonfand, E.; Forsland, L.; Motherwell, W. B.; Vazquez, S.; *Synlett.*, **2000**, 475.
52. Clark, A. J.; Coles, S. R.; Collis, A.; Debure, T.; Guy, C.; Murphy, N. P.; Wilson, P.; *Tetrahedron Letts.*, **2009**, 50, 5609-5612.

53. Clark, A. J.; Coles, S. R.; Collis, A.; Fullaway, D. R.; Murphy, N. P.; Wilson, P.; *Tetrahedron Letts.*, **2009**, 50, 6311-6314.
54. Hernan, A. G.; Horton, P. N.; Hursthouse, M. B.; Kilburn, J. D.; *J. Organometallic Chem.*, **2006**, 691, 1466-1475.
55. Clark, A. J.; Filik, R. J.; Haddleton, D. M.; Radigue, A.; Sanders, C. J.; *J. Org. Chem.*, **1999**, 64, 8954-8957.
56. Clark, A. J.; Geden, J. V.; Thom, S.; *J. Org. Chem.*, **2006**, 71, 1471-1479.
57. Motoyama, Y.; Kamo, K.; Yuasa, A.; Nagashima, H.; *Chem. Commun.*, **2010**, 46, 2256-2258.
58. Curran, D. P.; Hadida, S.; *J. Am. Chem. Soc.*, **1996**, 118, 2531.
59. Curran, D. P.; Hoshino, M.; *J. Org. Chem.*, **1996**, 61, 6480.
60. Curran, D. P.; Hadida, S.; He, M.; *J. Org. Chem.*, **1997**, 62, 6714.
61. De Campo, F.; Lastecoueres, D.; Vincent, J. M.; Verlhac, J. B.; *J. Org. Chem.*, **1999**, 64, 4969.
62. Wang, J. S.; Matyjaszewski, K.; *J. Am. Chem. Soc.*, **1995**, 117, 5614-5615.
63. Kato, M.; Kamigaito, M.; Sawamoto, M.; Higashimura, T.; *Macromolecules*, **1995**, 28, 1721-1723.
64. Matyjaszewski, K.; Jakubowski, W.; Min, K.; Tang, W.; Huang, J.; Braunecker, W. A.; Tsarevsky, N. V.; *Proc. Nat. Acad. Sci. U.S.A.*, **2006**, 103, 15309-15314.
65. De Vries, A.; Klumperman, B.; De Wet-Roos, D.; Sanderson R. D.; *Macromol. Chem. Phys.*, **2001**, 202, 1645-1648.
66. Jakubowski, W.; Min, K.; Matyjaszewski, K.; *Macromolecules*, **2006**, 39, 39-45.
67. Min, K.; Jakubowski, W.; Matyjaszewski, K.; *Macromol. Rapid Commun.*, **2006**, 27, 594-598.
68. Min, K.; Gao, H.; Matyjaszewski, K.; *J. Am. Chem. Soc.*, **2005**, 127, 3825-3830.
69. Quebatte, L.; Thommes, K.; Severin, K.; *J. Am. Chem. Soc.*, **2006**, 128, 7440-7441.
70. Eckenhoff, W. T.; Pintauer, T.; *Inorg. Chem.*, **2007**, 46, 5844-5846.
71. Eckenhoff, W. T.; Garrity, S. T.; Pintauer, T.; *Eur. J. Inorg. Chem.*, **2008**, 563-571.
72. Pintauer, T.; Eckenhoff, W. T.; Ricardo, C.; Balili, M. N. C.; Biernesser, A. B.; Noonan, S. J.; Taylor, M. J. W.; *Chem. Eur. J.*, **2009**, 15, 38-41.
73. Pintauer, T.; Matyjaszewski, K.; *Chem. Soc. Rev.*, **2008**, 37, 1087-1097.
74. Ricardo, C.; Pintauer, T.; *Chem. Commun.*, **2009**, 3029-3031.
75. Munoz-Molina, J. M.; Belderrain, T. R.; Perez, P. J.; *Inorg. Chem.*, **2010**, 49, 642-645.
76. Munoz-Molina, J. M.; Caballero, A.; Diaz-Requejo, M. M.; Trofimenko, S.; Belderrain, T. R.; Perez, P.; *J. Inorg. Chem.*, **2007**, 46, 7725.
77. Jones, K.; Thompson, M.; Wright, C.; *J. Chem. Soc. Chem. Comm.*, **1986**, 115.
78. Clark, A. J.; Jones, K.; *Tetrahedron Lett.*, **1989**, 30, 5485-5488.
79. Clark, A. J.; Jones, K.; *Tetrahedron*, **1992**, 48, 6875-6882.
80. Patel, V. F.; Pattenden, G.; *J. Chem. Soc. Perkin Trans 1*, **1990**, 2703-2708.
81. Boivin, J.; Yousfi, M.; Zard, S. Z.; *Tetrahedron Lett.*, **1994**, 35, 5629.
82. Iqbal, J.; Bhatia, B.; Nayyar, N. K.; *Chem. Rev.*, **1994**, 94, 519.

83. Motoyama, Y.; Hanada, S.; Shimamoto, K.; Nagashima, H.; *Tetrahedron*, **2006**, 62, 2779-2788.
84. Thommes, K.; Icli, B.; Scopelliti, R.; Severin, K.; *Chem. Eur. J.*, **2007**, 13, 6899-6907.
85. Quayle, P.; Fengas, D.; Richards, S.; *Synlett*, **2003**, 12, 1797-1800.
86. Faulkner, J.; Edlin, C. D.; Fengas, D.; Preece, I.; Quayle, P.; Richards, S.; *Tetrahedron Lett.*, **2005**, 46, 2381-2385.
87. Edlin, C. D.; Faulkner, J.; Quayle, P.; *Tetrahedron Lett.*, **2006**, 47, 1145-1151.
88. C. D. Edlin, J. Faulkner, D. Fengas, C. K. Knight, J. Parker, I. Preece, P. Quayle and S. N. Richards, *Synlett*, **2005**, 4, 572-576.
89. Cao, L.; Chaozhong, L.; *Tetrahedron Lett.*, **2008**, 49, 7380-7382.
90. Feray, L.; Bertrand, M. P.; *Eur. J. Org. Chem.*, **2008**, 3164-3170.
91. Jasperse, C.P.; Curran, D.P.; Fevig, T.L.; *Chem. Rev.*, **1991**, 91, 1237-1286.
92. Quirante, J.; Escolano C.; Merino, A.; Bonjoch, J.; *J. Org. Chem.*, **1998**, 63, 968-976.
93. De Buyck, L.; Forazto, C.; Ghelfi, F.; Mucci, A.; Nitti, P.; Pagnoni, U. M.; Parsons, A. F.; Pitacco, G.; Roncaglia, F.; *Tetrahedron Lett.*, **2006**, 47, 7759-7762.
94. Pattenden, G.; Rescourio, G.; *Org. Biomol. Chem.*, **2008**, 6, 3428-3438.
95. Corey, E. J.; Li, W. D. Z.; *Chem. Pharm. Bull.*, **1999**, 47, 1-10.
96. Masse, E. C.; Morgan, A. J.; Adams, J.; Panek, J. S.; *Eur. J. Org. Chem.*, **2000**, 2513-2528.
97. Kuo, Y. L.; Dhanasekaran, M.; Sha, C. K.; *J. Org. Chem.*, **2009**, 74, 2033-2038.
98. Cimino, G.; De Rosa, S.; De Stefano, S.; Sodano, G.; *Comp. Biochem. Physiol.*, **1982**, 73B, 471-474.
99. Pawlik, J. R. *Chem. Rev.*, **1993**, 93, 1911-1922.
100. Piers, E.; Yeung, B. W. A.; *Can. J. Chem.*, **1986**, 64, 2475-2476.
101. Piers, E.; Yeung, B. W. A.; Rettig, S. J.; *Tetrahedron*, **1987**, 43, 5521-4535.
102. Guevel, A.-C.; Hart, D. J.; *Synlett*, **1994**, 169-170.
103. Hart, D. J.; Lai, C.-S.; *Synlett*, **1989**, 49-51.
104. Chenera, B.; Chuang, C.-P.; Hart, D. J.; Lai, C.-S.; *J. Org. Chem.*, **1992**, 57, 2018-2029.
105. Guevel, A.-C.; Hart, D. J.; *J. Org. Chem.*, **1996**, 61, 473-479.
106. Felluga, F.; Forzato, C.; Ghelfi, F.; Nitti, P.; Pitacco, G.; Pagnoni, U. M.; Roncaglia, F.; *Tetrahedron: Asymmetry*, **2007**, 527-536.
107. Helliwell, M.; Fengas, D.; Knight, C. K.; Parker, J.; Quayle, P.; Raftery, J.; Richards, S. N.; *Tetrahedron Lett.*, **2005**, 46, 7129-7134.
108. Roncaglia, F.; Stevens, C. V.; Ghelfi, F.; Van Der Steen, M.; Pattarozzi, M.; De Buyck, L.; *Tetrahedron*, **2009**, 65, 1481-1487.
109. Weber, W.; Semar, M.; Anke, T.; Bross, M.; Steglich, W.; *Planta Med.*, **1992**, 58, 56-59.
110. Bellesia, F.; Danieli, C.; De Buyck, L.; Galeazzi, R.; Ghelfi, F.; Mucci, A.; Orena, M.; Pagnoni, U. M.; Parsons, A. F.; Roncaglia, F.; *Tetrahedron*, **2006**, 746-757.

111. Singh, S. B.; Zink, D. L.; Liesch, J. M.; Goetz, M. A.; Jenkins, R. G.; Nallin-Omstead, M.; Silverman, K. C.; Bills, G. F.; Mosley, R. T.; Gibbs, J. B.; Albers-Schonberg, G.; Lingham, R. B.; *Tetrahedron*, **1993**, 49, 5917–5926.
112. Singh, S. B.; Jayasuriya, H.; Silverman, K. C.; Bonfiglio, C. A.; Williamson, J. M.; Lingham, R. B.; *Bioorg. Med. Chem.*, **2000**, 8, 571–580.
113. Chikashita, H.; Ide, H.; Itoh, K.; *J. Org. Chem.*, **1986**, 51, 5400.
114. Tanner, D. D.; Chan, J. J.; *J. Org. Chem.*, **1989**, 54, 3842.
115. Dittmer, D. C.; Lombardo, A.; Batzold, F. H.; Greene, C. S.; *J. Org. Chem.*, **1976**, 41, 2976.
116. Naito, T.; Saito, S.; Ueda, M.; Miyata, O.; *Heterocycles*, **2005**, 65, 1857.
117. Cossy, J.; Ranaivosata, J. L.; Bellosta, V.; *Tetrahedron Lett.*, **1994**, 35, 8161.
118. Ishibashi, H.; Haruki, S.; Uchiyama, M.; Tamura, O.; Matsuo, J.; *Tetrahedron Lett.*, **2006**, 47, 6263–6266.
119. Ishibashi, H.; Sasaki, M.; Taniguchi, T.; *Tetrahedron*, **2008**, 64, 7771–7773.
120. Bhandal, H.; Patel, V. F.; Pattenden, G.; Russel; *J. Chem. Soc.; Perkin Trans 1*, **1990**, 2691–2702.
121. Samsel, E. G.; Kochi, J. K.; *J. Am. Chem. Soc.*, **1986**, 108, 4790.
122. Hill, C. L.; Whiteside, G. M.; *J. Am. Chem. Soc.*, **1974**, 96, 870.
123. Beckwith, A. L. J.; Meifs, C. F.; *J. Chem. Soc. Chem. Commun.*, **1981**, 595.
124. Stork, G.; Sher, P. M.; *J. Am. Chem. Soc.*, **1983**, 105, 6765.
125. Baldwin, J. E.; Kelly, D. R.; Ziegler, C. B.; *J. Chem. Soc. Chem. Commun.*, **1984**, 133.
126. Huhtasaari, M.; Schafer, H. J.; Becking, L.; *Angew. Chem. Int. Ed. Engl.*, **1984**, 23, 980.
127. Haddleton, D. M.; Jasieczek, C. B.; Hannon, M. J.; Shooter, A. J.; *Macromolecules*, **1997**, 30, 2190.
128. Haddleton, D. M.; Clark, A. J.; Crossman, M. C.; Duncalf, D. J.; Heming, A. M.; Morsley, S. R.; Shooter, A. J.; *Chem. Commun.*, **1997**, 1173.
129. Matyjaszewski, K.; Xia, J.; *Chem. Rev.*, **2001**, 101, 2921–2990.
130. Pintauer, T.; Matyjaszewski, K.; *Coordination Chemistry Reviews*, **2005**, 1155–1184.
131. Tang, W.; Kwak, Y.; Braunecker, W.; Tsarevsky, N. V.; Coote, M. L.; Matyjaszewski, K.; *J. Am. Chem. Soc.*, **2008**, 130, 10702–10713.
132. Gossage, R. A.; Van De Kuil, L. A.; Van Koten, G.; *Acc. Chem. Res.*, **1998**, 31, 423.
133. Severin, K.; *Curr. Org. Chem.*, **2006**, 10, 217.
134. Fischer, H.; *Chem. Rev.*, **2001**, 101, 3581–3610.
135. Zhang, H.; Klumperman, B.; Ming, W.; Fischer, H.; van der Lind, R.; *Macromolecules*, **2001**, 34, 6169–6173.
136. Tang, W.; Tsarevsky, N. V.; Matyjaszewski, K.; *J. Am. Chem. Soc.*, **2006**, 128, 1598–1604.
137. Tang, H.; Radosz, M.; Shen, Y.; *Macromol. Rapid. Commun.*, **2006**, 27, 1127–1131.

-
138. Tang, H.; Shen, Y.; Li, B. G.; Radosz, M.; *Macromol. Rapid. Commun.*, **2008**, 29, 1834-1838.
139. Tang, H.; Arulsamy, N.; Radosz, M.; Shen, Y.; Tsarevsky, N. V.; Braunecker, W.; Tang, W.; Matyjaszewski, K.; *J. Am. Chem. Soc.*, **2006**, 128, 16277-16285.
140. Jakubowski, W.; Matyjaszewski, K.; *Angew. Chem. Int. Ed.*, **2006**, 45, 4482-4486.
141. Matyjaszewski, K.; Dong, H.; Jakubowski, W.; Pietrasik, J.; Kusumo, A.; *Langmuir*, **2008**, 23, 4528-4531.
142. Bawn, C. E. H.; Mellish, S. F.; *Trans. Faraday. Soc.*, **1951**, 47, 1216.
143. Walling, C. J.; *Polym. Sci.*, **1954**, 14, 214.
144. Hammond, G. S.; Sen, J. N.; Boozer, C. E.; *J. Am. Chem. Soc.*, **1955**, 77, 3244.
145. Sasaki, H.; Nagayama, M.; *Appl. Polym. Chem.*, **1967**, 11, 2097.
146. MacCallum, J. R.; *J. Chem. Ed.*, **1971**, 48, 705.
147. Clayden, J.; Greeves, N.; Warren, S.; Wothers, P.; *Organic Chemistry*. Oxford University Press Inc.: New York. **2001**
148. Beckwith, A. L. J.; Goh, S. H.; *J. Chem. Soc. Chem. Commun.*, **1983**, 905.
149. Beckwith, A. L. J.; Goh, S. H.; *J. Chem. Soc. Chem. Commun.*, **1983**, 907.
150. Beckwith, A. J. L.; Abeywickrema, A. N.; *Tetrahedron Letts.*, **1986**, 109-112.
151. Beckwith, A. L. J.; Gara, W. B.; *J. Am. Chem. Soc.*, **1969**, 91, 5689.
152. Chung, S-K.; Chung, F-F.; *Tetrahedron Letts.*, **1979**, 2473.
153. Liu, Q.; Han, B.; Zhang, W.; Yang, L.; Liu, Z-L.; Yu, W.; *Synlett*, **2005**, 2248.
154. Barltrop, H.; Bradbury, D.; *J. Am. Chem. Soc.*, **1973**, 95, 5085.
155. Kropp, M.; Schuster, G. B.; *Tetrahedron Letts.*, **1987**, 5295.
156. Wiberg, E.; Henle W. Z. *Naturforsch. Teil B.*, **1952**, 7, 582.
157. Klingen, T. J. *Inorg. Chem.*, **1964**, 3, 1058.
158. Spokas, R. J.; James, B. D. *Inorganica Chimica Acta*, **1986**, 118, 99-104.
159. Sorrel, T. N.; Spillane, R. J. *Tetrahedron Letts.*, **1978**, 2473.
160. Fleet, G. W. T.; Harding P. J. C. *Tetrahedron Letts.*, **1981**, 22, 675.
161. Kunkely, H.; Vogler, A.; *Inorg. Chem. Commun.*, **2002**, 5, 239-241.
162. Kunkely, H.; Vogler, A.; *Journal of Photochemistry and Photobiology A: Chemistry*, **2002**, 147, 149-152.
163. Percec, V.; Guliashvili, D.; Ladislav, J. S.; Wistrand, A.; Stjerndahl, A.; Sienkowska, M. J.; Monteiro, M. J.; Sahoo, S. *J. Am. Chem. Soc.*, **2006**, 128, 14156-14165
164. Matyjaszewski, K.; Dong, H.; *Macromolecules*, **2008**, 41, 6868-6870.
165. Guliashvili, T.; Percec, V.; *J. Polym. Sci. Part A: Polym. Chem.*, **2007**, 45, 1607-1618.
166. Monteiro, M. J.; Guliashvili, T.; Percec, V.; *J. Polym. Sci. Part A: Polym. Chem.*, **2007**, 45, 1835-1847.
167. Lligadas, G.; Ladislav, J. S.; Guliashvili, T.; Percec, V.; *J. Polym. Sci. Part A: Polym. Chem.*, **2008**, 46, 278-288.
168. Matyjaszewski, K.; Tsarevsky, N. V.; Braunecker, W. A.; Dong, H.; Huang, J.; Jakubowski, W.; Kwak, Y.; Nicolay, R.; Tang, W.; Yoon, J. A. *Macromolecules*, **2007**, 40, 7795-7806.
169. Parsons A. F. *C. R. Acad. Sci. Paris, Chimie*, **2001**, 4, 391-400.

-
170. Bryans, J. S.; Chessum, E. A.; Parsons, A. F.; Ghelfi, F. *Tetrahedron Letts.*, **2001**, 42, 2901-2905.
171. Oki, M.; *The Chemistry of Rotational Isomers*. Springer-Verlag: New York, **1993**, Vol 30.
172. Cahn, R. S.; Ingold, C.; Prelog, V.; *Angew. Chem. Int. Ed.*, **1966**, 5, 385-415.
173. Christie, G. H.; Kenner, J.; *J. Chem. Soc. Trans.*, **1922**, 614-620.
174. Noyori, R.; *Angew. Chem. Int. Ed.*, **2002**, 41, 2008-2022.
175. Nicolaou, K. C.; Mitchell, H. J.; Jain, N. F.; Winssinger, N.; Hughes, R.; Bando, T.; *Angew. Chem. Int. Ed.*, **1999**, 38, 240-244.
176. Bringmann, G.; Harmsen, S.; Holenz, J.; Geuder, T.; Götz, R.; Keller, P. A.; Walter, R.; Hallock, Y. F.; Cardellina II, J. H.; Boyd, M. R.; *Tetrahedron*, **1994**, 50, 9643-9648.
177. Curran, D. P.; Qi, H.; Geib, S. J.; De Mello, N. C.; *J. Am. Chem. Soc.*, **1994**, 116, 3131-3132.
178. Curran, D. P.; Hale, G. R.; Geib, S. J.; Balog, A.; Cass, Q. B.; Degani, A. L. G.; Hernandez, M. Z.; Freitas, L. C. G.; *Tetrahedron Asymmetry*, **1997**, 8, 3955-3975.
179. Curran, D. P.; Chen, C. H. T.; Geib, S. J.; Lapierre, A. J. B.; *Tetrahedron*, **2004**, 60, 4413-4424.
180. Petit, M.; Geib, S. J.; Curran, D. P.; *Tetrahedron*, **2004**, 60, 7543-7552.
181. Lapierre, A. J. B.; Geib, S. J.; Curran, D. P.; *J. Am. Chem. Soc.*, **2007**, 129, 494-495.
182. Guthrie, D. B.; Damodaran, K.; Curran, D. P.; Wilson, P.; Clark, A. J.; *J. Org. Chem.*, **2009**, 74, 4262-4266.
183. Adler, T.; Bonjoch, J.; Clayden, J.; Lai, L.; Font-Bardia, M.; Pickworth, M.; Solans, X.; Sole, D.; Vallverdu, L.; *Org. Biomol. Chem.*, **2005**, 3, 3173-3183.
184. Ahmed, A.; Bragg, R. A.; Clayden, J.; Lai, L. W.; McCarthy, C.; Pink, J. H.; Westlund, N.; Yasin, S.; *Tetrahedron*, **1998**, 54, 13277-13294.
185. Betson, M. S.; Clayden, J.; Helliwell, M.; Johnson, P.; Lai, L. W.; Pink, J. H.; Stimson, C. C.; Vassiliou, M.; Yasin, S.; Youssef, L.; *Org. Biomol. Chem.*, **2006**, 424-443.
186. Clayden, J.; *Synlett*, **1998**, 810-816.
187. Clayden, J.; *Chem. Commun.*, **2004**, 127-135.
188. Clayden, J.; Foricher, Y. J. Y.; Helliwell, M.; Johnson, P.; Mitjans, D.; Vinader, V.; *Org. Biomol. Chem.*, **2006**, 444-454.
189. Clayden, J.; Lai, L. W.; *Angew. Chem. Int. Ed.*, **1999**, 38, 2556-2558.
190. Clayden, J.; Lai, L. W.; Helliwell, M.; *Tetrahedron*, **2004**, 60, 4399-4412.
191. Clayden, J.; Vallverdu, L.; Helliwell, M.; *Org. Biomol. Chem.*, **2006**, 2106-2118.
192. Bragg, R. A.; Clayden, J.; Morris, G. A.; Pink, J. H.; *Chem. Eur. J.*, **2002**, 8, 1279-1289.
193. Clayden, J.; Lai, L. W.; Helliwell, M.; *Tetrahedron Asymmetry*, **2001**, 12, 695-698.
194. Clayden, J.; Stimson, C. C.; Keenan, M.; Wheatley, A. E. H.; *Chem. Commun.*, **2004**, 228-229.
195. Adams, R.; Sundholm, N. K.; *J. Am. Chem. Soc.*, **1948**, 70, 2667-2673.

-
196. Stewart, W. E.; Siddell III, T. H.; *Chem. Rev.*, **1970**, 70, 517-551
197. Carey, F. A.; Sundberg, R. J.; *Advanced Organic Chemistry Part A; Structure and Mechanisms*. 4th ed; Kluwer Academic / Plenum Publishers: New York, 2000.
198. Curran, D. P.; Liu, W. D.; Chen, C. H. T.; *J. Am. Chem. Soc.*, **1999**, 121, 11012-11013.
199. Wunderlich, M. D.; Leung, L. K.; Sandberg, J. A.; Meyer, K. D.; Yoder, C. H.; *J. Am. Chem. Soc.*, **1978**, 100, 1500-1503.
200. Siddall, T. H.; Stewart, W. E.; Knight, F. D.; *J. Phys. Chem.*, **1970**, 74, 3580-3583.
201. Pedersen, B. F.; Pedersen, B.; *Tetrahedron Lett.*, **1965**, 6, 2996-3001.
202. Cass, Q. B.; Degani, A. L. G.; Tiritan, M. E.; Matlin, S. A.; Curran, D. P.; Balog, A.; *Chirality*, **1997**, 9, 109-112.
203. Petit, M.; Lapierre, A. J. B.; Curran, D. P.; *J. Am. Chem. Soc.*, **2005**, 127, 14994-14995.
204. Kawabata, T.; Yahiro, K.; Fuji, K.; *J. Am. Chem. Soc.*, **1991**, 113, 9694-9696.
205. Fuji, K.; Kawabata, T.; *Chem. Eur. J.*, **1998**, 4, 373-376.
206. Zhao, H.; Hsu, D. C.; Carlier, P. R.; *Synthesis*, **2005**, 1, 1-16.
207. Jones, K.; McCarthy, C.; *Tetrahedron Lett.*, **1989**, 30, 2657-2660.
208. Ates, A.; Curran, D. P.; *J. Am. Chem. Soc.*, **2001**, 123, 5130-5131.
209. Tamura, O.; Matsukida, H.; Toyao, A.; Takeda, Y.; Ishibashi, H.; *J. Org. Chem.*, **2002**, 67, 5537-5545.
210. Ishibashi, H.; Ishita, A.; Tamura, O.; *Tetrahedron Lett.*, **2002**, 43, 473-475.
211. Clark, A. J.; Dell, C. P.; McDonagh, J. P.; Geden J.; Mawdsley, P.; *Org. Lett.*, **2003**, 5, 2063-2066.
212. Chatgililoglu, C.; Ferreri, C.; Guerra, M.; Timokhin, V.; Froudakis, G.; Gimisis, T.; *J. Am. Chem. Soc.*, **2002**, 124, 10765-10772.
213. Curran, D. P.; Guthrie, D. B.; Geib, S. J.; *J. Am. Chem. Soc.*, **2008**, 130, 8437-8445.
214. Musa, O. M.; Horner, J. H.; Newcomb, M.; *J. Org. Chem.*, **1999**, 64, 1022-1025.
215. Chupp, J. P.; Olin, J. F.; *J. Org. Chem.*, **1967**, 32, 2297-2303.
216. Otani, Y.; Nagae, O.; Naruse, Y.; Inagaki, S.; Ohno, M.; Yamaguchi, K.; Yamamoto, G.; Uchiyama, M.; Ohwada, T.; *J. Am. Chem. Soc.*, **2003**, 125, 15199-15199.
217. Guthrie, D. B.; Ph.D Dissertation, Univeristy of Pittsburgh, **2008**.
218. Sandstrom, J.; *Dynamic NMR Spectroscopy*; Academic Press Inc.; New York, **1982**.
219. Mannschreck, A.; Vonderheid, C.; *Chem. Lett.*, **1977**, 6, 211-214.
220. Ahlbrect, H.; Becher, G.; Blecher, J.; Kalinowski, H. O.; Raab, W.; Mannschreck, A.; *Tetrahedron Lett.*, **1979**, 24, 2265-2268.
221. Reich, H. J.; *J. Chem. Ed. Software*, **1966**, 3D, 2.
222. Geise, B.; *Angew. Chem. Int. Ed.*, **1983**, 22, 753-764.
223. Yamada, S.; *Rev. Heteroatom. Chem.*, **1999**, 19, 203-236.

-
224. Bakmutov, V. I.; Babievshii, K. K.; Fedin, E. I.; *Acad. Sci. USSR*, **1981**, 4, 776-781.
225. Kaur, S.; Eberhardt, E. S.; Doucette, A.; Chase, A.; Dalby, C.; *J. Org. Chem.*, **2002**, 67, 3937-3940.
226. Faria, M. D. G.; Teixeira-Dias, J. J. C.; Fausto, R.; *Vibrational Spectroscopy*, **1991**, 2, 43-60.
227. Boar, R. B.; McGhie, J. F.; Robinson, M.; Barton, D. H. R.; Horwell, D. C.; Stick, R. V.; *J. Chem. Soc. Perkin Trans 1*, **1975**, 1237-1241.
228. Bayer, A.; Maier, M.; *Tetrahedron*, **2004**, 60, 6665-6677.
229. Zhao, H.; Vandenbossche, C. P.; Koenig, S. G.; Singh, S. P.; Bakale, R. P.; *Org Lett.*, **2008**, 3, 505-507.
230. Guan, Z. H.; Huang, K.; Yu, S.; Zhang, X.; *Org Lett.*, **2009**, 2, 481-483.
231. Burk, M. J.; Casy, G.; Johnson, N. B.; *J. Org. Chem.*, **1998**, 63, 6084.
232. Brettle, R.; Shibib, S. M.; Wheeler, K. J.; *J. Chem. Soc. Perkin Trans 1*, **1985**, 831-836.
233. Rodriguez, R.; Estiarte, M. A.; Diez, A.; Rubiralta, M.; Colell, A.; Garcia-Ruiz, C.; Fernandez-Checa, J. C.; *Tetrahedron*, **1996**, 52, 7727-7736.
234. El-Nabi, H. A. A.; *Tetrahedron*, **2000**, 56, 3013-3020.
235. Kagan, H. B.; *Tetrahedron*, **2003**, 59, 10351-10372.
236. Kakimoto, M.; Yamamoto, T.; Okawara, M.; *Tetrahedron Lett.*, **1979**, 623.
237. Oppolzer, W.; Ruiz-Montes, J.; *Helvetica Chimica Acta.*, **1993**, 1266-1274.
238. Ozaki, S.; Matsushita, H.; Ohmori, H.; *J. Chem. Soc. Perkin Trans 1*, **1993**, 2339-2344.
239. Mukherjee, S.; List, B.; *J. Am. Chem. Soc.*, **2007**, 129, 11336-11337.
240. Blid, J.; Brandt, P.; Somfai, P.; *J. Org. Chem.*, **2004**, 69, 3043-3049.
241. Yoshida, M.; Komatsuzaki, Y.; Ihara, M.; *Org. Lett.*, **2008**, 10, 2083-2086.
239. Shigeko, O.; Hidenori, M.; Hidenobu, O.; *J. Chem. Soc., Perkin Trans 1*, **1993**, 2339-44.
243. Liard, A.; Quiclet-Sire, B.; Zard, S. Z.; *Tetrahedron Lett.*, **1996**, 37, 5877-5880.
244. Naito, T.; Tada, Y.; Nishiguchi, Y.; Ninomiya, I.; *J. Chem. Soc., Perkin Trans 1*, **1985**, 487-91.
245. Paulvannan, K.; Stille, J. R.; *J. Org. Chem.*, **1992**, 57, 5319-5328.
246. Zhu, G.; Zhang, X.; *J. Org. Chem.*, **1998**, 63, 9590-9593,